The Role of Myc in Aging and Longevity in Mice

Jeffrey Walter Hofmann

B.S., Brown University, 2008

A dissertation submitted in partial fulfillment of the requirements for the degree of Doctor of Philosophy in the Division of Biology and Medicine at Brown University

Providence, Rhode Island

May 2014

This dissertation by Jeffrey Walter Hofmann is accepted in its present form by the Division of Biology and Medicine as satisfying the dissertation requirement for the degree of Doctor of Philosophy.

Date _____ _____

John M. Sedivy, Ph.D. (Advisor)

Recommended to the Graduate Council

Date _____ _____

Richard Freiman, Ph.D.

Date _____ _____

Marc Tatar, Ph.D.

Date _____ _____

Philip Gruppuso, M.D.

Date _____ _____

Andrzej Bartke Ph.D.

Approved by the Graduate Council

Date _____ _____

Peter Weber, Ph. D,

Dean of the Graduate School

Jeffrey Walter Hofmann
Curriculum Vitae

BIRTH: January 10, 1986,
Houston, Texas

EDUCATION:

Sc.B., Computational Biology, Brown University, 2008
MD/PhD Candidate, Brown University, 2016

AWARDS:

2005	Summer Research Assistantship Award (Brown University)
2007	Undergraduate Teaching and Research Award (Brown University)
2007	Royce Fellowship Award (Brown University)

GRANTS AWARDED:

10/2009	F30 NIH Grant: Wnt signaling in cellular senescence and aging

RESEARCH:

Undergraduate Research Assistant, May 2005 – May 2008
Department of Ecology and Evolutionary Biology, Brown University
Assisted Dr. David Rand with research involving mitochondrial genomics. Specific topics included:

Using bioinformatics to assess mitochondrial evolution in Drosophila.
Investigating the interaction between mitochondrial genotype and dietary restriction in longevity
Using Drosophila as a model organism to study Parkinson's Disease genetics.

Undergraduate Researcher, March 2007 – March 2008
Brown University international Genetically Engineered Machines (iGEM) team.
Worked on a team of 7 undergraduates, advised by Drs. Gary Wessel, Alex Brodsky, and Tayhas Palmore, to compete in an international synthetic biology competition. Specific topics included:

Engineering E. Coli to act as a lead sensing device
Developing a genetic tri-stable switch to be used in future E. Coli-based systems

Graduate Research, June 2008 – August 2008
Department of Orthopedics, Brown Medical School
Assisted Drs. Qian Chen and Xu Yang in researching the localization of the Shh protein and its role in chondrocyte development.

Graduate Research, June 2009 – Ongoing
Department of Molecular Biology, Cell Biology, and Biochemistry, Brown University
Working with Dr. John Sedivy to investigate the roles of Myc and Wnt signaling in cellular senescence and aging.

PRESENTATIONS:

10/2008	Poster at the international iGEM conference. "Creating Lead Sensing Bacteria."
2009-2010	Aging Interest Group (2009-2010). Organized and hosted lectures about aging
10/2011	Poster presented at the San Antonio Nathan Shock Conference on Aging. "The role of Myc in aging and inflammation."
12/2011	CCRI/Brown University Symposium. Lecture: "Gene Expression Analysis and Aging in Mice"
1/2012	Boston Aging Data Series: "Supply-side metabolism – fueling longevity?"
1/2012	Providence Area Aging Research Forum: "Supply-side metabolism – fueling longevity?"
8/2013	National MD/PhD Student Conference, Keystone Colorado. Poster: "Myc haploinsufficiency increases longevity and inhibits effects of aging"

PUBLICATIONS:

Montooth KL, Abt DN, Hofmann JW, Rand DM. Comparative genomics of Drosophila mtDNA: Novel features of conservation and change across functional domains and lineages. *Journal of Molecular Evolution* **69**, 94-114 (2009).

Hofmann J, in Le T, Larson A, eds. Flash Cards for First Aid for the USMLE Step 1 2010. On-line and mobile applications. http://www.usmlerx.com. Published March 2010.

Le T, Hofmann J, eds. First Aid Step 1 Express 2011 videos. http://www.usmlerx.com. Published October 2011.

Le T, Bhushan V, Tolles J, Hofmann J, eds. *First Aid for the USMLE Step 1* 2011. New York: The McGraw-Hill Companies, 2011.

Le T, Hofmann J, eds. First Aid Step 1 Express 2012 videos. http://www.usmlerx.com. Published May 2012.

Le T, Bhushan V, Hofmann J, Gayed PM, eds. *First Aid for the USMLE Step 1* 2012. New York: The McGraw-Hill Companies, 2012.

Sedivy JM, Kreiling JA, Neretti N, DeCecco M, Criscione SW, Hofmann JW, Zhao X, Ito T, Peterson A. Death by transposition – the enemy within? Bioessays, accepted 2013.

Hofmann JW, McBryan T, Adams PD, Sedivy JM. The effects of aging on the expression of Wnt pathway genes in mouse tissues. *Age*. 2014.

Acknowledgements

I would like to thank my advisor, John Sedivy, for his mentorship and research guidance which have helped me to grow as a scientist. I am also grateful to everyone in the Sedivy lab for always being friendly and collaborative, and for making each day in the lab something to look forward to. I appreciate the guidance of my committee members, Phil Gruppuso, Marc Tatar, and Rich Freiman, as well as other faculty who have always been willing to take a few minutes and chat about how things are going in the lab and offer their advice, including Nicola Neretti, Alex Brodsky, Stephen Helfand, and Rebecca Page. I would like to thank Andrzej Bartke for serving as my outside reader and taking the time to travel to Providence for my defense. I feel lucky to have supportive friends and family, both in the graduate school and otherwise, and would especially like to thank my father, Jeffrey Hofmann, for proofreading and providing feedback on my thesis. And lastly, none of this would have been possible without the past and present MCB administration, including Art Salomon, Elaine Butler, Judith Bender, and Tricia Serio.

Table of Contents

List of Tables

List of Figures

Chapter 1. Introduction

I. What is aging, and why do we age?

Aging plays a substantial role in the life of almost everyone alive today, and it has a dramatic impact on modern society as a whole. Herein, aging will be defined as functional decline in organ systems and homeostatic mechanisms and accumulation of pathological phenomena, which combine to increase frailty and mortality rate over time. Virtually all animal species age, and individuals within a species exhibit similar effects of aging and similar lifespans. Interestingly, different species age at remarkably different rates, and even closely related species can have lifespans that differ by orders of magnitude. For example, mice typically live for about two or three years, while other animals, such as bats and naked mole rats, often survive for two or three decades. We can therefore conclude that the rate of aging is at least partially based on genetics, and that genetic features exist which either permit rapid aging in short-lived species or slow down aging in long-lived species.

Investigating the causes of aging and ultimately intervening to mitigate their effects would provide tremendous benefits both to individual quality of life and to society as a whole, due to rapidly increasing costs of healthcare for the elderly. Aging is an incredibly complex process, but we can more effectively study how we age if we first consider why we age. From the perspective of evolutionary biology, it is curious that animals age at all. Any degree of aging decreases the window of time in which an animal can reproduce, and thereby decreases evolutionary fitness, or the likelihood of an individual to produce offspring and propagate its genetic lineage. Thus, one might wonder why evolutionary forces have not selected against the genetic causes of aging,

resulting in all species being much longer-lived and each individual producing more offspring throughout its lifespan.

There are several reasons that aging has evaded natural selection. One is described by the notion of antagonistic pleiotropy, first coined in 1957 (Williams 1957), which posits that heritable traits that increase fitness early in life (specifically before and during the reproductive periods) will be selected for even if they have deleterious effects later in life. This permits traits that decrease post-reproductive fitness to accumulate within a species. However, this does not account for the vast differences in lifespan between closely related species. This can be attributed to the role of extrinsic sources of mortality, namely predation, in shaping the lifespan of a species. For example, independent from aging, a mouse is likely to die within its first few years of life because it is an easy target for predators, whereas animals that can evade predators, for example by flying in the case of the bat, or burrowing underground in the case of the naked mole rat, can survive for a much longer period of time.

There is minimal evolutionary advantage in preserving health past the age at which most animals in a population would have already perished from an extrinsic threat, so the effects of aging will first present near this age and accelerate rapidly thereafter. This explains the epidemics of diseases associated with aging among humans in the most recent century, as extrinsic causes of mortality such as infection and starvation have been practically eliminated, allowing us to live into the years for which natural selection did not prepare us. It also suggests that aging did not evolve to its present state because its causes and effects are unavoidable (which would imply that developing therapies to treat them would be extraordinarily difficulty), but rather because there has been no

evolutionary drive to maintain health beyond a certain point. This is reason to believe that each aspect of aging will someday be treatable.

II. DNA damage and genomic instability

Although various species of animals have evolved to permit aging for similar reasons, the mechanisms by which they age and the effects of old age are not always consistent. Here, I will focus on the mouse, which exhibits many similarities to humans yet is easier to study due to its relatively short lifespan and ease of genetic manipulation. Aging in the mouse has been studied from its molecular roots up through its pathological outcomes, although our understanding of it remains incomplete. The etiology of aging is almost certainly multifactorial, as many mechanisms of aging have been proposed and verified. Quantitative measurement of aging is complicated by its diverse effects of varying magnitude and prevalence, so lifespan and mortality rates have emerged as the best quantitative approximations of the rate of aging. Accordingly, the effectiveness of anti-aging interventions is primarily evaluated by their ability to extend lifespan.

One of the most extensively studied causes of aging is oxidative stress. Reactive oxygen species (ROS) such as hydroperoxyl and hydroxyl radicals are generated as a byproduct of normal metabolic processes that utilize oxygen and cause damage to other molecules. The major source of ROS is the electron transport chain in mitochondria, which is particularly dangerous due to its close proximity to mitochondrial DNA (mtDNA). As mtDNA damage accumulates, the efficiency of aerobic respiration is impaired, creating a vicious cycle of accelerating oxidative damage within the

mitochondria and elsewhere in the cell (Bratic and Trifunovic, 2010). Cells have robust defense mechanisms against ROS, including the enzymes superoxide dismutase (SOD) and catalase, but they are not 100% effective.

It is well documented that oxidative damage accumulates with age (Bokov et al., 2004). Lipid peroxidation, often estimated by the concentration of F_2-isoprostanes, can disrupt cell membrane integrity and cause DNA damage that results in cancer (Marnett 1999). Protein oxidation, which is measured by looking at protein carbonyls, plays a role in the pathogenesis of a wide variety of diseases such as Alzheimer's disease and cataracts (Berlett and Stadtman, 1997). Perhaps the most notorious effect of ROS on cellular macromolecules is DNA damage, which increases with age in both nuclear and mitochondrial DNA and can be measured as the prevalence of 8-oxo-2'-deoxyguanosine (Hamilton et al., 2001). Most oxidative damage is irreversible, and it will therefore accumulate over time, although to a lesser extent in cells that regularly divide and thereby dilute out damaged molecules.

Reduced oxidative stress can be observed in many long-lived mouse models, although it is unclear whether it is a cause or effect of their extended longevity. Reducing ROS does not universally improve lifespan. For example, overexpressing copper/zinc superoxide dismutase (CuZnSOD) extends lifespan in *Drosophila*, but overexpression of antioxidant enzymes such as CuZnSOD, catalase, manganese superoxide dismutase, or glutathione peroxidase 4 in mice reduces oxidative stress but has no effect on lifespan (Perez et al., 2009). However, overexpression of catalase targeted to mitochondria has been shown to increase lifespan in mice, suggesting that oxidative stress, especially from the mitochondria, contributes to mortality (Schriner et al., 2005).

Another source of DNA damage that has been investigated for its role in aging is telomere attrition. With each round of cell division, the telomeres at the ends of chromosomes become shorter and can eventually be completely lost, allowing genomic DNA to become damaged during subsequent rounds of replication. While this serves as an important defense mechanism by limiting the proliferative capacity of cancer cells, the damage it causes to normal proliferating cells can impair their function and even result in chromosomal translocations that cause cancer. The telomerase reverse transcriptase (TERT) enzyme can extend telomeres and prevent such damage, but in many cases it is unable to keep up with telomere attrition, especially as its expression declines with age; thus telomeres shorten with age at an accelerating rate, including in stem cells, which ultimately diminishes tissue renewal (Flores et al., 2008).

TERT transgenic mice are highly susceptible to cancer, and they have a shorter lifespan than wild-type mice for reasons unrelated to aging. Therefore, TERT transgenic mice that also overexpress the tumor suppressor genes p53 and p16/Arf were created to observe the effects of improved telomere maintenance on longevity independent of cancer. Compared to mice that only overexpress the tumor suppressors, mice that also overexpress TERT have a slightly increased median lifespan but no change in maximum lifespan, and they also exhibit less age-related decline in subcutaneous adipose thickness, intestinal villi length, neuromuscular coordination, and glucose tolerance (Tomas-Loba et al., 2008). These benefits suggest that telomere attrition contributes to normal aging in mice.

Genomic instability can occur not only at the ends of chromosomes, but also throughout the genome. Transposable elements (TE) are genomic sequences found in all

species that can insert copies of themselves throughout the genome, causing genomic destabilization and ultimately tissue dysfunction (Sedivy et al., 2013). Transposition is rare in somatic tissues of young animals due to repression via heterochromatinization and silencing via micro RNA, small interfering RNA, and piwi-iinteracting RNA pathways, but both the rate of TE transcription and genomic TE copy number increase substantially with age (De Cecco et al., 2013). This is likely attributable to the age-dependent interconversion of euchromatic and heterochromatic regions, which results in repressed transcription of genes that should be expressed in a given cell, and activated expression of genes and non-genetic sequences (such as TEs) that are deleterious to the cell. Since about half of a mammalian genome is comprised of TEs, even nonspecific derepression can permit TE expression and proliferation (Sedivy et al., 2013).

Another recently discovered form of genomic disruption that increases with age is aneuploidy, which is the presence of a number of chromosomes that is not a multiple of the haploid set. Aneuploidy can arise from missegregation of chromosomes during mitosis, and the prevalence of aneuploid cells increases in a variety of tissues with age to such an extent that the majority of cells in many tissues are aneuploid in mice by the age of 24 months (Baker et al., 2013). In healthy cells, the mitotic checkpoint protein BubR1 has an essential role in proper chromosome segregation during mitosis, and mice that are hypomorphic for BubR1 are prone to aneuploidy and exhibit many features of aging in young animals, including short lifespan (Baker et al., 2004). The natural decline in BubR1 expression with age is likely responsible for increased aneuploidy. Mice transgenic for BubR1 have extended lifespan and healthspan, suggesting that the decline

in BubR1 and increase in aneuploidy with age contribute to age-dependent pathology and mortality (Baker et al., 2013).

Over the lifespan of an organism, DNA damage accumulates from all of the mechanisms described above, in addition to others, such as errors in DNA replication and exogenous sources such as radiation and chemical mutagens. Thousands of DNA lesions occur per day, but the vast majority are rapidly corrected. However, as animals age, the rate at which mutations occur increases, and the cell's capacity to repair them declines, resulting in accumulation of mutations at an accelerating rate (Li and Vijg, 2012). Many mutations are irreparable when the original sequence is lost, leaving the cell with no way to return to its original sequence. Damage to genetic loci can alter the function of proteins encoded by those genes, and damage to nearby regions can affect gene expression, both of which can have widespread effects on the cell.

III. Regulation of the cell cycle: cancer and senescence

Loss of function of tumor suppressor genes and overexpression of oncogenes can induce cancer. Cancer is the most common cause of death in laboratory mice, and its prevalence greatly increases with age. In most cases, cancer can also be found in mice that died from other causes. The most common type of cancer in C57BL/6 mice is lymphoma, which is rare before 12 months of age but almost ubiquitous in old age, and histiocytic sarcomas and lung, liver and pituitary tumors are also common. Common neoplasias that can give rise to cancer include adrenal subcapsular cell hyperplasia and

endometrial hyperplasia (Brayton 2009). Due to the high prevalence and lethality of cancer in mice, most long-lived mouse models are relatively cancer resistant.

To prevent cancer, tumor suppressor pathways such as the p53 pathway will respond to DNA damage by arresting the cell cycle until the damage can be repaired. If repair is not possible, either the cell will undergo apoptosis, or the prolonged DNA damage response will initiate a permanent cessation of replication, termed cellular senescence, through the p53/p21 or $p16^{INK4a}$/pRB signaling pathways. Cellular senescence is often the result of oncogene activation, such as constitutive H-RAS signaling, or reaching the end of the cell's replicative potential due to telomere attrition, and it is maintained by heterochromatinization, and therefore repression, of genes that mediate cell proliferation (Campisi 2013). In addition to preventing a neoplastic transformation, senescence also plays a role in tissue repair through paracrine signaling, termed the senescence-associated secretory phenotype (SASP).

Both p16 levels and the prevalence of senescent cells increase with age in many tissues, which is most likely due to a combination of more cells becoming senescent and fewer senescent cells being cleared by the immune system in old animals. Although senescent cells have beneficial roles in tissue physiology in the short term, they eventually become deleterious, and are linked to a surprising number of age-related pathologies, including osteoarthritis, insulin insensitivity, cardiovascular disease, and cognitive impairment. This is mostly attributable to the SASP, which promotes inflammation by secreting cytokines, chemokines, and matrix metalloproteases (MMP) into their local environment. Ironically, despite preventing cancer in the short term, the

SASP can later promote cancer initiating events by causing inflammation which leads to DNA damage, and by MMPs allowing cancer to spread (Campisi 2013).

Stem cells are particularly affected by perturbations of replicative capacity since the primary function of these cells is to proliferate. Hematopoietic stem cells (HSC), which give rise to all blood cells, have a 2 to 4 fold decrease in repopulation capacity in old mice relative to young, including when they are transplanted into a young animal, suggesting that this is a cell-intrinsic phenotype. Expression of p16 increases with age in HSCs, suggesting that the decline in HSC function is partially attributable to cellular senescence. There is also an increase in expression of myeloid-specific genes and a decrease in expression of lymphoid-specific genes, which results in both decreased differentiation of HSCs into common lymphoid progenitors (CLP), which give rise to B and T lymphocytes, and decreased proliferative potential of CLPs (Geiger and Rudolph, 2009).

IV. Immunosenescence and inflammation

Reduced capacity of HSCs to generate lymphoid cells is the basis for immunosenescence, which is the age-dependent functional decline and dysregulation of the immune system that particularly affects the adaptive immune system through involution of the thymus and cellular senescence of individual lymphocytes (Akbar and Henson, 2011). In C57BL/6 mice, the thymus begins to involute at 10 months of age and very little tissue remains by 20 months (Hsu et al., 2003). Since few T cells are produced

by the thymus in older animals, the T cell pool is maintained by the expansion of existing memory T cells, and this expansion is greater for cytotoxic CD8+ than regulatory CD4+ T cells (Goronzy and Weyand, 2005). Thus, the generation of naïve CD4+ T cells is greatly reduced in old animals. One of many deleterious effects of impaired CD4+ T cell generation is impaired "senescence surveillance", or immune-mediated clearance of senescent cells, and this allows senescent cells to persist and accumulate in old animals. Through this process, immunosenescence has been linked to a greater prevalence of cancers in mice, including hepatocellular carcinoma (Kang et al., 2011).

The innate immune system is also dysregulated with aging. In particular, baseline, or sterile, inflammation increases with age, as evidenced by increased levels of the cytokines interleukin-1, interleukin-6, TNFα, and CRP (Michaud et al., 2013). One cause of increased inflammation is the decrease in CD4+ T cells, specifically T_{reg} cells, which maintain self-tolerance and limit inflammation and autoimmunity (van Eden et al., 2013), so their decline results in a greater level of baseline inflammation with age (Franceschi et al., 2000). This is compounded by the intrinsically decreased ability of neutrophils to respond to chemotactic signals, which results in delayed migration to damaged or infected tissue and also impaired egress from that tissue. This creates more inflammation and is partially responsible for impaired wound healing in older mice (Shaw et al., 2013). Furthermore, as discussed above, senescent cells secrete cytokines, predominantly IL-8 and IL-6, which recruit neutrophils and drive local inflammation (Orjalo et al., 2009). Inflammation can be beneficial when properly regulated by orchestrating recruitment of immune cells to sites of infection or injury and mediating wound repair and tissue remodeling, but excessive inflammation is involved in the pathogenesis of many age-

related diseases, including sarcopenia (Degens 2010), Alzheimer's disease (Liu and Chan, 2014), osteoporosis (Lacativa and Farias, 2010), and insulin resistance (Shu et al., 2012).

V. Metabolism and aging

Metabolism at the molecular, cellular, and organismal level has been closely linked to aging. One of the original theories for a molecular basis of aging is the free radical theory, which proposes that free radicals produced by the mitochondria damage other molecules, and due to their proximity to the source of ROS, mitochondrial DNA and proteins receive a disproportionately large amount of oxidative damage (Harman 1972). This creates a vicious cycle by which damaged mitochondria are less efficient and produce more free radicals, which in turn cause even more damage as the organism ages. This theory has gained support over the years through data showing that, with age, mitochondria become larger and accumulate morphological abnormalities (Frenzel and Feimann, 1984), mitochondrial enzyme activity and membrane potential both decrease, and oxidative damage to mitochondrial DNA and proteins increases (Cottrell and Turnbull, 2000).

This originally led to the "rate of living" theory, which predicts that the more energy an individual consumes, the more damage will accumulate, and thus greater activity and a higher metabolic rate should decrease lifespan, but this has since been refuted (Bratic and Trifunovic, 2010). More recently, the "uncoupling to survive" theory has gained traction, which predicts that greater metabolic activity yields greater longevity

by easing the proton gradient across the inner mitochondrial membrane and thereby reducing production of ROS (Brand 2000). This is supported by experiments performed on mice that overexpress UCP1 in skeletal muscle and in mice treated with 2,4-dinitrophenol, both of which uncouple the proton gradient from ATP production and allow protons to leak across the inner membrane and dissipate energy as heat. Both interventions resulted in increased lifespan and metabolic rate (Caldeira da Silva et al., 2008; Gates et al., 2007), suggesting that although a high proton gradient may promote mitochondrial efficiency, it also contributes to aging. Consistent with this notion, exercise attenuates mtDNA damage in both neurons and skeletal muscle (Intlekofer and Cotman, 2013), and many long-lived mouse models have an increased metabolic rate and small body sizes, which require more uncoupling to generate enough heat to maintain their body temperature.

Uncoupling proteins are generally expressed in brown adipose tissue for the purpose of thermogenesis in response to a cold environment, but white adipose tissue (WAT) physiology is also closely linked with aging. Mice typically accumulate WAT through middle age, but rapidly lose it when they become very old. Furthermore, the distribution of WAT changes with age as the ratio of subcutaneous to visceral WAT decreases, and adipocytes in most WAT depots are smaller in older animals (Sackmann-Sala et al., 2012). This is consistent with the decline in expression of adipogenic transcription factors PPARG and CEBPA in WAT with age, and a reduced replicative capacity of old preadipocytes relative to young (Tchkonia et al., 2010). In other tissues, including skeletal muscle, liver, and bone, PPARG and CEBPA expression increase with

age and drive adipose accumulation, which impairs normal tissue function (Rosen et al., 2009; She et al., 2005; Taylor-Jones et al., 2002).

WAT plays a vital role in endocrine regulation of metabolism. Insulin resistance is typically associated with aging, and type 2 diabetes mellitus occurs when insulin secretion can no longer compensate for insulin resistance. This has widespread pathological effects, including neuropathy, renal failure, cardiovascular disease, and dementia. There is debate about whether insulin resistance is a natural progression of aging or whether it is secondary to obesity and physical inactivity that are common in elderly individuals and independent from aging itself. In some experiments in both humans and rodents, when cohorts are matched for activity and body mass index, age has no effect on insulin sensitivity (Amati et al., 2009; Barnard et al., 1992). There is also evidence that accumulation of intermuscular adipose contributes to insulin resistance in older mice (Freda et al., 2008).

However, other studies have shown that age may indeed affect insulin sensitivity. First, there is abundant evidence that inflammation in WAT mediates insulin resistance in obesity, and the age-dependent increase in inflammation does not require obesity or low physical activity (Tchkonia et al., 2010). Second, the hormone adiponectin increases insulin sensitivity and is primarily produced in WAT, and its secretion declines with age (Sackmann-Sala et al., 2012), which leads to insulin resistance (Yamauchi et al., 2001). Third, the adipogenic transcription factors PPARG and CEBPA have lower expression with age in WAT, as do their target genes, which contributes to insulin resistance. Lastly, there are several long-lived mouse models in which quantity of WAT is either unaffected or increased yet insulin sensitivity is also increased (Bartke et al., 2013; Martin-Montalvo

et al., 2013). In summary, these data support the notion that age affects insulin sensitivity through mechanisms which are relevant to WAT but not dependent on obesity.

VI. Calorie restriction

Many interventions in mice have been found to extend longevity, and the majority are related to metabolism. The most studied is calorie restriction (CR), in which restricting the amount of calories available to mice by 30% to 60% has been shown to increase both their median and maximum lifespan by over 50% (Sohal and Weindruch, 1996). It has been suggested that this effect is an artifact of laboratory conditions since mice are often overfed and sedentary, and thus CR is merely mimicking a more natural environment in which resources are scarce and mice are unlikely to become obese (Martin et al., 2010). However, given that the ultimate goal of aging research is to improve human health, and that humans also have unlimited access to food and are often sedentary, particularly in old age and in developed countries, learning from laboratory mice can still be quite beneficial. Recently, the lifespan-extending effects of CR have been challenged by a study which showed that among 41 recombinant inbred strains of mice, only a minority (5% for males, 21% for females) of strains had significant lifespan extension from CR, and lifespan reduction was even more common (26% for males, 26% for females) (Liao et al., 2010). In a separate study, CR in mice that were grandoffspring of wild-caught mice also had no increase in lifespan (Harper et al., 2006), suggesting that a positive response to CR might be an acquired trait after many generations of domestication in a laboratory. Clearly there is a genetic component to the effects of CR,

and some strains benefit more than others. However, by studying the effects of CR in strains to which it confers a large lifespan increase, it can be a useful tool to study aging.

For the better part of the last century, a variety of hypotheses have been proposed to explain how CR affects lifespan, and although the mechanisms remain incompletely understood, many important details have been established. CR preserves mitochondrial efficiency in old age and attenuates oxidative stress, including oxidative damage to DNA and proteins (Lanza et al., 2012; Yu 1996). Calorically restricted mice also have a lower prevalence of senescent cells, including in the liver and intestine (Wang et al., 2010), and they exhibit resistance to cancer (Harvey et al., 2013). As for metabolism, mice on CR diets have decreased serum glucose and insulin, increased adiponectin, and preserved insulin sensitivity later in life (Dean and Cartee, 1996; Harvey et al., 2013; Masoro et al., 1992). They also have less adipose tissue and reduced adipocytic infiltration of other organs, such as muscle (Masternak et al., 2005). All of these are benefits that contrast the effects of normal aging and are therefore likely to contribute to increased longevity.

The effects of CR on the immune system have also been extensively studied, but the overall picture is complicated. CR attenuates immunosenescence, specifically by increasing T cell output from the thymus and improving T cell proliferative capacity in old animals, and it also reduces PPARG activity in the thymus, which otherwise contributes to adipocytic infiltration and degeneration of the tissue (Yang et al., 2009). Inflammation is reduced in CR mice, particularly the response mediated by the Nf-κB signaling pathway (Chung et al., 2002; Harvey et al., 2013), which may be particularly beneficial for laboratory mice that are not exposed to pathogens. However, the immune systems of CR mice are worse at fighting bacterial, viral, and parasitic infections, which

is most likely attributable to the attenuated inflammatory response or perhaps other innate immune system deficits (Gardner 2005; Kristan 2007; Sun et al., 2001). While some effects of CR on the immune system are beneficial and others are deleterious, the overall effect on mice in a laboratory environment is positive.

Other benefits of CR include improved motor coordination in old age (Weindruch and Walford, 1988), attenuation of age-related cardiomyopathy (Yan et al., 2013), and reduced serum insulin-like growth factor 1 (IGF1) (Lee and Longo, 2011), which has been heavily linked to aging in mice and will be discussed below. One of the major drawbacks of CR as far as evolutionary fitness is reduced fecundity (Longo and Finch, 2003). In summary, CR has many effects which oppose aging in some strains of mice, and it is likely to extend lifespan through some combination of them rather than through a more specific mechanism.

VII. Somatotropic signaling

The somatotropic signaling axis has been heavily implicated in aging in mice. This endocrine signaling axis begins as growth hormone releasing hormone (GHRH) is released from hypothalamic neurons in a pulsatile manner and stimulates release of growth hormone (GH) from the anterior pituitary gland in the same pulsatile temporal pattern. GH has a variety of effects, most of which are anabolic and include long-bone growth during development, but one of the most notable effects in adults is stimulation of IGF1 secretion from the liver. The majority of circulating IGF1 is secreted by the liver as a result of GH signaling, although some is secreted by adipose tissue, and many tissues

exhibit non-GH dependent local IGF1 signaling. Like GH, IGF1 has many effects that are generally anabolic, and they include cell growth and proliferation, inhibition of apoptosis, and effects on cell metabolism since it uses the same signaling cascade as insulin: IGF1 and insulin both act through the insulin receptor substrate proteins IRS1 and IRS2 and ultimately influence gene expression through the FOXO family of transcription factors (Bartke et al., 2013). In the circulation, most IGF1 is in a complex with IGF binding proteins (IGFBP), which regulate the amount of free (active) IGF1, and protect it from degradation or clearance.

GH typically declines with age in mice, so a reasonable hypothesis might be that increasing it to the same levels observed in young mice would be beneficial, but in fact the opposite is true: perturbations in the somatotropic axis, including GH signaling, increase longevity in mice. Historically, the first example of this was the Snell dwarf mouse, which has impaired development of the pituitary gland due to a homozygous loss-of-function mutation in the gene *Pit1*. These mice are deficient in multiple pituitary hormones, including GH, prolactin (PRL), and thyroid stimulating hormone (TSH), and their median and maximum lifespan are each extended by about 40% (Flurkey et al., 2001). The Ames dwarf mouse also has impaired pituitary development, which in this case is due to a homozygous mutation in the gene *Prop1*, which functions upstream from *Pit1* in pituitary development, and thus results in the same endocrine deficiencies and a 50% increase in longevity (Brown-Borg et al., 1996). “Little” mice, which have a homozygous mutation in the growth hormone releasing hormone receptor (*Ghrhr*) in the pituitary and therefore are deficient in GH have increased median and maximum lifespan by about 25% and 15%, respectively (Flurkey et al., 2001), which suggests that the

lifespan extending effects in Snell and Ames dwarf mice are primarily due to their deficiency in GH rather than TSH or PRL. This is also supported by the 40-50% lifespan extension in growth hormone receptor (GHR) knockout mice (GHRKO) that has been observed in multiple laboratories and genetic backgrounds, which are IGF1 deficient but have elevated GH due to loss of negative feedback from IGF1 (Bartke et al., 2013). Even further downstream in the somatotropic axis, it has been observed that IGF1 receptor (IGF1R) heterozygous mice, IRS1 knockout mice, and IRS2 heterozygous mice also have extended longevity (Selman et al., 2008; Taguchi et al., 2007; Xu et al., 2014). Lastly, knocking out the gene pregnancy-associated plasma protein A (*Pappa),* whose normal function is to cleave IGFBPs and thereby increase the active form of IGF1, also extends longevity in mice (Conover and Bale, 2007).

All together, these experiments suggest that reduced IGF1 signaling is beneficial for lifespan. There are several proposed mechanisms for this. Many phenotypes have been measured in some of these mice and not others, and may or may not be universal, but considering them all together will provide an overall picture of the causes and effects of reduced somatotropic signaling in mice. These mouse models generally have greatly diminished body mass, a major effect of which is reduced body temperature despite increased brown adipose and a higher metabolic rate, which are likely attempts to generate heat (Hauck et al., 2001; Hunter et al., 1999). As discussed above, an increased metabolic rate can reduce the proton gradient across the inner mitochondrial membrane and thereby decrease ROS production, and consistent with this, these mice exhibit reduced oxidative damage (Brown-Borg et al., 2001; Sanz et al., 2002). Possibly through

this mechanism, these mice are also cancer resistant (Ikeno et al., 2003; Ikeno et al., 2009).

There are also several metabolic phenotypes, some of which may be related to the increased metabolic rate. Ames dwarf, Snell dwarf, Little, and GHRKO mice all have increased insulin sensitivity despite the fact that Snell and GHRKO mice are obese (Bartke et al., 2013). Snell dwarf mice have reduced hepatic cholesterol biogenesis (Boylston et al., 2004), and Ames dwarfs have reduced serum triglycerides and free fatty acids (Wang et al., 2006). Altogether, both carbohydrate and lipid metabolism are healthier. Regarding the immune system, Snell dwarf mice have delayed immunosenescence (Flurkey et al., 2001), and the HSC population of GHRKO mice has a higher percentage of very small embryonic-like stem cells (VSEL), which play an important role in bone marrow maintenance by giving rise to other HSCs (Ratajczak et al., 2011). GHRKO mice have reduced IL-6 in WAT (Masternak et al., 2012), and Ames dwarfs have reduced TNF-α expression in WAT (Wang et al., 2006). These benefits to the hematopoietic system may help the immune system as a whole, and anti-inflammatory effects in WAT may contribute to preserved insulin sensitivity in old age. Like CR, a major deficit in these mice is that many of these models have delayed puberty or otherwise afflicted reproductive capacity (Bartke et al., 2013).

VIII. mTOR signaling

Another major signaling pathway whose perturbation can result in increased longevity is the mechanistic target of rapamycin (mTOR) pathway. As its name suggests,

mTOR is inhibited by the drug rapamycin. This pathway is generally thought to couple nutrient availability with regulation of metabolic processes, but it has a wide array of other effects. mTOR functions in two different multiprotein complexes. mTOR complex 1 (mTORC1) regulates cell growth and translation by phosphorylating its substrates ribosomal S6 kinase (e.g. S6K1) and eukaryotic initiation factor eIF4E binding protein (4E-BP) in response to extracellular nutritional signals, including glucose and amino acids. mTOR complex 2 (mTORC2) influences cell survival and cytoskeletal organization through its substrates Akt and PKC-α in response to IGF1 and other growth factors (Laplante and Sabatini, 2012), and it is also involved in insulin signaling (Lamming et al., 2012). mTORC1 is acutely inhibited by rapamycin, while mTORC2 is only inhibited by long-term treatment with rapamycin (Zinzalla et al., 2011).

mTOR and many proteins in mTORC1 and mTORC2 are essential for development in mice, so complete knockout mice cannot be studied (Guertin et al., 2006). However, mTOR hypomorphic mice ($mTOR^{\Delta/\Delta}$) that express mTOR at 25% of normal levels have a 20% increase in lifespan (Wu et al., 2013). Rapamycin also increases lifespan in several different strains of mice (Harrison et al., 2009; Neff et al., 2013) making it the first drug that has been found to increase lifespan in mammals. Female mice knocked out for S6K1, which is directly downstream from mTORC1, are also long-lived, although males are not (Selman et al., 2009). Similarly, only female mice that are heterozygous for both mTOR and mLST8, which is a protein in both mTORC1 and mTORC2, have extended lifespan, although only mTORC1 signaling was found to be attenuated in these mice (Lamming et al., 2012). In summary, mTORC1 inhibition is able to extend lifespan and mTORC2 inhibition may not be required for this

effect. In fact, mTORC1 inhibition may increase lifespan in spite of the deleterious effects of mTORC2 inhibition. Contrary to what is observed in other long-lived mice, rapamycin causes glucose insensitivity and insulin resistance, which is mediated by increased hepatic PEPCK activity which induces gluconeogenesis. This effect is mediated by mTORC2 inhibition (Lamming et al., 2012).

Some of the mechanisms by which inhibition of mTOR signaling might extend lifespan are similar to those observed in CR and impairment of somatotropic signaling, although others are opposite to what is observed in these models. Due to numerous differences in endocrine signaling and metabolism, CR and rapamycin treatment are thought to increase longevity by mostly distinct mechanisms (Miller et al., 2013). $mTOR^{\Delta/\Delta}$, $S6K1^{-/-}$, and rapamycin-treated mice all have reduced body mass, $mTOR^{\Delta/\Delta}$ mice are resistant to oxidative stress and have less $p16^{Ink4A}$ expression, and $mTOR^{\Delta/\Delta}$ and rapamycin-treated mice are resistant to cancer (Miller et al., 2011; Neff et al., 2013; Selman et al., 2009; Wu et al., 2013). Both mTORC1 and mTORC2 promote adipogenesis, and adipose content is reduced in $S6K1^{-/-}$ mice (Lamming and Sabatini, 2013; Selman et al., 2009). However, deleterious metabolic effects include the insulin resistance mentioned above and hyperlipidemia in rapamycin-treated mice (Houde et al., 2010).

Rapamycin also has a mixture of beneficial and deleterious effects on the immune system. It has been used clinically for decades as an immunosuppressant to prevent rejection of organ transplants (Ingle et al., 2000). Specifically, it suppresses CD4+ T cell differentiation into subtypes such as Th_1 and Th_{17}, and suppresses dendritic cell maturation and their ability to produce IL6 and TNFα (Araki et al., 2011; Araki et al.,

2009). However, recent studies have also demonstrated immune strengthening effects. Both mTOR and $p16^{Ink4A}$ expression are greater in old than young HSCs, but rapamycin reduces $p16^{Ink4A}$ expression and restores the ability of old HSCs to reconstitute the bone marrow of irradiated mice, which is normally attenuated with age (Chen et al., 2009). Rapamycin also improves the differentiation of CD8+ T cells into memory T cells when responding to vaccination. It remains unclear whether rapamycin's effects on the immune system are favorable overall, but its apparent rejuvenation of HSCs and potential to decrease inflammation may contribute to increased longevity in these mice.

IX. *Pten*^{tg} mice

Phosphatase and tensin homolog (PTEN) is a tumor suppressor that inhibits the phosphoinositide 3 kinase (PI3K) signaling cascade, which otherwise partially acts through mTORC1 to stimulate cell survival, growth, and proliferation in response to anabolic signaling molecules like insulin and IGF1. mTORC1 can be indirectly inhibited by PTEN through the intermediaries AKT and TSC (Zoncu et al., 2011). This suggests that increasing expression of *Pten* would have similar effects as mTORC1 inhibition. To study the physiological effects of *Pten* overexpression, transgenesis was performed using the intact *Pten* genomic locus in a bacterial artificial chromosome, resulting in mice with approximately 2-fold greater *Pten* expression (Garcia-Cao et al., 2012). *Pten*^{tg} mice have reduced body mass, resistance to oncogenic transformation, and increased median and maximum longevity in both sexes (Ortega-Molina et al., 2012). While some of the increased longevity is undoubtedly attributable to cancer resistance, cancer-free *Pten*^{tg}

mice also lived longer than cancer-free wild type mice, suggesting other longevity-extending benefits in these mice. mTORC1 inhibition is also likely to contribute to their increased longevity, as many phenotypes are shared between these two models. However, *Pten*^{tg} mice have an increased metabolic rate and less oxidative stress and DNA damage in old animals, while mTORC1 hypomorphism or inhibition via rapamycin has no effect on these phenotypes. *Pten*^{tg} mice also have lower serum glucose and insulin, are more insulin sensitive, and have less serum IGF1, suggesting that their longevity extension may have common mechanisms with perturbation of the somatotropic signaling axis (Ortega-Molina et al., 2012). The authors also discuss the possibility that many phenotypes of *Pten*^{tg} mice are due to the observed repression of the oncogene MYC in these mice, since *Myc* hypomorphic mice also have reduced body mass and cancer resistance (Trumpp et al., 2001).

X. MYC

Myc is a member of a small family of three closely related genes that also includes *Mycn* and *Mycl1* (formerly designated as c-*Myc*, N-*Myc* and L-*Myc*, respectively). All encode helix-loop-helix leucine zipper transcription factors that are well conserved among metazoans (Meyer and Penn, 2008). The *Myc* gene is expressed in most cell types while the others show more tissue-specific expression. *Myc* was discovered as the transforming oncogene of the MC29 avian myelocytomatosis virus, and subsequently as the cellular proto-oncogene activated in Burkitt's lymphoma. Increased

expression of the MYC protein strongly promotes cell proliferation, and has been documented as a frequent event in a wide variety of human cancers (Dang 2012).

MYC activity is induced by a variety of growth factors, mitogens, and cytokines, through signaling mediators such as mTORC1 and PTEN (Garcia-Cao et al., 2012; Yecies and Manning, 2011), and is repressed by anti-proliferative signaling molecules such as transforming growth factor-β (TGFβ) (Pietenpol et al., 1990). By interacting with partners such as MAX and ZBTB17 (formerly known as MIZ1), MYC has the ability to either activate or repress transcription by binding to canonical (CACGTG, CATGTG) or noncanonical (CATGCG, CACGCG, CACGAG) E boxes in the promoters of its target genes (James and Eisenman, 2002; Meyer and Penn, 2008). Much effort has been focused on understanding how MYC influences signaling networks, and it has emerged as a major regulatory hub. By conservative estimates, 15-20% of all genes can be directly regulated by MYC, including genes that play key roles not only in the cell cycle, but also in metabolism, ribosome biogenesis, apoptosis, differentiation, and stem cell maintenance (Dang 2012). Recent reports have further expanded this repertoire by suggesting that MYC can amplify the expression of the majority of actively transcribed genes in any particular cell type, generally only increasing their expression by about 50%-100% (Lin et al., 2012; Nie et al., 2012).

In addition to its extensively studied roles in cancer, MYC is also critically involved with many essential cellular processes, and its knockout in the mouse results in early embryonic lethality. While age does not have a significant effect on *Myc* expression in any mouse tissue documented in the AGEMAP database (Zahn et al., 2007), many of the biological processes regulated by MYC have also been implicated in aging and age-

associated diseases. Perhaps the most obvious connection is that increased MYC expression promotes cancer, and cancer prevalence increases with age. In contrast, lowering normal MYC expression levels reduces sensitivity to oncogene transformation and enhances cellular senescence (Guney et al., 2006). MYC drives major anabolic pathways, including fatty acid, amino acid and nucleotide biosynthesis leading to cellular growth and proliferation, and promotes energy production through glycolysis and oxidative phosphorylation (Dang 2012). This contrasts some of the most well characterized and effective methods of extending lifespan, such as CR and reduction of IGF1 signaling.

MYC overexpression results in an increase in ROS and DNA damage, including double strand breaks (DSBs) (Vafa et al., 2002), which may contribute to the pathogenesis of aging. Stem cell populations decline in number and functionality with normal aging (Cho et al., 2008; Jang et al., 2011), while ectopic MYC expression depletes stem cell populations (Eilers and Eisenman, 2008). MYC may also affect the inflammatory state that accompanies aging, since it directly regulates expression of some cytokines (Whitfield and Soucek, 2012) and may influence the composition of the leukocyte population via its roles in proliferation and stem cell maintenance (Eilers and Eisenman, 2008; Wang et al., 2011).

XI. Experimental approach

The overall trend suggested by this large volume of evidence is that increased MYC activity promotes several distinct processes that have been connected with aging

and age-associated diseases. To address the role of MYC in aging, given that a complete loss of *Myc* is embryonic lethal while overexpression promotes cancer, we sought to establish a partial loss of function (hypomorphic) model in the mouse. We have previously noted that cells knocked out for one copy of the *Myc* gene (*Myc* heterozygotes) display a variety of mild but distinct phenotypes, including reduced rates of proliferation (Mateyak et al., 1997). This is because the cells do not compensate by upregulating the remaining *Myc* gene copy (or the *Mycn* or *Mycl1* genes), but continue to express approximately half the normal amounts of *Myc* mRNA. Similarly, heterozygous ($Myc^{+/-}$) mice appear normal and healthy, but have a 20% smaller body mass, which was attributed to reduced numbers (but not size) of cells (Trumpp et al., 2001).

While conditional ablation of *Myc* has been extensively investigated in the context of cancer as well as the development of multiple tissues, very few studies have examined the effects of constitutive hypomorphic alleles, and none addressed the consequences on aging. Here, we report that $Myc^{+/-}$ mice live significantly longer than their normal $Myc^{+/+}$ littermates, and they display ameliorated aging phenotypes across a variety of pathophysiological processes in multiple organs. The breadth of these phenotypes suggests that the increased longevity of $Myc^{+/-}$ mice is not attributable to the prevention of a specific fatal disease, but rather to the attenuation of fundamental underlying mechanisms of aging and therefore broadly increased healthspan.

Chapter 2. Materials and Methods

Mouse Husbandry

Mice with one floxed allele of *Myc* (*Myc*$^{+/flox}$) on a mixed 129 and C57BL/6 background (de Alboran et al., 2001) were obtained from Dr. Ignacio de Alboran, Department of Immunology and Oncology, University of Madrid, Spain. Upon receipt the mice were rederived and subsequently housed in a helicobacter-free barrier facility at Brown University. The floxed allele was converted to a germline deletion allele (*Myc*$^{+/-}$) by breeding heterozygous floxed animals with a germline-expressed Cre recombinase (also on a C57BL/6 background) obtained from Dr. Tomas Prolla, Departments of Genetics and Medical Genetics, University of Wisconsin, Madison. The line was backcrossed greater than 10 times to C57BL/6NCrl mice purchased from Charles River (strain code 027). The *Myc* deletion line has been propagated by breeding *Myc* heterozygous males (*Myc*$^{+/-}$) with C57BL/6NCrl females purchased from Charles River. These crosses produce the two genotypes (*Myc*$^{+/+}$ and *Myc*$^{+/-}$) and the two sexes at the expected Mendelian ratio (1:1).

Mice were produced and housed in a specific pathogen-free (SPF), AAALAC-certified barrier facility. The following pathogens are tested on a quarterly basis: Sendai virus (SEND), Pneumonia virus of mice (PVM), Mouse hepatitis virus (MHV), Minute virus of mice (MVM), Theiler's murine encephalomyelitis virus (TMEV), Reovirus 3 (REO), Mouse parvovirus (MPV), Mouse parvovirus (NS1), Epizootic diarrhea of infant mice (EDIM), Lymphocytic choriomeningitis virus (LCMV), Hantavirus (HTN), and *Mycoplasma pulmonis.* In addition, the following pathogens are tested on a yearly basis: Mouse adenovirus 1 & 2 (MAV), Ectromelia virus (ECTRO), K virus (K), Polyoma virus (POLY), Mouse thymic virus (MTLV), Murine cytomegalovirus (MCMV), Mouse Noro

virus (MNV), *Encephalitozoon cuniculi* (ECUN), Cilia-associated respiratory bacillus (CARB) and Helicobacter. The following strains of Helicobater are tested: *Helicobacter bilis, Helicobacter ganmani, Helicobacter hepaticus, Helicobacter rodentium, Helicobacter sp., Helicobacter trogontum, Helicobacter typhlonius.*

Animals are housed in plastic 27 cm x 27 cm cages which are held in HEPA-ventilated cage racks (maximum of 7 animals per cage). Animals are also housed in half-cages (maximum of 3 animals). Cages, bedding (Sani-chip hardwood bedding) and food (Purina Lab Chow # 5010) are sterilized by autoclaving. Food and water (also sterilized) are provided *ad libitum*. The same food is used for all animals, including pregnant and nursing mothers and weaned pups. Bedding is changed once per week. A light-dark cycle of 12 hours is used (7 AM On, 7 PM Off). Temperature is maintained at 70°F, and humidity at 50%.

Animals for the aging study were produced using the scheme described above, where $Myc^{+/-}$ males were mated with C57BL/6NCrl females purchased from Charles River. Females were purchased at 12 weeks of age and bred immediately. Two females were housed continuously with one male in a full (27 x 27 cm) cage. Females were replaced after producing 3-4 litters. A total of 7 males and 23 females were used to produce the cohorts for the aging study. Four cohorts were entered into the study: 42 $Myc^{+/+}$ males, 41 $Myc^{+/+}$ females, 42 $Myc^{+/-}$ males, and 42 $Myc^{+/-}$ females. Most of these animals were produced over a period of 7 months (11/17/07 to 9/9/08) by 6 males and 22 females (Table 3.2). A few animals (9 pups, 2 litters) were produced over the subsequent months by a new pair and used to top up the cohorts. Litters were weaned at 21 days of age, at which time tail snips were taken for PCR genotyping. Genomic DNA was

prepared from the tails as follows. A piece of tail ~5 mm in length was cut and lysed in 0.5 ml of buffer (10 mM Tris-HCl pH 8.0, 1 mM EDTA, 200 mM NaCl, 0.2% SDS) with 140 μg/ml proteinase K. Samples were shaken at 55°C until the tail was mostly dissolved, spun briefly to pellet bones and hair, and DNA was precipitated with an equal volume of isopropanol). Reactions were performed using the Promega GoTaq system (Fisher PRM7122) and primer pairs 1 and 2 (Appendix 3), using protocols provided by the manufacturer, run out on 1% agarose gels, and photographed after staining with ethidium bromide.

Animals were marked with ear tags, and separated by sex into full (27 x 27 cm) cages. Animals of the two genotypes ($Myc^{+/+}$ and $Myc^{+/-}$) were housed together. No animals were lost to fighting or accidental death. The first death occurred at 498 days (16.4 months) due to an apparent respiratory illness. Dermatitis did occur in very few of the animals but was successfully treated by spraying the affected area with 70% ethanol. No animals had to be euthanized or were deemed to have died due to dermatitis. A few animals (n=12) were euthanized for humane reasons (these animals were deemed to have lived to the end of their natural life spans and were thus not censored in the demographic analysis). The guidelines for euthanasia developed by the NIA Interventions Testing Program (ITP) were used (Miller et al., 2007), also see (Ladiges et al., 2009). Seven animals (4 $Myc^{+/+}$ females and 3 $Myc^{+/-}$ females) were sacrificed at approximately 30 months of age for the collection of tissue specimens, at which time they were in apparent good health. These animals were censored (at the age of sacrifice) in the demographic analysis (Table 3.2). No other animals were censored. The only procedures that were performed were periodic weighings (weekly in the first 6 months of life, and monthly

thereafter), rotarod tests on a few animals, and tail bleeds at a young age on a few animals.

Statistical and Demographic Analysis

Unless indicated otherwise data in graphs are shown as means. Error bars represent SEM (standard error of the mean). N indicates the number of animals per test group. For pairwise comparisons p values were calculated using the Student's t-test (two-tailed, assuming equal variance). Relevant p values are shown in the figures; if not shown, the values were >0.05. Lifespan data were analyzed using JMP software (SAS Institute), computing mean and median lifespans, SEM, percent increase of the median, and p values (log-rank test) for each cohort. Mortality rate was calculated as log (-log (survival)). Maximum lifespans were computed as described previously (Wang et al., 2004) by calculating the proportion of each cohort still alive when the total population had reached 90% mortality, and using Fisher’s exact test to determine statistical significance.

Procedures Performed on Live Animals

To score vaginal patency, female mice were examined daily from weaning (21 days) until vaginal opening was observed. Mice were held with the back feet against the cage wall and tail stretched up, and a sterile pipet tip was used to gently probe for vaginal opening. For rotarod tests, the apparatus used was from MedAssociates, Inc. (St Alban, VT). A

mouse was placed on the cylinder (rod) with high walls on both sides that forced the mouse to ambulate on the rod. The rod was at a height of 35 cm above the base, and was accelerated continuously from 4 to 40 revolutions per minute in 5 minutes. The trial was terminated at 6 minutes or when the animal fell from the rod. Falls were detected by a photobeam detector. Each mouse received three trials per day for three consecutive days. To assess metabolic rates, O_2 consumption and CO_2 production were measured using a fully automated comprehensive lab animal monitoring system (Oxymax Open Circuit Calorimeter, Columbus Instruments) equipped with 4 mouse chambers. Animals were transferred to the chambers (one per chamber) and allowed to acclimate for one day. Measurements were taken every 10 minutes continuously for a period of 3 days (72 hours). Food and water were provided ad libitum, and the animals were maintained on a normal light-dark cycle. For body temperature measurements an implantable temperature transponder system (IPTT-300, Bio Medic Data Systems) was used. The transponders were implanted under the skin on the back of the animals between the shoulder blades using the provided instrument. The animals were allowed to heal and recover for a minimum of one week after the implantation before measurements were commenced. The transponders were kept in the animals until they died or were euthanized for other reasons (such as collection of tissue specimens).

End of Life Pathology Examination

Cages were inspected each morning. Dead animals were removed from cages, opened, and examined macroscopically by a trained technician. A fraction of animals could not be

examined because they were too decomposed or disturbed by other animals. Organs were moved, turned or lifted with forceps for the examination but were not removed. All visible tumors, as well as any other observations were noted. The animals were then preserved in formalin by first opening the skull with scissors and then placing the whole carcass into formalin. After sufficient preservation the animals were shipped for examination by an expert pathologist (Dr. Yuji Ikeno, Barshop Institute for Longevity and Aging Studies, University of Texas Health Science Center at San Antonio). A detailed pathological record, including a histological examination of major organs, was prepared and is shown in Table 3.3. This examination confirmed most of the findings of the initial autopsy, but also showed that at a microscopic level, cancer was more widespread than was evident from the gross macroscopic examination. Most animals showed some evidence of lymphoma in at least one organ.

Harvesting of Tissues

Mice were euthanized in the morning (between 8 and 10 AM) by isofluorane anesthesia followed by cervical dislocation. Animals were brought to the laboratory in their holding cages and euthanized one by one for dissection. The dissection was performed as rapidly as possible following euthanasia by several trained staff members working in concert on one mouse. Major organs were removed, cut into appropriate size pieces, and either flash-frozen in liquid nitrogen, embedded and frozen in Tissue-Tek optimal temperature cutting compound (OCT, Sakura Finetek), or placed in formalin for preservation. Flash-frozen tissue samples and OCT blocks were stored at -80°C. After several days of formalin

fixation at room temperature, tissue fragments were transferred to 70% ethanol and stored at 4°C. Tissue specimens were embedded in paraffin by the Brown University Molecular Pathology Core Facility (http://brown.edu/Research/SRP/coreD.shtml). Blood was collected by cardiac puncture and either allowed to coagulate for the preparation of serum, or mixed with heparin for the preparation of plasma (20 μl of 0.225 mg/ml heparin per blood sample recovered from one mouse, 100-150 μl). The entire dissection and tissue harvest of one mouse took less than 5 minutes.

Histological Analysis

Paraffin-embedded specimens were sectioned at 5 μm thickness, deparaffinized, rehydrated, and stained with hematoxylin and eosin (H&E) using standard protocols. OCT-embedded specimens were cryosectioned at 8 μm thickness using a Leica CM3050S cryomicrotome and were used for the determination of fibrosis, cellular senescence, the lipid content of tissues, and visualization of macrophages in tissues. Fibrosis was detected using Masson's trichrome stain, and lipids were detected using the Oil Red O stain; both were performed using kits purchased from American MasterTech, following the supplier's protocols. Size and number of lipid droplets and total Oil Red O staining were quantified using ImageJ. Senescent cells were identified using the senescence-associated β-galactosidase protocol (Debacq-Chainiaux et al., 2009) as follows: 8 μm cryo-sections were incubated for 15 minutes at room temperature in 0.5% glutaraldehyde in phosphate-buffered saline (PBS), washed in PBS, stained for 16 hours at 37°C with X-gal (using a solution containing 0.16% potassium ferricyanide, 0.18%

potassium ferrocyanide, 0.88% NaCl, 0.019% $MgCl_2$, 0.17% citric acid, 0.11% Na_2HPO_4, and 0.1% X-gal carefully adjusted to pH 6.0), washed with PBS again, stained with nuclear fast red solution for 1 minute or Harris hematoxylin for 15 seconds (Sigma), washed with tap water, and mounted using aqueous mounting media (CCMount, Sigma). The values were expressed as the proportion (%) of SA-β-gal positive cells among total cells. The purpose of the counterstain was to allow the visualization of individual cells, and hence the scoring of total cells. In some experiments a different scoring procedure was used, in which the number of SA-β-gal positive cells was counted and expressed per one magnification field (typically 100x). This procedure was adopted because it was often difficult to accurately ascertain the number of individual cells (due to the weak nature of the counterstain). Unfortunately, a heavier counterstain obscured the often weak SA-β-gal staining. This alternate procedure was quite accurate if neighboring sections were stained with H&E to verify that equivalent tissue specimens were used from different animals. Immunofluorescence to detect macrophages was performed on frozen liver and adipose tissue sections as follow: 7 μm sections were air dried for 1 hour, fixed in acetone for 15 minutes, allowed to dry for 10 minutes, washed in PBS, incubated for 10 minutes in 10% serum, and then incubated with primary F4-80 antibody (AbD Serotec) overnight at 4°C. Slides were then washed 3 times with PBS, incubated with secondary antibody for 2 hours at room temperature, washed 3 more times with PBS, stained with 2 μg/μl DAPI for 30 minutes, washed 3 more times in PBS, and mounted (CCMount, Sigma). Immunofluorescence to detect apoptotic cells was performed as above for the detection of macrophages, except that 8 μm cryosections were fixed in 4% formaldehyde for 15 minutes, washed in PBS, incubated for 1 hour in 10% serum, and

then incubated with cleaved caspase-3 antibody (Cell Signaling, Cat. No. 9661) overnight at 4°C. Visualization of DNA damage foci by immunofluorescence staining of 53BP1 (antibody NB100-304, Novus Biologicals) in cryosections of tissues was performed as described (Jeyapalan et al., 2007; Jeyapalan and Sedivy, 2013).

Preparation of RNA, qPCR and Microarray Analysis

Fragments of tissues in the range of 20-50 mg were removed from samples kept at -80°C, carefully weighed on dry ice, and homogenized in Trizol reagent (Invitrogen) according to the supplier's instructions. Two homogenization methods were used. In the first, the tissue was hand-ground to a powder using a plastic homogenizer (Fisher 02-542-09) chilled in liquid nitrogen, and the powder was vigorously vortexed with Trizol reagent at room temperature. In the second, the tissue fragment was homogenized directly in Trizol reagent in a Fisher PowerGen 125 motorized homogenizer at room temperature. Both procedures yielded high quality RNA, but the second one was more convenient and is now the preferred method. For RT-qPCR, after recovery of total RNA from the Trizol reagent by isopropanol precipitation and purification using the RNeasy Mini kit (QIAGEN), its quality was assessed using an Agilent 2100 Bioanalyzer instrument, and the yield was quantified using a NanoDrop 2000 spectrophotometer. 1 µg of total RNA was reverse transcribed into cDNA in 50 µl reactions using the Taqman kit (Applied Biosystems), according to the manufacturer's protocol. 1 µl of this reaction was used in subsequent qPCR reactions, which were performed using the SYBR Green system (Applied Biosystems) on the ABI 7900 Fast Sequence Detection instrument, according to

the manufacturer's specifications. Primer sequences are listed in Appendix 3. *Gapdh* was used as the internal normalization control.

For microarray analysis, total RNA was prepared, checked for quality, and quantified as indicated above. Equal amounts of total RNA from 5 to 8 male animals were pooled to create a representative sample with a final concentration of 100 ng/ul (Kendziorski et al., 2005). The same animals were used for the analysis of all tissues. The pooled RNA samples were converted to cRNA targets using the 3' IVT Express kit from Affymetrix, hybridized to Mouse 1.0 Gene ST arrays, and scanned on a 3000 G7 scanner, all according to the manufacturer's protocols. These procedures were performed by the Brown University Genomics Core Facility (http://www.brown.edu/Research/CGP/core/). The data from all expression arrays were normalized using the Affymetrix Expression Console software package, and expression values for all genes were generated using the built-in RMA algorithm. False discovery rate (FDR) was calculated as indicated (Storey and Tibshirani, 2003). To identify functional categories that are enriched for differentially expressed genes, the microarray data were analyzed using the Ingenuity Pathway Analysis (IPA) software package (Ingenuity Systems). The GEO accession number for the microarray data is GSE55272.

Bone Density

L4 vertebrae were scanned using a Scanco Medical Micro-CT 40 system to acquire approximately 250 slices per sample at 10 μm resolution. The volume containing trabecular bone (cortical bone was omitted) was selected by someone blind to the age or

genotype of the mouse. The morphometric parameters of bone volume per total volume, trabecular spacing, and trabecular number, were computed for each vertebra, and the average, standard error, and p value (Student's t test) were determined for each cohort.

Cholesterol Determination

The Folch method (Folch et al., 1957) was used to extract lipids from tissues (liver) or serum. 23-30 mg pieces of liver were homogenized in 240 μl of methanol, to which 480 μl of chloroform was added. After shaking for 40 minutes, 145 μl of methanol was added and the samples were centrifuged at 14,000 rpm for 10 minutes. The liquid phase was transferred to a new tube, and 290 μl of chloroform and 252 μl of 0.9% NaCl (in water) were added. After centrifuging for 5 minutes at 2,000 rpm, the upper aqueous phase was discarded and the lower organic phase was transferred to a new tube and dried in a vacuum centrifuge. The dried residue was resuspended in 400 μl of reaction buffer from the Amplex Red Cholesterol kit (Molecular Probes, Invitrogen), which was then used as indicated by the manufacturer to quantify the cholesterol content in each sample.

Flow Cytometry of Peripheral Blood Lymphocytes

Blood was harvested at time of sacrifice by cardiac puncture into heparinized tubes and stored on ice until all mice were sacrificed. The samples were then centrifuged, the plasma was collected, the cell pellets were washed in Hank's balanced salt solution (HBSS, Life Technologies) containing 0.2% bovine serum albumin (BSA), and divided

into 4 separate samples (based on the mouse with the lowest recovered volume of blood). Residual blood was pooled and used for control staining. Four antibody combinations (all from Becton Dickinson) were used: 1) FITC-anti-CD3 (Cat. No. 553062)/PE-anti-CD4 (Cat. No. 553049, 2) FITC-anti-CD3/PE-anti-CD8 (Cat. No. 553033), 3) FITC-anti-CD44 (Cat. No. 553133)/PE-anti-CD4, and 4) FITC-anti-CD44/PE-anti-CD8. Cells were incubated on ice for 30 minutes in the staining cocktails (protected from light), washed twice in HBSS, 0.2% BSA, resuspended in 2 ml of FACS lysing solution (Becton Dickinson, Cat. No. 349202), and incubated for 10 minutes at room temperature to lyse the red blood cells. Cells were recovered by centrifugation and resuspended in HBSS, 0.2% BSA for analysis. Flow cytometry was performed using a Becton Dickinson FACSAria instrument in the Brown University Flow Cytometry and Sorting Facility (http://biomed.brown.edu/mmi/flow_facility).

Flow Cytometry of Bone Marrow

Bone marrow was flushed out of the long bones (femur and tibia) with PBS, 0.5% BSA, and gently passed several times through a 25 gauge syringe to create a single cell suspension. Cell numbers were counted using a hemocytometer, and $1x10^7$ cells were processed for flow cytometry. After centrifugation at 3000 rpm at 4°C for 5 minutes, cell pellets were resuspended in PBS, 0.5% BSA containing conjugated antibodies and incubated for 30 minutes on ice (protected from light). The antibodies used were: FITC-anti-CD34, PE-anti-CD127, PerCP Cy5.5-anti-Sca1, eFluor 780-anti-cKit, and APC-anti-Flt3, all purchased from eBioscience. A lineage cocktail using the pacific blue marker

was purchased from BioLegend. After staining the cells were washed twice in PBS, 0.5% BSA, and flow cytometry was performed as indicated above. Common lymphoid progenitors were defined as Lin^{-}, $Sca1^{+}$, $Flt3^{+}$, $CD127^{+}$; common myeloid progenitors were defined as Lin^{-}, $Sca1^{-}$, $cKit^{+}$, $CD34^{+}$, $CD127^{-}$; long-term HSCs were defined as Lin^{-}, $Sca1^{+}$, $cKit^{+}$, $CD34^{-}$, $Flt3^{-}$; and short term HSCs were defined as Lin^{-}, $Sca1^{+}$, $cKit^{+}$, $CD34^{+}$, $Flt3^{-}$.

Chromatin immunoprecipitation (ChIP)

The procedure was based on the Magna ChIP protocol (Millipore, Cat. No. 17-10085). Nuclei were isolated from intact frozen liver tissue. The tissue was homogenized in a Dounce homogenizer in buffer A1 (15 mM HEPES pH 7.5, 300 mM sucrose, 60 mM KCl, 15 mM NaCl, 2 mM EDTA, 0.5 mM EGTA, 0.15 mM spermine, 0.5 mM spermidine, 14 mM mercaptoethanol, and protease inhibitors) by douncing 5x with the loose pestle and 3x with the tight pestle. The homogenate was centrifuged at 1800 rpm for 5 min. The pellet was resuspended in buffer A2 (A1 + 0.5% NP-40) and gently layered on top of a cushion of buffer B (A1 made with 60% sucrose). Nuclei were collected by centrifugation at 2500 rpm, and resuspended in ice-cold PBS supplemented with protease inhibitors to a final concentration of $2x10^{6}$ nuclei/ml. For each immunoprecipitation, $2x10^{6}$ nuclei were crosslinked at room temperature for 10 min. with 1% formaldehyde, quenched with glycine, and washed twice with ice-cold PBS containing protease inhibitors. Pellets of crosslinked, washed nuclei were resuspended in 100 µl of lysis buffer and sonicated with a Bioruptor UCD-200 (Diagenode) instrument,

set to pulse on high (30 sec. sonication followed by 30 sec. rest) for a total time of 10 min. Next, tubes were spun to remove debris and diluted ten-fold with ChIP dilution buffer containing protease inhibitors. A 1% aliquot of each chromatin preparation was saved as input for further quantification; the remainder was split into two 500 µl reactions, antibody was added (5 µg of anti-c-Myc, clone N-262, Santa Cruz, Cat. No. sc-764), followed by 20 µl of magnetic protein A beads. Immunoprecipitations were performed overnight at 4°C with constant rotation. The immunocomplexes were carefully washed as described in the Magna ChIP protocol (1x low salt wash buffer, 1x high salt wash buffer, 1x LiCl wash buffer, and 2x TE buffer). DNA was recovered by a 2 hr. digestion with proteinase K at 65°C, followed immediately by a 10 min. incubation at 95°C. The recovered DNA was cleaned up by phenol/chloroform extraction and ethanol precipitation and finally resuspended in 16 µl TE. Yields were quantified with Qubit 2.0 dsDNA HS assay kit (Invitrogen, Cat. No. Q32851) and normalized either to starting cell number or input DNA.

Measurement of Serum Analytes

Leptin, adiponectin, and cytokines were measured using the Mouse Adipokine panel, the Mouse Adiponectin single-plex assay, and the Mouse Cytokine/Chemokine panel I (catalog numbers MADPKMAG-71K, MADPNMAG-70K-01, and MCYTOMAG-70K, respectively), all of which use the Luminex magnetic bead system (Millipore). Serum IGF1 was measured using the IGF1 Mouse ELISA Kit, (catalog # ab100695, Abcam) according to the manufacturer's suggested protocol. Serum β-hydroxybutyrate was

measured using the β-hydroxybutyrate LiquiColor Procedure (Catalog # 2440, STANBIO) according to the manufacturer's suggested protocol.

Insulin Sensitivity and Glucose Tolerance Tests

For insulin sensitivity tests and glucose tolerance tests, blood glucose was measured using the Abbot AlphaTRAK glucometer. Test strips used with the glucometer were touched directly to fresh blood from a small cut in the tail vein after wiping away the first drop of blood with a sterile gauze pad. The first measurement was taken before glucose or insulin were injected, and then every 15 or 30 minutes thereafter. Glucose and insulin were administered by intraperitoneal injection. For glucose tolerance tests, 2 grams of glucose were injected per kilogram of body mass, and for insulin sensitivity tests, 1.25 units for females or 2 units of insulin for males were injected per kilogram of body mass.

Chapter 3.

The Life and Death of *Myc*$^{+/-}$ Mice

I. Generation of MYC hypomorphic mice

The overarching goal of this project was to investigate the role of MYC in the aging process by comparing longevity and age-related phenotypes between wild-type and MYC hypomorphic mice. To develop a constitutively hypomorphic *Myc* model, we started with mice in which all coding exons of one copy of the gene were flanked with LoxP sites (de Alboran et al., 2001). We converted the floxed allele to a deletion by breeding to a line expressing Cre recombinase in the germline, and subsequently backcrossed onto the C57BL/6 background for 10 generations. The heterozygous knockout was confirmed using PCR of the *Myc* locus, which revealed half as much *Myc* DNA in knock-out cells (Figure 3.1A). The effect of the $Myc^{+/-}$ genotype on MYC mRNA and protein abundance was confirmed by quantitative RT-PCR (qPCR) and immunoblotting analysis of primary tail fibroblasts established from adult mice. In both cases approximately half of normal ($Myc^{+/+}$) levels of mRNA and protein were observed (Figure 3.1B and 3.1D). Furthermore, chromatin immunoprecipitation (ChIP) with MYC antibody of liver extracts from $Myc^{+/-}$ animals reproducibly gave lower yields, indicating that in vivo a smaller fraction of DNA was bound by MYC (Figure 3.1C).

II. $Myc^{+/-}$ mice have increased longevity

To study the effects of reduced MYC activity on longevity, large cohorts of both sexes and genotypes were maintained in a specific pathogen free (SPF) barrier facility and allowed to die of natural causes. Analysis of the lifespan data revealed a highly significant increase in median lifespan: 10.7% for males, 20.9% for females, and 15.1%

for both sexes combined (Figure 3.2A, Tables 3.1 and 3.2). We do not know the reason for the greater apparent effect in females; we note, however, that control (*Myc*$^{+/+}$) females were shorter lived than males, an observation that has been reported in several colonies of C57BL/6 mice (Thewes et al., 2008). Thus, while *Myc*$^{+/+}$ males lived 8.8% longer than *Myc*$^{+/+}$ females, *Myc*$^{+/-}$ males and females had equivalent lifespans. The lifespans of the *Myc*$^{+/+}$ animals in our colony are among the longest reported (Yuan et al., 2009). Maximum lifespan was also commensurately increased, and the significance of this observation was confirmed using the method of Allison (Wang et al., 2004), showing that nearly all of the mice from the total cohort to survive to the longest-lived decile were of the *Myc*$^{+/-}$ genotype. The instantaneous mortality rate was lower for *Myc*$^{+/-}$ mice across all ages for which death was observed (Figure 3.2B), indicating that the increase in median lifespan reflects a consistent effect across all ages rather than the influence of a subset of animals with particularly long or short lifespans.

III. *Myc*$^{+/-}$ mice are smaller and develop and reproduce normally

Myc$^{+/-}$ mice are healthy, robust and can be group-housed with their *Myc*$^{+/+}$ littermates without any adverse consequences. Animals of both sexes are 15-20% smaller as adults (Figure 3.3A). These differences were apparent at weaning (3 weeks), and the growth (weight) curves of *Myc*$^{+/+}$ and *Myc*$^{+/-}$ mice were parallel over time. Several genetically modified long-lived lines are also smaller, such as Ames or Snell dwarf mice (Bartke and Westbrook, 2012), GHRKO mice (Junnila et al., 2013), or *Pten*^{tg} mice (Ortega-Molina et al., 2012). Mass has been noted as a predictor of longevity in mice,

although this effect is strain specific (Anisimov et al., 2004). In our study, there was no correlation between longevity and the weight attained by individual mice within any cohort (Figure 3.3B), suggesting that the reduced mass of *Myc*$^{+/-}$ mice is not responsible for their increased longevity.

The decreased size of *Myc*$^{+/-}$ mice is proportional across all parts of the body. At 5 months of age, the mass ratio of major organs to total body weight was not significantly different between genotypes (Figure 3.3C). Of particular interest was adipose tissue, since in several long-lived mouse models reduced adiposity has been associated with longevity (Streeper et al., 2012). In this regard, *Myc*$^{+/-}$ and *Myc*$^{+/+}$ mice have a similar proportion of adipose tissue relative to total body volume, and also have similar proportions of visceral and subcutaneous adipose depots (Figure 3.3D). Consistent with this finding, *Myc*$^{+/-}$ and *Myc*$^{+/+}$ mice had similar levels of both leptin and adiponectin in serum at both 6 and 22 months, implying similar adipose tissue function (Figure 3.4A and 3.4B). The reduced size of *Myc*$^{+/-}$ mice may be due to their lower levels of serum IGF1, which we documented in both young and old animals (Figure 3.4C). IGF1 levels are positively correlated with body mass, and decreased insulin/IGF signaling promotes longevity in several model organisms (Hamilton et al., 1994).

The concept of a tradeoff between longevity and reproduction, namely that increased longevity may bear the cost of decreased efficacy or duration of reproductive ability, has been widely discussed. For example in mice, long-lived GHRKO females show delayed vaginal patency, a measure of the onset of puberty (Danilovich et al., 1999). We thus asked whether the increased longevity of *Myc*$^{+/-}$ mice comes at the expense of reduced fecundity. We found that matings between either *Myc*$^{+/-}$ males and

Myc$^{+/+}$ females or *Myc*$^{+/-}$ females and *Myc*$^{+/+}$ males produce normal numbers of pups of each genotype, and, contrary to expectation, *Myc*$^{+/-}$ mice have a slightly earlier age of vaginal patency (Figure 3.4D). In aggregate, these data indicate that the increased longevity of *Myc*$^{+/-}$ mice is not influenced by either slower reproductive development or reduced fecundity.

IV. *Myc*$^{+/-}$ mice show decreased prevalence of cancer

Cancer is the predominant cause of mortality in laboratory mice, and *Myc* heterozygosity has been shown to decrease tumor prevalence and delay progression to carcinoma (Athineos and Sansom, 2010). To investigate whether the increased longevity of *Myc*$^{+/-}$ mice is attributable to cancer resistance, we performed autopsies on all adequately preserved mice at time of death and noted macroscopically visible tumors. A subset of these mice was subjected to a histopathological analysis of 18 tissues by a veterinary pathologist. Common non-neoplastic age-associated pathological findings such as glomerulonephritis and amyloid deposits were similarly prevalent at time of death in each genotype. The spectrum of hyperproliferative pathologies was typical of the C57BL/6 strain of mice and very similar in both genotypes: in order from most to least prevalent, lymphoma, hepatocellular carcinoma, endometrial hyperplasia, and adrenal subcapsular cell hyperplasia were most common (Table 3.3).

Myc$^{+/-}$ mice generally had a lower prevalence and grade of cancer, as well as of hyperplasias which give rise to cancer. Although the proportion of mice with lymphoma in at least one tissue was very high and unaffected by genotype, the number of tissues

affected was lower in *Myc*$^{+/-}$ mice (Figure 3.5A). For example, very few *Myc*$^{+/-}$ mice had lymphoma in more than 5 tissues, whereas in most *Myc*$^{+/+}$ mice lymphoma was detected in at least 6 tissues. The prevalence and severity of adrenal subcapsular cell hyperplasia (which often progresses to adenoma), endometrial hyperplasia (a risk factor for endometrial cancer), and hepatocellular carcinoma, were also lower in *Myc*$^{+/-}$ mice (Figure 3.5B). The absence of high grade hyperproliferative disease, other than lymphoma, in *Myc*$^{+/-}$ mice is noteworthy, as it suggests that the *Myc*$^{+/-}$ genotype attenuates tumor progression. The percentage of mice with macroscopically observable tumors on autopsy was significantly lower in *Myc*$^{+/-}$ mice (53.7%) compared to *Myc*$^{+/+}$ mice (73.4%, p=0.03) (Figure 3.5C). Overall, these results indicate that *Myc*$^{+/-}$ mice have decreased susceptibility to cancer progression.

To investigate whether the increased longevity of *Myc*$^{+/-}$ mice could be attributed to these cancer phenotypes, longevity was assessed in animals that were deemed not to have died from hyperproliferative disease (Table 3.4). Cancer is unlikely to have been a determinant of lifespan in these mice, so genotype should only affect their lifespan via mechanisms unrelated to cancer. The numbers of completely cancer-free mice were too small to conduct a meaningful analysis, but many mice only had low grade lymphoma in only one or two tissues, which is not likely to be a cause of death. Therefore, criteria other than complete absence of cancer were used to designate subsets of animals for the survival analysis, most of which were related to lymphoma due to its high prevalence. Analysis of all cohorts defined by these criteria demonstrated significant ($p<0.05$) lifespan increases in *Myc*$^{+/-}$ mice, which were similar in magnitude to those observed in the complete longevity dataset. It has also been found that reducing cancer prevalence

alone does not significantly extend lifespan in mice (Laposa et al., 2003). This, and additional data from multiple organ systems presented below, indicates that deceleration of cancer in *Myc*$^{+/-}$ mice does not fully account for their increased longevity, and therefore other effects of this genotype are likely to contribute to their longer lifespan.

V. Healthspan in *Myc*$^{+/-}$ mice

The pathological effects of aging in several organ systems were found to be attenuated in *Myc*$^{+/-}$ mice. Cardiac fibrosis increases with age and in diabetes and obesity, and has been found to be reduced in several long-lived mouse models (Dai et al., 2009; Yan et al., 2013). *Myc*$^{+/-}$ mice had less cardiac fibrosis in old age than *Myc*$^{+/+}$ animals (Figure 3.6A). Musculoskeletal and neurological performance decline with age, and the rotarod test (the duration of time that mice are able to remain on an accelerating rotating rod) is a frequently used measure of motor coordination that reflects these parameters. Old *Myc*$^{+/-}$ mice were able to remain on the rotarod nearly twice as long as *Myc*$^{+/+}$ animals of the same age (Figure 3.6B), indicating an attenuation of the effects of aging on motor function. An important component of healthspan in females is osteoporosis (Syed and Melim, 2011), which we assessed in L4 vertebrae using micro computed tomography (micro-CT). In *Myc*$^{+/+}$ females, both bone volume and trabecular number declined with age, whereas trabecular spacing increased (Figure 3.6C), all of which are hallmarks of osteoporosis. Using all these parameters, old *Myc*$^{+/-}$ mice were indistinguishable from young *Myc*$^{+/+}$ animals, indicating that *Myc*$^{+/-}$ females do not develop osteoporosis by 22 months of age. In summary, *Myc*$^{+/-}$ mice are less sensitive to the effects of aging on their

heart and neuromusculoskeletal systems. The diversity of tissues and organ systems in which aging-related diseases were attenuated, as well as the fact that lifespan is extended independent of cancer susceptibility, suggest that *Myc*$^{+/-}$ mice live longer due to broad resistance to the effects of age rather than resistance to a particular lethal disease.

Figure 3.1

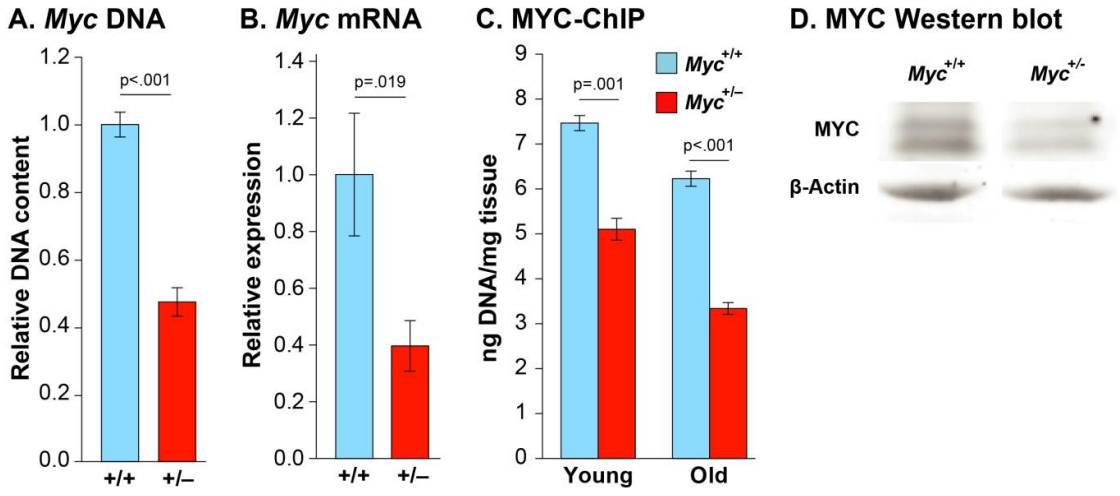
A. Myc DNA
Relative DNA content
1.2
1.0
0.8
0.6
0.4
0.2
0.0
p<.001
+/+
+/–
B. Myc mRNA
Relative expression
1.4
1.2
1.0
0.8
0.6
0.4
0.2
0.0
p=.019
+/+
+/–
C. MYC-ChIP
ng DNA/mg tissue
9
8
7
6
5
4
3
2
1
0
p=.001
p<.001
Myc+/+
Myc+/–
Young
Old
D. MYC Western blot
Myc+/+
Myc+/-
MYC
β-Actin

Figure 3.1. Expression of MYC mRNA and protein in *Myc*$^{+/-}$ cells and tissues

(A) q-PCR with primer pairs 3 and 4 (Appendix 3) on genomic DNA (liver) obtained from *Myc*$^{+/-}$ (red) and *Myc*$^{+/+}$ (blue) mice, to validate the sensitivity and accuracy of detection of our qPCR assays.

(B) *Myc* mRNA expression in early passage mouse tail fibroblasts (MTF) derived from *Myc*$^{+/-}$ and *Myc*$^{+/+}$ mice, measured by q-RT-PCR (Appendix 3) and normalized to *Gapdh* (n=5 for each genotype).

(C) Yields of chromatin immunoprecipitations using anti-MYC antibody from extracts of young (5 month) and old (25 month) liver tissues. DNA was recovered from the pulled down chromatin, quantified using the Qubit HS DNA assay, and normalized to mass of starting tissue samples (n=3 for each genotype at each age). The antibody was from Santa Cruz (sc-764x), also known as N262.

(D) Western blot showing MYC protein in MTF extracts, with β-actin shown as a loading control. The antibody was obtained from Epitomics (Cat. No. 1472-1) and the experiments were performed as described previously (Kreiling et al., 2011).

Figure 3.2

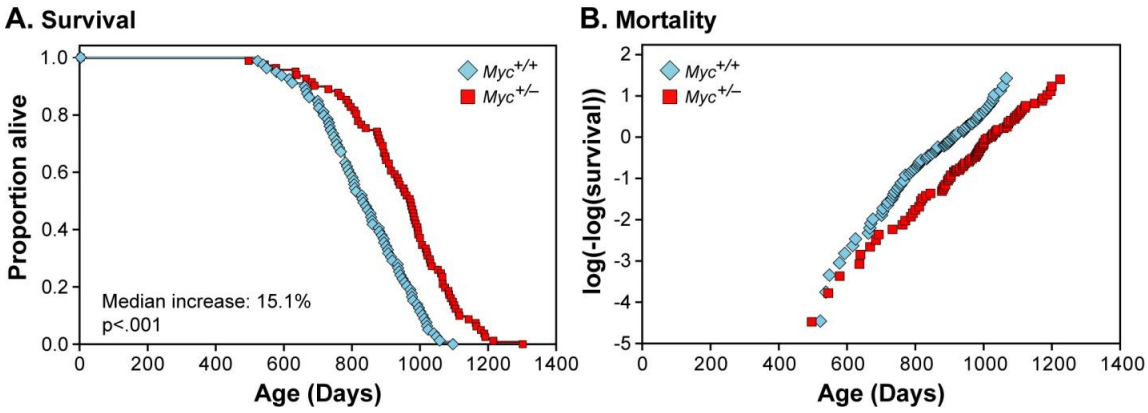
A. Survival
Proportion alive
1.0
0.8
0.6
0.4
0.2
0.0
0
200
400
600
800
1000
1200
1400
Age (Days)
Myc+/+
Myc+/–
Median increase: 15.1%
p<.001
B. Mortality
log(-log(survival))
2
1
0
-1
-2
-3
-4
-5
0
200
400
600
800
1000
1200
1400
Age (Days)
Myc+/+
Myc+/–

Figure 3.2. *Myc*$^{+/-}$ mice have extended longevity

(A) Survival of *Myc*$^{+/+}$ (blue) and *Myc*$^{+/-}$ (red) mice. Males and females were combined. N=79 *Myc*$^{+/+}$ and 81 *Myc*$^{+/-}$ animals. Each data point represents 1 animal.

(B) The same dataset expressed as the natural log of instantaneous mortality for *Myc*$^{+/+}$ and *Myc*$^{+/-}$ mice. Males and females were combined as above.

Table 3.1. Summary of lifespan data

Sex	Genotype	N[1]	Mean[2]	SE[3]	Median[4]	Increase[5]	P (med)[6]	N (max)[7]	P (max)[8]
Female	*Myc*$^{+/-}$	39	945.53	27.4	979	20.9%	<.0001	8	.0053
	Myc$^{+/+}$	37	829.12	20.2	810			0	
Male	*Myc*$^{+/-}$	42	953.07	22.3	975	10.7%	.0006	7	.057
	Myc$^{+/+}$	42	854.74	22.3	881			1	
All	*Myc*$^{+/-}$	81	949.32	17.5	976	15.1%	<.0001	15	.0003
	Myc$^{+/+}$	79	842.32	15.1	848			1	

Table 3.1. Summary of lifespan data

[1]Number of animals in cohort.

[2]Mean (average) lifespan (days).

[3]Standard error of the mean.

[4]Median lifespan (days).

[5]Increase of median lifespan in *Myc*$^{+/-}$ animals (in percent).

[6]P value of the median lifespan increase calculated using the long-rank test.

[7]Number of animals in the longest lived decile.

[8]P value of increased maximum lifespan; Fisher's exact test was applied to N (max) values. Log-rank statistics and SE were computed using JMP10 software.

Table 3.2. Lifespan data[1]

			Age at death			Actual date of:			
Mouse	Genotype	Sex	Days	Months	Censor[2]	Birth	Death	Mother[3]	Father[3]
859	Myc+/–	F	498	16.4	0	6/17/2008	10/28/2009	15, 16	3
869	Myc+/–	F	546	17.9	0	6/19/2008	12/17/2009	13, 14	2
850	Myc+/–	F	579	19.0	0	6/9/2008	1/9/2010	11, 12	1
582	Myc+/–	F	636	20.9	0	11/16/2007	8/13/2009	1, 2	1
882	Myc+/–	F	684	22.5	0	11/19/2008	10/4/2010	23	7
890	Myc+/–	F	769	25.3	0	1/3/2009	2/11/2011	23	7
742	Myc+/–	F	791	26.0	0	2/10/2008	4/11/2010	3, 4	2
880	Myc+/–	F	814	26.8	0	11/19/2008	2/11/2011	23	7
695	Myc+/–	F	842	27.7	0	1/10/2008	5/1/2010	7, 8	5
839	Myc+/–	F	878	28.9	0	5/20/2008	10/15/2010	19, 20	5
600	Myc+/–	F	892	29.3	0	11/18/2007	4/28/2010	7, 8	5
852	Myc+/–	F	892	29.3	0	6/9/2008	11/18/2010	11, 12	1
580	Myc+/–	F	900	29.6	0	11/16/2007	5/4/2010	1, 2	1
728	Myc+/–	F	910	29.9	0	2/1/2008	7/30/2010	5, 6	3
733	Myc+/–	F	910	29.9	0	2/3/2008	8/1/2010	9, 10	6
777	Myc+/–	F	913	30.0	1	2/22/2008	8/23/2010	21, 22	6
694	Myc+/–	F	916	30.1	0	1/10/2008	7/14/2010	7, 8	5
758	Myc+/–	F	919	30.2	1	2/16/2008	8/23/2010	1, 2	1
744	Myc+/–	F	925	30.4	1	2/10/2008	8/23/2010	3, 4	2
734	Myc+/–	F	927	30.5	0	2/3/2008	8/18/2010	9, 10	6
692	Myc+/–	F	935	30.7	0	1/10/2008	8/2/2010	7, 8	5
663	Myc+/–	F	953	31.3	0	12/27/2007	8/6/2010	5, 6	3
623	Myc+/–	F	971	31.9	0	12/6/2007	8/3/2010	5, 6	4
851	Myc+/–	F	979	32.2	0	6/9/2008	2/13/2011	11, 12	1
671	Myc+/–	F	982	32.3	0	12/27/2007	9/4/2010	5, 6	4
770	Myc+/–	F	983	32.3	0	2/19/2008	10/29/2010	15, 16	3
621	Myc+/–	F	986	32.4	0	12/6/2007	8/18/2010	5, 6	4
714	Myc+/–	F	989	32.5	0	1/23/2008	10/8/2010	9, 10	6
853	Myc+/–	F	994	32.7	0	6/9/2008	2/28/2011	11, 12	1
682	Myc+/–	F	1001	32.9	0	12/28/2007	9/24/2010	1, 2	1
586	Myc+/–	F	1021	33.6	0	11/16/2007	9/2/2010	1, 2	1
821	Myc+/–	F	1036	34.1	0	4/12/2008	2/12/2011	17, 18	4
743	Myc+/–	F	1063	34.9	0	2/10/2008	1/8/2011	3, 4	2
601	Myc+/–	F	1067	35.1	0	11/18/2007	10/20/2010	7, 8	5
597	Myc+/–	F	1068	35.1	0	11/18/2007	10/21/2010	7, 8	5
730	Myc+/–	F	1087	35.7	0	2/1/2008	1/23/2011	5, 6	3
735	Myc+/–	F	1106	36.4	0	2/3/2008	2/13/2011	9, 10	6
783	Myc+/–	F	1115	36.7	0	3/11/2008	3/31/2011	11, 12	1
721	Myc+/–	F	1165	38.3	0	1/23/2008	4/2/2011	1, 2	1
628	Myc+/–	F	1167	38.4	0	12/13/2007	2/22/2011	9, 10	6
588	Myc+/–	F	1217	40.0	0	11/16/2007	3/17/2011	1, 2	1
759	Myc+/–	F	1303	42.8	0	2/16/2008	9/11/2011	1, 2	1
881	Myc+/+	F	551	18.1	0	11/19/2008	5/24/2010	23	7
716	Myc+/+	F	580	19.1	0	1/23/2008	8/25/2009	9, 10	6
778	Myc+/+	F	626	20.6	0	2/22/2008	11/9/2009	21, 22	6
722	Myc+/+	F	667	21.9	0	1/23/2008	11/20/2009	1, 2	1
626	Myc+/+	F	670	22.0	0	12/13/2007	10/13/2009	9, 10	6
771	Myc+/+	F	676	22.2	0	2/19/2008	12/26/2009	15, 16	3
595	Myc+/+	F	704	23.1	0	11/18/2007	10/22/2009	7, 8	5
868	Myc+/+	F	719	23.6	0	6/19/2008	6/8/2010	13, 14	2
599	Myc+/+	F	734	24.1	0	11/18/2007	11/21/2009	7, 8	5
757	Myc+/+	F	736	24.2	0	2/16/2008	2/21/2010	1, 2	1
870	Myc+/+	F	739	24.3	0	6/19/2008	6/28/2010	13, 14	2
622	Myc+/+	F	749	24.6	0	12/6/2007	12/24/2009	5, 6	4
665	Myc+/+	F	756	24.9	0	12/27/2007	1/21/2010	5, 6	3
666	Myc+/+	F	764	25.1	0	12/27/2007	1/29/2010	5, 6	3
891	Myc+/+	F	769	25.3	0	1/3/2009	2/11/2011	23	7
768	Myc+/+	F	782	25.7	0	2/19/2008	4/11/2010	15, 16	3

			Age at death			Actual date of:			
Mouse	Genotype	Sex	Days	Months	Censor[2]	Birth	Death	Mother[3]	Father[3]
854	Myc+/+	F	796	26.2	0	6/9/2008	8/14/2010	11, 12	1
584	Myc+/+	F	803	26.4	0	11/16/2007	1/27/2010	1, 2	1
784	Myc+/+	F	807	26.5	0	3/20/2008	6/5/2010	11, 12	1
719	Myc+/+	F	808	26.6	0	1/23/2008	4/10/2010	1, 2	1
780	Myc+/+	F	810	26.6	0	3/10/2008	5/29/2010	13, 14	2
715	Myc+/+	F	830	27.3	0	1/23/2008	5/2/2010	9, 10	6
685	Myc+/+	F	835	27.4	0	12/28/2007	4/11/2010	1, 2	1
704	Myc+/+	F	856	28.1	0	1/13/2008	5/18/2010	7, 8	5
729	Myc+/+	F	861	28.3	0	2/1/2008	6/11/2010	5, 6	3
789	Myc+/+	F	862	28.3	0	3/20/2008	7/30/2010	11, 12	1
788	Myc+/+	F	886	29.1	1	3/20/2008	8/23/2010	11, 12	1
782	Myc+/+	F	893	29.4	1	3/11/2008	8/21/2010	11, 12	1
775	Myc+/+	F	896	29.5	0	2/22/2008	8/6/2010	21, 22	6
736	Myc+/+	F	902	29.7	0	2/3/2008	7/24/2010	9, 10	6
781	Myc+/+	F	908	29.8	0	3/11/2008	9/5/2010	11, 12	1
776	Myc+/+	F	913	30.0	1	2/22/2008	8/23/2010	21, 22	6
693	Myc+/+	F	936	30.8	0	1/10/2008	8/3/2010	7, 8	5
672	Myc+/+	F	940	30.9	0	12/27/2007	7/24/2010	5, 6	4
598	Myc+/+	F	944	31.0	0	11/18/2007	6/19/2010	7, 8	5
723	Myc+/+	F	961	31.6	1	1/23/2008	9/10/2010	1, 2	1
587	Myc+/+	F	978	32.1	0	11/16/2007	7/21/2010	1, 2	1
664	Myc+/+	F	981	32.2	0	12/27/2007	9/3/2010	5, 6	3
720	Myc+/+	F	1022	33.6	0	1/23/2008	11/10/2010	1, 2	1
585	Myc+/+	F	1025	33.7	0	11/16/2007	9/6/2010	1, 2	1
583	Myc+/+	F	1042	34.3	0	11/16/2007	9/23/2010	1, 2	1
660	Myc+/–	M	639	21.0	0	12/27/2007	9/26/2009	5, 6	3
766	Myc+/–	M	667	21.9	0	2/19/2008	12/17/2009	15, 16	3
878	Myc+/–	M	692	22.7	0	11/19/2008	10/12/2010	23	7
724	Myc+/–	M	732	24.1	0	2/1/2008	2/2/2010	5, 6	3
561	Myc+/–	M	761	25.0	0	11/14/2007	12/14/2009	3, 4	2
625	Myc+/–	M	785	25.8	0	12/13/2007	2/5/2010	9, 10	6
701	Myc+/–	M	798	26.2	0	1/13/2008	3/21/2010	7, 8	5
732	Myc+/–	M	809	26.6	0	2/3/2008	4/22/2010	9, 10	6
879	Myc+/–	M	814	26.8	0	11/19/2008	2/11/2011	23	7
613	Myc+/–	M	819	26.9	0	11/27/2007	2/23/2010	5, 6	3
579	Myc+/–	M	829	27.3	0	11/16/2007	2/22/2010	1, 2	1
571	Myc+/–	M	875	28.8	0	11/14/2007	4/7/2010	5, 6	4
702	Myc+/–	M	881	29.0	0	1/13/2008	6/12/2010	7, 8	5
678	Myc+/–	M	885	29.1	0	12/28/2007	5/31/2010	1, 2	1
670	Myc+/–	M	895	29.4	0	12/27/2007	6/9/2010	5, 6	4
555	Myc+/–	M	901	29.6	0	11/14/2007	5/3/2010	5, 6	3
557	Myc+/–	M	938	30.8	0	11/14/2007	6/9/2010	5, 6	3
620	Myc+/–	M	942	31.0	0	12/6/2007	7/5/2010	5,6	4
754	Myc+/–	M	956	31.4	0	2/16/2008	9/29/2010	1, 2	1
762	Myc+/–	M	962	31.6	0	2/19/2008	10/8/2010	15, 16	3
679	Myc+/–	M	974	32.0	0	12/28/2007	8/28/2010	1, 2	1
691	Myc+/–	M	976	32.1	0	1/10/2008	9/12/2010	7, 8	5
690	Myc+/–	M	995	32.7	0	1/10/2008	10/1/2010	7, 8	5
610	Myc+/–	M	996	32.7	0	11/25/2007	8/17/2010	3, 4	2
699	Myc+/–	M	1001	32.9	0	1/8/2008	10/5/2010	3, 4	2
565	Myc+/–	M	1007	33.1	0	11/14/2007	8/17/2010	5, 6	4
727	Myc+/–	M	1018	33.5	0	2/1/2008	11/15/2010	5, 6	3
740	Myc+/–	M	1023	33.6	0	2/10/2008	11/29/2010	3, 4	2
737	Myc+/–	M	1030	33.9	0	2/10/2008	12/6/2010	3, 4	2
594	Myc+/–	M	1032	33.9	0	11/18/2007	9/15/2010	7, 8	5
755	Myc+/–	M	1054	34.6	0	2/16/2008	1/5/2011	1, 2	1
577	Myc+/–	M	1067	35.1	0	11/16/2007	10/18/2010	1, 2	1
764	Myc+/–	M	1075	35.3	0	2/19/2008	1/29/2011	15, 16	3
592	Myc+/–	M	1085	35.7	0	11/18/2007	11/7/2010	7, 8	5
559	Myc+/–	M	1092	35.9	0	11/14/2007	11/10/2010	3, 4	2

Mouse	Genotype	Sex	Age at death		Censor[2]	Actual date of:		Mother[3]	Father[3]
			Days	Months		Birth	Death		
767	Myc+/–	M	1098	36.1	0	2/19/2008	2/21/2011	15, 16	3
756	Myc+/–	M	1102	36.2	0	2/16/2008	2/22/2011	1, 2	1
659	Myc+/–	M	1117	36.7	0	12/27/2007	1/17/2011	5, 6	3
566	Myc+/–	M	1144	37.6	0	11/14/2007	1/1/2011	5, 6	4
648	Myc+/–	M	1180	38.8	0	12/18/2007	3/12/2011	3, 4	2
731	Myc+/–	M	1190	39.1	0	2/3/2008	5/8/2011	9, 10	6
568	Myc+/–	M	1193	39.2	0	11/14/2007	2/19/2011	5, 6	4
713	Myc+/+	M	525	17.3	0	1/23/2008	7/1/2009	9, 10	6
572	Myc+/+	M	541	17.8	0	11/14/2007	5/8/2009	5, 6	4
669	Myc+/+	M	595	19.6	0	12/27/2007	8/13/2009	5, 6	4
718	Myc+/+	M	618	20.3	0	1/23/2008	10/2/2009	1, 2	1
700	Myc+/+	M	663	21.8	0	1/13/2008	11/6/2009	7, 8	5
658	Myc+/+	M	701	23.0	0	12/27/2007	11/27/2009	5, 6	3
688	Myc+/+	M	705	23.2	0	1/10/2008	12/15/2009	7, 8	5
573	Myc+/+	M	718	23.6	0	11/14/2007	11/1/2009	5, 6	4
686	Myc+/+	M	730	24.0	0	1/10/2008	1/9/2010	7, 8	5
725	Myc+/+	M	746	24.5	0	2/1/2008	2/16/2010	5, 6	3
765	Myc+/+	M	757	24.9	0	2/19/2008	3/17/2010	15, 16	3
887	Myc+/+	M	769	25.3	0	1/3/2009	2/11/2011	23	7
889	Myc+/+	M	769	25.3	0	1/3/2009	2/11/2011	23	7
591	Myc+/+	M	787	25.9	0	11/18/2007	1/13/2010	7, 8	5
697	Myc+/+	M	791	26.0	0	1/8/2008	3/9/2010	3, 4	2
556	Myc+/+	M	814	26.8	0	11/14/2007	2/5/2010	5, 6	3
717	Myc+/+	M	832	27.4	0	1/23/2008	5/4/2010	1, 2	1
558	Myc+/+	M	843	27.7	0	11/14/2007	3/6/2010	5, 6	3
649	Myc+/+	M	848	27.9	0	12/18/2007	4/14/2010	3, 4	2
676	Myc+/+	M	858	28.2	0	12/28/2007	5/4/2010	1, 2	1
612	Myc+/+	M	880	28.9	0	11/27/2007	4/25/2010	5, 6	3
560	Myc+/+	M	882	29.0	0	11/14/2007	4/14/2010	3, 4	2
687	Myc+/+	M	889	29.2	0	1/10/2008	6/17/2010	7, 8	5
760	Myc+/+	M	895	29.4	0	2/19/2008	8/2/2010	15, 16	3
761	Myc+/+	M	907	29.8	0	2/19/2008	8/14/2010	15, 16	3
779	Myc+/+	M	916	30.1	0	3/10/2008	9/12/2010	13, 14	2
739	Myc+/+	M	920	30.2	0	2/10/2008	8/18/2010	3, 4	2
624	Myc+/+	M	937	30.8	0	12/13/2007	7/7/2010	9, 10	6
570	Myc+/+	M	950	31.2	0	11/14/2007	6/21/2010	5, 6	4
689	Myc+/+	M	957	31.5	0	1/10/2008	8/24/2010	7, 8	5
567	Myc+/+	M	963	31.7	0	11/14/2007	7/4/2010	5, 6	4
677	Myc+/+	M	973	32.0	0	12/28/2007	8/27/2010	1, 2	1
569	Myc+/+	M	977	32.1	0	11/14/2007	7/18/2010	5, 6	4
696	Myc+/+	M	993	32.6	0	1/8/2008	9/27/2010	3, 4	2
773	Myc+/+	M	998	32.8	0	2/22/2008	11/16/2010	21, 22	6
738	Myc+/+	M	1002	32.9	0	2/10/2008	11/8/2010	3, 4	2
578	Myc+/+	M	1009	33.2	0	11/16/2007	8/21/2010	1, 2	1
698	Myc+/+	M	1014	33.3	0	1/8/2008	10/18/2010	3, 4	2
593	Myc+/+	M	1020	33.5	0	11/18/2007	9/3/2010	7, 8	5
753	Myc+/+	M	1050	34.5	0	2/16/2008	1/1/2011	1, 2	1
726	Myc+/+	M	1059	34.8	0	2/1/2008	12/26/2010	5, 6	3
562	Myc+/+	M	1098	36.1	0	11/14/2007	11/16/2010	3, 4	2

Table 3.2 Lifespan data

[1]Individual lifespan data for all mice used in the analysis of longevity.

[2]A few animals were removed from the cohort before their natural death to harvest tissues or other experiments. These animals were censored at the time of removal.

[3]Matings were set up in large cages with 2 females and one male (see Extended Experimental Procedures). The identity of the father and both potential mothers are shown for each mouse.

Figure 3.3

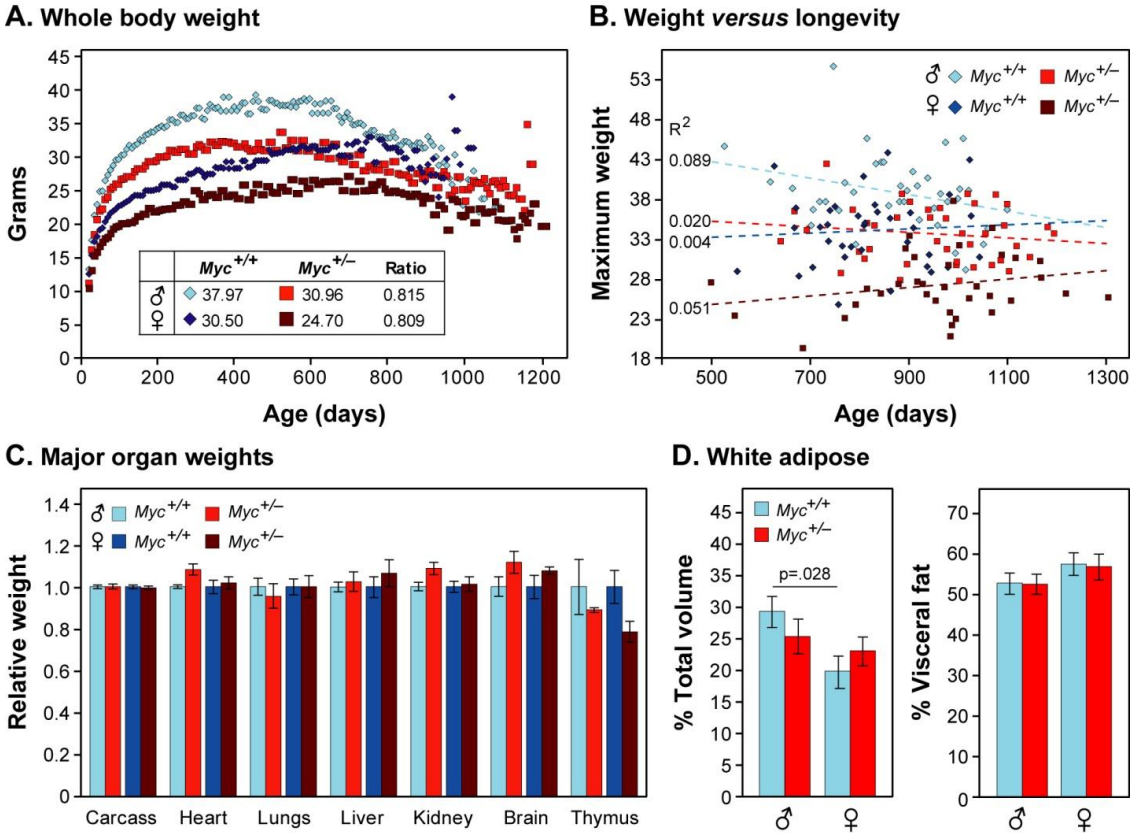
A. Whole body weight
Grams
Age (days)
Myc+/+
Myc+/–
Ratio
♂ 37.97 30.96 0.815
♀ 30.50 24.70 0.809
B. Weight versus longevity
Maximum weight
Age (days)
R2
0.089
0.020
0.004
0.051
C. Major organ weights
Relative weight
Carcass
Heart
Lungs
Liver
Kidney
Brain
Thymus
D. White adipose
% Total volume
p=.028
% Visceral fat

Figure 3.3. Effects of *Myc*$^{+/-}$ genotype on body mass and composition

(A) Lifelong trends of whole body weights. Four cohorts were scored: *Myc*$^{+/+}$ males (n=39), *Myc*$^{+/+}$ females (n=41), *Myc*$^{+/-}$ males (n=36) and *Myc*$^{+/+}$ females (n=35). Animals were weighed weekly and median weights using a 3-week sliding window are shown. Inset shows weights at 500 days (grams), and the relative weights of *Myc*$^{+/-}$ animals.

(B) Correlations between the maximum achieved weight and age at death for individual mice. The same cohorts as in (A) above are shown. R^2 values and linear regressions (dashed lines) summarize the correlations within each cohort.

(C) Relative organ weights. Major organs were removed and weighed. Organ mass values are expressed as ratios to total body weight, additionally normalized to *Myc*$^{+/+}$ for each tissue. All animals were 5 months of age (n=6 for each genotype and sex).

(D) Relative adiposity. Freshly sacrificed animals were scanned by microCT imaging. Left: volume occupied by all white adipose tissue is shown as percent of total volume of the animal. Right: volume of visceral adipose is shown as percent of total adipose. The same animals as in (C) above were used.

Figure 3.4

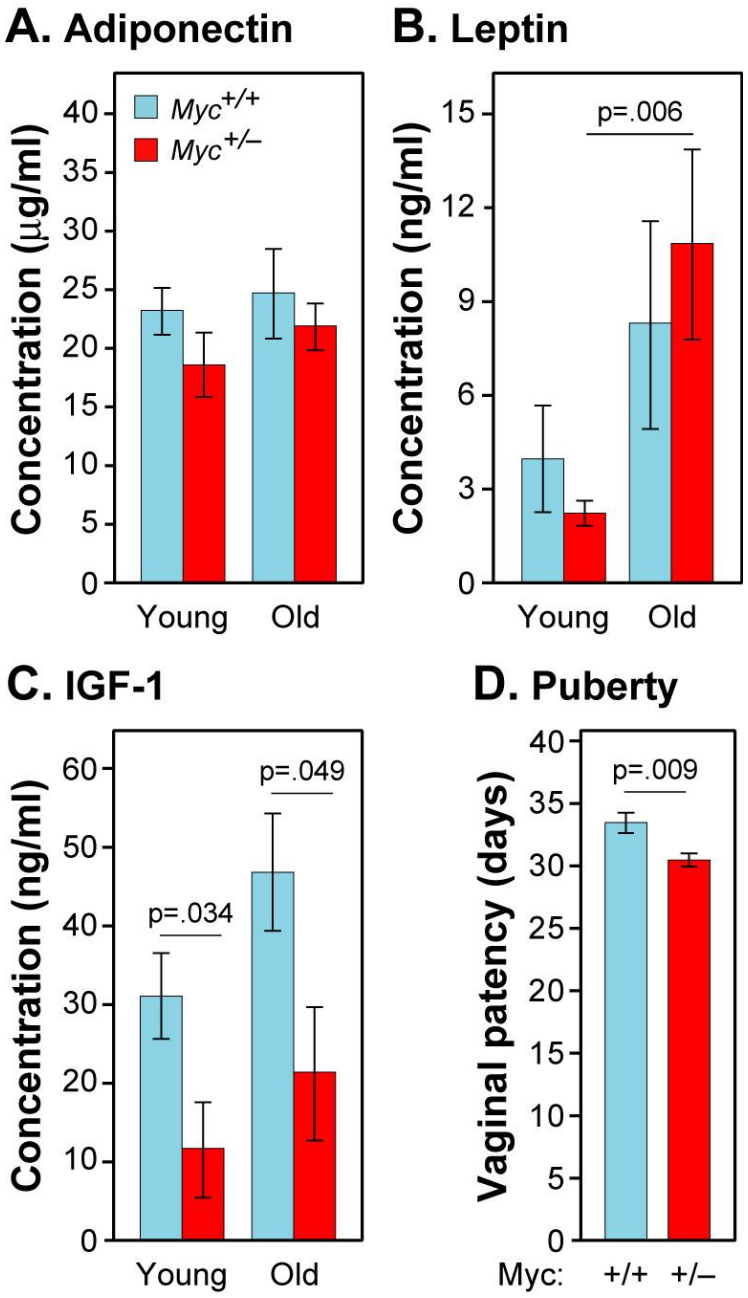
A. Adiponectin
Concentration (μg/ml)
Myc+/+
Myc+/–
Young
Old
B. Leptin
Concentration (ng/ml)
p=.006
Young
Old
C. IGF-1
Concentration (ng/ml)
p=.034
p=.049
Young
Old
D. Puberty
Vaginal patency (days)
p=.009
Myc: +/+ +/–

Figure 3.4. Effects of *Myc*$^{+/-}$ genotype on some metabolic hormones and sexual maturation

(A-C) Concentrations of adiponectin, leptin, and IGF1 in the plasma of 5 month and 22 month old females. Animals were starved overnight prior to the collection of blood samples in the morning. N=5-12 animals for each cohort.

(D) Age of vaginal patency (days) for *Myc*$^{+/+}$ and *Myc*$^{+/-}$ female mice. N=19 *Myc*$^{+/+}$ and 12 *Myc*$^{+/-}$ animals.

Table 3.3. End of life pathological and histological examination[1]

Mouse	Tumor	Myc	Sex	Heart	Salivary	Brain	Kidney	Liver	Spleen	Lung
587	0	+/+	F	ly 2	ly 3		ly 1, gn 2	ly 3	ly 3	ly 3
664	+	+/+	F		ly 3		gn 1, ly 2	ly 3	ly 2	ly 2
672	0	+/+	F					ly 2, necr 3	ly 3	
693	0	+/+	F		ly 2			hepcar 5	ly 3	
736	0	+/+	F		li 2	min 1	gn 2, li 2	hep 3, necr 2		pneum 5, aba 5
789	0	+/+	F		ly 2		ly 2	ly 2	ly 2	ly 2
583	+	+/+	F		ly 1	min 1	gn 3 amyl	hepcar 2, ly 3	ly 3	ly 2
720	0	+/+	F		ly 4	min 1	ly 3, gn 2	ly 2	ly 3	ly 3
1092	0	+/+	F		ly 3		gn 2, ly 2	ly 2	ly 2	ly 2
775	0	+/+	F		ly 4		gn 2, ly 2	ly 1	ly 4	ly 3
773	0	+/+	M			min 2	gn 2	ly 3	ly 2	ly 2
569	0	+/+	M		ly 2		ly 2, gn 1	ly 3	ly 3	ly 4
578	0	+/+	M		ly 2		ly 2, gn 3	ly 1	ly 2	ly 3
593	0	+/+	M				gn 1	ly 2, hemoma 3	ly 1	
689	+	+/+	M		ly 1		ly 1, gn 1	ly 3	ly 1	ly 1
739	+	+/+	M		li 1		li 2	hepcar 4		
760	+	+/+	M		ly 2		gn 1, ly 1	ly 4	ly 2	ly 2, aba 1
562	0	+/+	M				gn 3 amyl	hepcar 3, ly 2		ec 4 al 4
696	0	+/+	M				gn 1, li 2,	ly 3	ly 3	
738	+	+/+	M				gn 2	ly 4	ly 2	ly 2, li 1
992	N/A	+/+	M		li 3		gn5 - amyl, li3			aba 3, al 3, li 3
994	N/A	+/+	M		li 3		gn 4 - amyl, li 3			li 3
621	0	+/–	F		ly 2		gn 1, ly 1	ly 2	ly 3	
623	0	+/–	F				gn 2, ly 2		ly 2	si 3
671	0	+/–	F				gn 1, li 1		ly 2	ly 2
692	+	+/–	F				gn 1	ly 3	ly 2	ly 1
694	0	+/–	F				gn 1, li 1	ly 1	ly 4	
733	+	+/–	F		m		ly 1	ly 4	ly 4	ly 4
734	+	+/–	F					ly 3	ly 3	ly 3
597	0	+/–	F		li 1		gn 3, ly 2		ly 1	ly 2, ec 3, al 3
601	+	+/–	F				gn 2, li 1	ly 3	ly 2	li 1
682	+	+/–	F				gn 2, li 1	ly 3	ly 4	ly 2, aba 1
714	0	+/–	F	ly 1	ly 3	min 2	ly 1, gn 1		ly 3	ly 3
1091	N/A	+/–	F		ly 2		gn 1, ly 2		ly 1	ly 2
588	0	+/–	F				inep3, min4, gn1	necr 4	ly 2	ly 2, ec 2
628	0	+/–	F				gn 1, hem 2	ly 3	ly 2	ly 2
721	0	+/–	F				gn 2			ec 1
735	0	+/–	F			min 1	gn 2	ly 3	ly 2	
851	+	+/–	F	amyl 2	amyl 1	min 1	gn 5. amyl 5	ly 3	ly 1	
759	0	+/–	F				gn 4, amyl 2			
839	+	+/–	F				gn 3	ly 2	ly 2	ly 2, aba 1
565	+	+/–	M				li 1	ly 3		
610	+	+/–	M					ly 3	ly 3	ly 2
679	+	+/–	M				gn 2	ly 4		
559	0	+/–	M	throm 2	li 1	min 1	li 1, min 1	ly 4, necr 4	necr 2	ec 3, al 2
592	0	+/–	M		li 1		li 1	ly 2	ly 5	
594	0	+/–	M				gn 2,li 1	ly 4		ly 1
690	0	+/–	M				gn 1, min 1			ec 2
691	0	+/–	M			min 1	gn 1			aba 1
699	0	+/–	M		li 1	min 2	gn 2, li 1	necr 2, hepcar 2	ly 2	ly 1
737	+	+/–	M			min 3	gn 2, min 1, li 1	ly 3	ly 1	
740	+	+/–	M		li 1		gn 2	ly 4	ly 2	
755	0	+/–	M		ly 4		gn 2	ly 3	ly 2	
762	0	+/–	M				gn 2, ly 1	ly 4	ly 3	ly 4, aba 4
878	0	+/–	M				gn 1			
991	N/A	+/–	M				gn 4 - amyl			
993	N/A	+/–	M		li 3		gn 5 - amyl			li 1
568	0	+/–	M		ly 1	min 2	gn 2. min 1	ly 3	ly 2	ly 2
648	+	+/–	M				gn 2	ly 3	ly 2	ly 2, ec 2
731	0	+/–	M	cm 1			gn 4, min 1	ly 3	ly 2,hmsc 4	
756	+	+/–	M		ly 1		gn 1, min 1	ly 3	ly 2	
764	0	+/–	M	amyl 4	amyl 3		gn 2	ly 3	ly 2	
767	0	+/–	M	amyl 4	amyl 1	min 1	gn 3, min 1	ly 3		

Mouse	Pancreas	Pituitary	Thymus	Thyroid	Adrenal gland	Testis/ovary	Other repro.
587			fsch		sh 1		ly 2
664			m			hem 4	endohyper 3
672					sh 3		endohyper 3
693	ly 2				sh 3	tsadn 4, ly 3	ly 3, endohyper 3
736	atrophy 4			fch 2	sh 1	tsadn 2,cyst2	endohyper 2
789					sh 3		endohyper 2
583			m		sh 1		
720		adn 3			sh 3	ly 2	ly 2
1092	ly 2				sh 3, amyl 1		endohyper 4
775		adn 3			sh 1		endohyper 2
773					sh 2		
569			m			ly 1	ly 2
578			m				si 3
593				m			
689							si 2
739		m			sh 1		
760	ly 1						
562							
696							granuloma 3
738							si 2
992			hyperplasia 2	m	amyl 4		
994		m			amyl 3		
621			m				
623			m		sh 3	tsadn 4	
671			m		sh 1		
692		m			sh 2		endohyper 2
694					sh 2		ly 2, endohyper 1
733	m	m	ly 1	m	ly 2, sh 1	m	ly 3
734							
597		adn 3					
601			m				
682			m		sh 2		ly 3
714	m		ly 3				
1091				negative	sh 2		
588		adn 3				m	
628					sh 1		endohyper 2
721				hyperplasia 2		m	endohyper 2
735						m	
851				amyl 2	amyl 3		endohyper 1
759			m	cyst 1		cyst 4	
839		m		m			
565			m	m			si 4
610			m	m			si 5
679					m		
559			m				
592			m				ly 2
594		m					si 2
690			m				
691			m				
699							
737							
740							
755	m			m			
762							si 2
878							
991					amyl 3		
993					amyl 3		
568				m	m		
648							
731		adn 2					cyst 3
756				m	m		cyst 4
764				amyl 5	m	spgran 1	adn 4,si 2, cyst 4
767				m	amyl 4		cyst 5

Mouse	Urinary	LNs[2]	Stomach	Intestine	Others
587	ly 2	ly 2			
664	ly 1	ly 3			
672		ly 3		ly 1	
693	ly 2	ly 5		ly 1	
736					
789	ly 1	ly 5	ly 2		
583		ly 1		ly 1	
720	ly 3	ly 5	gastritis 3		
1092	ly 2	ly 2		li 1	
775		ly 4	ly 5	ly 5	
773		ly 1	ly 1	ly 2	
569	ly 1	ly 3	m	m	
578		ly 1			
593		ly 1		li 1	
689		ly 1		ly 2	
739					
760		ly 2			
562				li 1	
696		ly 1		li 1	
738		ly 1		li 2	
992	m			amyl 5, li 1	
994				amyl 5, li 3	
621		ly 2			
623		ly 1			
671		ly 5		li 1	
692		ly 1		li 2	si 2 - trachea
694		ly 5		ly 1	
733		ly 4		ly 1	
734		ly 2		li 1	
597		ly 1			
601	li 1	ly 5			
682		ly 4			
714		ly 5		li 1	
1091		ly 2		li 1	
588				ly 1	
628		ly 4			
721					
735		ly 5			
851		m		ly 2, amyl 3	
759				amyl 5	
839		ly 1		ly 1	
565			m	m	
610	si 4			ly 1	
679				li 1	
559					
592		ly 5			
594					cyst skin 2
690		m		li 1	
691		ly 3		li 1	
699		ly 1		ly 1	
737				li 1	
740		ly 2			
755		ly 5			
762		ly 4			
878				li 1	
991				li 1	
993					
568		ly 1			
648		ly 3			
731		ly 2			
756		ly 1		ly 2	
764		ly 1	amyl 1	amyl 3	
767		m	amyl 3		

Table 3.3. End of life pathological and histological examination

[1]Summary of pathological findings in 18 tissues assessed by an expert veterinary pathologist (Y. Ikeno). The analysis included a histological examination of major organs. Severity is described on a scale of 1 (least) to 5 (greatest). See Table 3.2 for ages of death.

[2]Abbreviation LNs designates Lymph Nodes

Abbreviations of pathological observations used:

aba - alveolar/bronchiolar adenoma
adn - adenoma
al - alveolar proteinosis
amyl - amyloid
cm - cardiomyopathy
ec - eosinophilic crystals
endohyper - endometrial hyperplasia
fch - follicular cell hyperplasia
fsch - focal squamous cell hyperplasia
gn - glomerulonephritis
hem - hemorrhage
hemoma – hemangioma
hep - hepatitis
hmsc - hemangiosarcoma
hepcar - hepatocellular carcinoma
inep - interstitial nephritis
li - lymphocytic infiltrate
ly - lymphoma
m - missing
min - mineralization
necr - necrosis
sh - subcapsular hyperplasia
si - suppurative inflammation
spgran - sperm granuloma
throm - thrombus
tsadn - tubulostromal adenoma

Figure 3.5

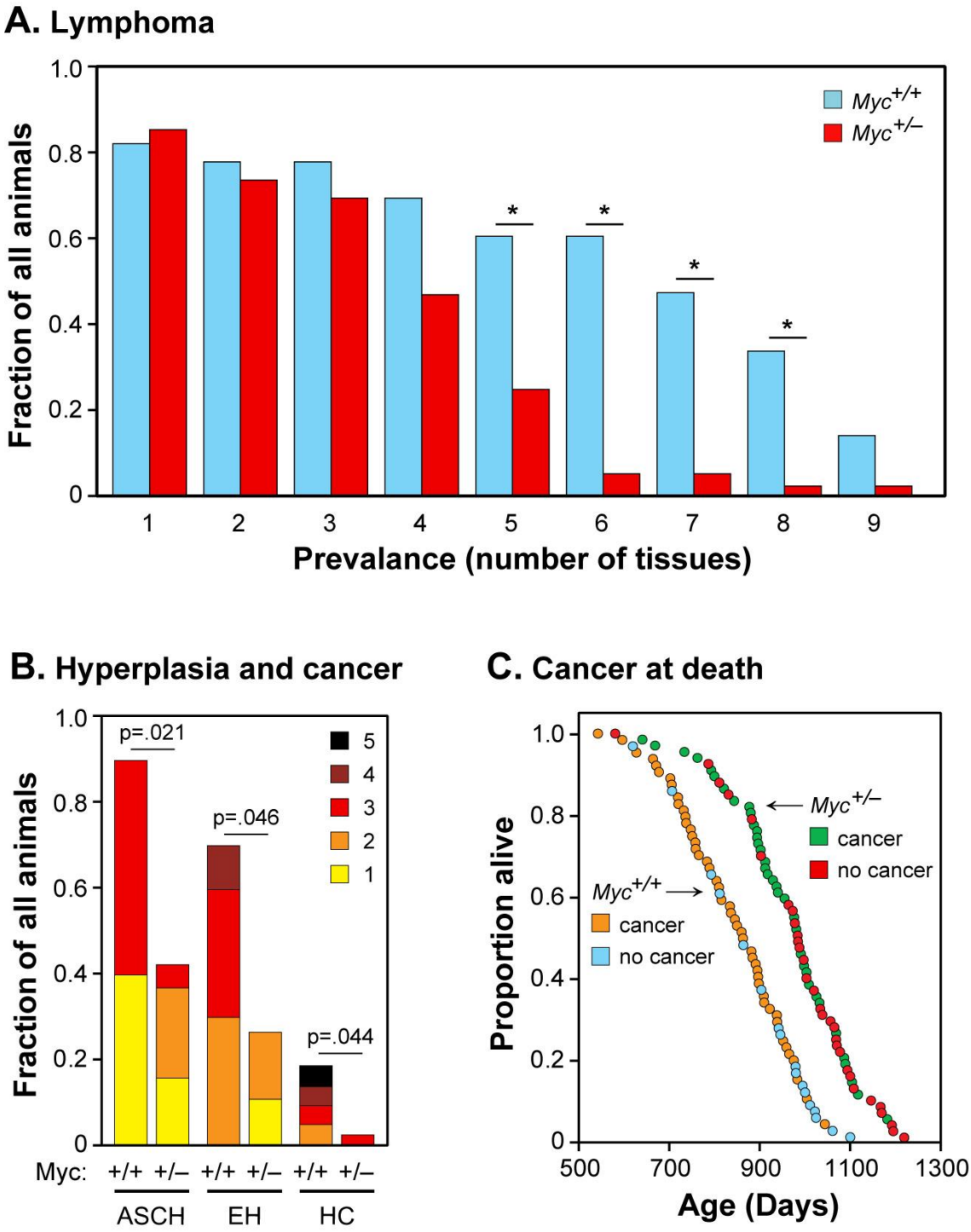
A. Lymphoma
Fraction of all animals
1.0
0.8
0.6
0.4
0.2
0
Myc+/+
Myc+/–
*
*
*
*
1
2
3
4
5
6
7
8
9
Prevalance (number of tissues)
B. Hyperplasia and cancer
Fraction of all animals
p=.021
p=.046
p=.044
5
4
3
2
1
Myc: +/+ +/– +/+ +/– +/+ +/–
ASCH
EH
HC
C. Cancer at death
Proportion alive
Myc+/–
cancer
no cancer
Myc+/+
cancer
no cancer
500
700
900
1100
1300
Age (Days)

Figure 3.5. Cancer is ameliorated in *Myc*$^{+/-}$ mice

(A) The fraction of mice of each genotype that had lymphoma present in the given (or greater) number of tissues. 18 tissues were assessed at the time of death. N=22 for *Myc*$^{+/+}$ and 41 for *Myc*$^{+/-}$ animals. Significance was calculated using Fisher's exact test. Asterisks (*) indicate $p \leq 0.05$.

(B) Prevalence and severity of adrenal subcapsular cell hyperplasia (ASCH, females), endometrial hyperplasia (EH, females), and hepatocellular carcinoma (HC, both sexes) at time of death. Severity is described on a scale of 1 (least) to 5 (greatest). The same histopathological dataset was used in both panels.

(C) Incidence of macroscopic cancer noted at time of autopsy; 73.4% and 53.7% for *Myc*$^{+/+}$ and *Myc*$^{+/-}$ animals, respectively (p=0.03). Each data point represents 1 animal and the presence or absence of cancer is noted by the color code. N=64 *Myc*$^{+/+}$ and 67 *Myc*$^{+/-}$ animals.

Table 3.4. Longevity of cancer resistant animals

Type of examination	Criteria	Increase[1]	P (med)[2]	N *Myc*$^{+/+}$ [3]	N *Myc*$^{+/-}$ [4]
Histological[4]	All in this set	12.28%	0.0001	19	25
	Did not die of lymphoma	16.7%	0.0339	7	6
	Lymphoma in < 5 tissues	11.23%	0.0016	7	21
	All tissues have lymphoma grade ≤ 3	13.35%	0.0001	13	15
	All tissues have lymphoma grade ≤ 2	17.19%	0.0308	6	6
	0 or 1 site with lymphoma grade ≥ 3	14.27%	0.0001	11	18
Macroscopic[5]	All in this set	14.2%	<.0001	64	67
	No gross tumors detected at death	9.6%	0.005	17	31

Table 3.4. Longevity of cancer resistant animals

[1]The increase in lifespan of *Myc*$^{+/-}$ relative to *Myc*$^{+/+}$ mice for sets of mice least likely to have died from cancer.

[2]P value of the median lifespan increase computed using the long-rank test (JMP10 software).

[3]Number of *Myc*$^{+/+}$ and [4]*Myc*$^{+/-}$ animals in the cohort under consideration.

[4]Mice were fixed in formalin upon death, and lymphoma was graded on a scale of 1 (least) to 5 (greatest) in 18 tissues.

[5]All adequately preserved mice were examined by autopsy.

Figure 3.6

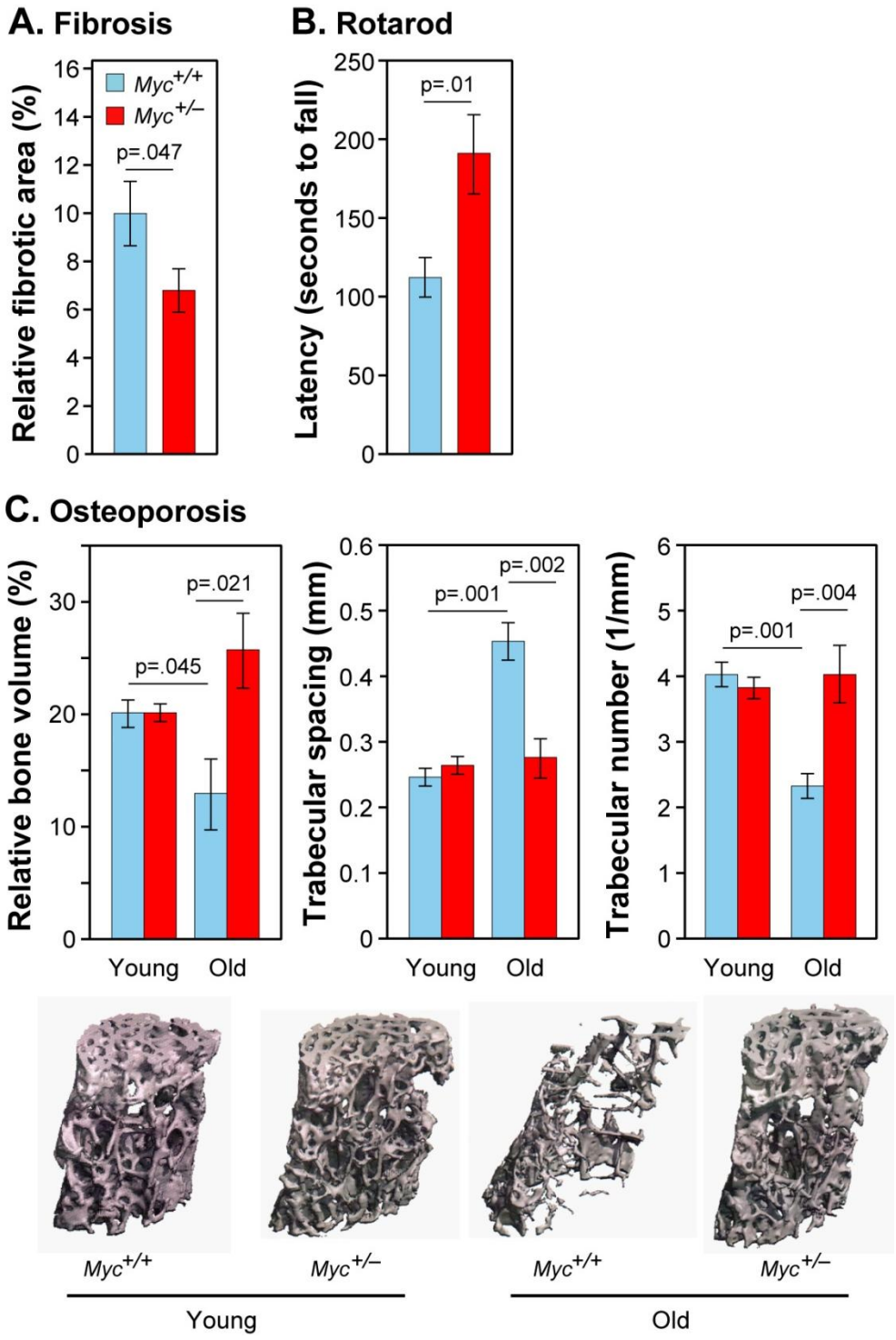
A. Fibrosis
Relative fibrotic area (%)
Myc+/+
Myc+/–
p=.047
B. Rotarod
Latency (seconds to fall)
p=.01
C. Osteoporosis
Relative bone volume (%)
p=.045
p=.021
Trabecular spacing (mm)
p=.001
p=.002
Trabecular number (1/mm)
p=.001
p=.004
Young
Old
Myc+/+
Myc+/–
Young
Old

Figure 3.6. Slower degeneration of the cardiac and musculoskeletal systems in *Myc*$^{+/-}$ mice

(A) Cardiac fibrosis was scored in ventricular cross sections of 22-24 month old mice of both sexes using Masson's trichrome staining. N=11 for *Myc*$^{+/+}$ and 14 for *Myc*$^{+/-}$ animals.

(B) Rotarod performance of 24 month old male *Myc*$^{+/+}$ and *Myc*$^{+/-}$ mice. N=4 for *Myc*$^{+/+}$ and 3 for *Myc*$^{+/-}$ animals. Animals of average weight were chosen for the tests, and their performance was corrected for their weight.

(C) Parameters of bone density for 5 month and 22 month old females were assessed using micro-CT analysis. N=3-7 animals for each group. Representative images are shown from each cohort.

Chapter 4.

Mechanisms of Lifespan Extension in *Myc*$^{+/-}$ Mice

I. Searching for a mechanism

Myc$^{+/-}$ mice live longer than their wild-type littermates, and show reduced effects of aging, including resistance to cancer, osteoporosis, cardiac fibrosis, and deterioration of motor coordination. Since MYC has never before been associated with longevity or any age-related pathology, with the exception of cancer, the mechanistic link between *Myc* expression and these observed effects is unclear and requires investigation. Understanding these mechanisms will provide greater insight into MYC, aging, and age-related diseases, and therefore is applicable to human health. Unfortunately, it is impossible to claim with certainty which effects of *Myc* hypomorphism are causally related to increased longevity and which are merely byproducts. However, studying the normal age-associated changes in these mice may reveal whether each is likely to play a role in the observed longevity increase, and identification of phenotypes not formerly associated with aging may suggest new avenues through which aging occurs.

II. Microarray gene expression analysis points to a novel expression signature and changes in metabolism and the immune system

To begin our investigation of mechanisms through which lifespan is increased in *Myc*$^{+/-}$ mice, microarray expression profiling was performed on liver, skeletal muscle, and white adipose (gonadal) tissues in 5 month and 24 month old animals. A principal component analysis revealed that the first component was tissue, the second age, and the third genotype, representing 61.6%, 30.0%, and 2.9% of the total variability between cohorts, respectively (Figure 4.1A). The relatively small effect of the *Myc*$^{+/-}$ genotype is

notable, accounting for 10-fold fewer expression changes than those attributable to age (see Appendix 1 for the list of genes changing with genotype).

If the increased longevity of *Myc*$^{+/-}$ mice results from a broad attenuation of aging, their transcriptomes would be expected to change less over time across multiple tissues. We thus extracted from our datasets the number of genes, for each genotype and tissue, which are differentially expressed between 5 and 24 months, as well as the average change in expression across all genes with age. While the majority of genes that are differentially expressed between young and old mice were the same for both genotypes, both the number of differentially expressed genes and the average change in expression with age were lower in *Myc*$^{+/-}$ animals for the three tissues examined (Figure 4.1B). This reduction in the apparent aging of the transcriptome suggests that *Myc*$^{+/-}$ mice are long-lived because of widespread changes that increase healthspan rather than a specific disease-mitigating effect. Furthermore, this suggests that the changes observed in the microarray dataset are relevant to the connection between *Myc* and aging.

The software package Ingenuity Pathway Analysis (IPA) was used to identify genetic networks that were enriched for differentially expressed genes. The categories most enriched across all three tissues were generally related to the immune system and metabolism, especially that of lipids (Figure 4.2). We also evaluated which upstream regulators could be responsible for these effects based on the level of expression of their target genes (Table 4.1). When sorted by significance for the effect of genotype in old animals, regulators of lipid metabolism and the immune system were prominently enriched. Transcription factors that regulate lipid biosynthesis and adipogenic fate were predicted to become more active with age in the liver and skeletal muscle, in which

adipogenesis and lipid accumulation are considered pathogenic, and less active with age in adipose tissue. These changes were reversed in old *Myc*$^{+/-}$ tissues: liver showed decreased predicted activity of SREBF1 and SREBF2; adipose showed increased activity of SREBF1, SREBF2, and PPARG; and muscle showed decreased activity of SREBF1, PPARG, and CEBPA. This suggests that the adipocytic infiltration of muscle which normally occurs with age and may contribute to the pathogenesis of sarcopenia (Vettor et al., 2009) could be attenuated in *Myc*$^{+/-}$ mice. The effects of numerous immune system regulators including interferon alpha, beta, and gamma, interleukins 1, 1b, 2, 4, 5, 6, 12a, 12b, 13, 15, 27 and 29, colony stimulating factors 1 and 2, and NF-κB, were almost universally predicted to increase with age in all three tissues. The most interesting genotype effects were in muscle, in which the age-associated changes were predicted to be counteracted in *Myc*$^{+/-}$ mice. As inflammation and lipid metabolism are well known to be involved in the pathologies of aging, these data suggest that *Myc*$^{+/-}$ mice may live longer, at least in part, due to changes in immune and/or metabolic processes.

Xenobiotic metabolism enzymes (XME) are expressed in response to, and subsequently act to remove, ingested or endogenously created toxic metabolites. Expression of many XME genes increases with age and is further elevated in male mice that are long-lived due to genetic, pharmacologic, or dietary interventions; female mice express these genes at an elevated and mostly constant level (Dias et al., 2014; Roy et al., 2014). The XME gene expression signature in male *Myc*$^{+/-}$ mice did not recapitulate well the signatures observed in several known mouse longevity models (Table 4.2). This *in silico* analysis is consistent with the results of stress tests performed in cell culture with tail fibroblasts established from adult *Myc*$^{+/-}$ mice (Figure 4.3), which did not display

increased resistance to any of the stressors previously documented to be counteracted by cells from a variety of long-lived mice or other species. While XME gene expression did increase with age in male *Myc*$^{+/-}$ mice, it increased less than in *Myc*$^{+/+}$ animals, raising the interesting possibility that *Myc*$^{+/-}$ animals may experience less xenobiotic stress as they age. We also note that compared to other longevity models, some of which display very pronounced changes in XME gene expression, the changes in our animals were very modest (Table 4.2).

In a broader meta-analysis, we compared our gene expression datasets with those of other lifespan and healthspan extending interventions: CR and treatments with resveratrol, metformin or rapamycin (Martin-Montalvo et al., 2013; Pearson et al., 2008). While some of these interventions show considerable overlap with one another in differentially expressed genes, for example, CR and metformin (Martin-Montalvo et al., 2013), none were similar to the *Myc*$^{+/-}$ signature (Figure 4.1C, Figure 4.4). A meta-analysis based on Gene Ontology (GO) pathways also failed to indicate substantial overlap (Figure 4.5). As before, CR and metformin showed much greater similarity to each other than either with *Myc*$^{+/-}$. The few universally enriched GO terms, however, further implicated metabolism and inflammation; for example, in muscle the only commonly enriched GO term was *immune response*, while in liver *high density lipoprotein binding* and *hormone activity* were two of only five enriched GO terms. A comparison of differentially expressed genes between *Myc*$^{+/-}$ mice and rapamycin treated mice was made later based on a slightly different algorithm, which used a minimum fold change of 1.5 and a maximum FDR of .3 as thresholds for differential expression. Only 2 genes were commonly upregulated, whereas 219 and 12 genes were upregulated only in

Myc$^{+/-}$ or rapamycin-treated mice, respectively; and 0 genes were commonly downregulated, whereas 154 and 37 genes were downregulated only in *Myc*$^{+/-}$ or rapamycin-treated mice, respectively. These findings suggest that the mechanisms by which *Myc*$^{+/-}$ mice liver longer than their *Myc*$^{+/+}$ counterparts are mostly distinct from the longevity-extending mechanisms of calorie restriction, resveratrol, rapamycin, or metformin, and provide further evidence that the immune system and metabolism are underlying factors.

III. Metabolism in *Myc*$^{+/-}$ mice

Lipid metabolism was identified as one of the main functional categories affected by the *Myc*$^{+/-}$ genotype at the level of transcription in the analysis of microarray data from several different tissues, as described above. Several parameters of metabolism are affected by age in mice, including metabolic rate, ROS production, WAT distribution, adipocytic infiltration of non-adipose tissues, and insulin resistance. As described in chapter 3, *Myc*$^{+/-}$ mice have no difference in WAT quantity, distribution, or function (as determined by serum leptin and adiponectin levels) compared to wild-type mice. To increase the sensitivity of further experiments designed to assess metabolism in these mice, several dietary conditions were used to stress the mice. Normal mouse chow is mostly comprised of carbohydrates to mimic a natural murine diet, and we also fed mice a high fat diet (HFD) or a high fat and cholesterol diet (HFD-C) for 14 weeks, starting at 3 months of age (see table 4.3 for dietary composition).

To investigate the effect of age and diet on lipid metabolism, we assessed hepatic lipid droplets (LDs), which are spherical organelles that are bound by a phospholipid monolayer and primarily contain triglycerides and cholesterol esters. While a single large LD may comprise nearly the entirety of an adipocyte, many smaller LDs are typically present in other cell types, such as hepatocytes. In addition to storing fatty acids and cholesterol (Schaffer 2003), LDs regulate triglyceride metabolism and store proteins in their membranes which counteracts their aggregation (Fujimoto and Parton, 2011). Since LD activities occur predominantly at their surface, total surface area rather than volume is a relevant measure of their functional capacity. For example, individual LD size, but not aggregate volume, has been shown to decrease as a result of endurance exercise (He et al., 2004).

We used the lipid stain Oil Red O to compare liver sections from 5 and 24 month old male mice that were fed a standard diet, and 6 month old mice that were fed a HFD. While total hepatic LD area decreased by about 2-fold in $Myc^{+/+}$ animals with age (Figure 4.6A), average LD size increased by over 3.5-fold (Figure 4.6B). In contrast, total LD content in $Myc^{+/-}$ mice did not change, and LD size increased with age to a lesser extent. The relative preservation of LD surface area with age in $Myc^{+/-}$ animals suggests that it may contribute to their healthy aging. It is also consistent with increased expression of genes involved in LD biogenesis in our expression datasets from $Myc^{+/-}$ liver (*Plin2*, *Cidec*, *Fitm1*). Surprisingly, on the HFD, $Myc^{+/-}$ mice had more total ORO staining and larger lipid droplets than $Myc^{+/+}$, suggesting that they are more sensitive to this diet. The role of MYC in regulating lipid metabolism is not well defined, and there are contradicting reports in the literature. It has previously been documented that MYC can

activate *de novo* palmitate synthesis (Morrish et al., 2010) in fibroblasts, yet others have shown that MYC causes cells to preferentially consume fatty acids rather than glucose (Fan et al., 2010), or that MYC inhibition causes lipids to accumulate in tumor cells (Zirath et al., 2013).

In vivo, hepatic lipid accumulation may also result from phenomena extrinsic to the liver, and in this scenario, the effect of diet on body mass and liver mass may explain why $Myc^{+/-}$ mice have more lipid accumulation on a HFD. Body mass increases substantially when mice are fed a HFD, and this is mostly attributable to increased mass of adipose depots. $Myc^{+/-}$ males gained significantly less weight than $Myc^{+/+}$ on the HFD (Figure 4.7A), suggesting that their adipose depots are not accumulating as much fat as $Myc^{+/+}$. This is consistent with the known roles of MYC in cellular growth and proliferation, since reduced *Myc* expression may limit expansion of adipocytes in response to energy availability. Liver mass increased over the course of the HFD as well, and the increase in $Myc^{+/-}$ was greater in $Myc^{+/+}$, which is consistent with the ORO histology described above. In sum, this suggests that in $Myc^{+/-}$ mice, adipose tissue may have been less able to accommodate such a high quantity of lipids as rapidly as in $Myc^{+/+}$ mice, forcing some lipids to accumulate in the liver instead. Though this may be considered a drawback of the $Myc^{+/-}$ genotype, it would be unlikely to affect mice in their natural environment where they consume very low fat diets.

Another important healthspan parameter of lipid metabolism is cholesterol. Cholesterol levels in mouse liver increase with age (Bose et al., 2005), and some interventions that promote longevity, such as CR, result in decreased cholesterol synthesis (Tsuchiya et al., 2004). In our microarray datasets the expression of cholesterol

biosynthetic genes increased with age in *Myc*$^{+/+}$ mice. In contrast, almost all genes in this pathway showed lower expression in *Myc*$^{+/-}$ animals, which we confirmed by qRT-PCR (Figure 4.8A); this included the rate limiting enzyme, HMG-CoA reductase, and the master transcriptional regulator of the genes in this pathway, SREBF2. Furthermore, the amount of both esterified and non-esterified cholesterol was lower in *Myc*$^{+/-}$ liver, where cholesterol is synthesized and stored, and in serum, where its overabundance causes vascular and tissue damage (Figure 4.8B). Also *Apoa4* (Duverger et al., 1996) and *Lipc* (Annema and Tietge, 2011), showed higher expression in old *Myc*$^{+/-}$ liver, implying that *Myc*$^{+/-}$ mice may be better at clearing harmful lipids from the circulation. Although C57BL/6 mice do not develop atherosclerosis on a normal diet, high cholesterol is pathogenic in several aging related diseases in mice, including Alzheimer's disease (Puglielli et al., 2001), impaired immune function (Rivnay et al., 1979), and diabetes (Ishikawa et al., 2008), suggesting that reduced cholesterol could be involved in the increased longevity of *Myc*$^{+/-}$ mice. One of the goals of the HFD-C diet experiment was to assess atherosclerosis in these mice, but unfortunately none of the mice developed an appreciable amount of atherosclerosis during the 14-week dietary treatment. This may be worth repeating in the future using *Myc*$^{+/-}$ mice that are also knocked out for apolipoprotein E (ApoE) or the low-density lipoprotein receptor (LDLR). Those mouse models are both highly prone to atherosclerotic lesions, which may be ameliorated by the cholesterol-lowering effects of *Myc* hypomorphism.

Metabolic rate, as measured by O_2 consumption and CO_2 production, declines during normal aging, and is increased by CR and in the long lived Ames and GHR-KO dwarf mice (Bartke and Westbrook, 2012). Interestingly, old *Myc*$^{+/-}$ mice were found to

have a significantly higher metabolic rate than *Myc*$^{+/+}$ animals (Figure 4.9). Young *Myc*$^{+/-}$ mice showed a trend in the same direction, which however was not statistically significant. The respiratory quotient, which is the ratio of CO_2 eliminated to O_2 consumed, was not affected by genotype, which suggests that there is no difference in the ratio of carbohydrates to fatty acids used to generate ATP. Old *Myc*$^{+/-}$ animals also had higher water consumption and a trend towards higher food consumption (Figure 4.10A,B). Animals of both genotypes had equivalent body temperatures (Figure 4.10C), suggesting that the higher metabolic rate of *Myc*$^{+/-}$ mice may be used to thermoregulate their smaller body mass (which would be expected to predispose to hypothermia). The increase in metabolic rate was accompanied by a small but significant increase in mitochondrial copy number in skeletal muscle of old animals (Figure 4.11); no change was observed in liver. The preservation of metabolic rate into old age combined with the increased mitochondrial copy number in *Myc*$^{+/-}$ mice may reflect increased fatty acid oxidation, which in turn may reduce lipid accumulation in tissues such as the liver and skeletal muscle. Thus, these results may contribute to increased longevity by maintaining tissue health and function in old age.

Insulin sensitivity declines with age in laboratory mice, and several long-lived mouse models have been shown to maintain insulin sensitivity into old age better than their controls (see Chapter 1). This improved insulin sensitivity is presumed to promote health and longevity in these mice. We assessed both insulin sensitivity and glucose tolerance in young and old mice, and in all three dietary conditions described above. In these experiments, either insulin or glucose was administered by intraperitoneal injection, and glucose levels were then measured in blood acquired from the tail over several time

intervals. There was no significant effect of either age or genotype on baseline blood glucose levels or on glucose tolerance on a standard diet (Figure 4.12A,B). This suggests that neither insulin sensitivity nor blood glucose levels contribute to increased longevity in *Myc*$^{+/-}$ mice.

Both the high fat and high fat with cholesterol diets impair glucose tolerance and increase baseline glucose levels, and after 14 weeks on either diet, *Myc*$^{+/-}$ mice respond differently than *Myc*$^{+/+}$ to glucose or insulin administration. Glucose tolerance is improved (i.e. faster return to baseline) in *Myc*$^{+/-}$ males relative to *Myc*$^{+/+}$ after the HFD-C diet, although females on the same diet and both sexes on the HFD exhibited no genotype effects (Figure 4.12C, D). Surprisingly, *Myc*$^{+/-}$ females and males are less sensitive to insulin after either diet relative to *Myc*$^{+/+}$ (Figure 4.12E, F), which is opposite from the increased insulin sensitivity observed in many other long-lived mouse models. It also seemingly contradicts the improved glucose tolerance in HFD-C males, which suggested a greater response to insulin. While the causes and effects of reduced insulin sensitivity in *Myc*$^{+/-}$ mice remain unclear, these experiments demonstrate that increased insulin sensitivity does not contribute to greater longevity in *Myc*$^{+/-}$ mice, nor is improved insulin sensitivity required to extend lifespan in mice.

A final metabolic parameter that we measured was β-hydroxybutyrate concentration in serum. β-hydroxybutyrate is a ketone body produced in the mitochondria and secreted from the liver in response to hypoglycemia. It can be used as an energy source in other tissues, particularly the brain, during a period of fasting or nutrient deprivation. A recent report has shown that β-hydroxybutyrate concentration in serum is increased in several long-lived mouse models, including CR and Ames dwarf

mice (Wijeyesekera et al., 2012). Furthermore, there is evidence that a ketogenic diet, which promotes energy transport via ketone bodies rather than more conventional molecules such as glucose, has a neuroprotective effect during aging (Balietti et al., 2010). Since β-hydroxybutyrate levels increase dramatically in response to fasting, we measured its concentration in serum from young and old mice of each genotype after either a 0 hour, 7 hour, or 24 hour fast (Figure 4.13). Interestingly, β-hydroxybutyrate levels were greater in old than young $Myc^{+/+}$ mice after a 7 hour fast, and there was a nonsignificant trend in the same direction after a 24 hour fast, suggesting that the substrate preference of older animals may be shifted in favor of ketogenesis. However, there was no significant difference between $Myc^{+/-}$ and $Myc^{+/+}$ mice at either age after any duration of fasting. Therefore, this is unlikely to play a role in healthspan or longevity of $Myc^{+/-}$ mice.

IV. The immune system is protected from aging in *Myc*$^{+/-}$ mice

Myc hypomorphism may increase healthspan by attenuating immunosenescence, which results, in part, from thymic involution as well as senescence of some T cell populations (Akbar and Henson, 2011). Since few T cells are produced by the thymus in older animals, the T cell pool is maintained by the expansion of existing memory T cells, which is greater for cytotoxic CD8+ than regulatory CD4+ T cells (Goronzy and Weyand, 2005). Naïve T cells do not proliferate. This results in a lower ratio of naïve to memory T cells, a lower ratio of CD4+ to CD8+ T cells, and fewer total T cells in old

animals. We used flow cytometry to quantify the proportions of different T cell subsets in the peripheral circulation of our mice.

As previously reported, the ratios of both CD4+ to CD8+ T cells and of naïve to memory T cells declined with age in normal ($Myc^{+/+}$) mice, but both were unaffected by age in $Myc^{+/-}$ animals (Figure 4.14B, C). We found no effect of genotype on total T cell levels (Figure 4.14A), however this should be interpreted as no change in T cell count relative to all lymphocytes, since these flow cytometry data were analyzed after filtering for cells that were included within a lymphocyte gate. If normalized instead to blood volume or all blood cells, it is possible that total T cells may also differ between genotypes. These results indicate that aging $Myc^{+/-}$ animals can maintain phenotypically younger and presumably healthier proportions of T cell populations, and hence a more functional adaptive immune system. It has previously been shown that T cell proliferation in response to activation *in vitro* is positively correlated with MYC expression (Trumpp et al., 2001), suggesting that the increased ratio of naïve to memory T cells may be caused by decreased proliferation of memory T cells.

To investigate the mechanism by which T cell proportions are affected in $Myc^{+/-}$ mice, we next examined age related changes in the bone marrow and thymus where T cells develop and mature. In C57BL/6 mice the thymus begins to involute at 10 months of age and very little tissue remains by 20 months. We assessed 16 month old animals and found that neither the loss of mass with age, adiposity, or proportion of senescent cells in the thymus was affected by genotype (Figure 4.15). Hence, the changes in T cell subsets are unlikely to be caused by differential thymic involution. Hematopoietic stem cells (HSC) in the bone marrow are comprised of several subpopulations: long term

HSCs (LT-HSC) differentiate into short term HSCs (ST-HSC), which can then differentiate into either common myeloid progenitors (CMP) or common lymphoid progenitors (CLP), the latter of which give rise to T cells and other lymphocytes. With normal aging, the CLP/CMP ratio decreases by about 3-fold (Cho et al., 2008). Flow cytometry of HSCs showed that 16 month old $Myc^{+/-}$ mice had a higher CLP/CMP ratio relative to $Myc^{+/+}$ animals (Figure 4.14D,E). This is further evidence for decelerated aging of the hematopoietic system, and may be responsible for the observed changes in T cell proportions (Guo et al., 2009). Consistent with this, we found that $Myc^{+/-}$ mice have a lower ratio of ST-HSC to LT-HSC (Figure 4.14F), suggesting that LT-HSC can persist in greater numbers and/or functional capacity into old age.

Sterile inflammation, which is a baseline level of inflammation in the absence of infection, is a multi-systemic contributor to age-related pathology. As described above, genes and genetic pathways related to inflammation were identified as differentially regulated between $Myc^{+/-}$ and $Myc^{+/+}$ mice in our microarray data. The cytokines CRP, TNFa, CXCL10, CCL21c, KC, MCP1, MCP5, MMP9, TGF1B, IFNγ, IL1a, IL1Ra, IL4, IL6, IL12, GCSF, and MCSF were measured in serum, liver, and skeletal muscle to determine whether and how inflammation was affected in these mice. These cytokines were selected because of their known roles in inflammation and because of their differential expression in the microarray data. Two different types of assays were conducted: serum samples from old mice were sent to Aushon BioSystems, Inc, for multiplex cytokine analysis, and serum, skeletal muscle, and liver samples from a separate group of both young and old mice were analyzed in-house using the Milliplex magnetic bead multiplex assay (Millipore).

In both skeletal muscle and liver, the concentration of several cytokines was greater in old relative to young animals, which is consistent with the known increase in inflammation with age. However, analysis of serum using either the Aushon or Milliplex approach revealed no significant differences between the two genotypes in any of the cytokines measured (Figure 4.16). We also investigated macrophages, which orchestrate inflammation within tissues, by using immunofluorescence with an antibody to the macrophage surface marker F4-80 in both liver and adipose tissues in old mice. There was no difference in macrophage prevalence between the two genotypes (Figure 4.17A, C). Furthermore, we measured the total white blood cell counts in blood from old females, and again found no difference between genotypes (Figure 4.17B). In summary, these results suggest that amelioration of inflammation is not a major contributor to increased lifespan in *Myc*$^{+/-}$ mice. However, given the strong inflammatory signature in our microarrays, it is possible that parts of inflammatory pathways that we did not yet measure, such as NF-κB signaling or the relative prevalence of different macrophage subtypes, may be affected in *Myc*$^{+/-}$ mice.

V. *Myc*$^{+/-}$ mice do not show changes in pathways linked with macromolecular damage

A commonly invoked cause of aging is the accumulation of damage to macromolecules, particularly from oxidative stress. Genotoxic stress, manifested as various forms of DNA damage, increases dramatically with age (Hoeijmakers 2009). We examined the frequency of DNA damage foci, a commonly used measure of DNA

double-strand breaks, and while we saw clear evidence of the previously reported age-associated increase (Berlett and Stadtman, 1997), the *Myc* genotype had no effect (Figure 4.18A). Genotoxic stress and other forms of damage can lead to apoptosis, which has been found to rise with age in several tissues (Chao et al., 1997). While we observed an increase in the prevalence of apoptotic cells with age, the changes were equivalent in $Myc^{+/+}$ and $Myc^{+/-}$ animals (Figure 4.18B). Genotoxic stress is also a major trigger of cellular senescence, which is increasingly believed to have important links with aging (Hamilton et al., 2001). As with apoptosis, however, the *Myc* genotype did not affect the age-associated increase in cellular senescence (Figure 4.19).

The cyclin-dependent kinase inhibitors p21 (*Cdkn1a*) and p16 (*Cdkn2a*) are important regulators of senescence. p21 is a downstream effector in the p53 pathway, and is strongly upregulated by DNA damage and stresses such as reactive oxygen species (ROS). p16 is a regulator of the pRb pathway, and in contrast to p21 it does not respond rapidly to these stimuli. Both p21 and p16 were upregulated with aging (Figure 4.20). The expression of p21 was unaffected by the *Myc* genotype, whereas the expression of p16 was significantly lower in $Myc^{+/-}$ animals at both ages (although p16 is often used as a marker of cellular senescence, its regulation is not well understood, and likely affected in other contexts). F_2-isoprostanes, products of lipid peroxidation, are a sensitive and accurate biomarker of oxidative status. As expected, we found that levels of F_2-isoprostanes rose with age, but the changes were the same in $Myc^{+/+}$ and $Myc^{+/-}$ animals (Figure 4.21). Hence, $Myc^{+/-}$ animals do not seem to be protected from age-associated increases in ROS, or from the consequences of this and other forms of stress, such as DNA damage, apoptosis and senescence.

Figure 4.1

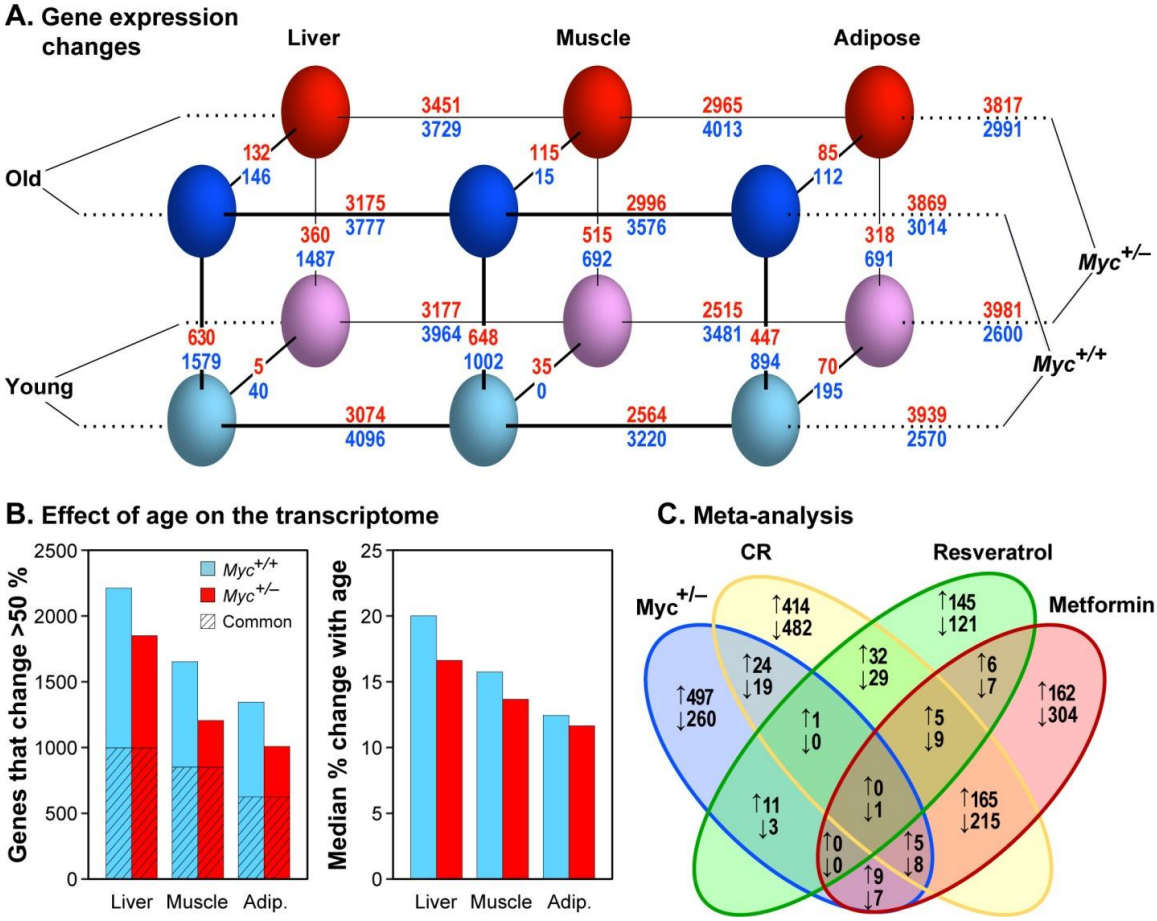
A. Gene expression changes
Liver
Muscle
Adipose
Old
Young
Myc+/–
Myc+/+
3451
3729
2965
4013
3817
2991
132
146
115
15
85
112
3175
3777
2996
3576
3869
3014
360
1487
515
692
318
691
3177
3964
2515
3481
3981
2600
630
1579
5
40
648
1002
35
0
447
894
70
195
3074
4096
2564
3220
3939
2570
B. Effect of age on the transcriptome
Genes that change >50 %
Myc+/+
Myc+/–
Common
Liver Muscle Adip.
Median % change with age
Liver Muscle Adip.
C. Meta-analysis
CR
Resveratrol
Myc+/–
Metformin
↑414 ↓482
↑145 ↓121
↑497 ↓260
↑24 ↓19
↑32 ↓29
↑6 ↓7
↑162 ↓304
↑1 ↓0
↑5 ↓9
↑0 ↓1
↑11 ↓3
↑165 ↓215
↑0 ↓0
↑5 ↓8
↑9 ↓7

Figure 4.1. Gene expression changes in *Myc*$^{+/-}$ mice

(A) Schematic representation of all observed gene expression changes. Three parameters were compared (in various combinations): genotype (*Myc*$^{+/+}$, *Myc*$^{+/-}$), age (5 months, 24 months) and tissue (liver, skeletal muscle, white adipose). Genotype, age, and tissue comparisons are connected with diagonal, vertical and horizontal lines, respectively. The number of genes changing expression is shown above and below each line. Red numbers designate genes upregulated in *Myc*$^{+/+}$ *versus Myc*$^{+/-}$ animals (*i.e.* MYC activated genes), while blue numbers represent genes upregulated in *Myc*$^{+/-}$ *versus Myc*$^{+/+}$ animals (*i.e.* MYC repressed genes). A 1.5-fold cutoff and a FDR threshold of <5% were used to calculate the number of genes changing expression. N=5-8 male animals in each group.

(B) Effect of age on the transcriptome. Left panel: the number of genes whose expression changes with age by more than 50% (in either direction); right panel: the median change in expression with age (expressed as %) across all expressed genes (the reciprocal was used for genes whose expression decreased with age). The hatched area (left panel) represents common differentially expressed genes between the two genotypes.

(C) Meta-analysis of gene expression changes in different longevity models. Differentially expressed genes in our datasets (*Myc*$^{+/-}$ *versus Myc*$^{+/+}$ animals) were compared with genes similarly recovered in studies of calorie restriction (*versus* ad libitum feeding), and metformin or resveratrol feeding (*versus* untreated controls) (Martin-Montalvo et al., 2013; Pearson et al., 2008). Upward arrows indicate genes upregulated in the long-lived condition (and conversely for the downward arrows). In all cases genes differentially expressed in liver of old male mice were compared. A

comparison of skeletal muscle data showed the same trends; data for adipose were not reported by the other groups. The significant overlap between calorie restriction and metformin treatments has been previously reported (Martin-Montalvo et al., 2013). For additional clarity, Venn diagrams of pairwise comparisons are shown in Figure 4.4.

Figure 4.2

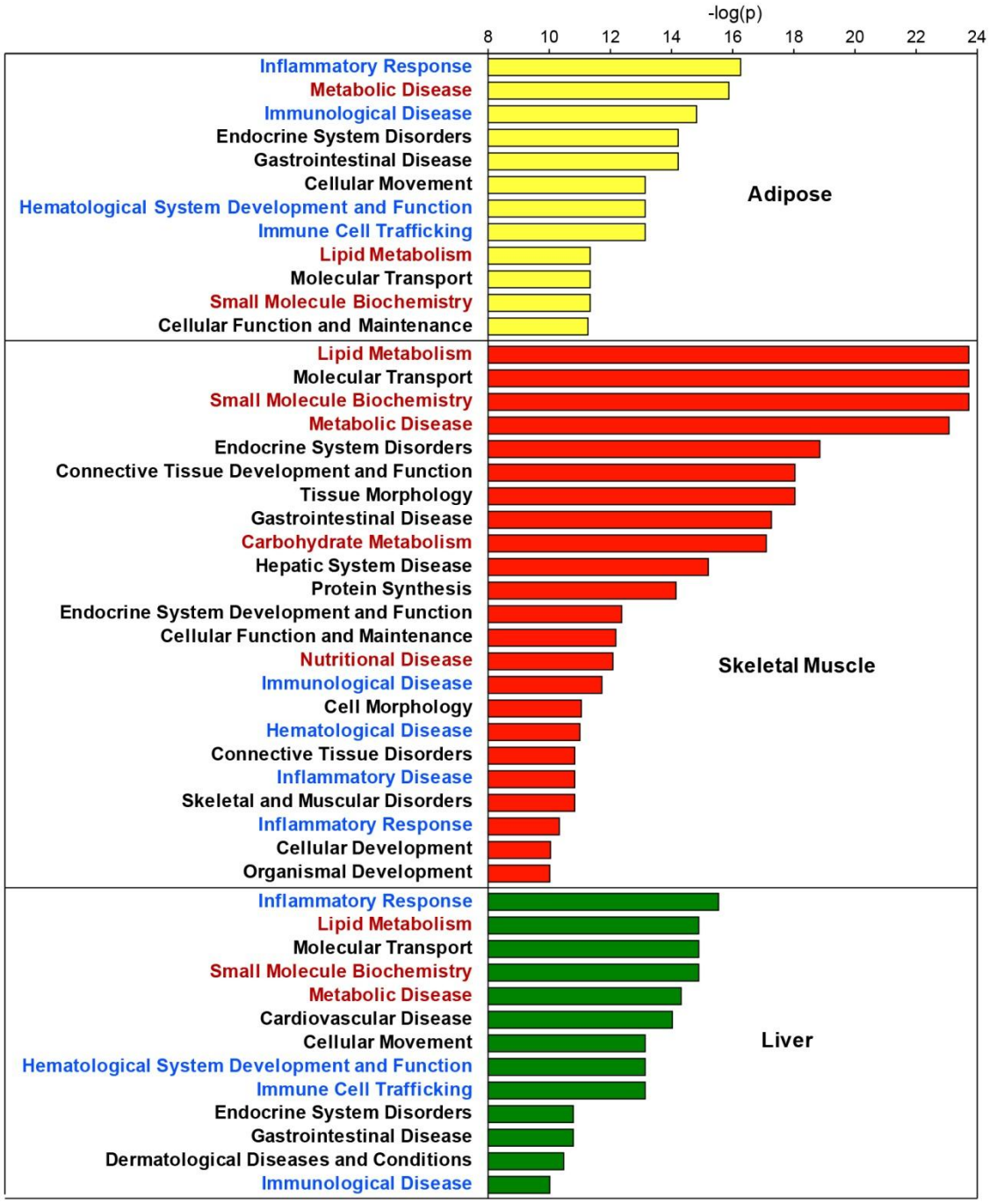
-log(p)
8
10
12
14
16
18
20
22
24
Inflammatory Response
Metabolic Disease
Immunological Disease
Endocrine System Disorders
Gastrointestinal Disease
Cellular Movement
Hematological System Development and Function
Immune Cell Trafficking
Lipid Metabolism
Molecular Transport
Small Molecule Biochemistry
Cellular Function and Maintenance
Adipose
Lipid Metabolism
Molecular Transport
Small Molecule Biochemistry
Metabolic Disease
Endocrine System Disorders
Connective Tissue Development and Function
Tissue Morphology
Gastrointestinal Disease
Carbohydrate Metabolism
Hepatic System Disease
Protein Synthesis
Endocrine System Development and Function
Cellular Function and Maintenance
Nutritional Disease
Immunological Disease
Cell Morphology
Hematological Disease
Connective Tissue Disorders
Inflammatory Disease
Skeletal and Muscular Disorders
Inflammatory Response
Cellular Development
Organismal Development
Skeletal Muscle
Inflammatory Response
Lipid Metabolism
Molecular Transport
Small Molecule Biochemistry
Metabolic Disease
Cardiovascular Disease
Cellular Movement
Hematological System Development and Function
Immune Cell Trafficking
Endocrine System Disorders
Gastrointestinal Disease
Dermatological Diseases and Conditions
Immunological Disease
Liver

Figure 4.2. Pathway level analysis of gene expression changes in *Myc*$^{+/-}$ mice

Functional categories that were significantly enriched for differentially expressed genes in old (24 months) animals between *Myc*$^{+/-}$ and *Myc*$^{+/+}$ genotypes were determined using IPA (Ingenuity) software. For each tissue the IPA categories are listed in order of significance (-log of the p value). A significance threshold was calculated for each tissue as 2 standard deviations below the mean of 4 minimum p values from random sets of the same number of genes subjected to the same analysis. Categories labeled in blue are related to the immune system, and categories in red are related to metabolism.

Table 4.1. Upstream regulators implicated by analysis of microarray data[1]

Upstream Regulator	Liver				Adipose				Skeletal Muscle			
	ΔGenotype[2]		ΔAge[3]		ΔGenotype[2]		ΔAge[3]		ΔGenotype[2]		ΔAge[3]	
	Young	Old	+/+	+/–	Young	Old	+/+	+/–	Young	Old	+/+	+/–
SREBF1	3.0	-2.9	1.0	0.0	3.4	3.6	-2.8	-2.2	0.0	-2.9	3.8	3.5
PPARG	3.3	1.1	-1.9	0.0	-1.1	3.0	-3.9	-2.3	0.0	-4.6	3.2	3.3
SREBF2	1.9	-3.3	1.1	0.0	2.6	2.9	-3.1	-2.1	0.0	-1.9	4.4	3.7
SCAP	2.1	-2.5	0.5	0.0	1.8	3.0	-3.2	-2.1	0.0	-2.2	4.1	3.1
INSIG1	-2.8	2.3	-3.7	-5.0	-4.1	-1.9	-0.5	-1.6	0.0	3.4	-5.7	-2.9
Tretinoin	2.5	2.0	5.1	6.6	3.5	-0.9	4.3	4.9	0.0	-4.3	3.0	0.8
INSIG2	0.0	2.6	0.7	0.0	-1.0	-2.2	2.2	0.7	0.0	2.2	-2.3	-1.9
THRB	1.7	-1.7	-0.1	0.0	-1.3	2.8	-1.8	-0.2	0.0	-2.2	0.7	0.0
PPARA	2.3	3.9	-1.2	2.4	-0.4	-0.4	-2.5	-1.2	0.2	-2.4	2.1	2.5
IL5	1.1	-1.4	6.0	4.8	3.5	2.0	3.3	2.4	0.0	-2.9	2.7	1.3
OSM	1.9	-2.4	5.8	4.4	3.7	2.8	3.0	1.3	-1.4	0.8	1.1	0.5
CSF2	1.4	0.2	8.3	7.7	5.2	-2.8	7.6	3.8	0.0	-2.9	4.6	1.9
MITF	0.0	2.4	2.2	0.0	0.9	-1.5	2.1	1.0	0.0	-1.9	2.6	1.8
NR1H3	0.0	-2.5	-0.5	0.0	-0.3	1.2	-0.5	-0.2	0.0	-2.0	1.9	1.5
Arachidonic acid	-1.1	2.1	2.2	0.8	0.2	-1.3	1.0	0.7	0.0	2.2	-1.3	-0.6
LDL	2.0	1.6	3.5	4.2	3.6	-1.4	3.2	1.0	0.0	-2.5	2.7	1.9
MAPK9	0.9	0.5	0.0	1.4	-0.1	2.4	0.1	0.8	0.0	-2.6	1.0	0.8
TGM2	0.0	1.9	5.3	5.6	4.4	0.7	5.5	4.0	0.0	-2.8	5.0	2.3
CD44	1.1	1.7	3.7	4.0	1.9	-2.4	4.5	1.5	0.0	-1.3	1.3	0.0
L-glutamic acid	2.4	0.9	2.6	0.0	1.7	1.8	-0.5	-0.4	0.0	-2.6	1.8	1.5
FGF21	0.0	-0.9	-0.2	0.0	0.0	1.7	-0.5	0.4	0.0	-2.6	1.0	0.7
ESR1	0.4	0.5	1.8	2.7	1.4	-2.2	0.2	-1.0	0.0	-2.6	0.2	0.0
EGR1	2.0	1.4	3.0	3.4	2.3	2.4	1.7	0.0	0.0	-1.4	0.4	-1.2
AICAR	0.8	1.5	-0.6	0.0	-1.7	-2.6	-0.1	-0.6	0.0	-1.1	0.0	0.0
ARNT2	0.0	2.7	0.0	0.0	2.9	0.0	2.7	2.7	0.0	-2.4	2.2	2.6
SIM1	0.0	2.7	0.0	0.0	3.1	0.0	2.8	3.0	0.0	-2.4	1.9	2.5
ATP7B	1.0	-2.7	-1.2	0.0	1.0	2.4	-3.0	-0.9	0.0	0.0	3.3	2.7
RAF1	1.2	2.6	2.2	4.0	2.2	0.5	1.0	0.3	0.0	-2.0	0.8	-1.2
HRG	0.0	2.4	3.6	3.4	1.9	-2.6	2.5	1.3	0.0	0.0	0.3	-2.1
IGF1	2.0	-1.9	2.1	0.0	2.9	0.7	1.5	-0.5	0.0	-2.5	-0.4	-0.9
IL4	1.2	2.0	4.7	4.8	4.0	0.5	3.6	0.1	0.0	-2.5	3.9	1.2
VEGFA	0.0	2.1	1.9	1.9	1.7	0.3	1.3	0.8	0.0	-2.6	-0.7	-2.5
Sterol	0.0	2.4	0.0	0.0	-1.2	-1.9	2.9	1.0	0.0	0.6	-1.5	0.0
CSF1	0.0	0.9	5.6	5.3	4.2	-1.6	4.0	1.9	0.0	-2.4	2.9	0.8
F2	2.6	1.3	5.4	0.0	3.4	1.3	4.2	1.5	0.0	-2.1	0.0	-1.3
HOXA10	-1.3	-1.4	-0.3	0.0	-0.1	0.4	-1.3	-2.2	0.0	3.0	-2.8	-1.0
MED13	-2.6	0.0	1.4	0.0	0.0	-2.2	3.2	1.3	0.0	2.5	-3.5	-2.3
Cholesterol	0.8	1.2	2.8	3.5	1.6	-3.3	3.1	2.1	0.0	0.2	0.3	-1.0
PPARGC1B	0.0	-2.7	0.7	0.0	0.9	0.0	-1.5	-0.1	0.0	-2.0	1.9	2.5
NR1I2	3.5	-1.0	2.2	0.0	-0.3	1.1	-3.1	-1.1	2.0	-2.6	2.5	0.0
CDKN1A	0.0	-1.9	-0.4	-1.5	-0.1	2.7	-1.9	0.0	0.0	0.0	0.0	0.0
PDGF BB	2.6	-1.0	4.2	0.0	4.6	-0.9	5.1	1.5	0.0	-2.7	0.2	-0.7
IL22	0.0	-2.9	3.7	2.9	1.7	-1.6	2.8	0.4	0.0	0.0	0.0	0.0
MAP2K1	0.0	0.7	4.0	0.0	2.9	-1.5	3.0	0.4	0.0	-2.4	1.3	0.0
MAP4K4	-2.6	0.0	1.5	0.0	1.5	-2.0	6.9	4.8	0.0	2.6	-0.5	-1.8
P38 MAPK	2.6	1.8	4.3	4.8	3.7	-0.8	5.1	1.8	0.0	-2.0	0.1	-0.8
IFNAR1	0.0	2.1	1.9	3.6	1.2	-0.4	4.0	3.9	0.0	-2.0	2.2	0.0
ANGPT2	2.0	0.7	2.7	0.0	2.6	2.4	0.3	-0.4	0.0	-1.4	0.1	-1.5
POR	-2.2	1.4	-2.5	-3.1	-2.6	-3.0	0.8	0.9	0.0	0.1	-2.9	-1.4
CFTR	-1.1	2.9	-2.0	0.0	-1.3	-0.4	-2.2	-0.8	0.0	-1.1	-0.1	0.0

Table 4.1. Upstream regulators implicated by analysis of microarray data

[1]IPA (Ingenuity) software was used to analyze microarray expression data sets to predict upstream regulators. All the values shown are z-scores generated by the software. Values greater than 2 or less than -2 are considered meaningful. Rows were sorted by the sum of absolute values of z-scores for the genotype effect in old (24 month old) mice, and the first 50 upstream regulators are shown For the complete table of all upstream regulators for which there is a meaningful difference between genotypes in at least one tissue, see Appendix 2.

[2]Changes due to genotype (ΔGenotype columns). Red shading indicates a stronger effect in $Myc^{+/-}$ *versus* $Myc^{+/+}$ animals (*i.e.* effectors/regulators whose influence is more pronounced in $Myc^{+/-}$ tissues). Conversely, blue shading indicates a stronger effect in $Myc^{+/+}$ *versus* $Myc^{+/-}$ animals (*i.e.* effectors/regulators whose influence is more pronounced in $Myc^{+/+}$ tissues). The intensity of the shading illustrates the relative magnitude of the effect.

[3]Changes due to age (ΔAge columns). Red shading indicates a stronger effect in old (24 month old) relative to young (5 month old) animals (*i.e.* effectors/regulators whose influence is more pronounced in old tissues). Conversely, blue shading indicates a stronger effect in young *versus* old animals (*i.e.* effectors/regulators whose influence is more pronounced in young tissues). The intensity of the shading illustrates the relative magnitude of the effect.

Table 4.2. Expression patterns of xenobiotic metabolism genes in long-lived mice[1]

Gene expression values[2]

Gene	CR[3]	CL[4]	Rapa[5]	tBHQ[6]	CA[7]	Little[8]	Snell[9]	GHRKO[10]	ΔGenotype[11] Young[12]	ΔGenotype[11] Old[13]	ΔAge[11] +/+[14]	ΔAge[11] +/–[15]
Cyp1a1	2.9	1.9	2.4	2.4	-	1.7	1.4	1.2	1.0	1.1	0.7	0.8
Cyp1a2	1.4	1.6	0.9	1.7	-	1.1	1.4	0.9	0.9	1.1	0.9	1.1
Cyp2a4	9	1.8	1.2	2.9	5.1	3.4	6.8	3.5	0.9	1.3	0.8	1.1
Cyp2a5	9.4	1.8	1.2	3.5	-	-	-	-	0.9	1.4	0.9	1.3
Cyp2b10	6	2.1	0.7	12	4.4	21	2	8.8	1.6	1.0	1.4	0.9
Cyp2b13	368	2.6	6.4	9	32	7715	205	201	1.4	0.3	6.0	1.1
Cyp2b9	276	4.7	12	57	473	4127	16	61	1.6	0.5	5.8	1.8
Cyp2c37	1.6	0.5	0.9	3.6	-	2.6	5.7	0.8	0.9	1.1	1.4	1.6
Cyp2c38	1.6	1.4	1.5	1.9	0.9	2	2.7	2.2	1.8	1.0	2.8	1.6
Cyp3a11	0.6	0.8	1.8	1.9	-	1	1.1	0.9	1.0	1.0	1.1	1.1
Cyp3a41	1.8	1.4	1.5	1.5	-	-	-	0.7	1.0	0.5	2.4	1.2
Cyp4a10	4.6	3	3	3.9	5.1	6.8	11	3.1	1.2	1.4	1.3	1.6
Cyp4a14	210	24	44	43	72	26	20	24	1.5	2.3	1.5	2.2
Fmo3	379	5.7	4	14	124	128	314	11	0.9	0.4	5.1	2.2
Fmo4	3.3	1.9	1.4	1.6	3.4	3	1.8	1.9	1.2	0.7	2.0	1.3
Hao2	9.1	3.6	4.7	3.5	-	-	11	17	1.1	1.2	1.2	1.3
Mt1	4.9	2.3	0.8	11	7.5	4.4	25	36	2.3	0.4	3.7	0.7
Mt2	1.9	1.8	0.6	30	-	-	29	51	2.2	0.6	3.1	0.9
Por	5.8	1.5	1.8	1.1	4	2.4	1.1	1.4	0.9	1.0	1.0	1.1
Geomean[16]	8.4	2.2	2.1	5.1	12.7	12.0	7.8	5.6	1.2	0.9	1.8	1.2

Correlation coefficients[17]

ΔGenotype	CR	CL	Rapa	tBHQ	CA	Little	Snell	GHRKO	ΔGenotype Young	ΔGenotype Old	ΔAge +/+	ΔAge +/–
Young	0.073	0.325	-0.06	0.514	0.009	0.382	0.442	0.624		-0.253	0.605	-0.042
Old	-0.138	-0.04	0.026	-0.118	-0.296	-0.375	-0.368	-0.316	-0.253		-0.763	0.163

P values[18]

ΔGenotype	CR	CL	Rapa	tBHQ	CA	Little	Snell	GHRKO	ΔGenotype Young	ΔGenotype Old	ΔAge +/+	ΔAge +/–
Young	0.76	0.174	0.802	0.024	0.978	0.16	0.075	0.005		0.296	0.006	0.8641
Old	0.573	0.869	0.914	0.631	0.376	0.168	0.145	0.201	0.296		0.0001	0.5045

Table 4.2. Expression patterns of xenobiotic metabolism genes in long-lived mice

[1]Data in columns 3-10 were taken from (Steinbaugh et al., 2012), and in columns 12-15 from our microarray datasets.

[2]Fold-change in the expression of the listed xenobiotic metabolism genes, in the liver of several strains of long-lived mice, or mice subjected to the indicated treatments.

[3]CR, calorie restricted.

[4]CL, crowded litter.

[5]Rapa, rapamycin treated.

[6]tBHQ, *tert*butylhydroquinone treated.

[7]CA, cholic acid treated.

[8]Little, mice mutated in the growth hormone releasing hormone receptor (also known as "little" mice).

[9]Snell dwarf mice.

[10]GHRKO, growth hormone receptor knockout mice.

[11]Red and blue shading is used to highlight changes of 1.5-fold (or greater) in our datasets: red, increased expression; blue, decreased expression.

[12]Genotype effect in young mice, 5 month old $Myc^{+/-}$ mice *versus* 5 month old $Myc^{+/+}$ mice.

[13]Genotype effect in old mice, 24 month old $Myc^{+/-}$ mice *versus* 24 month old $Myc^{+/+}$ mice.

[14]Aging effect in $Myc^{+/+}$ mice, 24 month old $Myc^{+/+}$ mice *versus* 5 month old $Myc^{+/+}$ mice.

[15]Aging effect in $Myc^{+/-}$ mice, 24 month old $Myc^{+/-}$ mice *versus* 5 month old $Myc^{+/-}$ mice.

[16]The geometric mean for all listed genes of each mouse model (column).

[17]The Spearman correlation coefficient (R) is provided for the comparisons between the effect of the $Myc^{+/-}$ genotype at young age (top row) or old age (bottom row) and each mouse model (column). Comparisons for which $R > 0.5$ are shaded grey.

[18]The P values are provided for all the comparisons for which the correlation coefficients were calculated. Comparisons for which $p<0.05$ are considered significant and are shaded grey.

Figure 4.3

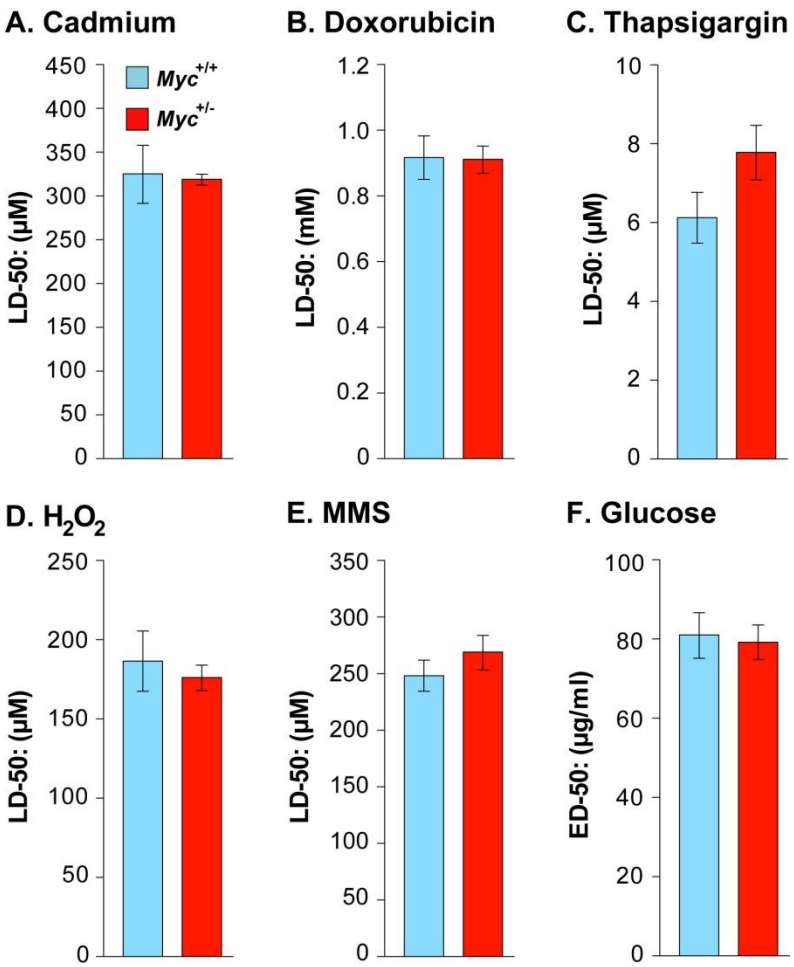
A. Cadmium
B. Doxorubicin
C. Thapsigargin
D. H_2O_2
E. MMS
F. Glucose
$Myc^{+/+}$
$Myc^{+/-}$
LD-50: (µM)
LD-50: (mM)
ED-50: (µg/ml)
0
50
100
150
200
250
300
350
400
450
0.2
0.4
0.6
0.8
1.0
1.2
2
4
6
8
10
20
40
60
80

Figure 4.3. Resistance of mouse tail fibroblasts to chemical or metabolic stresses

Cultures were treated with (A) cadmium, (B) doxorubicin, (C) thapsigargin, (D) hydrogen peroxide (H_2O_2,) or (E) methyl methane sulfonate (MMS), and the concentrations that were lethal for 50% of the cells (LD-50) are shown. (F) The concentration of glucose that reduced metabolic activity by 50% is shown. Tail biopsies of 10 mice of each genotype were shipped to the laboratory of Dr. R.A. Miller (University of Michigan) where fibroblasts were established and tested in cell culture as previously described (Harper et al., 2007). Data are shown as means with SEM. None of the changes between in $Myc^{+/-}$ and $Myc^{+/+}$ cells were statistically significant.

Figure 4.4

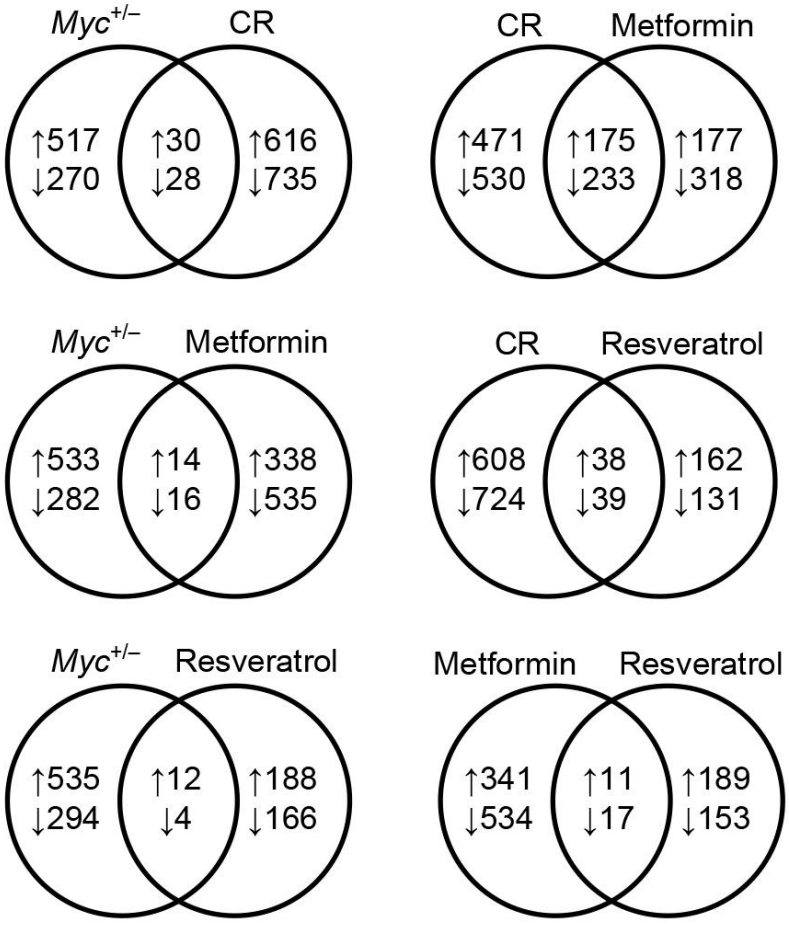
Myc+/–
CR
↑517
↓270
↑30
↓28
↑616
↓735
CR
Metformin
↑471
↓530
↑175
↓233
↑177
↓318
Myc+/–
Metformin
↑533
↓282
↑14
↓16
↑338
↓535
CR
Resveratrol
↑608
↓724
↑38
↓39
↑162
↓131
Myc+/–
Resveratrol
↑535
↓294
↑12
↓4
↑188
↓166
Metformin
Resveratrol
↑341
↓534
↑11
↓17
↑189
↓153

Figure 4.4. Gene level meta-analysis of expression changes in different longevity models

The data presented in Figure 4.1C are shown here as all possible pairwise comparisons. Differentially expressed genes in our datasets ($Myc^{+/-}$ *versus* $Myc^{+/+}$ animals) were compared with genes similarly recovered in studies of calorie restriction (*versus* ad libitum feeding), and metformin or resveratrol feeding (*versus* untreated controls). Upward arrows indicate genes upregulated in the long-lived condition (and conversely for the downward arrows). Our datasets were transferred to the laboratory of Dr. R. de Cabo (National Institute on Aging) where they were compared to previously reported datasets (Martin-Montalvo et al., 2013; Pearson et al., 2008). Raw data were subjected to Z-normalization as described (Perez et al., 2009; Schriner et al., 2005). Analysis of the normalized Z-scores of all of the detectable probes in the samples was performed using DIANE 6.0 (http://www.grc.nia.nih.gov/branches/rrb/dna/diane_software.pdf). Significant genes were selected by the Z-test <0.05, FDR <0.30, as well as Z-ratio >1.5 in both directions and analysis of variance P-value <0.05.

Figure 4.5

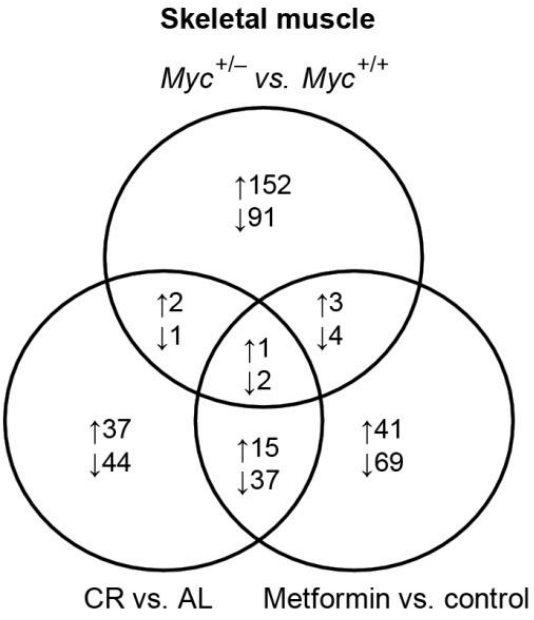

Common depleted
GO0005096: GTPase activator activity
GO0007165: Signal transduction

Common enriched
GO0006955: Immune response

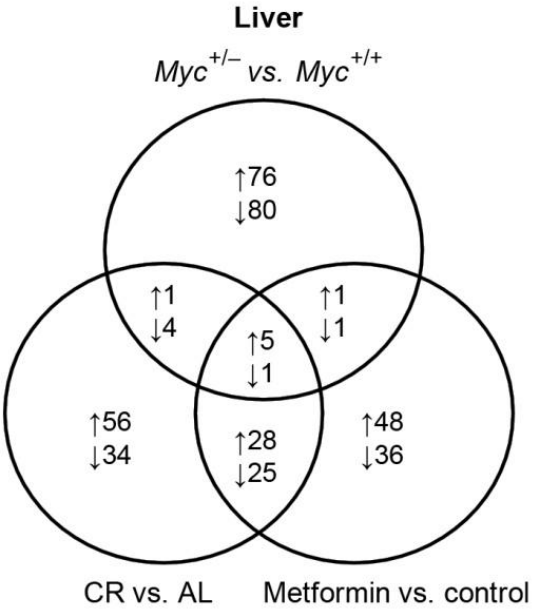

Common depleted
GO0032020: ISG15 protein conjugation

Common enriched
GO0004872: Receptor activity
GO0005179: Hormone activity
GO0007165: Signal transduction
GO0007608: Sensory perception of smell
GO0008035: High density lipoprotein binding

Figure 4.5. Pathway level meta-analysis of expression changes in different longevity models The number of GO terms that were significantly enriched or depleted in our microarray datasets (*Myc*$^{+/-}$ *versus Myc*$^{+/+}$ animals) were compared with GO terms similarly recovered in studies of calorie restriction (*versus* ad libitum feeding), and metformin feeding (*versus* untreated controls). Data were analyzed in the laboratory of R. de Cabo as previously indicated (Martin-Montalvo et al., 2013). Upward arrows indicate enriched GO categories in the long-lived condition (and conversely for the downward arrows). GO terms that were enriched or depleted in all three comparisons are listed on the right. All experiments considered only old male mice, and used liver or skeletal muscle data.

Table 4.3. Comparison of diets

	Standard[1]	HFD[2]	HFD-C[3]
Protein	28.8	18.4	18.4
Carbohydrate	58.5	21.3	21.3
Fat	12.7	60.3	60.3

	HFD[2]	HFD-C[3]
Casein	265	265
L-cystine	4	4
Maltodextrin	160	160
Sucrose	90	90
Lard	310	310
Soybean Oil	30	30
Cellulose	65.5	48
Mineral Mix	48	48
Calcium phosphate, dibasic	3.4	3.4
Vitamin mix	21	21
Choline bitartrate	3	3
Sodium cholate	0	5
Cholesterol	0	12.5

Table 4.3. Comparison of diets

The first table lists the percentage of kilocalories derived from each source.

The second table lists the quantity of each substance listed as grams per kilogram of food.

[1]Purina laboratory autoclavable rodent diet 5010

[2]Harlan laboratories Teclad diet TD.06414

[3]Harlan laboratories Teclad diet TD.110823

Figure 4.6

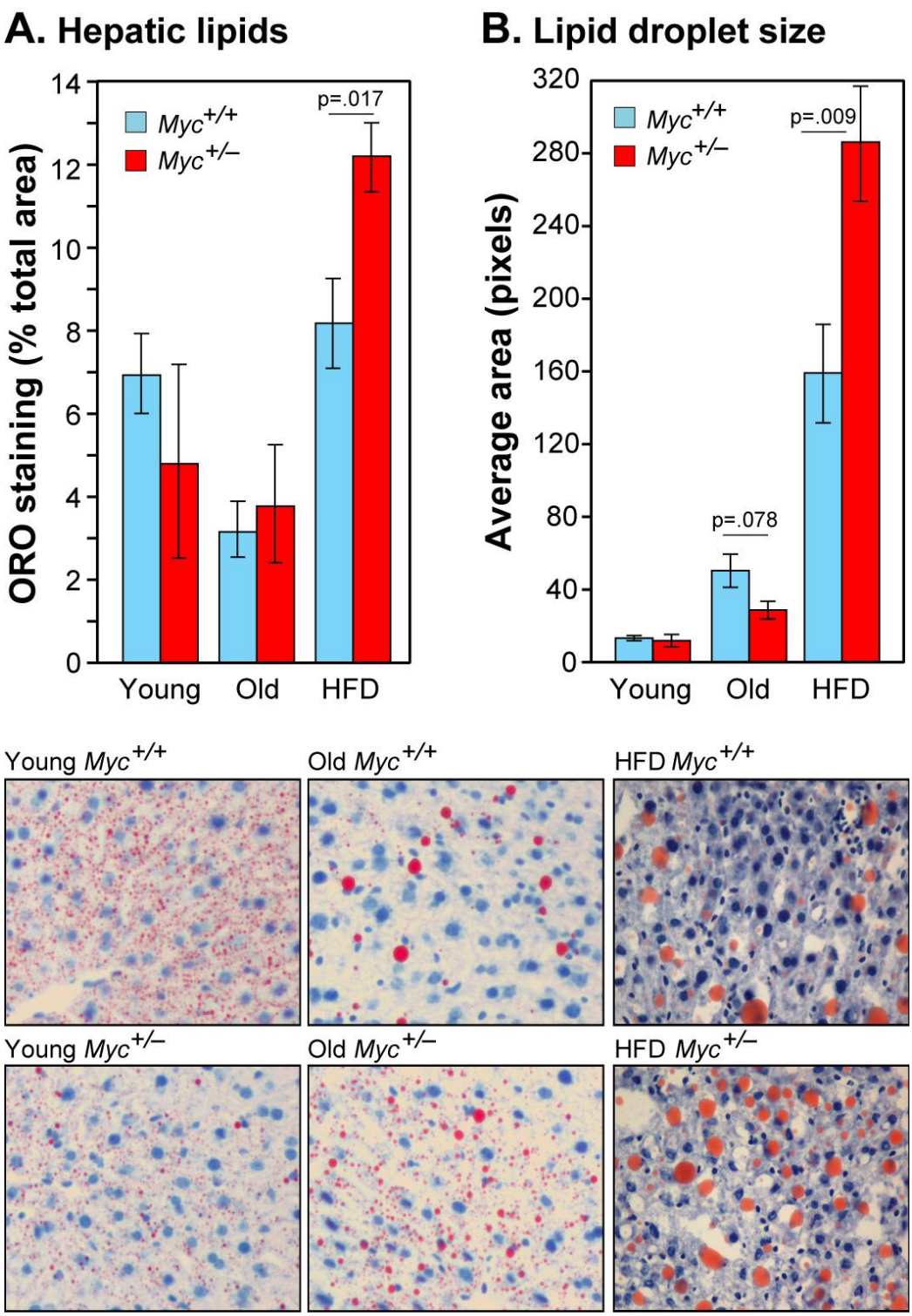
A. Hepatic lipids
ORO staining (% total area)
14
12
10
8
6
4
2
0
Myc+/+
Myc+/–
p=.017
Young
Old
HFD
B. Lipid droplet size
Average area (pixels)
320
280
240
200
160
120
80
40
0
Myc+/+
Myc+/–
p=.009
p=.078
Young
Old
HFD
Young Myc+/+
Old Myc+/+
HFD Myc+/+
Young Myc+/–
Old Myc+/–
HFD Myc+/–

Figure 4.6 Oil Red O staining in young, old, and HFD liver

(A) Lipid content was assessed in liver sections of 5 month and 24 month old male mice, and 6 month old males fed a high fat diet, using Oil Red O staining. Total cross sectional area per field was scored. N=6 for each standard diet cohort, and 11 for wild-type and 7 for $Myc^{+/-}$ mice from the high fat diet cohorts.

(B) Average size of lipid droplets of the animals analyzed in panel A. Specimens were stained with Oil Red O and hematoxylin ($p = .078$ for the comparison of old $Myc^{+/+}$ and $Myc^{+/-}$ animals). Representative images are shown from each cohort.

Figure 4.7

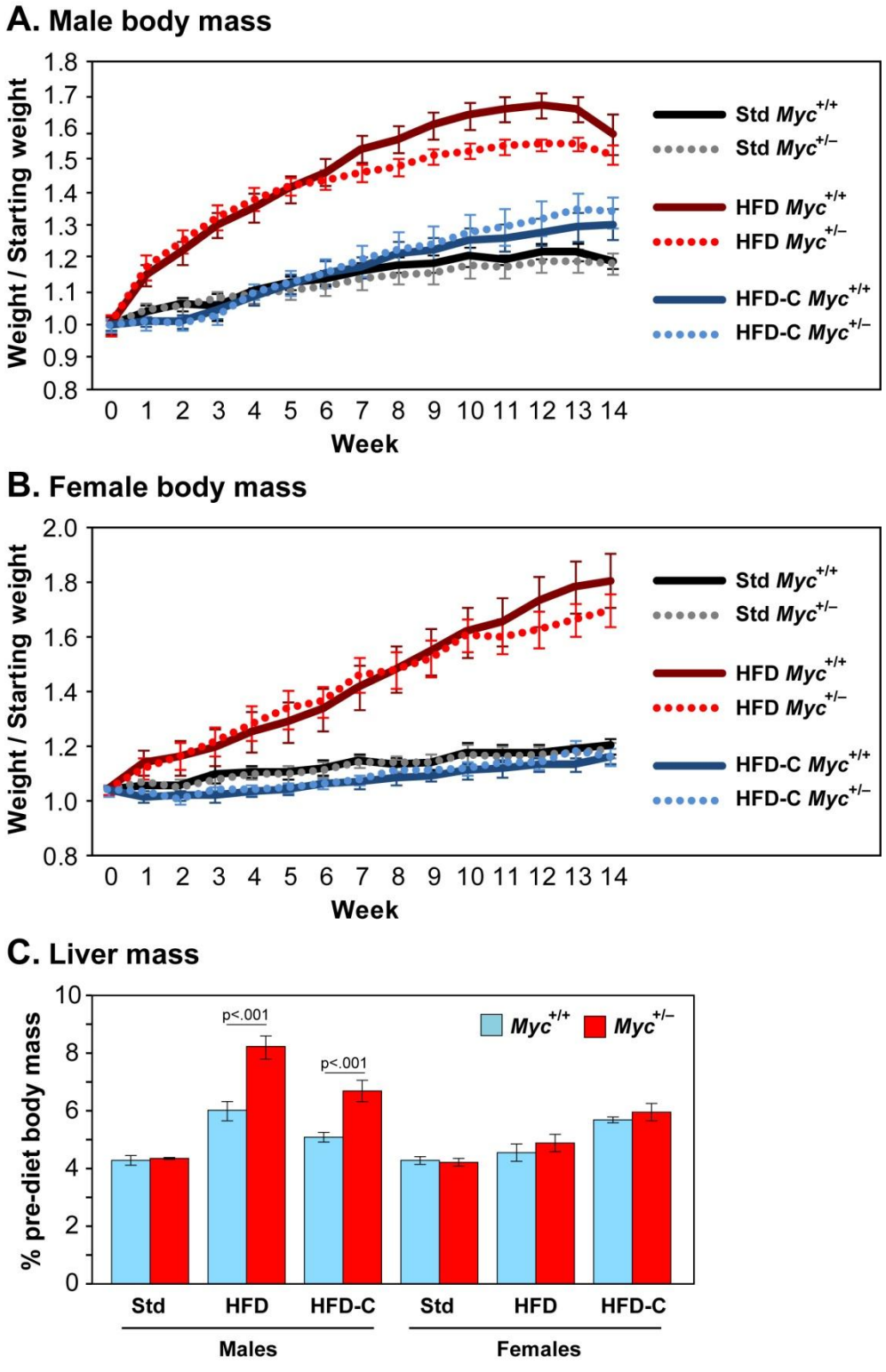
A. Male body mass
Weight / Starting weight
1.8
1.7
1.6
1.5
1.4
1.3
1.2
1.1
1.0
0.9
0.8
0 1 2 3 4 5 6 7 8 9 10 11 12 13 14
Week
Std Myc+/+
Std Myc+/–
HFD Myc+/+
HFD Myc+/–
HFD-C Myc+/+
HFD-C Myc+/–
B. Female body mass
Weight / Starting weight
2.0
1.8
1.6
1.4
1.2
1.0
0.8
0 1 2 3 4 5 6 7 8 9 10 11 12 13 14
Week
Std Myc+/+
Std Myc+/–
HFD Myc+/+
HFD Myc+/–
HFD-C Myc+/+
HFD-C Myc+/–
C. Liver mass
% pre-diet body mass
10
8
6
4
2
0
p<.001
p<.001
Myc+/+
Myc+/–
Std
HFD
HFD-C
Std
HFD
HFD-C
Males
Females

Figure 4.7. Effects of diet and genotype on liver and body mass

Body mass of males (A) and females (B) normalized to body mass before segregation by diet. “Std” refers to the standard diet, “HFD” is the high fat diet, and “HFD-C” is the high fat diet with cholesterol, as described in table 4.3. Mice were on a given diet for 14 weeks beginning at 3 months of age. Each cohort of a specific sex, genotype, and diet included between 8 and 13 mice. Average and standard error of the mean are shown at each one-week interval.

C) For the same cohorts of mice as (A) and (B), the post-diet liver mass was determined as a percentage of pre-diet body mass. Average and standard error of the mean are shown.

Figure 4.8

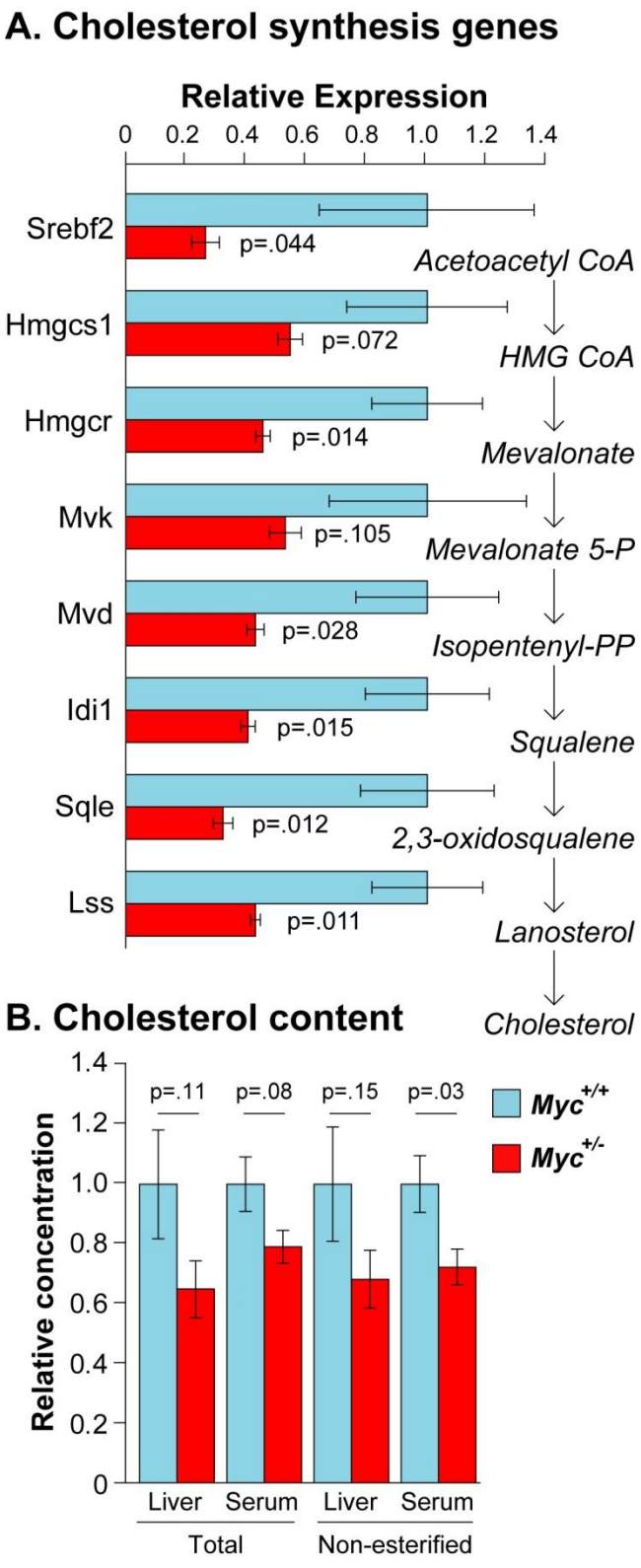
A. Cholesterol synthesis genes
Relative Expression
0
0.2
0.4
0.6
0.8
1.0
1.2
1.4
Srebf2
p=.044
Hmgcs1
p=.072
Hmgcr
p=.014
Mvk
p=.105
Mvd
p=.028
Idi1
p=.015
Sqle
p=.012
Lss
p=.011
Acetoacetyl CoA
HMG CoA
Mevalonate
Mevalonate 5-P
Isopentenyl-PP
Squalene
2,3-oxidosqualene
Lanosterol
Cholesterol
B. Cholesterol content
Relative concentration
p=.11
p=.08
p=.15
p=.03
Myc+/+
Myc+/-
Liver
Serum
Liver
Serum
Total
Non-esterified

Figure 4.8. Decreased cholesterol synthesis in *Myc*$^{+/-}$ mice

(A) Expression of genes in the cholesterol synthesis pathway was measured by q-RT-PCR in livers of 24 month old male mice. Primer sequences are listed in Appendix 3 (primer pairs 7-14). N=4 for each group. Genes (right side) are ordered to correspond with the steps of the enzymatic pathway. Substrates and products are listed on the left.

(B) Concentration of total and non-esterified cholesterol in liver extracts and plasma of 24 month old male animals was measured using the Folch method. N=5-6 for each group or condition tested.

Figure 4.9

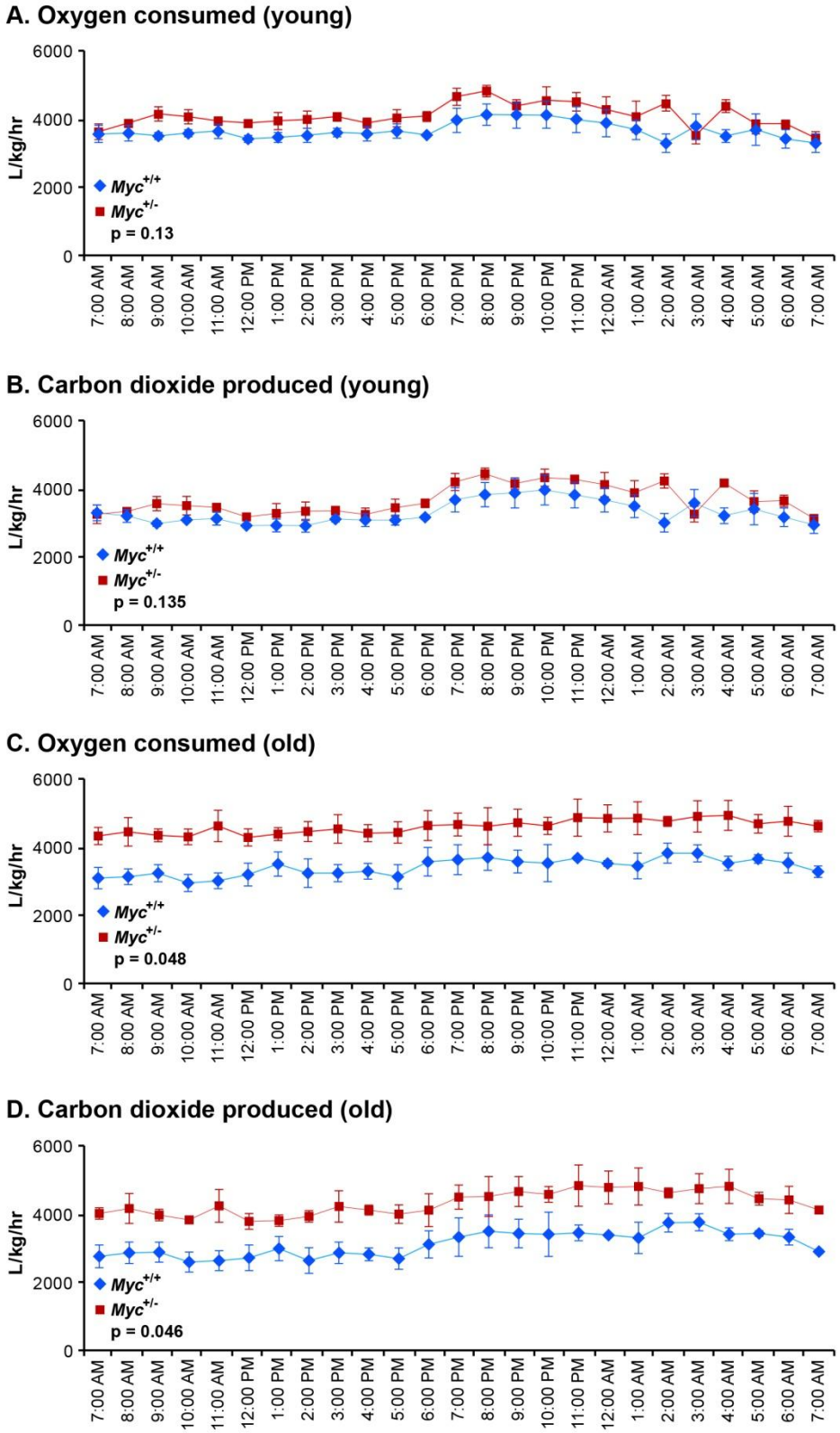
A. Oxygen consumed (young)
L/kg/hr
6000
4000
2000
0
Myc+/+
Myc+/-
p = 0.13
7:00 AM
8:00 AM
9:00 AM
10:00 AM
11:00 AM
12:00 PM
1:00 PM
2:00 PM
3:00 PM
4:00 PM
5:00 PM
6:00 PM
7:00 PM
8:00 PM
9:00 PM
10:00 PM
11:00 PM
12:00 AM
1:00 AM
2:00 AM
3:00 AM
4:00 AM
5:00 AM
6:00 AM
7:00 AM
B. Carbon dioxide produced (young)
L/kg/hr
6000
4000
2000
0
Myc+/+
Myc+/-
p = 0.135
7:00 AM
8:00 AM
9:00 AM
10:00 AM
11:00 AM
12:00 PM
1:00 PM
2:00 PM
3:00 PM
4:00 PM
5:00 PM
6:00 PM
7:00 PM
8:00 PM
9:00 PM
10:00 PM
11:00 PM
12:00 AM
1:00 AM
2:00 AM
3:00 AM
4:00 AM
5:00 AM
6:00 AM
7:00 AM
C. Oxygen consumed (old)
L/kg/hr
6000
4000
2000
0
Myc+/+
Myc+/-
p = 0.048
7:00 AM
8:00 AM
9:00 AM
10:00 AM
11:00 AM
12:00 PM
1:00 PM
2:00 PM
3:00 PM
4:00 PM
5:00 PM
6:00 PM
7:00 PM
8:00 PM
9:00 PM
10:00 PM
11:00 PM
12:00 AM
1:00 AM
2:00 AM
3:00 AM
4:00 AM
5:00 AM
6:00 AM
7:00 AM
D. Carbon dioxide produced (old)
L/kg/hr
6000
4000
2000
0
Myc+/+
Myc+/-
p = 0.046
7:00 AM
8:00 AM
9:00 AM
10:00 AM
11:00 AM
12:00 PM
1:00 PM
2:00 PM
3:00 PM
4:00 PM
5:00 PM
6:00 PM
7:00 PM
8:00 PM
9:00 PM
10:00 PM
11:00 PM
12:00 AM
1:00 AM
2:00 AM
3:00 AM
4:00 AM
5:00 AM
6:00 AM
7:00 AM

Figure 4.9. Oxygen consumption and carbon dioxide production by live animals

The volume of O_2 consumed and CO_2 produced were measured in metabolic chambers (Columbus Instruments). The data were averaged for each hour over a 24-hour total monitoring period and normalized to the body mass of each animal. Animals of both sexes were used. N=4 per genotype for young (5 months) animals; n=3 for old (24 months) animals. Animals were transferred to the laboratory of Dr. H. Xu (Rhode Island Hospital), where they were tested in metabolic chambers as previously described (Marnett 1999). Statistical significance was calculated by the repeated measured analysis of variance method (RM-ANOVA) using IBM SPSS software. SEM is shown for each time point.

Figure 4.10

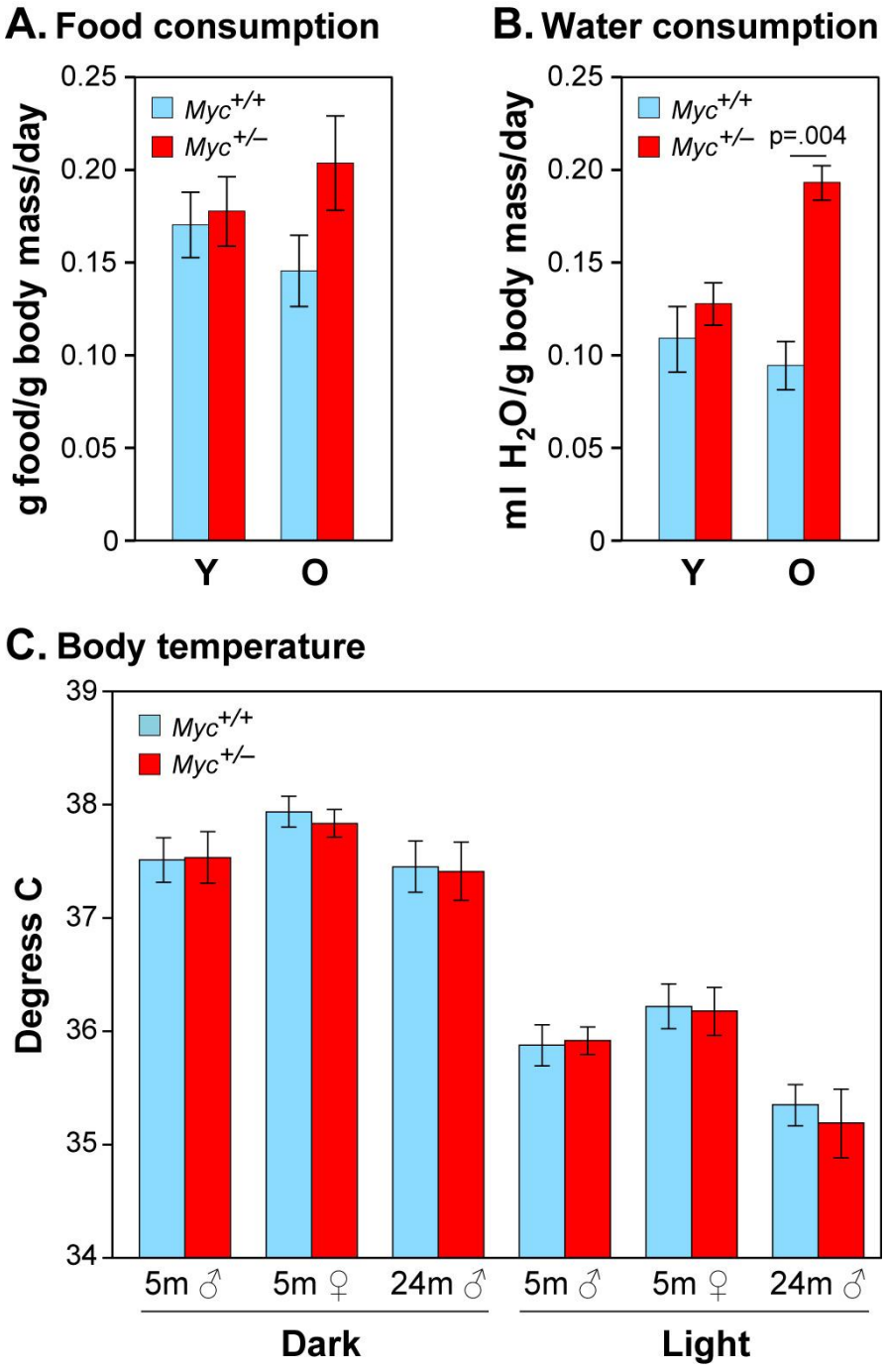
A. Food consumption
g food/g body mass/day
0.25
0.20
0.15
0.10
0.05
0
Myc+/+
Myc+/–
Y
O
B. Water consumption
ml H2O/g body mass/day
p=.004
C. Body temperature
Degress C
39
38
37
36
35
34
5m ♂
5m ♀
24m ♂
Dark
Light

Figure 4.10. Food and water consumption and body temperature

A, B) These data were acquired concomitantly with the O_2 consumption and CO_2 production data shown in Figure 4.9. P=.140 for the comparison of food consumption in old animals.

C) Temperature was measured in young (5 months) and old (24 months) mice using an implantable temperature transponder system (IPTT-300, Bio Medic Data Systems). The transponders were read by a hand-held IPTT 7009 reader without disturbing the animals (taking them out of their cages; when needed animals were individually housed). Light cycle measurements were taken during the day when the mice were asleep. Dark cycle measurements were taken late at night or early in the morning when the mice were active. For each type of measurement, readings were taken on three separate, successive days. N=6-7 for young animals. For old males, n=5 for the *Myc*$^{+/+}$ group and 4 for the *Myc*$^{+/-}$ group.

Figure 4.11

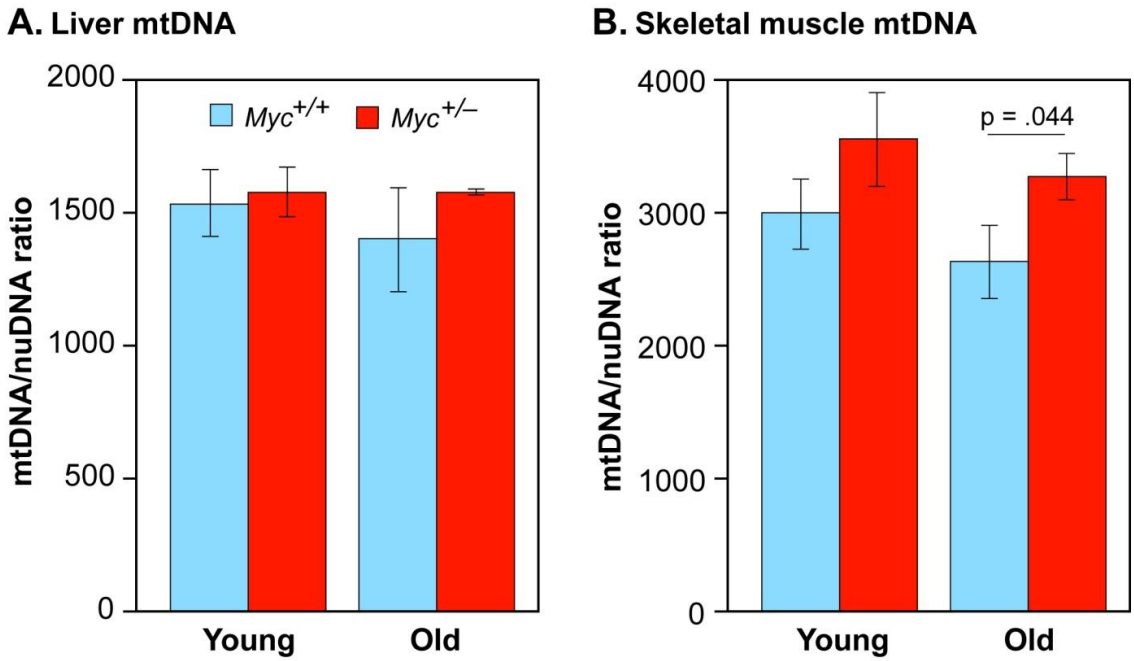
A. Liver mtDNA
2000
1500
1000
500
0
mtDNA/nuDNA ratio
Myc+/+
Myc+/–
Young
Old
B. Skeletal muscle mtDNA
4000
3000
2000
1000
0
mtDNA/nuDNA ratio
p = .044
Young
Old

Figure 4.11. Mitochondrial DNA copy number

(A) Total DNA was prepared from liver tissue of young (5 months) and old (30 months) female mice of both genotypes. N=4 for each young group, and 3 for each old group.

(B) Total DNA was prepared from skeletal muscle tissue of young (5 months) and old (22 months) female mice of both genotypes. N=4 for each young group, and 6 for each old group.

Amounts of mitochondrial and nuclear sequences were measured by qPCR using primers to mitochondrial DNA (cytochrome C gene, primer pair 5, Appendix 3) and to unique, single copy nuclear sequences (primer pair 3, Appendix 3). Relative copy number of mitochondria was calculated as the ratio of mitochondrial to nuclear signals.

Figure 4.12

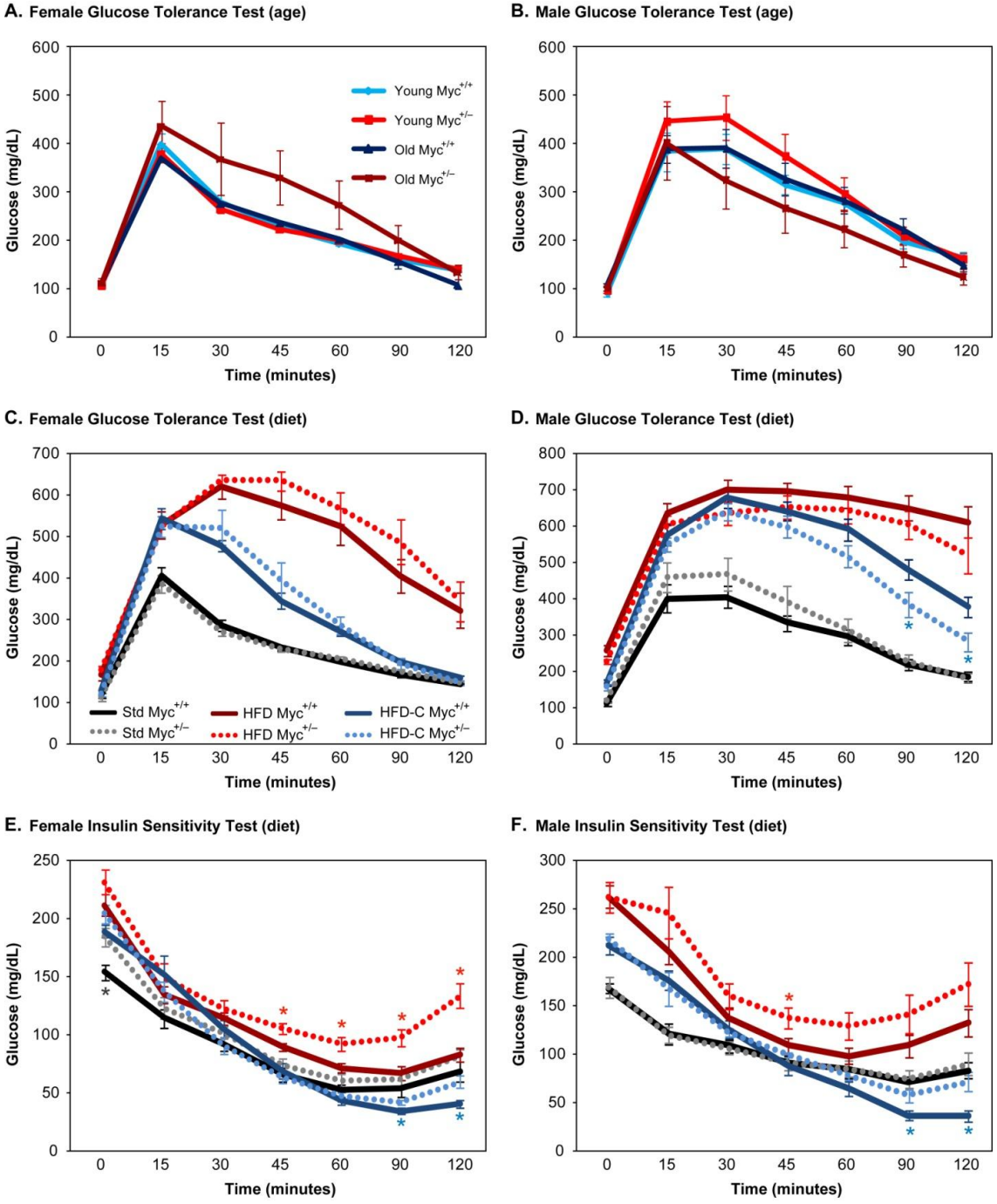
A. Female Glucose Tolerance Test (age)
B. Male Glucose Tolerance Test (age)
C. Female Glucose Tolerance Test (diet)
D. Male Glucose Tolerance Test (diet)
E. Female Insulin Sensitivity Test (diet)
F. Male Insulin Sensitivity Test (diet)
Glucose (mg/dL)
Time (minutes)
Young Myc+/+
Young Myc+/–
Old Myc+/+
Old Myc+/–
Std Myc+/+
Std Myc+/–
HFD Myc+/+
HFD Myc+/–
HFD-C Myc+/+
HFD-C Myc+/–

Figure 4.12. Insulin sensitivity and glucose tolerance

Glucose tolerance tests were performed by intraperitoneal injection of an amount of glucose proportional to body mass, followed by measurement of glucose in blood collected from tail bleeds at several intervals over two hours. The first measurement was taken before glucose administration, and other time points represent the duration that had elapsed since the injection. Several different cohorts of $Myc^{+/-}$ and $Myc^{+/+}$ mice were compared: A) female and B) male 5 month (young) and 22 month (old) mice; and C) females and D) males on a standard (Std), high fat (HFD), or high fat and cholesterol (HFD-C) diet. Insulin sensitivity tests were performed by intraperitoneal injection of insulin followed by blood glucose measurements as described above, using the same mice for (E) and (F) as in (C) and (D), respectively. Glucose tolerance was measured in the morning after a 14 hour overnight fast, and insulin sensitivity was measured in the afternoon after a 6 hour fast. N = 9-12 mice for young mice for each diet, and 5 old males of each genotype, and 3 $Myc^{+/-}$ and 2 $Myc^{+/+}$ old females. Mean and standard error are shown for each time point for each cohort, and asterisks indicate $p < .05$ in a two-tailed t-test between the two genotypes for the condition of the corresponding color.

Figure 4.13

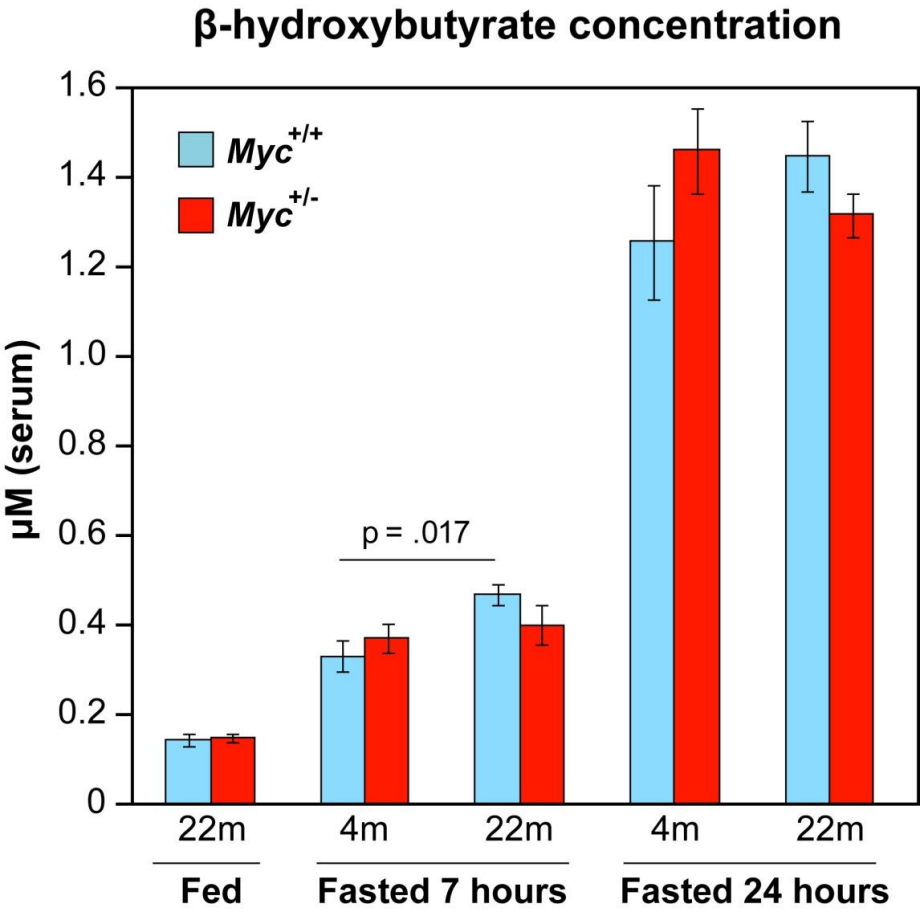
β-hydroxybutyrate concentration
μM (serum)
1.6
1.4
1.2
1.0
0.8
0.6
0.4
0.2
0
Myc+/+
Myc+/-
p = .017
22m
4m
22m
4m
22m
Fed
Fasted 7 hours
Fasted 24 hours

Figure 4.13. β-hydroxybutyrate concentration

β-hydroxybutyrate was measured in serum of 4 and 22 month old female mice after 0, 7, or 24 hours of fasting. Blood was collected at the end of the "awake" period (8:00 am) for the 0 and 24 hour time points, and in the latter half of the "sleeping" period (3:00 pm) for the 7 hour time point. N = 9 young *Myc*$^{+/+}$, 7 young *Myc*$^{+/-}$, 5 old *Myc*$^{+/+}$, and 4 old *Myc*$^{+/-}$. Mean and standard error are shown for each cohort.

Figure 4.14

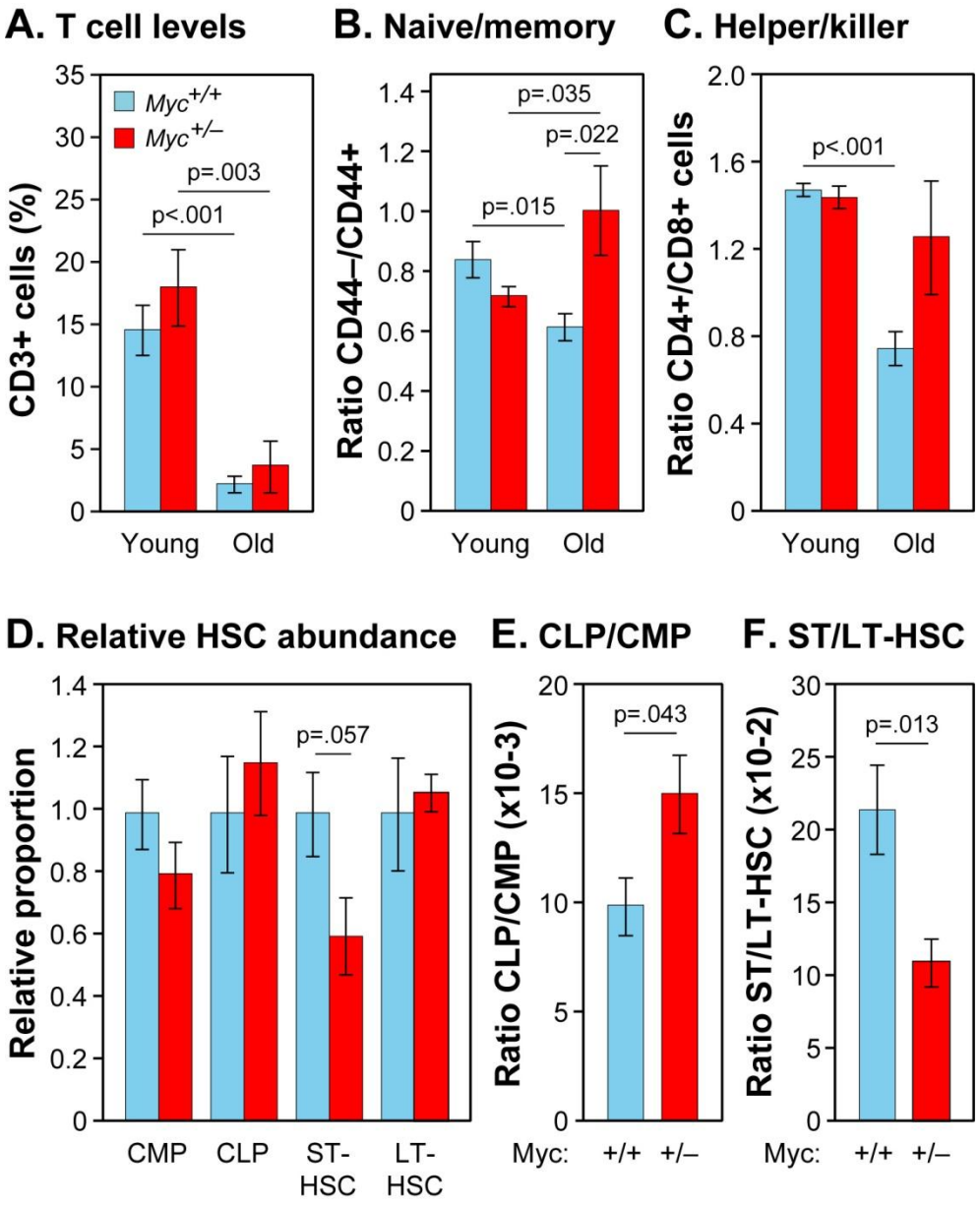
A. T cell levels
B. Naive/memory
C. Helper/killer
Myc+/+
Myc+/–
CD3+ cells (%)
p=.003
p<.001
Ratio CD44–/CD44+
p=.035
p=.022
p=.015
Ratio CD4+/CD8+ cells
p<.001
Young
Old
D. Relative HSC abundance
E. CLP/CMP
F. ST/LT-HSC
Relative proportion
p=.057
CMP
CLP
ST-HSC
LT-HSC
Ratio CLP/CMP (x10-3)
p=.043
Myc: +/+ +/–
Ratio ST/LT-HSC (x10-2)
p=.013

Figure 4.14. Markers of immunosenescence are decreased in *Myc*$^{+/-}$ mice

(A) Total T cell levels ($CD3^+$) were scored as a % of total peripheral lymphocytes in 5 month and 24 month old male mice using flow cytometry.

(B) The ratio of naive to memory T cells ($CD44^-/CD44^+$), and

(C) the ratio of helper to killer T cells ($CD4^+/CD8^+$) were measured in the same samples. N=12 young and 8 old animals for each genotype.

(D) Proportions of common myeloid progenitors (CMP; Lin^-, $Sca1^-$, $cKit^+$, $CD34^+$, $CD127^-$), common lymphoid progenitors (CLP; Lin^-, $Sca1^+$, $Flt3^+$, $CD127^+$), short-term hematopoietic stem cells (ST-HSC; Lin^-, $Sca1^+$, $cKit^+$, $CD34^+$, $Flt3^-$), and long-term hematopoietic stem cells (LT-HSC; Lin^-, $Sca1^+$, $cKit^+$, $CD34^-$, $Flt3^-$) were scored as % of Lin^- cells in bone marrow recovered from long bones (tibia and femur) of 16 month old female mice using flow cytometry. Data are shown normalized to the *Myc*$^{+/+}$ condition for each comparison.

(E) The ratio of CLP to CMP, and

(F) the ratio of ST-HSC to LT-HSC were measured in the same samples. N=6 for each genotype.

Figure 4.15

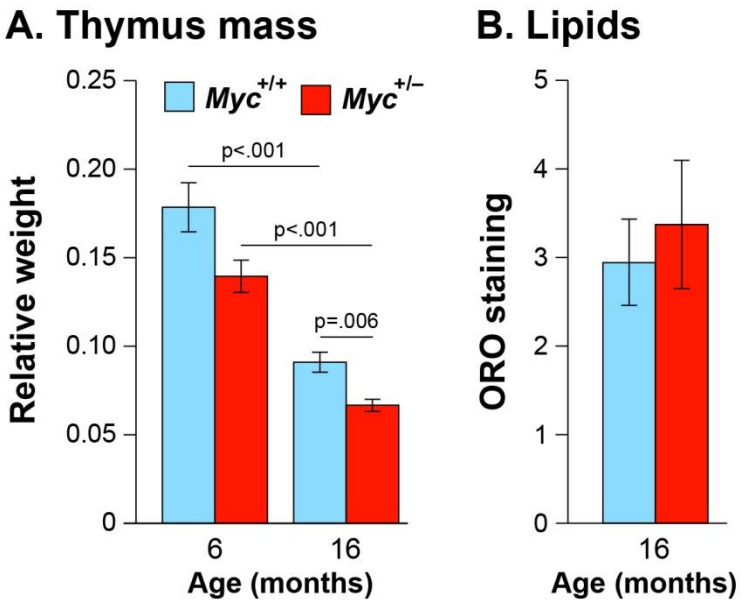
A. Thymus mass
B. Lipids
Myc+/+
Myc+/–
p<.001
p<.001
p=.006
Relative weight
ORO staining
0.25
0.20
0.15
0.10
0.05
0
5
4
3
2
1
0
6
16
16
Age (months)
Age (months)

Figure 4.15. Evaluation of age-associated thymic involution

(A) Relative organ weight. Thymuses were carefully dissected out and weighed. The values are expressed as ratios to total body weight. Note that in this series of experiments young and old cohorts were 6 months and 16 months of age, respectively. All animals were females, N=3-7 per group.

(B) Relative adiposity. Thymic involution is accompanied by a progressive lipid infiltration of the tissue. Lipid content was assessed in sections of dissected thymus tissue, which were stained with Oil Red O. The values are expressed as the % stained area per total field. All animals were females, N=7-10 per group.

For an evaluation of cellular senescence during thymic involution see Figure 4.19E.

Figure 4.16

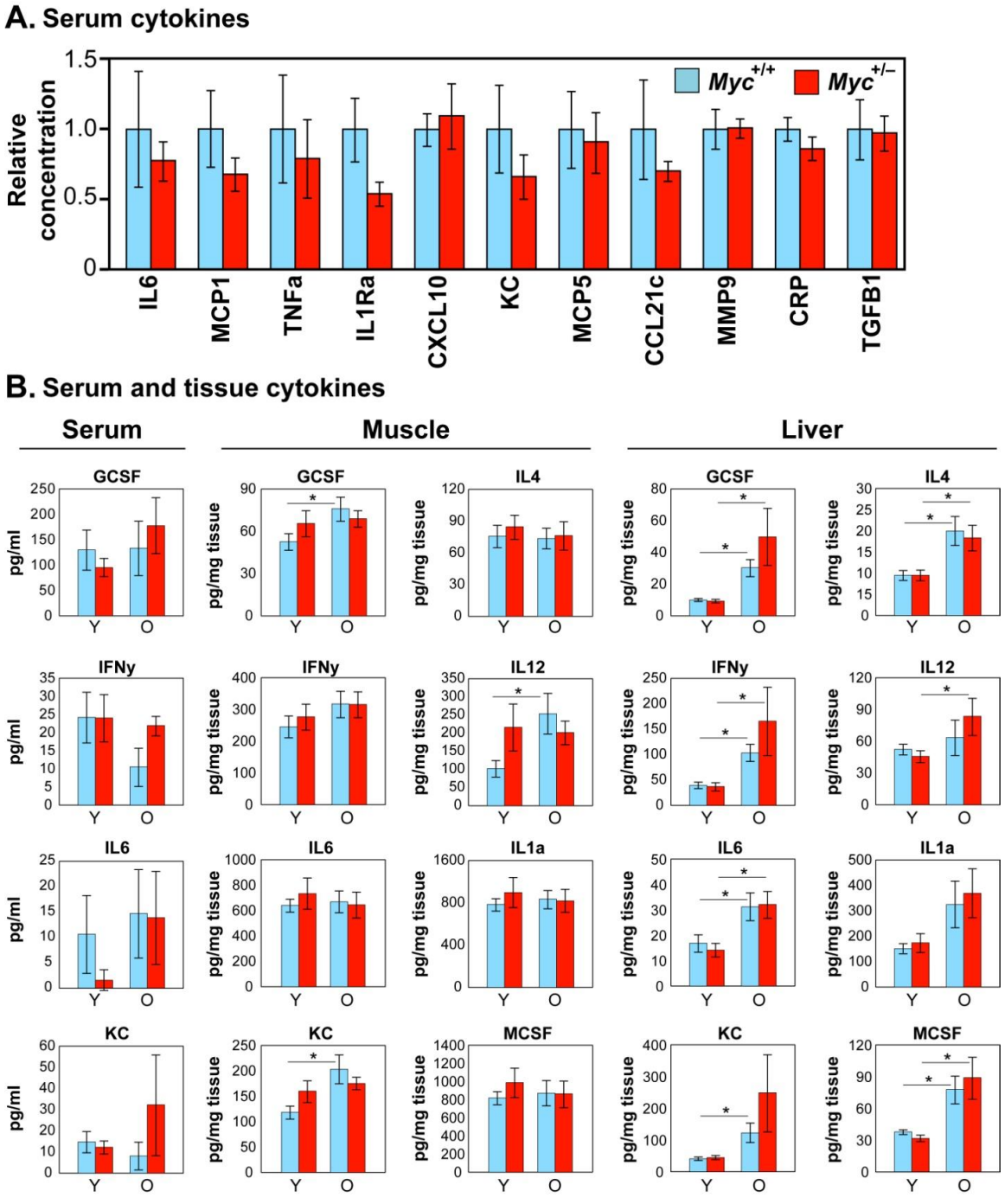
A. Serum cytokines
Relative concentration
Myc+/+
Myc+/−
IL6
MCP1
TNFa
IL1Ra
CXCL10
KC
MCP5
CCL21c
MMP9
CRP
TGFB1
B. Serum and tissue cytokines
Serum
Muscle
Liver
GCSF
IL4
IFNy
IL12
IL6
IL1a
KC
MCSF
pg/ml
pg/mg tissue
Y
O

Figure 4.16. Cytokines

A) Serum from 24 month old mice was sent to Aushon BioSystems, Inc. for quantification of cytokines using a custom multiplex biomarker testing system. N = 8 (4 males and 4 females) for each genotype. Data have been normalized to the average of $Myc^{+/+}$ for each cytokine, and average and standard error of the mean are shown.

B) Serum, skeletal muscle, and liver samples from 6 month (Y) and 22 month (O) females were analyzed using the Luminex multiplex assay system (Millipore). N = 8 for each genotype of young mice and 6 for each genotype of old mice. Average and standard error are shown for each cohort. Blue and red bars represent $Myc^{+/+}$ and $Myc^{+/-}$ mice, respectively. A p value < .05 produced by a two-tailed t-test is denoted by an asterisk (*).

Figure 4.17

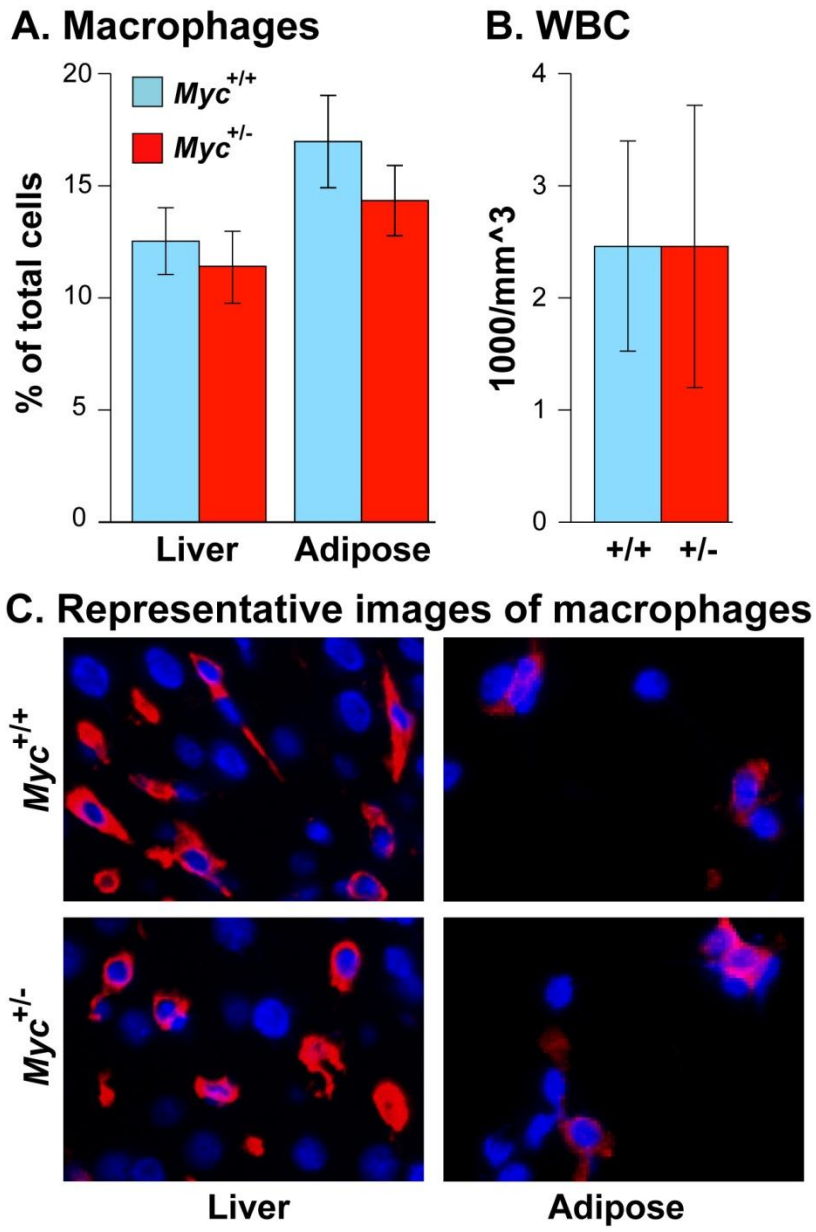
A. Macrophages
B. WBC
% of total cells
20
15
10
5
0
Myc+/+
Myc+/-
Liver
Adipose
1000/mm^3
4
3
2
1
0
+/+
+/-
C. Representative images of macrophages
Myc+/+
Myc+/-
Liver
Adipose

Figure 4.17. Presence of macrophages in tissues and total white blood cell counts

(A) The proportion of macrophages to other cells in the liver and white adipose tissue of 24 month old male animals was assessed by immunofluorescence staining of macrophages with the F4-80 antibody (AbD Serotec). Total cells were scored as DAPI-positive nuclei. 3-5 slides were scored for each liver, and 2-4 slides for each adipose sample. N=5 $Myc^{+/+}$ and 6 $Myc^{+/-}$ animals; the same animals were used to analyze both tissues.

(B) White blood cell counts were measured using a scil Vet abc Plus veterinary hematology analyzer. Blood samples from six 22 month old females of each genotype were used.

(C) Representative images of F4-80 macrophage staining are shown for each genotype and tissue. These are magnified and cropped from the original versions, and are meant to represent staining quality, not cell number.

Figure 4.18

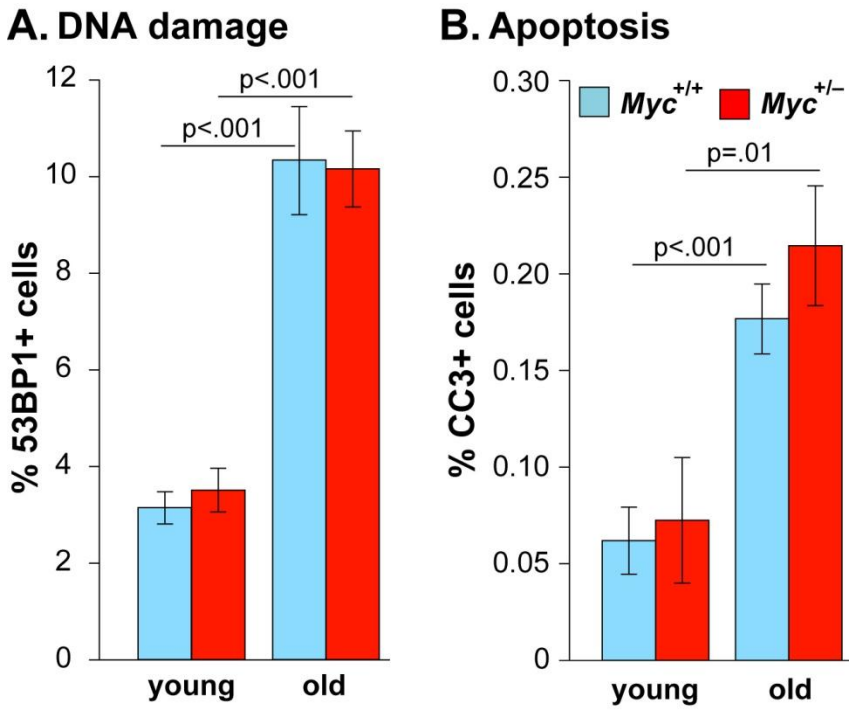
A. DNA damage
% 53BP1+ cells
12
10
8
6
4
2
0
p<.001
p<.001
young
old
B. Apoptosis
% CC3+ cells
0.30
0.25
0.20
0.15
0.10
0.05
0
Myc+/+
Myc+/–
p=.01
p<.001
young
old

Figure 4.18. DNA damage (double strand breaks) and apoptosis

A) 53BP1-positive cells were scored as % of total cells in liver specimens of 5 and 25 month old male animals. Cryosections were stained with antibody to the 53BP1 protein (antibody NB100-304, Novus Biologicals) and visualized by immunofluorescence. Total cells were scored as DAPI-positive nuclei. An average of 370 well-defined nuclei (min=258, max=468) were scored for each specimen. A nucleus was considered positive if it contained at least one large focus. N=5 young $Myc^{+/+}$ animals, and 6 for the other groups.

B) Cryosections of liver tissue specimens from 6 and 22 month old female animals were stained with an antibody specific for the cleaved form of caspase-3 (antibody 9661, Cell Signaling) and visualized by immunofluorescence. Total cells were scored as DAPI-positive nuclei. A total of approximately 3,000 cells in 3 separate sections were counted for each animal. The values are expressed as the proportion (%) of positive cells among total cells. N=8 young and 6 old animals of each genotype.

Figure 4.19

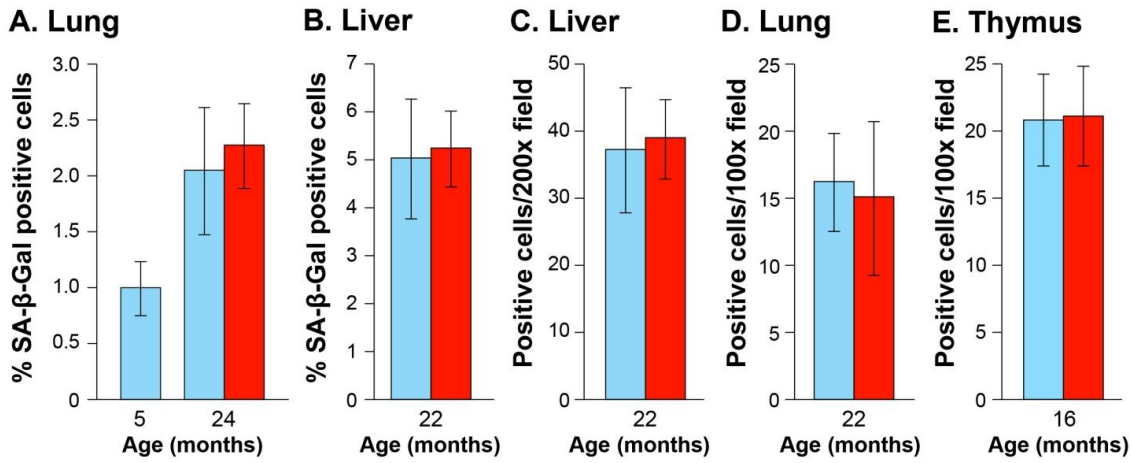
A. Lung
% SA-β-Gal positive cells
3.0
2.5
2.0
1.5
1.0
0.5
0
5
24
Age (months)
B. Liver
% SA-β-Gal positive cells
7
6
5
4
3
2
1
0
22
Age (months)
C. Liver
Positive cells/200x field
50
40
30
20
10
0
22
Age (months)
D. Lung
Positive cells/100x field
25
20
15
10
5
0
22
Age (months)
E. Thymus
Positive cells/100x field
25
20
15
10
5
0
16
Age (months)

Figure 4.19. Prevalence of Cellular Senescence in Tissues

(A) Cryosections of lung tissue specimens from male animals were processed using the senescence-associated β-galactosidase histochemical staining protocol (Debacq-Chainiaux et al., 2009). Sections were counterstained with nuclear fast red solution to allow the visualization of individual cells. The values are expressed as the proportion (%) of SA-β-gal positive cells among total cells. N=2 young (5 months) *Myc*$^{+/+}$ animals, 6 old *Myc*$^{+/+}$ animals and 8 old *Myc*$^{+/-}$ animals.

(B) SA-β-gal positive cells were assessed in liver tissue of a different group of old female animals. The same scoring procedure was used as in panel A. N=6 for each genotype.

(C) SA-β-gal positive cells were scored in the same liver specimens as in panel B using an alternate procedure, namely, as the number of positive cells per one 200x magnification field. The two scoring methods produced very similar results.

(D) SA-β-gal positive cells were assessed in lung tissue of the same group of old female animals as in panel B, using the scoring procedure from panel C. The values are expressed as the number of positive cells per one 100x magnification field.

(E) SA-β-gal positive cells were scored in thymus tissue of another group of old female animals (see Figure 4.15). The values are expressed as the number of positive cells per one 100x magnification field. N = 6-10 for each genotype.

Figure 4.20

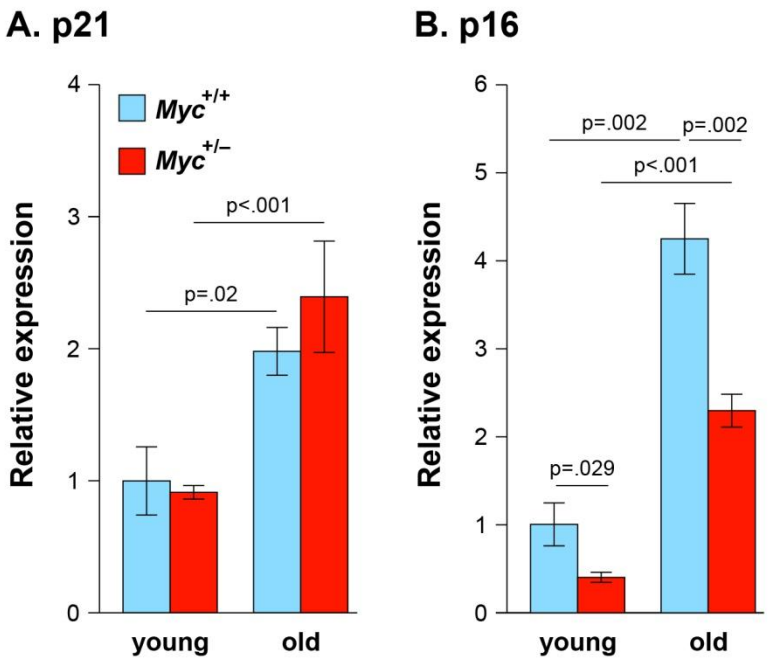
A. p21
B. p16
Relative expression
Myc+/+
Myc+/–
p<.001
p=.02
p=.002
p=.002
p<.001
p=.029
young
old
young
old
0
1
2
3
4
5
6

Figure 4.20. Age-associated induction of the *Cdkn1a* (p21) and *Cdkn2a* (p16) genes

(A) Expression of the p21 mRNA was measured by q-RT-PCR in livers of 6 and 22 month old female mice using primer pair 15 (Appendix 3) and normalized to *Gapdh*. N=9 young and 6 old animals of each genotype.

(B) Expression of the p16 mRNA was measured using the same specimens and procedures with primer pair 16.

Figure 4.21

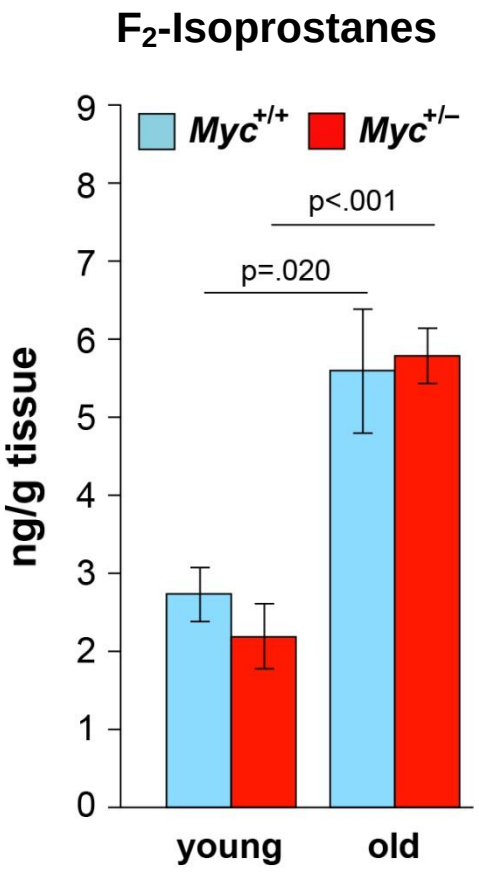
F2-Isoprostanes
Myc+/+
Myc+/–
p<.001
p=.020
ng/g tissue
0
1
2
3
4
5
6
7
8
9
young
old

Figure 4.21. Levels of F_2-Isoprostanes in tissues

F_2-isoprostane levels in liver tissues of 5 and 23-27 month old male animals were measured using the gas chromatography and mass spectrometry method. Tissue samples were flash-frozen at the time of sacrifice and shipped to the laboratory of Dr. H. Van Remmen (Barshop Institute) where they were analyzed as previously indicated (Ward et al., 2005). N=4 animals per each young group, and 5 and 7 for old $Myc^{+/+}$ and $Myc^{+/-}$ animals, respectively.

Chapter 5. Discussion

I. MYC and aging

MYC is a highly pleiotropic transcription factor that directly regulates 15-20% of the transcriptome (Dang 2012). MYC impinges on numerous pathways, and its activity promotes cell proliferation, accumulation of mass, energy metabolism and a variety of anabolic functions. *Myc*$^{+/-}$ mice have significantly extended median and maximum lifespans in both sexes and a reduced mortality rate across all ages relative to their normal *Myc*$^{+/+}$ littermates. *Myc* haploinsufficiency in *Drosophila* also extends lifespan, pointing to a deep conservation of the underlying processes (Greer et al., 2013). *Myc*$^{+/-}$ mice display ameliorated aging phenotypes across a variety of pathophysiological processes in multiple organs, the breadth of which suggests that their increased longevity is not attributable to the prevention of a specific fatal disease, but rather to the attenuation of fundamental underlying mechanisms of aging and therefore broadly increased healthspan.

Aging *Myc*$^{+/-}$ mice have a lower prevalence of cancer, healthier lipid and cholesterol metabolism, a higher metabolic rate, stronger bones, less fibrosis, improved motor control, and reduced immunosenescence compared to their normal littermates. All of these phenotypes oppose the effects of normal aging and are shared with many other long-lived mouse models (Table 5.1). For example, CR and Ames dwarf mice also have an increased metabolic rate (Bartke and Westbrook, 2012); CR and metformin-treated mice have lower cholesterol (Martin-Montalvo et al., 2013; Tsuchiya et al., 2004); CR, Ames dwarf, and mice fed rapamycin or metformin are cancer resistant (Jalland et al., 2013; Pratheeshkumar et al., 2010; Samadder et al., 2011; Szczesny et al., 2010); and CR, Ames dwarf, and metformin-treated mice have better motor coordination (Martin-Montalvo et al., 2013; Xie et al., 2012; Yamamoto et al., 2013). All of these long-lived

models show reduced body mass. However, *Myc* hypomorphic mice also exhibit contrasting phenotypes to other long-lived models; for example, rapamycin administration increases serum cholesterol and does not improve motor coordination (Pratheeshkumar et al., 2010), Ames dwarf mice have decreased bone density (Song et al., 2012), and CR reduces fecundity (Liu et al., 2014). Importantly, compared to other longevity extending interventions, all of which compromise some aspects of healthy physiology, we have to date not found any significant physiological deficits in $Myc^{+/-}$ mice.

Low serum IGF-1 levels are almost universally observed in long-lived mice, including CR, $Pten^{tg}$, GHRKO, and Ames and Snell dwarf mice, and IGF-1 signaling is reduced in $Igf1r^{+/-}$, $Irs1^{-/-}$, and $Pappa^{-/-}$ mice (Table 5.1). Since reducing GH/IGF-1 signaling is able to extend lifespan and elicit many of the phenotypes described above, it seems likely that it contributes to the benefits observed in $Myc^{+/-}$ mice. However, due to some of the contrasting phenotypes of $Myc^{+/-}$ mice, reduced IGF-1 is probably only one of several mechanisms responsible for lifespan and healthspan extension.

Insulin signaling is also often connected with longevity extension in many model organisms, including mice. Insulin sensitivity decreases with age, and is improved in several long-lived mouse models, including CR, Ames dwarf, GHRKO, and metformin-treated mice, suggesting that it contributes to increased longevity. However, in other long-lived mice, insulin signaling is directly perturbed, such as $Irs1^{-/-}$, $Irs2^{+/-}$, and fat-specific insulin receptor knockout (FIRKO) (Bluher et al., 2003). Furthermore, mice that are heterozygous for a non-functional insulin receptor, and therefore less sensitive to insulin, have a normal lifespan (Shimizu et al., 2011), and mice that are knocked out for

protein tyrosine phosphatase 1B, and are therefore more sensitive to insulin, have reduced longevity (Nelson et al., 2012). The *Myc*$^{+/-}$ genotype has no effect on insulin sensitivity on a normal diet, and reduces insulin sensitivity on a high fat diet. In aggregate, it appears that increased longevity can be associated with increased, decreased, or normal insulin sensitivity, and modulating insulin sensitivity in either direction does not consistently increase lifespan in mice. This suggests that insulin signaling may not be as closely linked to longevity in mice as once thought, or as is the case in other model organisms. Moreover, effects on the insulin signaling pathway may be unrelated to lifespan in some long-lived mice.

Production of ROS increases with age and can damage important macromolecules such as DNA and proteins. Although manipulation of these pathways has not yet achieved robust lifespan extension in mammals (Shukla et al., 2013), a stress resistance signature is a component of several important longevity models (CR, reduced somatotrophic signaling, metformin treatment, Table 5.1). The XME pathway, which promotes the removal of ingested or endogenous toxic metabolites, has been strongly linked with longevity in invertebrate models (Hamilton et al., 1994), and to a more limited extent in the mouse (Dias et al., 2014). Although the expression of some XME genes in liver increased less with age in male *Myc*$^{+/-}$ than *Myc*$^{+/+}$ mice, this effect was of much smaller magnitude than in other long-lived models. In agreement, fibroblasts from *Myc*$^{+/-}$ mice did not display increased resistance in culture to a variety of chemical stressors.

To further evaluate the effects of cellular stress in *Myc*$^{+/-}$ animals we looked for changes in the production of ROS (F_2 isoprostanes), as well as some notable

consequences of ROS exposure (DNA DSB, apoptosis, cellular senescence, p21 and p16 induction). Although in all cases we observed the expected age-associated increases, with the exception of p16 expression, we did not observe a significant effect of the *Myc*$^{+/-}$ genotype. Taken together, these results indicate that *Myc*$^{+/-}$ mice can achieve impressive gains in longevity without significant improvements in the efficacy of stress management pathways. It is important to note that long-lived *Myc*$^{+/-}$ *Drosophila* had a lower rate of spontaneous mutations, which was concluded to be the primary reason for their extended longevity (Greer et al., 2013). This does not necessarily contradict our data, since we measured DSBs rather than spontaneous point mutations. Therefore, a more comprehensive investigation of DNA mutations in *Myc*$^{+/-}$ mice should be considered as a future investigation.

Considering all the major longevity models no set of phenotypes or pathways emerges as a unifying correlation. In other words, animals can achieve extended lifespan by displaying an amelioration of some, but not all age-associated pathophysiologies. Aging is increasingly being viewed as a segmental process (Guerrero-Castilla et al., 2014), and the phenotypes of *Myc* hypomorphic animals are consistent with this notion. In agreement, a meta-analysis of gene expression showed very limited overlap between *Myc*$^{+/-}$ mice and CR, metformin or resveratrol treatments (with the exception of a few pathways related to metabolism and the immune system), even though the same analysis previously revealed connections between CR and metformin treatment (Martin-Montalvo et al., 2013). This underscores the apparently unique nature of the *Myc*$^{+/-}$-elicited lifespan extension.

The mechanisms by which reduced *Myc* expression results in the phenotypes described above, and how or if each contributes to increased longevity, remain incompletely understood. The vast number of genes and pathways regulated by MYC and the multifactorial nature of aging complicate this investigation. However, consideration of the evolution of aging may point us in the right direction. The tangible benefits observed in $Myc^{+/-}$ mice raise the question of why reduced MYC signaling has not been naturally selected for in evolution, especially in light of the absence of reproductive deficits. One explanation is that the natural level of *Myc* may be optimized for fitness in the wild, but a lower level is better suited for longevity in a laboratory.

In a natural setting, the smaller body size of $Myc^{+/-}$ mice would make them more susceptible to hypothermia and predation, and the immune and metabolic effects could increase risk of infection or starvation. Furthermore, there is little selective pressure to increase longevity in the wild, since few mice survive into old age due to extrinsic factors, thus the physiological benefits observed in these experiments would never be realized in wild mice. However, in the lab, there are no predators, no extreme temperatures, no pathogens, abundant food and water, and less need for physical activity, allowing the benefits of this genotype to outweigh the costs. Though the artifactual attributes of a laboratory environment may be perceived to marginalize our findings, they actually mimic human environments in first world countries: food and water are abundantly available, death from predation and hypothermia are almost nonexistent, many individuals are sedentary, and although our environments are not sterile, most infections can be treated with antibiotics or supportive care. Therefore, genetic

modifications that benefit a laboratory mouse would be expected to provide similar benefits to modern humans.

A general theme emerging from aging studies in multiple species is that "less is better": less food, less “growth” (somatotropic/IGF1) signaling, less anabolic activity, less protein translation, etc., and MYC certainly fits well in this paradigm. The majority of genes studied for their promotion of longevity act in signaling pathways and encode components that include hormones, receptors, protein kinases, phosphatases and adaptor proteins. Transcription factors have been relatively underrepresented, and MYC is unique because of the vast size of its regulome. The *Myc* gene is strongly upregulated by mitogens, and by virtue of its widespread targets constitutes the “gas pedal” that allows a cell to double its mass every 18-24 hours. It is thus not surprising that MYC is necessary during embryonic development, and that its deregulated expression strongly promotes cancer.

Several phenotypes of $Myc^{+/-}$ mice are known to be causally related to one another, and some phenotypes have already been connected to *Myc* or aging. By connecting these relationships together, we can create a set of possible mechanisms by which longevity is extended in these mice (Figure 5.1). MYC is most known for its role in cancer, and cancer is the leading of cause of death in laboratory mice, therefore relative cancer-resistance must contribute to increased longevity in $Myc^{+/-}$ mice. MYC is also involved in stem cell maintenance, especially that of HSCs (Eilers and Eisenman, 2008; Laurenti et al., 2009), which is probably why $Myc^{+/-}$ mice have delayed immunosenescence of T cell populations. This, in turn, can contribute to cancer resistance and also might prevent the age-associated increase in inflammation, which is

pathogenic in many diseases that contribute to mortality in mice. We found that decreasing *Myc* expression reduces the amount that other genes' expression changes with age, and from our expression data we can predict that adipogenic transcription factors are less active outside of adipose tissue, and more active in adipose tissue in old $Myc^{+/-}$ mice relative to $Myc^{+/+}$. These effects oppose the normal effects of aging on these transcription factors, and may prevent hepatosteatosis, increased serum cholesterol, and accumulation of adipose in muscle and other tissues, all of which otherwise cause disease and possibly death, and certainly decrease healthspan. Serum IGF1 is decreased in $Myc^{+/-}$ mice, and given the role of IGF1 in other long-lived mice, it is likely that this contributes to their increased longevity. Specifically, reducing IGF1 has been shown to delay osteoporosis (Moerth et al., 2007) and decrease body mass (Stratikopoulos et al., 2008). However, other phenotypes of mice with reduced IGF1 secretion or sensitivity are mostly distinct from those of $Myc^{+/-}$ mice, suggesting that reduced IGF1 may not strongly influence their lifespan. Lastly, through reduced IGF1 signaling and reduced cellular proliferation, $Myc^{+/-}$ mice have a smaller body mass, which likely explains their increased metabolic rate. A higher metabolic rate has also been observed in several other long-lived mouse models, and has been correlated with greater longevity in a cohort of outbred mice (Speakman et al., 2004), suggesting that this may also contribute to increased longevity in $Myc^{+/-}$ mice. There are of course many other possible mechanisms by which longevity is extended in these mice that we have not yet investigated, and some will be discussed below.

II. Future directions

We have learned a great deal about MYC, aging, and the relationship between them through the experiments described above, but there are several pieces to this story that we have not yet investigated. Both this project and existing literature on MYC and aging suggest several additional hypotheses that can be tested.

A fascinating caveat to aging is that somatic tissues in an organism will always decline in similar ways and at similar rates among individuals of a species, and yet the germline does not "age" or deteriorate over multiple generations. This can be explained by one of two possibilities: either aging is entirely caused by molecular insults from which the germline is completely protected, or the germline has the unique ability to repair or reset itself and thereby remove the effects of aging. Each of these has powerful implications. If the first is true, it suggests that future research could discover how the germline is shielded from molecular damage, and we could apply this to treat or prevent the diseases of aging. If the second is true, then discovery of the germline's reset mechanism and what it resets would reveal a primary underlying cause of aging. The first possibility seems unlikely, since all molecular damage that is associated with aging (e.g. oxidative damage, DNA mutations, protein aggregation, and chromosomal instability) can occur in the germline. However, assuming the genome is relatively unmodified, there are a number of possible ways that other cellular damage can be prevented from affecting future generations.

One possibility is that damaged molecules can be diluted out through successive rounds of division. However, even rapidly dividing somatic cells will eventually become

impaired, such as HSCs, so there must be a cause of aging that the germline has a unique method for reversing in order to eternally maintain their function. A likely candidate is epigenetic modification of the genome. The epigenome, including histone variants and methylation or acetylation of histones and DNA, changes with age in several tissues in mice and humans (Hidalgo and Gonzalez, 2013; Kreiling et al., 2011; Pegoraro and Misteli, 2009; Rodrigues et al., 2014). It is also reset during early development (Surani et al., 2007). This is consistent with epigenetic changes driving a substantial portion of aging from which the germline is immune. MYC has widespread effects on the epigenome both by recruiting chromatin modifying enzymes when it binds to DNA and by driving the expression of such enzymes, most notably histone acetyltransferase GCN5 (Knoepfler et al., 2006). The effects of MYC on chromatin have not been studied in the context of aging, but given the reduced effects of age on global gene expression in $Myc^{+/-}$ mice, it would not be surprising if chromatin was widely altered in these mice. Future experiments that compare the epigenome of $Myc^{+/-}$ with $Myc^{+/+}$ mice and then determine whether these changes oppose those of normal aging would clarify the role of epigenetic modification in lifespan extension of $Myc^{+/-}$ mice, and thereby in the aging process itself.

Another longevity-extending mechanism that is supported by existing evidence is preservation of stem cell function. Many, if not all, tissues rely on cell renewal via proliferation and differentiation of tissue-specific stem cells. In many cases, the quantity and/or function of stem cells declines with age, including the bone marrow, skeletal muscle, and brain (Cho et al., 2008; Hamilton et al., 2013; Jang et al., 2011). MYC's role in cancer suggests that it promotes an undifferentiated state, and therefore helps maintain stem cell populations. This is supported by the discovery that MYC is one of 4 factors,

along with Oct3/4, Sox2, and Klf4, which in combination have the remarkable ability to revert fibroblasts into embryonic stem cells (Takahashi and Yamanaka, 2006).

However, recent studies have shown that MYC can be detrimental to the aging of stem cell populations. As described above, HSCs in *Myc*$^{+/-}$ mice resist the decline in lymphoid progenitors that normally occurs with age. This is consistent with previous research on MYC in HSCs which showed that conditional elimination of *Myc* expression in the bone marrow prevented HSCs from differentiating and caused them to accumulate (Wilson et al., 2004). MYC is also known to be involved throughout the process of hematopoietic maturation, possibly mediated by its chromatin modifying effects in these cells (Laurenti et al., 2009). Thus, *Myc* hypomorphism might preserve HSCs for a longer period of time at the cost of reduced hematopoietic output of differentiated cells. MYC has also been shown to stimulate differentiation in epidermal stem cells (Watt et al., 2008), and ectopic expression of *Myc* results in their depletion (Waikel et al., 2001). These results suggest a balance in which greater *Myc* expression promotes differentiation and reduced *Myc* expression allows maintenance of the stem cell population.

It would therefore be interesting to investigate stem cells in tissues outside of the bone marrow in *Myc*$^{+/-}$ mice. A commonly studied stem cell population in aging mice is that of satellite cells in skeletal muscle, which have a reduced myogenic capacity with age in response to injury (Cousin et al., 2013). Neural stem cells in the subventricular zone also decline with age, resulting in impaired cognition and olfaction (Hamilton et al., 2013). The improved performance of old *Myc*$^{+/-}$ mice on the rotarod test suggests healthier neuromusculoskeletal function, and it would be interesting to investigate whether this results from healthier stem cells in these tissues. This could be studied by

measuring the quantity of stem cells in skeletal muscle, brain, and other tissues at young and old ages in each genotype of mice, and also assessing whether transplanted stem cells from old *Myc*$^{+/-}$ into old *Myc*$^{+/+}$ tissue have greater tissue repair capacity following an acute injury.

Chromosomal instability, which is the inability to maintain the same chromosomal content from one cell to its progeny through cell division, is another contributor to aging in mice. Specifically, this results in aneuploid cells, which have an unbalanced chromosome number that is not a multiple of the original haploid set. The prevalence of aneuploid cells increases with age as the mechanisms that mitigate chromosomal instability, most notably expression of the gene *Bubr1*, decline in old animals (Ricke and van Deursen, 2013). This can lead to cancer or otherwise impaired cell and tissue function, with a variety of specific effects depending on the affected chromosome and cell type. The importance of chromosomal instability in aging and cancer is highlighted by experiments in which mice that overexpress *Bubr1* were shown to have a reduced prevalence of aneuploid cells, resistance to cancer, and increased longevity (Baker et al., 2013).

There is evidence that MYC contributes to chromosomal instability in mice. Overexpression of MYC promotes a “mutator phenotype” in which DNA damage, including DSBs, is more frequent, and it can force cells through cell cycle checkpoints to replicate even in cases of genomic damage or failed chromosomal segregation (Li and Dang, 1999; Li et al., 2012; Prochownik 2008). While the effect of physiologic levels of MYC on chromosomal instability have not yet been investigated as thoroughly, it would not be surprising if MYC contributes to it in normal tissues. Therefore, the hypothesis

that *Myc*$^{+/-}$ mice are partially protected from chromosomal instability would be interesting to explore. This could be tested by using fluorescence *in situ* hybridization to quantify the percentage of cells aneuploid for each of several chromosomes in young and old mice from each genotype.

Although *Myc* is ubiquitously expressed, its family members *Mycn* and *Mycl1* are expressed in a complex and mosaic fashion in many tissues. Given that *Mycn* and *Mycl1* can substitute for *Myc* in many cell-based and biochemical assays, the overall level of MYC activity in a given cell type or tissue, and how this would be impacted by loss of one *Myc* allele, is not known. Although it is possible that the phenotypes of *Myc*$^{+/-}$ mice predominantly originate from one cell type or tissue and are mediated in an endocrine manner, given the diverse and widespread nature of these effects we think this is unlikely. Furthermore, cell-autonomous effects are clearly apparent in cell culture.

Many of the phenotypes that we observed could be accounted for by effects in adipose tissue and the hematopoietic system, and there are many tissues and organ systems in which *Myc* hypomorphism might not be beneficial, or might even be detrimental. As floxed *Myc* alleles are available (de Alboran et al., 2001; Trumpp et al., 2001), investigating the effects of tissue-specific reduction of MYC activity would be of considerable interest. Similarly, the relationship between lifespan and healthspan benefits and the level of MYC activity is not known. We tested a heterozygous (*Myc*$^{+/-}$) condition that resulted in ~50% levels of MYC mRNA and protein. Given that *Myc* hypomorphs down to ~25% expression are viable, it would be interesting to find the peak of the dose-response curve between MYC and longevity and ask whether animals at this level of expression continue to accrue healthspan benefits.

The results of this research could be most easily and directly applied to human health via pharmacological inhibition of MYC. This would also be a useful method to study MYC in aging or otherwise, since it could be applied at any age, dosage, or duration of treatment. The search for a MYC inhibitor has been ongoing for years due to its potential to treat many types of cancer (Wang et al., 2008), and the recently discovered role of MYC in aging would make such a drug all the more consequential. Unfortunately, MYC has proven difficult to target due to the way it interacts with its targets. It does not have a catalytic domain that can be blocked, but instead has interfaces for protein-protein interactions that have a number of high affinity sites for each domain. However, targeting some of these sites may be sufficient to reduce MYC activity (Prochownik and Vogt, 2010).

Other approaches include indirectly inhibiting MYC function by targeting its coactivator, MAX, or inhibiting *Myc* expression by targeting the bromodomain-containing protein BRD4 that recruits transcription factors to the *Myc* promoter. The most promising drug in the latter category, JQ1, has been shown to arrest proliferation in several cancer models that are dependent on MYC overexpression (Fowler et al., 2014). However, JQ1 has variable effects on different cell types, and it is not specific to MYC. Another drug, diclofenac, has recently been shown to reduce *Myc* expression and cell proliferation in a variety of cancer cell lines (Gottfried et al., 2013). Diclofenac has been in clinical use for decades as a non-steroidal anti-inflammatory drug, and like other NSAIDs, it inhibits cyclooxygenase enzymes I and II, but it has a variety of other mechanisms of action (Gan 2010). It would be interesting to study the effects of JQ1 and diclofenac on age-related phenotypes in mice, and eventually in humans. Unfortunately, a

small molecule that is a specific MYC inhibitor has not yet been discovered. However, if MYC inhibition in humans proves to be beneficial, it may soon be possible to use gene therapy to accomplish this. Gene therapy could be better than pharmacologic inhibition due to its permanence and the ability to target individual tissues separately.

Based mostly on cell culture studies it was widely believed that MYC is not expressed at all in quiescent cells, but it is now apparent that it is present in the majority of postmitotic tissues (albeit at low levels). Our discovery that long-term reduction of MYC activity robustly extends lifespan greatly extends our understanding of the biology regulated by this fascinating gene. Given the variety of other physiological benefits, particularly resistance to cancer, a healthier immune system, and improved musculoskeletal fitness, further studies of MYC and its targets should be an interesting avenue to explore in human medicine.

Table 5.1. Phenotypes of long-lived mice

						IGF1						mTOR			GH		
	Aging	*Myc*$^{+/-}$	CR	Metformin	*Pten*^{tg}	*Irs1*$^{-/-}$	*IGF1R*$^{+/-}$	*Pappa*$^{-/-}$	*Irs2*$^{+/-}$	*bIrs2*$^{+/-}$	*bIrs2*$^{-/-}$	Rapamycin	*Mtor*$^{\Delta/\Delta}$	*S6K1*$^{-/-}$	GHRKO	Snell	Ames
Median lifespan		↑	↑[36]	↑[28]	↑[41]	↑[43]	↑[49]	↑[52]	↑[56]	↑[56]	↑[56]	↑[22]	↑[58]	↑[59]	↑[60]	↑[14]	↑[14]
Maximum lifespan		↑	↑[36]	↑=[28]	↑[41]	↑[43]	=[49]	↑[52]	↑[56]	↑[56]	↑[56]	↑[22]	↑[58]	↑[59]	↑[60]	↑[14]	↑[14]
Body mass	↓	↓	↓[4]	↑↓[28]	↓[41]	↓[43]	↓[50]	↓[53]	=[57]	=[56]	=[56]	↓[23]	↓[58]	↓[59]	↓[14]	↓[14]	↓[14]
Adiposity	↑	=	↓[5]	=[28]	↓[41]	↓[43]				↑[56]	↑[56]		=[58]	↓[59]	↑[2]	↑[14]	=[15]
Metabolic rate	↓	↑	↑[35]	=[28]	↑[41]	=[43]	=[50]			↓[56]	↓[56]	=[24]	=[58]		↑[16]	↓[35]	↑[16]
Body temperature	=[1]	=	↓[6]	↑[28]	=[41]	↑[43]						=[24]			↓[2]	↓[35]	↓[2]
Cholesterol	↑	↓	↓[34]	↓[28]	↓[41]			=[52]				↑[24]					
Cancer	↑	↓	↓[4]	↓[29]	↓[41]	↑[44]	=[51]	↓[52]				↓[24]	↓[58]	=[59]	↓[14]	↓[14]	↓[17]
Serum IGF-1	=[2]	↓	↓[6]		↓[41]	=[43]	↑[49]	=[52]						=[59]	↓[60]	↓[14]	↓[2]
Fibrosis	↑	↓	↓[37]	↓[30]								=[23]					
DNA damage	↑	=	↓[8]	↓[31]								=[24]					↓[18]
Endogenous oxidative stress	↑	=	↓[9]	↓[28]								=[24]	↓[58]		=[14]		↓[14]
Susceptibility to chemical stress	↑[3]	=		↑[32]			↑↓[51]					↓[25]			↓[19]	↓[19]	↓[19]
Fertility	↓	=	↓[6]				=[50]	↓[55]		=[56]	↓[56]	↓[24]			↓[14]	↓[14]	↓[14]
Motor coordination	↓	↑	↑[10]	↑[28]	↑[41]	↑[43]						=[24]	↑[58]	↑[59]			↑[20]
Bone density	↓	↑	↑↓[11]			↑[43]						=[24]	↓[58]	↑[59]	↓[61]		↓[21]
Senescence	↑	=	↓[12]									↓[26]					
Apoptosis	↑	=	↑[13]	↑[33]			↓[51]					=[27]					
Mitochondrial number	=	=↑	=[8]	=[28]	↑[42]							=[46]					=[45]
Inflammation	↑[38]	↑↓	↓[4]	↓[28]								↓[47]			↓[62]		
Susceptibility to infection	↑[39]		↑[40]									↓[48]	↑[58]			↑[2]	
Insulin sensitivity	↓[63]	↓=	↑[65]	↑[28]		↓[43]	↓[51]		↑[56]	↓[56]	↓[56]	↓[24]	=[58]	↑[2]	↑[60]		↑[2]
Baseline glucose	↑=[64]	=	↓[66]	=[28]		↓=[43]	↑=[51]		↓[56]			=[24]	=[58]	=[67]	↓[60]		↓[68]

Table 5.1. Phenotypes of long-lived mice

Summary of common phenotypes in long-lived mice. ↑: greater effect; ↓: reduced effect; =: equal effect. Multiple or conflicting effects are indicated by a combination of the above. Column 1 shows the effects of normal aging in mice. References in the table are:

[1](Piao et al., 2005); [2](Ohnishi et al., 2011); [3](Lopez-Diazguerrero et al., 2005); [4](Jalland et al., 2013); [5](Trivedi and Jena, 2013a); [6](Liu et al., 2014); [7](Ye et al., 2013); [8](Yamamoto et al., 2013); [9](Yang et al., 2013); [10](Doreswamy et al., 2004); [11](Jeng et al., 2013); [12](Campagnaro et al., 2013); [13](Tonini et al., 2013); [14](Bartke and Brown-Borg, 2004); [15](Trivedi and Jena, 2013b); [16](Zhou et al., 2004); [17](Samadder et al., 2011); [18](Tasaki et al., 2013); [19](Gao et al., 2013); [20](Rani et al., 2012); [21](Song et al., 2012); [22](Tsuzuki et al., 2011a); [23](Zhang et al., 2011); [24](Pratheeshkumar et al., 2010); [25](Hwang et al., 2010); [26](Wong et al., 2011); [27](Liao et al., 2010); [28](Martin-Montalvo et al., 2013); [29](Szczesny et al., 2010); [30](Lovell et al., 2009); [31](Li et al., 2010); [32](Ishii et al., 2009); [33](Tripathi and Jena, 2009); [34](Tsuchiya et al., 2004); [35](Bartke and Westbrook, 2012); [36](Mercken et al., 2012); [37](Yan et al., 2013); [38](Narasimhaiah et al., 2005); [39](Reliene et al., 2004); [40](Das et al., 2013); [41](Ortega-Molina et al., 2012); [42](Garcia-Cao et al., 2012); [43](Selman et al., 2008); [44](Tripathi and Jena, 2008); [45](Xie et al., 2012); [46](Jeng and Wells, 2010); [47](McCallum et al., 2011); [48](Wang et al., 2011); [49](Okamoto et al., 2008); [50](Holzenberger et al., 2003); [51](Bokov et al., 2011); [52](Wang et al., 2006); [53](Yuan et al., 2006); [54](Kuroiwa et al., 2007); [55](Gudkov et al., 2006); [56](Taguchi et al., 2007); [57](Russo et al., 2004); [58](Guerrero-Castilla et al., 2014); [59](Ringvoll et al., 2006); [60](Coschigano et al., 2003); [61](Sinha and Roy, 2011); [62](Tsuzuki et al., 2011b); [63](Gonzalez-Rodriguez et al., 2012); [64](Rogers et al., 2012); [65](Heilbronn and Ravussin, 2003); [66](Barger et al., 2003); [67](Um et al., 2004); [68](Borg et al., 1995).

Figure 5.1

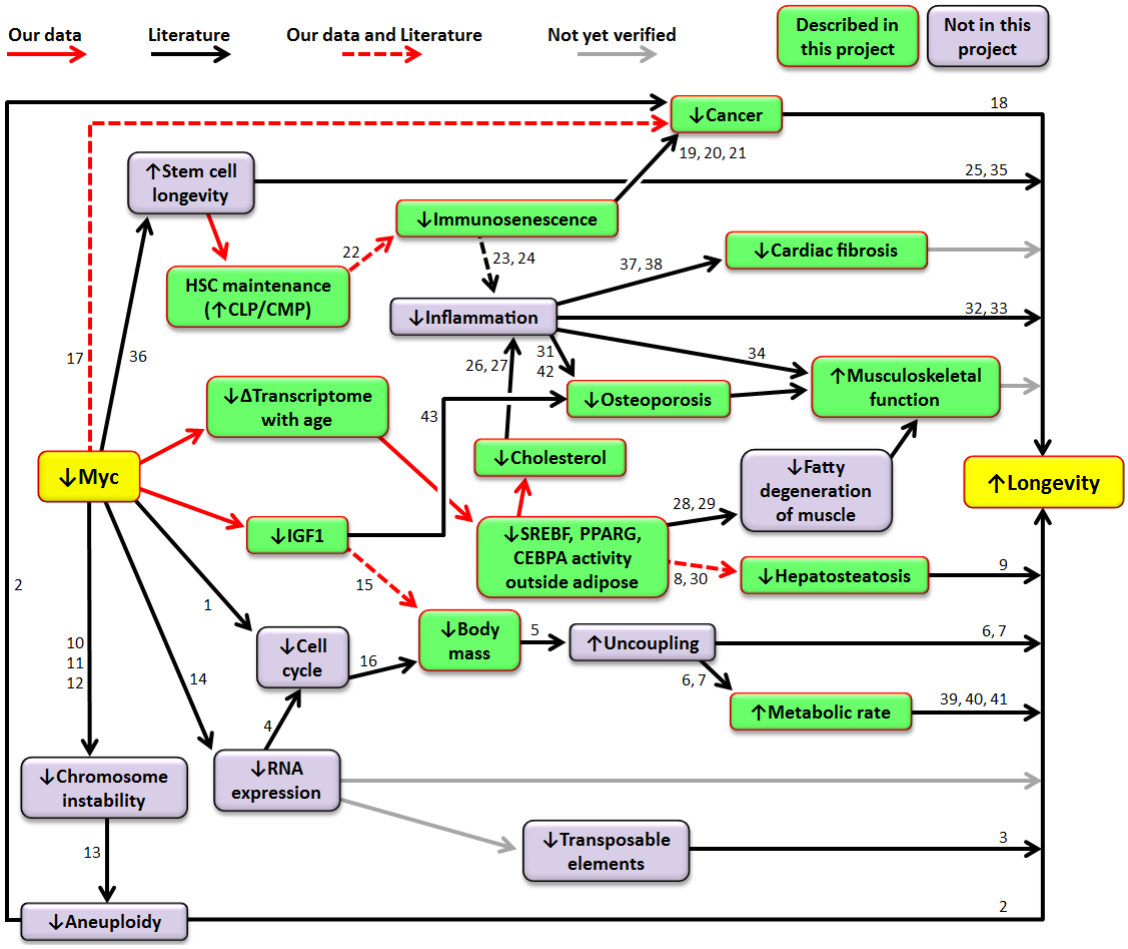
Our data
Literature
Our data and Literature
Not yet verified
Described in this project
Not in this project
↓Cancer
↑Stem cell longevity
↓Immunosenescence
HSC maintenance (↑CLP/CMP)
↓Inflammation
↓Cardiac fibrosis
↓Osteoporosis
↑Musculoskeletal function
↓ΔTranscriptome with age
↓Cholesterol
↓Myc
↓IGF1
↓SREBF, PPARG, CEBPA activity outside adipose
↓Fatty degeneration of muscle
↑Longevity
↓Hepatosteatosis
↓Cell cycle
↓Body mass
↑Uncoupling
↑Metabolic rate
↓Chromosome instability
↓RNA expression
↓Transposable elements
↓Aneuploidy
18
19, 20, 21
25, 35
22
23, 24
37, 38
32, 33
17
36
26, 27
31
42
34
43
28, 29
2
15
8, 30
9
1
10
11
12
5
6, 7
14
16
6, 7
39, 40, 41
4
13
3
2

Figure 5.1. Pathways to health

This figure summarizes some of the phenotypes observed in *Myc*$^{+/-}$ mice and connects them to suggest how *Myc* hypomorphism causes longevity extension. Green boxes indicate phenotypes that were observed in *Myc*$^{+/-}$ mice, and purple boxes are phenotypes that are hypothesized to exist in *Myc*$^{+/-}$ mice given evidence from the literature.

The references listed are:

[1](Hanson et al., 1994); [2](Ricke and van Deursen, 2013); [3](Sedivy et al., 2013); [4](Marguerat and Bahler, 2012); [5](Cannon and Nedergaard, 2004); [6] (Speakman et al., 2004); [7](Mookerjee et al., 2010); [8](Frith et al., 1983); [9](Matteoni et al., 1999); [10](Li et al., 2012); [11](Li and Dang, 1999); [12](Prochownik 2008); [13](Potapova et al., 2013); [14](Loven et al., 2012); [15](Stratikopoulos et al., 2008); [16](Trumpp et al., 2001); [17](Dang 2012); [18](Storer 1966); [19](Kang et al., 2011); [20](Baldwin 1955); [21](Pawelec et al., 2010); [22](Geiger et al., 2013); [23](Michaud et al., 2013); [24](Sauce et al., 2009); [25](Jang et al., 2011); [26](Huang et al., 2007); [27](Wouters et al., 2008); [28](Hu et al., 1995); [29](Vettor et al., 2009); [30](She et al., 2005); [31](Lacativa and Farias, 2010); [32](Goto 2008); [33](Alonso-Fernandez and De la Fuente, 2011); [34](Degens 2010); [35](Cho et al., 2008); [36](Eilers and Eisenman, 2008); [37](Shen et al., 2014); [38](Wang et al., 2014); [39](Westbrook et al., 2009); [40](Hasek et al., 2010); [41](Speakman et al., 2004); [42](Polzer et al., 2010); [43](Moerth et al., 2007).

References

Akbar AN, Henson SM (2011) Are senescence and exhaustion intertwined or unrelated processes that compromise immunity? Nat Rev Immunol *11*(4):289-295

Alonso-Fernandez P, De la Fuente M (2011) Role of the immune system in aging and longevity. Curr Aging Sci *4*(2):78-100

Amati F, Dube JJ, Coen PM, Stefanovic-Racic M, Toledo FG, Goodpaster BH (2009) Physical inactivity and obesity underlie the insulin resistance of aging. Diabetes Care *32*(8):1547-1549

Anisimov VN, Arbeev KG, Popovich IG, Zabezhinksi MA, Rosenfeld SV, Piskunova TS, Arbeeva LS, Semenchenko AV, Yashin AI (2004) Body weight is not always a good predictor of longevity in mice. Exp Gerontol *39*(3):305-319

Annema W, Tietge UJ (2011) Role of hepatic lipase and endothelial lipase in high-density lipoprotein-mediated reverse cholesterol transport. Curr Atheroscler Rep *13*(3):257-265

Araki K, Ellebedy AH, Ahmed R (2011) TOR in the immune system. Curr Opin Cell Biol *23*(6):707-715

Araki K, Turner AP, Shaffer VO, Gangappa S, Keller SA, Bachmann MF, Larsen CP, Ahmed R (2009) mTOR regulates memory CD8 T-cell differentiation. Nature *460*(7251):108-112

Athineos D, Sansom OJ (2010) Myc heterozygosity attenuates the phenotypes of APC deficiency in the small intestine. Oncogene *29*(17):2585-2590

Baker DJ, Dawlaty MM, Wijshake T, Jeganathan KB, Malureanu L, van Ree JH, Crespo-Diaz R, Reyes S, Seaburg L, Shapiro V*, et al.* (2013) Increased expression of BubR1 protects against aneuploidy and cancer and extends healthy lifespan. Nat Cell Biol *15*(1):96-102

Baker DJ, Jeganathan KB, Cameron JD, Thompson M, Juneja S, Kopecka A, Kumar R, Jenkins RB, de Groen PC, Roche P*, et al.* (2004) BubR1 insufficiency causes early onset of aging-associated phenotypes and infertility in mice. Nat Genet *36*(7):744-749

Baldwin RW (1955) Immunity to methylcholanthrene-induced tumours in inbred rats following atrophy and regression of the implanted tumours. Br J Cancer *9*(4):652-657

Balietti M, Casoli T, Di Stefano G, Giorgetti B, Aicardi G, Fattoretti P (2010) Ketogenic diets: an historical antiepileptic therapy with promising potentialities for the aging brain. Ageing Res Rev *9*(3):273-279

Barger JL, Walford RL, Weindruch R (2003) The retardation of aging by caloric restriction: its significance in the transgenic era. Exp Gerontol *38*(11-12):1343-1351

Barnard RJ, Lawani LO, Martin DA, Youngren JF, Singh R, Scheck SH (1992) Effects of maturation and aging on the skeletal muscle glucose transport system. Am J Physiol *262*(5 Pt 1):E619-626

Bartke A, Brown-Borg H (2004) Life extension in the dwarf mouse. Curr Top Dev Biol *63*189-225

Bartke A, Sun LY, Longo V (2013) Somatotropic signaling: trade-offs between growth, reproductive development, and longevity. Physiol Rev *93*(2):571-598

Bartke A, Westbrook R (2012) Metabolic characteristics of long-lived mice. Front Genet *3*288

Berlett BS, Stadtman ER (1997) Protein oxidation in aging, disease, and oxidative stress. J Biol Chem *272*(33):20313-20316

Bluher M, Kahn BB, Kahn CR (2003) Extended longevity in mice lacking the insulin receptor in adipose tissue. Science *299*(5606):572-574

Bokov A, Chaudhuri A, Richardson A (2004) The role of oxidative damage and stress in aging. Mech Ageing Dev *125*(10-11):811-826

Bokov AF, Garg N, Ikeno Y, Thakur S, Musi N, DeFronzo RA, Zhang N, Erickson RC, Gelfond J, Hubbard GB*, et al.* (2011) Does reduced IGF-1R signaling in Igf1r+/- mice alter aging? PLoS One *6*(11):e26891

Borg KE, Brown-Borg HM, Bartke A (1995) Assessment of the primary adrenal cortical and pancreatic hormone basal levels in relation to plasma glucose and age in the unstressed Ames dwarf mouse. Proc Soc Exp Biol Med *210*(2):126-133

Bose C, Bhuvaneswaran C, Udupa KB (2005) Age-related alteration in hepatic acyl-CoA: cholesterol acyltransferase and its relation to LDL receptor and MAPK. Mech Ageing Dev *126*(6-7):740-751

Boylston WH, Gerstner A, DeFord JH, Madsen M, Flurkey K, Harrison DE, Papaconstantinou J (2004) Altered cholesterologenic and lipogenic transcriptional profile in livers of aging Snell dwarf (Pit1dw/dwJ) mice. Aging Cell *3*(5):283-296

Brand MD (2000) Uncoupling to survive? The role of mitochondrial inefficiency in ageing. Exp Gerontol *35*(6-7):811-820

Bratic I, Trifunovic A (2010) Mitochondrial energy metabolism and ageing. Biochim Biophys Acta *1797*(6-7):961-967

Brayton C (2009). Spontaneous Diseases in Commonly Used Mouse Strains / Stocks (http://www.hopkinsmedicine.org).

Brown-Borg H, Johnson WT, Rakoczy S, Romanick M (2001) Mitochondrial oxidant generation and oxidative damage in Ames dwarf and GH transgenic mice. J Am Aging Assoc *24*(3):85-96

Brown-Borg HM, Borg KE, Meliska CJ, Bartke A (1996) Dwarf mice and the ageing process. Nature *384*(6604):33

Caldeira da Silva CC, Cerqueira FM, Barbosa LF, Medeiros MH, Kowaltowski AJ (2008) Mild mitochondrial uncoupling in mice affects energy metabolism, redox balance and longevity. Aging Cell *7*(4):552-560

Campagnaro BP, Tonini CL, Nogueira BV, Casarini DE, Vasquez EC, Meyrelles SS (2013) DNA damage and augmented oxidative stress in bone marrow mononuclear cells from Angiotensin-dependent hypertensive mice. Int J Hypertens *2013*305202

Campisi J (2013) Aging, cellular senescence, and cancer. Annu Rev Physiol *75*685-705

Cannon B, Nedergaard J (2004) Brown adipose tissue: function and physiological significance. Physiol Rev *84*(1):277-359

Chao CC, Ma YS, Stadtman ER (1997) Modification of protein surface hydrophobicity and methionine oxidation by oxidative systems. Proc Natl Acad Sci U S A *94*(7):2969-2974

Chen C, Liu Y, Zheng P (2009) mTOR regulation and therapeutic rejuvenation of aging hematopoietic stem cells. Sci Signal *2*(98):ra75

Cho RH, Sieburg HB, Muller-Sieburg CE (2008) A new mechanism for the aging of hematopoietic stem cells: aging changes the clonal composition of the stem cell compartment but not individual stem cells. Blood *111*(12):5553-5561

Chung HY, Kim HJ, Kim KW, Choi JS, Yu BP (2002) Molecular inflammation hypothesis of aging based on the anti-aging mechanism of calorie restriction. Microsc Res Tech *59*(4):264-272

Conover CA, Bale LK (2007) Loss of pregnancy-associated plasma protein A extends lifespan in mice. Aging Cell *6*(5):727-729

Coschigano KT, Holland AN, Riders ME, List EO, Flyvbjerg A, Kopchick JJ (2003) Deletion, but not antagonism, of the mouse growth hormone receptor results in severely decreased body weights, insulin, and insulin-like growth factor I levels and increased life span. Endocrinology *144*(9):3799-3810

Cottrell DA, Turnbull DM (2000) Mitochondria and ageing. Curr Opin Clin Nutr Metab Care *3*(6):473-478

Cousin W, Ho ML, Desai R, Tham A, Chen RY, Kung S, Elabd C, Conboy IM (2013) Regenerative capacity of old muscle stem cells declines without significant accumulation of DNA damage. PLoS One *8*(5):e63528

Dai DF, Santana LF, Vermulst M, Tomazela DM, Emond MJ, MacCoss MJ, Gollahon K, Martin GM, Loeb LA, Ladiges WC*, et al.* (2009) Overexpression of catalase targeted to mitochondria attenuates murine cardiac aging. Circulation *119*(21):2789-2797

Dang CV (2012) MYC on the path to cancer. Cell *149*(1):22-35

Danilovich N, Wernsing D, Coschigano KT, Kopchick JJ, Bartke A (1999) Deficits in female reproductive function in GH-R-KO mice; role of IGF-I. Endocrinology *140*(6):2637-2640

Das JK, Sarkar S, Hossain SU, Chakraborty P, Das RK, Bhattacharya S (2013) Diphenylmethyl selenocyanate attenuates malachite green induced oxidative injury through antioxidation & inhibition of DNA damage in mice. Indian J Med Res *137*(6):1163-1173

de Alboran IM, O'Hagan RC, Gartner F, Malynn B, Davidson L, Rickert R, Rajewsky K, DePinho RA, Alt FW (2001) Analysis of C-MYC function in normal cells via conditional gene-targeted mutation. Immunity *14*(1):45-55

De Cecco M, Criscione SW, Peterson AL, Neretti N, Sedivy JM, Kreiling JA (2013) Transposable elements become active and mobile in the genomes of aging mammalian somatic tissues. Aging (Albany NY) *5*(12):867-883

Dean DJ, Cartee GD (1996) Brief dietary restriction increases skeletal muscle glucose transport in old Fischer 344 rats. J Gerontol A Biol Sci Med Sci *51*(3):B208-213

Debacq-Chainiaux F, Erusalimsky JD, Campisi J, Toussaint O (2009) Protocols to detect senescence-associated beta-galactosidase (SA-betagal) activity, a biomarker of senescent cells in culture and in vivo. Nat Protoc *4*(12):1798-1806

Degens H (2010) The role of systemic inflammation in age-related muscle weakness and wasting. Scand J Med Sci Sports *20*(1):28-38

Dias AT, Rodrigues BP, Porto ML, Gava AL, Balarini CM, Freitas FP, Palomino Z, Casarini DE, Campagnaro BP, Pereira TM*, et al.* (2014) Sildenafil ameliorates oxidative stress and DNA damage in the stenotic kidneys in mice with renovascular hypertension. J Transl Med *12*(1):35

Doreswamy K, Shrilatha B, Rajeshkumar T, Muralidhara (2004) Nickel-induced oxidative stress in testis of mice: evidence of DNA damage and genotoxic effects. J Androl *25*(6):996-1003

Duverger N, Tremp G, Caillaud JM, Emmanuel F, Castro G, Fruchart JC, Steinmetz A, Denefle P (1996) Protection against atherogenesis in mice mediated by human apolipoprotein A-IV. Science *273*(5277):966-968

Eilers M, Eisenman RN (2008) Myc's broad reach. Genes Dev *22*(20):2755-2766

Fan Y, Dickman KG, Zong WX (2010) Akt and c-Myc differentially activate cellular metabolic programs and prime cells to bioenergetic inhibition. J Biol Chem *285*(10):7324-7333

Flores I, Canela A, Vera E, Tejera A, Cotsarelis G, Blasco MA (2008) The longest telomeres: a general signature of adult stem cell compartments. Genes Dev *22*(5):654-667

Flurkey K, Papaconstantinou J, Miller RA, Harrison DE (2001) Lifespan extension and delayed immune and collagen aging in mutant mice with defects in growth hormone production. Proc Natl Acad Sci U S A *98*(12):6736-6741

Folch J, Lees M, Sloane Stanley GH (1957) A simple method for the isolation and purification of total lipides from animal tissues. J Biol Chem *226*(1):497-509

Fowler T, Ghatak P, Price DH, Conaway R, Conaway J, Chiang CM, Bradner JE, Shilatifard A, Roy AL (2014) Regulation of MYC expression and differential JQ1 sensitivity in cancer cells. PLoS One *9*(1):e87003

Franceschi C, Bonafe M, Valensin S, Olivieri F, De Luca M, Ottaviani E, De Benedictis G (2000) Inflamm-aging. An evolutionary perspective on immunosenescence. Ann N Y Acad Sci *908*244-254

Freda PU, Shen W, Heymsfield SB, Reyes-Vidal CM, Geer EB, Bruce JN, Gallagher D (2008) Lower visceral and subcutaneous but higher intermuscular adipose tissue depots in patients with growth hormone and insulin-like growth factor I excess due to acromegaly. J Clin Endocrinol Metab *93*(6):2334-2343

Frenzel H, Feimann J (1984) Age-dependent structural changes in the myocardium of rats. A quantitative light- and electron-microscopic study on the right and left chamber wall. Mech Ageing Dev *27*(1):29-41

Frith CH, Highman B, Burger G, Sheldon WD (1983) Spontaneous lesions in virgin and retired breeder BALB/c and C57BL/6 mice. Lab Anim Sci *33*(3):273-286

Fujimoto T, Parton RG (2011) Not just fat: the structure and function of the lipid droplet. Cold Spring Harb Perspect Biol *3*(3):

Gan TJ (2010) Diclofenac: an update on its mechanism of action and safety profile. Curr Med Res Opin *26*(7):1715-1731

Gao H, Dong Y, Meng C, Guan W, Liu Y, Xing G (2013) Investigation of organic pollutants in wastewater-irrigated soil and its DNA damage and oxidative damage on mice. Environ Monit Assess *185*(3):2475-2482

Garcia-Cao I, Song MS, Hobbs RM, Laurent G, Giorgi C, de Boer VC, Anastasiou D, Ito K, Sasaki AT, Rameh L*, et al.* (2012) Systemic elevation of PTEN induces a tumor-suppressive metabolic state. Cell *149*(1):49-62

Gardner EM (2005) Caloric restriction decreases survival of aged mice in response to primary influenza infection. J Gerontol A Biol Sci Med Sci *60*(6):688-694

Gates AC, Bernal-Mizrachi C, Chinault SL, Feng C, Schneider JG, Coleman T, Malone JP, Townsend RR, Chakravarthy MV, Semenkovich CF (2007) Respiratory uncoupling in skeletal muscle delays death and diminishes age-related disease. Cell Metab *6*(6):497-505

Geiger H, de Haan G, Florian MC (2013) The ageing haematopoietic stem cell compartment. Nat Rev Immunol *13*(5):376-389

Geiger H, Rudolph KL (2009) Aging in the lympho-hematopoietic stem cell compartment. Trends Immunol *30*(7):360-365

Gonzalez-Rodriguez A, Mas-Gutierrez JA, Mirasierra M, Fernandez-Perez A, Lee YJ, Ko HJ, Kim JK, Romanos E, Carrascosa JM, Ros M*, et al.* (2012) Essential role of protein tyrosine phosphatase 1B in obesity-induced inflammation and peripheral insulin resistance during aging. Aging Cell *11*(2):284-296

Goronzy JJ, Weyand CM (2005) T cell development and receptor diversity during aging. Curr Opin Immunol *17*(5):468-475

Goto M (2008) Inflammaging (inflammation + aging): A driving force for human aging based on an evolutionarily antagonistic pleiotropy theory? Biosci Trends *2*(6):218-230

Gottfried E, Lang SA, Renner K, Bosserhoff A, Gronwald W, Rehli M, Einhell S, Gedig I, Singer K, Seilbeck A*, et al.* (2013) New aspects of an old drug--diclofenac targets MYC and glucose metabolism in tumor cells. PLoS One *8*(7):e66987

Greer C, Lee M, Westerhof M, Milholland B, Spokony R, Vijg J, Secombe J (2013) Myc-dependent genome instability and lifespan in Drosophila. PLoS One *8*(9):e74641

Gudkov SV, Shtarkman IN, Smirnova VS, Chernikov AV, Bruskov VI (2006) Guanosine and inosine display antioxidant activity, protect DNA in vitro from oxidative damage induced by reactive oxygen species, and serve as radioprotectors in mice. Radiat Res *165*(5):538-545

Guerrero-Castilla A, Olivero-Verbel J, Marrugo-Negrete J (2014) Heavy metals in feral mice from coal-mining areas of Colombia and expression of genes related to oxidative stress, DNA damage and exposure to metals. Mutat Res

Guertin DA, Stevens DM, Thoreen CC, Burds AA, Kalaany NY, Moffat J, Brown M, Fitzgerald KJ, Sabatini DM (2006) Ablation in mice of the mTORC components raptor, rictor, or mLST8 reveals that mTORC2 is required for signaling to Akt-FOXO and PKCalpha, but not S6K1. Dev Cell *11*(6):859-871

Guney I, Wu S, Sedivy JM (2006) Reduced c-Myc signaling triggers telomere-independent senescence by regulating Bmi-1 and p16(INK4a). Proc Natl Acad Sci U S A *103*(10):3645-3650

Guo Y, Niu C, Breslin P, Tang M, Zhang S, Wei W, Kini AR, Paner GP, Alkan S, Morris SW*, et al.* (2009) c-Myc-mediated control of cell fate in megakaryocyte-erythrocyte progenitors. Blood *114*(10):2097-2106

Hamilton KK, Lee K, Doetsch PW (1994) Detection and characterization of eukaryotic enzymes that recognize oxidative DNA damage. Methods Enzymol *234*33-44

Hamilton LK, Joppe SE, L MC, Fernandes KJ (2013) Aging and neurogenesis in the adult forebrain: what we have learned and where we should go from here. Eur J Neurosci *37*(12):1978-1986

Hamilton ML, Van Remmen H, Drake JA, Yang H, Guo ZM, Kewitt K, Walter CA, Richardson A (2001) Does oxidative damage to DNA increase with age? Proc Natl Acad Sci U S A *98*(18):10469-10474

Hanson KD, Shichiri M, Follansbee MR, Sedivy JM (1994) Effects of c-myc expression on cell cycle progression. Mol Cell Biol *14*(9):5748-5755

Harman D (1972) The biologic clock: the mitochondria? J Am Geriatr Soc *20*(4):145-147

Harper JM, Leathers CW, Austad SN (2006) Does caloric restriction extend life in wild mice? Aging Cell *5*(6):441-449

Harper JM, Salmon AB, Leiser SF, Galecki AT, Miller RA (2007) Skin-derived fibroblasts from long-lived species are resistant to some, but not all, lethal stresses and to the mitochondrial inhibitor rotenone. Aging Cell *6*(1):1-13

Harrison DE, Strong R, Sharp ZD, Nelson JF, Astle CM, Flurkey K, Nadon NL, Wilkinson JE, Frenkel K, Carter CS*, et al.* (2009) Rapamycin fed late in life extends lifespan in genetically heterogeneous mice. Nature *460*(7253):392-395

Harvey AE, Lashinger LM, Otto G, Nunez NP, Hursting SD (2013) Decreased systemic IGF-1 in response to calorie restriction modulates murine tumor cell growth, nuclear factor-kappaB activation, and inflammation-related gene expression. Mol Carcinog *52*(12):997-1006

Hasek BE, Stewart LK, Henagan TM, Boudreau A, Lenard NR, Black C, Shin J, Huypens P, Malloy VL, Plaisance EP*, et al.* (2010) Dietary methionine restriction enhances metabolic flexibility and increases uncoupled respiration in both fed and fasted states. Am J Physiol Regul Integr Comp Physiol *299*(3):R728-739

Hauck SJ, Hunter WS, Danilovich N, Kopchick JJ, Bartke A (2001) Reduced levels of thyroid hormones, insulin, and glucose, and lower body core temperature in the growth hormone receptor/binding protein knockout mouse. Exp Biol Med (Maywood) *226*(6):552-558

He J, Goodpaster BH, Kelley DE (2004) Effects of weight loss and physical activity on muscle lipid content and droplet size. Obes Res *12*(5):761-769

Heilbronn LK, Ravussin E (2003) Calorie restriction and aging: review of the literature and implications for studies in humans. Am J Clin Nutr *78*(3):361-369

Heininger U, Cotter PA, Fescemyer HW, Martinez de Tejada G, Yuk MH, Miller JF, Harvill ET (2002) Comparative phenotypic analysis of the Bordetella parapertussis isolate chosen for genomic sequencing. Infect Immun *70*(7):3777-3784

Hidalgo I, Gonzalez S (2013) New epigenetic pathway for stemness maintenance mediated by the histone methyltransferase Ezh1. Cell Cycle *12*(3):383-384

Hoeijmakers JH (2009) DNA damage, aging, and cancer. N Engl J Med *361*(15):1475-1485

Holzenberger M, Dupont J, Ducos B, Leneuve P, Geloen A, Even PC, Cervera P, Le Bouc Y (2003) IGF-1 receptor regulates lifespan and resistance to oxidative stress in mice. Nature *421*(6919):182-187

Houde VP, Brule S, Festuccia WT, Blanchard PG, Bellmann K, Deshaies Y, Marette A (2010) Chronic rapamycin treatment causes glucose intolerance and hyperlipidemia by upregulating hepatic gluconeogenesis and impairing lipid deposition in adipose tissue. Diabetes *59*(6):1338-1348

Hsu HC, Zhang HG, Li L, Yi N, Yang PA, Wu Q, Zhou J, Sun S, Xu X, Yang X*, et al.* (2003) Age-related thymic involution in C57BL/6J x DBA/2J recombinant-inbred mice maps to mouse chromosomes 9 and 10. Genes Immun *4*(6):402-410

Hu E, Tontonoz P, Spiegelman BM (1995) Transdifferentiation of myoblasts by the adipogenic transcription factors PPAR gamma and C/EBP alpha. Proc Natl Acad Sci U S A *92*(21):9856-9860

Huang H, Liu T, Rose JL, Stevens RL, Hoyt DG (2007) Sensitivity of mice to lipopolysaccharide is increased by a high saturated fat and cholesterol diet. J Inflamm (Lond) *4*22

Hunter WS, Croson WB, Bartke A, Gentry MV, Meliska CJ (1999) Low body temperature in long-lived Ames dwarf mice at rest and during stress. Physiol Behav *67*(3):433-437

Hwang YJ, Jeung YS, Seo MH, Yoon JY, Kim DY, Park JW, Han JH, Jeong SH (2010) Asian dust and titanium dioxide particles-induced inflammation and oxidative DNA damage in C57BL/6 mice. Inhal Toxicol *22*(13):1127-1133

Ikeno Y, Bronson RT, Hubbard GB, Lee S, Bartke A (2003) Delayed occurrence of fatal neoplastic diseases in ames dwarf mice: correlation to extended longevity. J Gerontol A Biol Sci Med Sci *58*(4):291-296

Ikeno Y, Hubbard GB, Lee S, Cortez LA, Lew CM, Webb CR, Berryman DE, List EO, Kopchick JJ, Bartke A (2009) Reduced incidence and delayed occurrence of fatal neoplastic diseases in growth hormone receptor/binding protein knockout mice. J Gerontol A Biol Sci Med Sci *64*(5):522-529

Ingle GR, Sievers TM, Holt CD (2000) Sirolimus: continuing the evolution of transplant immunosuppression. Ann Pharmacother *34*(9):1044-1055

Intlekofer KA, Cotman CW (2013) Exercise counteracts declining hippocampal function in aging and Alzheimer's disease. Neurobiol Dis *57*47-55

Ishii Y, Okamura T, Inoue T, Tasaki M, Umemura T, Nishikawa A (2009) Dietary catechol causes increased oxidative DNA damage in the livers of mice treated with acetaminophen. Toxicology *263*(2-3):93-99

Ishikawa M, Iwasaki Y, Yatoh S, Kato T, Kumadaki S, Inoue N, Yamamoto T, Matsuzaka T, Nakagawa Y, Yahagi N*, et al.* (2008) Cholesterol accumulation and diabetes in pancreatic beta-cell-specific SREBP-2 transgenic mice: a new model for lipotoxicity. J Lipid Res *49*(12):2524-2534

Jalland CM, Benestad SL, Ersdal C, Scheffler K, Suganthan R, Nakabeppu Y, Eide L, Bjoras M, Tranulis MA (2013) Accelerated clinical course of prion disease in mice compromised in repair of oxidative DNA damage. Free Radic Biol Med *68C*1-7

James L, Eisenman RN (2002) Myc and Mad bHLHZ domains possess identical DNA-binding specificities but only partially overlapping functions in vivo. Proc Natl Acad Sci U S A *99*(16):10429-10434

Jang YC, Sinha M, Cerletti M, Dall'Osso C, Wagers AJ (2011) Skeletal muscle stem cells: effects of aging and metabolism on muscle regenerative function. Cold Spring Harb Symp Quant Biol *76*101-111

Jeng W, Loniewska MM, Wells PG (2013) Brain glucose-6-phosphate dehydrogenase protects against endogenous oxidative DNA damage and neurodegeneration in aged mice. ACS Chem Neurosci *4*(7):1123-1132

Jeng W, Wells PG (2010) Reduced 3,4-methylenedioxymethamphetamine (MDMA, Ecstasy)-initiated oxidative DNA damage and neurodegeneration in prostaglandin H synthase-1 knockout mice. ACS Chem Neurosci *1*(5):366-380

Jeyapalan JC, Ferreira M, Sedivy JM, Herbig U (2007) Accumulation of senescent cells in mitotic tissue of aging primates. Mech Ageing Dev *128*(1):36-44

Jeyapalan JC, Sedivy JM (2013) How to measure RNA expression in rare senescent cells expressing any specific protein such as p16Ink4a. Aging (Albany NY) *5*(2):120-129

Kang TW, Yevsa T, Woller N, Hoenicke L, Wuestefeld T, Dauch D, Hohmeyer A, Gereke M, Rudalska R, Potapova A*, et al.* (2011) Senescence surveillance of pre-malignant hepatocytes limits liver cancer development. Nature *479*(7374):547-551

Knoepfler PS, Zhang XY, Cheng PF, Gafken PR, McMahon SB, Eisenman RN (2006) Myc influences global chromatin structure. EMBO J *25*(12):2723-2734

Kreiling JA, Tamamori-Adachi M, Sexton AN, Jeyapalan JC, Munoz-Najar U, Peterson AL, Manivannan J, Rogers ES, Pchelintsev NA, Adams PD*, et al.* (2011) Age-associated increase in heterochromatic marks in murine and primate tissues. Aging Cell *10*(2):292-304

Kristan DM (2007) Chronic calorie restriction increases susceptibility of laboratory mice (Mus musculus) to a primary intestinal parasite infection. Aging Cell *6*(6):817-825

Kuroiwa Y, Umemura T, Nishikawa A, Kanki K, Ishii Y, Kodama Y, Masumura K, Nohmi T, Hirose M (2007) Lack of in vivo mutagenicity and oxidative DNA damage by flumequine in the livers of gpt delta mice. Arch Toxicol *81*(1):63-69

Lacativa PG, Farias ML (2010) Osteoporosis and inflammation. Arq Bras Endocrinol Metabol *54*(2):123-132

Lamming DW, Sabatini DM (2013) A Central role for mTOR in lipid homeostasis. Cell Metab *18*(4):465-469

Lamming DW, Ye L, Katajisto P, Goncalves MD, Saitoh M, Stevens DM, Davis JG, Salmon AB, Richardson A, Ahima RS*, et al.* (2012) Rapamycin-induced insulin resistance is mediated by mTORC2 loss and uncoupled from longevity. Science *335*(6076):1638-1643

Lanza IR, Zabielski P, Klaus KA, Morse DM, Heppelmann CJ, Bergen HR, 3rd, Dasari S, Walrand S, Short KR, Johnson ML*, et al.* (2012) Chronic caloric restriction preserves mitochondrial function in senescence without increasing mitochondrial biogenesis. Cell Metab *16*(6):777-788

Laplante M, Sabatini DM (2012) mTOR signaling in growth control and disease. Cell *149*(2):274-293

Laposa RR, Henderson JT, Wells PG (2003) Tetracycline-dependent regulation of formamidopyrimidine DNA glycosylase in transgenic mice conditionally reduces oxidative DNA damage in vivo. FASEB J *17*(10):1343-1345

Laurenti E, Wilson A, Trumpp A (2009) Myc's other life: stem cells and beyond. Curr Opin Cell Biol *21*(6):844-854

Lee C, Longo VD (2011) Fasting vs dietary restriction in cellular protection and cancer treatment: from model organisms to patients. Oncogene *30*(30):3305-3316

Lewis JG, Hamilton T, Adams DO (1986) The effect of macrophage development on the release of reactive oxygen intermediates and lipid oxidation products, and their ability to induce oxidative DNA damage in mammalian cells. Carcinogenesis *7*(5):813-818

Li Q, Dang CV (1999) c-Myc overexpression uncouples DNA replication from mitosis. Mol Cell Biol *19*(8):5339-5351

Li W, Vijg J (2012) Measuring genome instability in aging - a mini-review. Gerontology *58*(2):129-138

Li Z, Owonikoko TK, Sun SY, Ramalingam SS, Doetsch PW, Xiao ZQ, Khuri FR, Curran WJ, Deng X (2012) c-Myc suppression of DNA double-strand break repair. Neoplasia *14*(12):1190-1202

Li Z, Piao F, Liu S, Wang Y, Qu S (2010) Subchronic exposure to arsenic trioxide-induced oxidative DNA damage in kidney tissue of mice. Exp Toxicol Pathol *62*(5):543-547

Liao CY, Rikke BA, Johnson TE, Diaz V, Nelson JF (2010a) Genetic variation in the murine lifespan response to dietary restriction: from life extension to life shortening. Aging Cell *9*(1):92-95

Liao YJ, Jin YP, Lin L, Tang H (2010b) [Determination of oxidative damage on DNA in brain and kidney of mice induced by anti-tumor agent of cisplatin]. Zhongguo Ying Yong Sheng Li Xue Za Zhi *26*(2):180-181

Lin CY, Loven J, Rahl PB, Paranal RM, Burge CB, Bradner JE, Lee TI, Young RA (2012) Transcriptional amplification in tumor cells with elevated c-Myc. Cell *151*(1):56-67

Liu B, Chen X, Wang ZQ, Tong WM (2014) DNA damage and oxidative injury are associated with hypomyelination in the corpus callosum of newborn Nbn(CNS-del) mice. J Neurosci Res *92*(2):254-266

Liu L, Chan C (2014) The role of inflammasome in Alzheimer's disease. Ageing Res Rev

Longo VD, Finch CE (2003) Evolutionary medicine: from dwarf model systems to healthy centenarians? Science *299*(5611):1342-1346

Lopez-Diazguerrero NE, Luna-Lopez A, Gutierrez-Ruiz MC, Zentella A, Konigsberg M (2005) Susceptibility of DNA to oxidative stressors in young and aging mice. Life Sci *77*(22):2840-2854

Lovell MA, Xiong S, Lyubartseva G, Markesbery WR (2009) Organoselenium (Sel-Plex diet) decreases amyloid burden and RNA and DNA oxidative damage in APP/PS1 mice. Free Radic Biol Med *46*(11):1527-1533

Loven J, Orlando DA, Sigova AA, Lin CY, Rahl PB, Burge CB, Levens DL, Lee TI, Young RA (2012) Revisiting global gene expression analysis. Cell *151*(3):476-482

Marguerat S, Bahler J (2012) Coordinating genome expression with cell size. Trends Genet *28*(11):560-565

Marnett LJ (1999) Lipid peroxidation-DNA damage by malondialdehyde. Mutat Res *424*(1-2):83-95

Martin-Montalvo A, Mercken EM, Mitchell SJ, Palacios HH, Mote PL, Scheibye-Knudsen M, Gomes AP, Ward TM, Minor RK, Blouin MJ*, et al.* (2013) Metformin improves healthspan and lifespan in mice. Nat Commun *4*2192

Martin B, Ji S, Maudsley S, Mattson MP (2010) "Control" laboratory rodents are metabolically morbid: why it matters. Proc Natl Acad Sci U S A *107*(14):6127-6133

Masoro EJ, McCarter RJ, Katz MS, McMahan CA (1992) Dietary restriction alters characteristics of glucose fuel use. J Gerontol *47*(6):B202-208

Masternak MM, Al-Regaiey KA, Del Rosario Lim MM, Bonkowski MS, Panici JA, Przybylski GK, Bartke A (2005) Caloric restriction results in decreased expression of peroxisome proliferator-activated receptor superfamily in muscle of normal and long-lived growth hormone receptor/binding protein knockout mice. J Gerontol A Biol Sci Med Sci *60*(10):1238-1245

Masternak MM, Bartke A, Wang F, Spong A, Gesing A, Fang Y, Salmon AB, Hughes LF, Liberati T, Boparai R*, et al.* (2012) Metabolic effects of intra-abdominal fat in GHRKO mice. Aging Cell *11*(1):73-81

Mateyak MK, Obaya AJ, Adachi S, Sedivy JM (1997) Phenotypes of c-Myc-deficient rat fibroblasts isolated by targeted homologous recombination. Cell Growth Differ *8*(10):1039-1048

Matteoni CA, Younossi ZM, Gramlich T, Boparai N, Liu YC, McCullough AJ (1999) Nonalcoholic fatty liver disease: a spectrum of clinical and pathological severity. Gastroenterology *116*(6):1413-1419

McCallum GP, Siu M, Ondovcik SL, Sweeting JN, Wells PG (2011) Methanol exposure does not lead to accumulation of oxidative DNA damage in bone marrow and spleen of mice, rabbits or primates. Mol Carcinog *50*(3):163-172

Mercken EM, Carboneau BA, Krzysik-Walker SM, de Cabo R (2012) Of mice and men: the benefits of caloric restriction, exercise, and mimetics. Ageing Res Rev *11*(3):390-398

Meyer N, Penn LZ (2008) Reflecting on 25 years with MYC. Nat Rev Cancer *8*(12):976-990

Michaud M, Balardy L, Moulis G, Gaudin C, Peyrot C, Vellas B, Cesari M, Nourhashemi F (2013) Proinflammatory cytokines, aging, and age-related diseases. J Am Med Dir Assoc *14*(12):877-882

Miller RA, Harrison DE, Astle CM, Baur JA, Boyd AR, de Cabo R, Fernandez E, Flurkey K, Javors MA, Nelson JF*, et al.* (2011) Rapamycin, but not resveratrol or simvastatin, extends life span of genetically heterogeneous mice. J Gerontol A Biol Sci Med Sci *66*(2):191-201

Miller RA, Harrison DE, Astle CM, Fernandez E, Flurkey K, Han M, Javors MA, Li X, Nadon NL, Nelson JF*, et al.* (2013) Rapamycin-mediated lifespan increase in mice is dose and sex dependent and metabolically distinct from dietary restriction. Aging Cell

Moerth C, Schneider MR, Renner-Mueller I, Blutke A, Elmlinger MW, Erben RG, Camacho-Hubner C, Hoeflich A, Wolf E (2007) Postnatally elevated levels of insulin-like growth factor (IGF)-II fail to rescue the dwarfism of IGF-I-deficient mice except kidney weight. Endocrinology *148*(1):441-451

Mookerjee SA, Divakaruni AS, Jastroch M, Brand MD (2010) Mitochondrial uncoupling and lifespan. Mech Ageing Dev *131*(7-8):463-472

Morrish F, Noonan J, Perez-Olsen C, Gafken PR, Fitzgibbon M, Kelleher J, VanGilst M, Hockenbery D (2010) Myc-dependent mitochondrial generation of acetyl-CoA contributes to fatty acid biosynthesis and histone acetylation during cell cycle entry. J Biol Chem *285*(47):36267-36274

Narasimhaiah R, Tuchman A, Lin SL, Naegele JR (2005) Oxidative damage and defective DNA repair is linked to apoptosis of migrating neurons and progenitors during cerebral cortex development in Ku70-deficient mice. Cereb Cortex *15*(6):696-707

Neff F, Flores-Dominguez D, Ryan DP, Horsch M, Schroder S, Adler T, Afonso LC, Aguilar-Pimentel JA, Becker L, Garrett L*, et al.* (2013) Rapamycin extends murine lifespan but has limited effects on aging. J Clin Invest *123*(8):3272-3291

Nelson JF, Strong R, Bokov A, Diaz V, Ward W (2012) Probing the relationship between insulin sensitivity and longevity using genetically modified mice. J Gerontol A Biol Sci Med Sci *67*(12):1332-1338

Nie Z, Hu G, Wei G, Cui K, Yamane A, Resch W, Wang R, Green DR, Tessarollo L, Casellas R*, et al.* (2012) c-Myc is a universal amplifier of expressed genes in lymphocytes and embryonic stem cells. Cell *151*(1):68-79

Ohnishi S, Saito H, Suzuki N, Ma N, Hiraku Y, Murata M, Kawanishi S (2011) Nitrative and oxidative DNA damage caused by K-ras mutation in mice. Biochem Biophys Res Commun *413*(2):236-240

Okamoto Y, Chou PH, Kim SY, Suzuki N, Laxmi YR, Okamoto K, Liu X, Matsuda T, Shibutani S (2008) Oxidative DNA damage in XPC-knockout and its wild mice treated with equine estrogen. Chem Res Toxicol *21*(5):1120-1124

Orjalo AV, Bhaumik D, Gengler BK, Scott GK, Campisi J (2009) Cell surface-bound IL-1alpha is an upstream regulator of the senescence-associated IL-6/IL-8 cytokine network. Proc Natl Acad Sci U S A *106*(40):17031-17036

Ortega-Molina A, Efeyan A, Lopez-Guadamillas E, Munoz-Martin M, Gomez-Lopez G, Canamero M, Mulero F, Pastor J, Martinez S, Romanos E*, et al.* (2012) Pten positively regulates brown adipose function, energy expenditure, and longevity. Cell Metab *15*(3):382-394

Osterod M, Hollenbach S, Hengstler JG, Barnes DE, Lindahl T, Epe B (2001) Age-related and tissue-specific accumulation of oxidative DNA base damage in 7,8-dihydro-8-oxoguanine-DNA glycosylase (Ogg1) deficient mice. Carcinogenesis *22*(9):1459-1463

Pawelec G, Derhovanessian E, Larbi A (2010) Immunosenescence and cancer. Crit Rev Oncol Hematol *75*(2):165-172

Pearson KJ, Baur JA, Lewis KN, Peshkin L, Price NL, Labinskyy N, Swindell WR, Kamara D, Minor RK, Perez E*, et al.* (2008) Resveratrol delays age-related deterioration and mimics transcriptional aspects of dietary restriction without extending life span. Cell Metab *8*(2):157-168

Pegoraro G, Misteli T (2009) The central role of chromatin maintenance in aging. Aging (Albany NY) *1*(12):1017-1022

Perez VI, Bokov A, Van Remmen H, Mele J, Ran Q, Ikeno Y, Richardson A (2009) Is the oxidative stress theory of aging dead? Biochim Biophys Acta *1790*(10):1005-1014

Piao F, Ma N, Hiraku Y, Murata M, Oikawa S, Cheng F, Zhong L, Yamauchi T, Kawanishi S, Yokoyama K (2005) Oxidative DNA damage in relation to neurotoxicity in the brain of mice exposed to arsenic at environmentally relevant levels. J Occup Health *47*(5):445-449

Pietenpol JA, Holt JT, Stein RW, Moses HL (1990) Transforming growth factor beta 1 suppression of c-myc gene transcription: role in inhibition of keratinocyte proliferation. Proc Natl Acad Sci U S A *87*(10):3758-3762

Polzer K, Joosten L, Gasser J, Distler JH, Ruiz G, Baum W, Redlich K, Bobacz K, Smolen JS, van den Berg W*, et al.* (2010) Interleukin-1 is essential for systemic inflammatory bone loss. Ann Rheum Dis *69*(1):284-290

Potapova TA, Zhu J, Li R (2013) Aneuploidy and chromosomal instability: a vicious cycle driving cellular evolution and cancer genome chaos. Cancer Metastasis Rev *32*(3-4):377-389

Pratheeshkumar P, Raphael TJ, Kuttan G (2010) Protective role of perillic acid against radiation-induced oxidative stress, cytokine profile, DNA damage, and intestinal toxicity in mice. J Environ Pathol Toxicol Oncol *29*(3):199-212

Prochownik EV (2008) c-Myc: linking transformation and genomic instability. Curr Mol Med *8*(6):446-458

Prochownik EV, Vogt PK (2010) Therapeutic Targeting of Myc. Genes Cancer *1*(6):650-659

Puglielli L, Konopka G, Pack-Chung E, Ingano LA, Berezovska O, Hyman BT, Chang TY, Tanzi RE, Kovacs DM (2001) Acyl-coenzyme A: cholesterol acyltransferase modulates the generation of the amyloid beta-peptide. Nat Cell Biol *3*(10):905-912

Rani V, Neumann CA, Shao C, Tischfield JA (2012) Prdx1 deficiency in mice promotes tissue specific loss of heterozygosity mediated by deficiency in DNA repair and increased oxidative stress. Mutat Res *735*(1-2):39-45

Ratajczak J, Shin DM, Wan W, Liu R, Masternak MM, Piotrowska K, Wiszniewska B, Kucia M, Bartke A, Ratajczak MZ (2011) Higher number of stem cells in the bone marrow of circulating low Igf-1 level Laron dwarf mice--novel view on Igf-1, stem cells and aging. Leukemia *25*(4):729-733

Reliene R, Fischer E, Schiestl RH (2004) Effect of N-acetyl cysteine on oxidative DNA damage and the frequency of DNA deletions in atm-deficient mice. Cancer Res *64*(15):5148-5153

Ricke RM, van Deursen JM (2013) Aneuploidy in health, disease, and aging. J Cell Biol *201*(1):11-21

Ringvoll J, Nordstrand LM, Vagbo CB, Talstad V, Reite K, Aas PA, Lauritzen KH, Liabakk NB, Bjork A, Doughty RW*, et al.* (2006) Repair deficient mice reveal mABH2 as the primary oxidative demethylase for repairing 1meA and 3meC lesions in DNA. EMBO J *25*(10):2189-2198

Rivnay B, Globerson A, Shinitzky M (1979) Viscosity of lymphocyte plasma membrane in aging mice and its possible relation to serum cholesterol. Mech Ageing Dev *10*(1-2):71-79

Rodrigues HF, Souza TA, Ghiraldini FG, Mello ML, Moraes AS (2014) Increased age is associated with epigenetic and structural changes in chromatin from neuronal nuclei. J Cell Biochem *115*(4):659-665

Rogers NH, Landa A, Park S, Smith RG (2012) Aging leads to a programmed loss of brown adipocytes in murine subcutaneous white adipose tissue. Aging Cell *11*(6):1074-1083

Rosen CJ, Ackert-Bicknell C, Rodriguez JP, Pino AM (2009) Marrow fat and the bone microenvironment: developmental, functional, and pathological implications. Crit Rev Eukaryot Gene Expr *19*(2):109-124

Roy SS, Chakraborty P, Bhattacharya S (2014) Intervention in cyclophosphamide induced oxidative stress and DNA damage by a flavonyl-thiazolidinedione based organoselenocyanate and evaluation of its efficacy during adjuvant therapy in tumor bearing mice. Eur J Med Chem *73*195-209

Russo MT, De Luca G, Degan P, Parlanti E, Dogliotti E, Barnes DE, Lindahl T, Yang H, Miller JH, Bignami M (2004) Accumulation of the oxidative base lesion 8-hydroxyguanine in DNA of tumor-prone mice defective in both the Myh and Ogg1 DNA glycosylases. Cancer Res *64*(13):4411-4414

Sackmann-Sala L, Berryman DE, Lubbers ER, Vesel CB, Troike KM, List EO, Munn RD, Ikeno Y, Kopchick JJ (2012) Decreased insulin sensitivity and increased oxidative damage in wasting adipose tissue depots of wild-type mice. Age (Dordr) *34*(5):1225-1237

Samadder A, Chakraborty D, De A, Bhattacharyya SS, Bhadra K, Khuda-Bukhsh AR (2011) Possible signaling cascades involved in attenuation of alloxan-induced oxidative stress and hyperglycemia in mice by ethanolic extract of Syzygium jambolanum: drug-DNA interaction with calf thymus DNA as target. Eur J Pharm Sci *44*(3):207-217

Sanz A, Bartke A, Barja G (2002) Long-lived Ames dwarf mice: Oxidative damage to mitochondrial DNA in heart and brain. J Am Aging Assoc *25*(3):119-122

Sauce D, Larsen M, Fastenackels S, Duperrier A, Keller M, Grubeck-Loebenstein B, Ferrand C, Debre P, Sidi D, Appay V (2009) Evidence of premature immune aging in patients thymectomized during early childhood. J Clin Invest *119*(10):3070-3078

Schaffer JE (2003) Lipotoxicity: when tissues overeat. Curr Opin Lipidol *14*(3):281-287

Schriner SE, Linford NJ, Martin GM, Treuting P, Ogburn CE, Emond M, Coskun PE, Ladiges W, Wolf N, Van Remmen H*, et al.* (2005) Extension of murine life span by overexpression of catalase targeted to mitochondria. Science *308*(5730):1909-1911

Sedivy JM, Kreiling JA, Neretti N, De Cecco M, Criscione SW, Hofmann JW, Zhao X, Ito T, Peterson AL (2013) Death by transposition - the enemy within? Bioessays *35*(12):1035-1043

Selman C, Lingard S, Choudhury AI, Batterham RL, Claret M, Clements M, Ramadani F, Okkenhaug K, Schuster E, Blanc E*, et al.* (2008) Evidence for lifespan extension and delayed age-related biomarkers in insulin receptor substrate 1 null mice. FASEB J *22*(3):807-818

Selman C, Tullet JM, Wieser D, Irvine E, Lingard SJ, Choudhury AI, Claret M, Al-Qassab H, Carmignac D, Ramadani F*, et al.* (2009) Ribosomal protein S6 kinase 1 signaling regulates mammalian life span. Science *326*(5949):140-144

Shaw AC, Goldstein DR, Montgomery RR (2013) Age-dependent dysregulation of innate immunity. Nat Rev Immunol *13*(12):875-887

She H, Xiong S, Hazra S, Tsukamoto H (2005) Adipogenic transcriptional regulation of hepatic stellate cells. J Biol Chem *280*(6):4959-4967

Shen JZ, Morgan J, Tesch GH, Fuller PJ, Young MJ (2014) CCL2-Dependent Macrophage Recruitment Is Critical for Mineralocorticoid Receptor-Mediated Cardiac Fibrosis, Inflammation, and Blood Pressure Responses in Male Mice. Endocrinology *155*(3):1057-1066

Shimizu T, Baba T, Ogawara M, Shirasawa T (2011) Lifespan and glucose metabolism in insulin receptor mutant mice. J Aging Res *2011*315640

Shu CJ, Benoist C, Mathis D (2012) The immune system's involvement in obesity-driven type 2 diabetes. Semin Immunol *24*(6):436-442

Shukla RK, Kumar A, Vallabani NV, Pandey AK, Dhawan A (2013) Titanium dioxide nanoparticle-induced oxidative stress triggers DNA damage and hepatic injury in mice. Nanomedicine (Lond)

Sinha D, Roy M (2011) Antagonistic role of tea against sodium arsenite-induced oxidative DNA damage and inhibition of DNA repair in Swiss albino mice. J Environ Pathol Toxicol Oncol *30*(4):311-322

Sohal RS, Weindruch R (1996) Oxidative stress, caloric restriction, and aging. Science *273*(5271):59-63

Song MF, Li YS, Kasai H, Kawai K (2012) Metal nanoparticle-induced micronuclei and oxidative DNA damage in mice. J Clin Biochem Nutr *50*(3):211-216

Speakman JR, Talbot DA, Selman C, Snart S, McLaren JS, Redman P, Krol E, Jackson DM, Johnson MS, Brand MD (2004) Uncoupled and surviving: individual mice with high metabolism have greater mitochondrial uncoupling and live longer. Aging Cell *3*(3):87-95

Steinbaugh MJ, Sun LY, Bartke A, Miller RA (2012) Activation of genes involved in xenobiotic metabolism is a shared signature of mouse models with extended lifespan. Am J Physiol Endocrinol Metab *303*(4):E488-495

Storer JB (1966) Longevity and gross pathology at death in 22 inbred mouse strains. J Gerontol *21*(3):404-409

Stratikopoulos E, Szabolcs M, Dragatsis I, Klinakis A, Efstratiadis A (2008) The hormonal action of IGF1 in postnatal mouse growth. Proc Natl Acad Sci U S A *105*(49):19378-19383

Streeper RS, Grueter CA, Salomonis N, Cases S, Levin MC, Koliwad SK, Zhou P, Hirschey MD, Verdin E, Farese RV, Jr. (2012) Deficiency of the lipid synthesis enzyme, DGAT1, extends longevity in mice. Aging (Albany NY) *4*(1):13-27

Sun D, Muthukumar AR, Lawrence RA, Fernandes G (2001) Effects of calorie restriction on polymicrobial peritonitis induced by cecum ligation and puncture in young C57BL/6 mice. Clin Diagn Lab Immunol *8*(5):1003-1011

Surani MA, Hayashi K, Hajkova P (2007) Genetic and epigenetic regulators of pluripotency. Cell *128*(4):747-762

Syed FA, Melim T (2011) Rodent models of aging bone: an update. Curr Osteoporos Rep *9*(4):219-228

Szczesny B, Tann AW, Mitra S (2010) Age- and tissue-specific changes in mitochondrial and nuclear DNA base excision repair activity in mice: Susceptibility of skeletal muscles to oxidative injury. Mech Ageing Dev *131*(5):330-337

Taguchi A, Wartschow LM, White MF (2007) Brain IRS2 signaling coordinates life span and nutrient homeostasis. Science *317*(5836):369-372

Takahashi K, Yamanaka S (2006) Induction of pluripotent stem cells from mouse embryonic and adult fibroblast cultures by defined factors. Cell *126*(4):663-676

Tasaki M, Kuroiwa Y, Inoue T, Hibi D, Matsushita K, Ishii Y, Maruyama S, Nohmi T, Nishikawa A, Umemura T (2013) Oxidative DNA damage and in vivo mutagenicity caused by reactive oxygen species generated in the livers of p53-proficient or -deficient gpt delta mice treated with non-genotoxic hepatocarcinogens. J Appl Toxicol *33*(12):1433-1441

Taylor-Jones JM, McGehee RE, Rando TA, Lecka-Czernik B, Lipschitz DA, Peterson CA (2002) Activation of an adipogenic program in adult myoblasts with age. Mech Ageing Dev *123*(6):649-661

Tchkonia T, Morbeck DE, Von Zglinicki T, Van Deursen J, Lustgarten J, Scrable H, Khosla S, Jensen MD, Kirkland JL (2010) Fat tissue, aging, and cellular senescence. Aging Cell *9*(5):667-684

Thewes S, Moran GP, Magee BB, Schaller M, Sullivan DJ, Hube B (2008) Phenotypic screening, transcriptional profiling, and comparative genomic analysis of an invasive and non-invasive strain of Candida albicans. BMC Microbiol *8*187

Tomas-Loba A, Flores I, Fernandez-Marcos PJ, Cayuela ML, Maraver A, Tejera A, Borras C, Matheu A, Klatt P, Flores JM*, et al.* (2008) Telomerase reverse transcriptase delays aging in cancer-resistant mice. Cell *135*(4):609-622

Tonini CL, Campagnaro BP, Louro LP, Pereira TM, Vasquez EC, Meyrelles SS (2013) Effects of Aging and Hypercholesterolemia on Oxidative Stress and DNA Damage in Bone Marrow Mononuclear Cells in Apolipoprotein E-deficient Mice. Int J Mol Sci *14*(2):3325-3342

Tripathi DN, Jena GB (2008) Ebselen attenuates cyclophosphamide-induced oxidative stress and DNA damage in mice. Free Radic Res *42*(11-12):966-977

Tripathi DN, Jena GB (2009) Intervention of astaxanthin against cyclophosphamide-induced oxidative stress and DNA damage: a study in mice. Chem Biol Interact *180*(3):398-406

Trivedi PP, Jena GB (2013a) Role of alpha-lipoic acid in dextran sulfate sodium-induced ulcerative colitis in mice: studies on inflammation, oxidative stress, DNA damage and fibrosis. Food Chem Toxicol *59*339-355

Trivedi PP, Jena GB (2013b) Ulcerative colitis-induced hepatic damage in mice: studies on inflammation, fibrosis, oxidative DNA damage and GST-P expression. Chem Biol Interact *201*(1-3):19-30

Trumpp A, Refaeli Y, Oskarsson T, Gasser S, Murphy M, Martin GR, Bishop JM (2001) c-Myc regulates mammalian body size by controlling cell number but not cell size. Nature *414*(6865):768-773

Tsuchiya T, Dhahbi JM, Cui X, Mote PL, Bartke A, Spindler SR (2004) Additive regulation of hepatic gene expression by dwarfism and caloric restriction. Physiol Genomics *17*(3):307-315

Tsuzuki T, Piao JS, Isoda T, Sakumi K, Nakabeppu Y, Nakatsu Y (2011a) Oxidative stress-induced tumorigenesis in the small intestines of DNA repair-deficient mice. Health Phys *100*(3):293-294

Tsuzuki T, Piao JS, Nakatsu Y (2011b) [Oxidative DNA damage-induced intestinal tumorigenesis in Mutyh-deficient mice]. Nihon Rinsho *69 Suppl 3*137-142

Um SH, Frigerio F, Watanabe M, Picard F, Joaquin M, Sticker M, Fumagalli S, Allegrini PR, Kozma SC, Auwerx J*, et al.* (2004) Absence of S6K1 protects against age- and diet-induced obesity while enhancing insulin sensitivity. Nature *431*(7005):200-205

Vafa O, Wade M, Kern S, Beeche M, Pandita TK, Hampton GM, Wahl GM (2002) c-Myc can induce DNA damage, increase reactive oxygen species, and mitigate p53 function: a mechanism for oncogene-induced genetic instability. Mol Cell *9*(5):1031-1044

van Eden W, van Herwijnen M, Wagenaar J, van Kooten P, Broere F, van der Zee R (2013) Stress proteins are used by the immune system for cognate interactions with anti-inflammatory regulatory T cells. FEBS Lett *587*(13):1951-1958

Vettor R, Milan G, Franzin C, Sanna M, De Coppi P, Rizzuto R, Federspil G (2009) The origin of intermuscular adipose tissue and its pathophysiological implications. Am J Physiol Endocrinol Metab *297*(5):E987-998

Waikel RL, Kawachi Y, Waikel PA, Wang XJ, Roop DR (2001) Deregulated expression of c-Myc depletes epidermal stem cells. Nat Genet *28*(2):165-168

Wang C, Li Q, Redden DT, Weindruch R, Allison DB (2004) Statistical methods for testing effects on "maximum lifespan". Mech Ageing Dev *125*(9):629-632

Wang C, Maddick M, Miwa S, Jurk D, Czapiewski R, Saretzki G, Langie SA, Godschalk RW, Cameron K, von Zglinicki T (2010) Adult-onset, short-term dietary restriction reduces cell senescence in mice. Aging (Albany NY) *2*(9):555-566

Wang D, Zhong Y, Luo X, Wu S, Xiao R, Bao W, Yang W, Yan H, Yao P, Liu L (2011a) Pu-erh black tea supplementation decreases quinocetone-induced ROS generation and oxidative DNA damage in Balb/c mice. Food Chem Toxicol *49*(2):477-484

Wang H, Mannava S, Grachtchouk V, Zhuang D, Soengas MS, Gudkov AV, Prochownik EV, Nikiforov MA (2008) c-Myc depletion inhibits proliferation of human tumor cells at various stages of the cell cycle. Oncogene *27*(13):1905-1915

Wang J, Geiger H, Rudolph KL (2011b) Immunoaging induced by hematopoietic stem cell aging. Curr Opin Immunol *23*(4):532-536

Wang L, Li YL, Zhang CC, Cui W, Wang X, Xia Y, Du J, Li HH (2014) Inhibition of Toll-like receptor 2 reduces cardiac fibrosis by attenuating macrophage-mediated inflammation. Cardiovasc Res *101*(3):383-392

Wang XF, Xing ML, Shen Y, Zhu X, Xu LH (2006a) Oral administration of Cr(VI) induced oxidative stress, DNA damage and apoptotic cell death in mice. Toxicology *228*(1):16-23

Wang Z, Al-Regaiey KA, Masternak MM, Bartke A (2006b) Adipocytokines and lipid levels in Ames dwarf and calorie-restricted mice. J Gerontol A Biol Sci Med Sci *61*(4):323-331

Ward WF, Qi W, Van Remmen H, Zackert WE, Roberts LJ, 2nd, Richardson A (2005) Effects of age and caloric restriction on lipid peroxidation: measurement of oxidative stress by F2-isoprostane levels. J Gerontol A Biol Sci Med Sci *60*(7):847-851

Watt FM, Frye M, Benitah SA (2008) MYC in mammalian epidermis: how can an oncogene stimulate differentiation? Nat Rev Cancer *8*(3):234-242

Weindruch R, Walford RL (1988). The Retardation of Aging and Disease by Dietary Restriction (Springfield, IL: Charles C. Thomas).

Westbrook R, Bonkowski MS, Strader AD, Bartke A (2009) Alterations in oxygen consumption, respiratory quotient, and heat production in long-lived GHRKO and Ames dwarf mice, and short-lived bGH transgenic mice. J Gerontol A Biol Sci Med Sci *64*(4):443-451

Whitfield JR, Soucek L (2012) Tumor microenvironment: becoming sick of Myc. Cell Mol Life Sci *69*(6):931-934

Wijeyesekera A, Selman C, Barton RH, Holmes E, Nicholson JK, Withers DJ (2012) Metabotyping of long-lived mice using 1H NMR spectroscopy. J Proteome Res *11*(4):2224-2235

Williams GC (1957) Pleiotropy, natural selection, and the evolution of senescence. Evolution *11*398–411

Wilson A, Murphy MJ, Oskarsson T, Kaloulis K, Bettess MD, Oser GM, Pasche AC, Knabenhans C, Macdonald HR, Trumpp A (2004) c-Myc controls the balance between hematopoietic stem cell self-renewal and differentiation. Genes Dev *18*(22):2747-2763

Wong YT, Gruber J, Jenner AM, Tay FE, Ruan R (2011) Chronic resveratrol intake reverses pro-inflammatory cytokine profile and oxidative DNA damage in ageing hybrid mice. Age (Dordr) *33*(3):229-246

Wouters K, van Gorp PJ, Bieghs V, Gijbels MJ, Duimel H, Lutjohann D, Kerksiek A, van Kruchten R, Maeda N, Staels B*, et al.* (2008) Dietary cholesterol, rather than liver steatosis, leads to hepatic inflammation in hyperlipidemic mouse models of nonalcoholic steatohepatitis. Hepatology *48*(2):474-486

Wu JJ, Liu J, Chen EB, Wang JJ, Cao L, Narayan N, Fergusson MM, Rovira, II, Allen M, Springer DA*, et al.* (2013) Increased mammalian lifespan and a segmental and tissue-specific slowing of aging after genetic reduction of mTOR expression. Cell Rep *4*(5):913-920

Xie G, Zhang J, Xiao Y, Han Y, Liu N, Li B, Mu Y, Han S, Huang P, Sun Z (2012) [Effects of CdTe QDs on oxidative stress and DNA damage of liver cells in mice]. Wei Sheng Yan Jiu *41*(1):31-34, 39

Xu J, Gontier G, Chaker Z, Lacube P, Dupont J, Holzenberger M (2014) Longevity effect of IGF-1R(+/-) mutation depends on genetic background-specific receptor activation. Aging Cell *13*(1):19-28

Yamamoto ML, Chapman AM, Schiestl RH (2013) Effects of side-stream tobacco smoke and smoke extract on glutathione- and oxidative DNA damage repair-deficient mice and blood cells. Mutat Res *749*(1-2):58-65

Yamauchi T, Kamon J, Waki H, Terauchi Y, Kubota N, Hara K, Mori Y, Ide T, Murakami K, Tsuboyama-Kasaoka N*, et al.* (2001) The fat-derived hormone adiponectin reverses insulin resistance associated with both lipoatrophy and obesity. Nat Med *7*(8):941-946

Yan L, Gao S, Ho D, Park M, Ge H, Wang C, Tian Y, Lai L, De Lorenzo MS, Vatner DE*, et al.* (2013a) Calorie restriction can reverse, as well as prevent, aging cardiomyopathy. Age (Dordr) *35*(6):2177-2182

Yan L, Gao S, Ho D, Park M, Ge H, Wang C, Tian Y, Lai L, De Lorenzo MS, Vatner DE*, et al.* (2013b) Calorie restriction can reverse, as well as prevent, aging cardiomyopathy. Age (Dordr)

Yang H, Youm YH, Dixit VD (2009) Inhibition of thymic adipogenesis by caloric restriction is coupled with reduction in age-related thymic involution. J Immunol *183*(5):3040-3052

Yang L, Zhang B, Yuan Y, Li C, Wang Z (2013) Oxidative stress and DNA damage in utero and embryo implantation of mice exposed to carbon disulfide at peri-implantation. Hum Exp Toxicol

Ye X, Ji Z, Wei C, McHale CM, Ding S, Thomas R, Yang X, Zhang L (2013) Inhaled formaldehyde induces DNA-protein crosslinks and oxidative stress in bone marrow and other distant organs of exposed mice. Environ Mol Mutagen *54*(9):705-718

Yecies JL, Manning BD (2011) Transcriptional control of cellular metabolism by mTOR signaling. Cancer Res *71*(8):2815-2820

Yu BP (1996) Aging and oxidative stress: modulation by dietary restriction. Free Radic Biol Med *21*(5):651-668

Yuan J, Liu H, Zhou LH, Zou YL, Lu WQ (2006) Oxidative stress and DNA damage induced by a drinking-water chlorination disinfection byproduct 3-chloro-4-(dichloromethyl)-5-hydroxy-2(5H)-furanone (MX) in mice. Mutat Res *609*(2):129-136

Yuan R, Tsaih SW, Petkova SB, Marin de Evsikova C, Xing S, Marion MA, Bogue MA, Mills KD, Peters LL, Bult CJ*, et al.* (2009) Aging in inbred strains of mice: study design and interim report on median lifespans and circulating IGF1 levels. Aging Cell *8*(3):277-287

Zahn JM, Poosala S, Owen AB, Ingram DK, Lustig A, Carter A, Weeraratna AT, Taub DD, Gorospe M, Mazan-Mamczarz K*, et al.* (2007) AGEMAP: a gene expression database for aging in mice. PLoS Genet *3*(11):e201

Zhang H, Xie C, Spencer HJ, Zuo C, Higuchi M, Ranganathan G, Kern PA, Chou MW, Huang Q, Szczesny B*, et al.* (2011) Obesity and hepatosteatosis in mice with enhanced oxidative DNA damage processing in mitochondria. Am J Pathol *178*(4):1715-1727

Zhou GD, Randerath K, Donnelly KC, Jaiswal AK (2004) Effects of NQO1 deficiency on levels of cyclopurines and other oxidative DNA lesions in liver and kidney of young mice. Int J Cancer *112*(5):877-883

Zinzalla V, Stracka D, Oppliger W, Hall MN (2011) Activation of mTORC2 by association with the ribosome. Cell *144*(5):757-768

Zirath H, Frenzel A, Oliynyk G, Segerstrom L, Westermark UK, Larsson K, Munksgaard Persson M, Hultenby K, Lehtio J, Einvik C*, et al.* (2013) MYC inhibition induces metabolic changes leading to accumulation of lipid droplets in tumor cells. Proc Natl Acad Sci U S A *110*(25):10258-10263

Zoncu R, Efeyan A, Sabatini DM (2011) mTOR: from growth signal integration to cancer, diabetes and ageing. Nat Rev Mol Cell Biol *12*(1):21-35

Appendices

Appendix 1. Genotype-associated gene expression changes from microarray experiments[1]

			Liver		Muscle		Adipose	
ID	Symbol	Name	Young	Old	Young	Old	Young	Old
		Number of genes with **increased**/**decreased** expression in $Myc^{+/+}$ cells[2]	5/40	132/146	35/0	115/15	70/195	85/112
76509	1600029D21Rik	RIKEN cDNA 1600029D21 gene					2.04	5.24
69327	1700007K13Rik	RIKEN cDNA 1700007K13 gene					1.79	3.14
67082	1700011H14Rik	RIKEN cDNA 1700011H14 gene					2.13	
69380	1700013G24Rik	RIKEN cDNA 1700013G24 gene						-1.85
329375	1700101E01Rik	RIKEN cDNA 1700101E01 gene						1.72
69068	1810011O10Rik	RIKEN cDNA 1810011O10 gene	-2.04					
70261	2010110P09Rik	RIKEN cDNA 2010110P09 gene		-1.61				
67373	2210010C04Rik	RIKEN cDNA 2210010C04 gene		-5.14				
66528	2210020M01Rik	RIKEN cDNA 2210020M01 gene					1.50	
69504	2310001H12Rik	RIKEN cDNA 2310001H12 gene					1.62	
70458	2610318N02Rik	RIKEN cDNA 2610318N02 gene						-2.50
380654	4930485B16Rik	RIKEN cDNA 4930485B16 gene						2.70
75861	4930571K23Rik	RIKEN cDNA 4930571K23 gene						-1.55
70977	4931407G18Rik	RIKEN cDNA 4931407G18 gene						-2.80
66765	4933411K16Rik	RIKEN cDNA 4933411K16 gene						-1.63
66761	4933417A18Rik	RIKEN cDNA 4933417A18 gene		1.90			1.55	
67531	5730408K05Rik	RIKEN cDNA 5730408K05 gene		1.62				
105892	9030619P08Rik	RIKEN cDNA 9030619P08 gene	-2.03					
619326	9130409I23Rik	RIKEN cDNA 9130409I23 gene	-1.86					
319942	A530016L24Rik	RIKEN cDNA A530016L24 gene				2.48		
12780	Abcc2	ATP-binding cassette, sub-family C (CFTR/MRP), member 2					-1.77	
107476	Acaca	Acetyl-Coenzyme A carboxylase alpha				2.02		-1.62
104112	Acly	ATP citrate lyase				1.67		-1.86
11428	Aco1	Aconitase 1				1.54		
26897	Acot1	Acyl-CoA thioesterase 1		-3.36				
171210	Acot2	Acyl-CoA thioesterase 2		-1.82				
11433	Acp5	Acid phosphatase 5, tartrate resistant				2.44		
56318	Acpp	Acid phosphatase, prostate		2.27			1.52	
94180	Acsbg1	Acyl-CoA synthetase bubblegum family member 1						1.75
233799	Acsm2	Acyl-CoA synthetase medium-chain family member 2						-2.93
20216	Acsm3	Acyl-CoA synthetase medium-chain family member 3				2.53	1.66	
60525	Acss2	Acyl-CoA synthetase short-chain family member 2						-1.81
380660	Acss3	Acyl-CoA synthetase short-chain family member 3	-1.72			1.55		
11459	Acta1	Actin, alpha 1, skeletal muscle		1.97				-2.16
11468	Actg2	Actin, gamma 2, smooth muscle, enteric						-1.63
269275	Acvr1c	Activin A receptor, type IC				2.52		
23792	Adam23	A disintegrin and metallopeptidase domain 23		1.59				
11497	Adam3	A disintegrin and metallopeptidase domain 3 (cyritestin)						-1.89
11500	Adam7	A disintegrin and metallopeptidase domain 7						-2.88
11501	Adam8	A disintegrin and metallopeptidase domain 8					-1.66	1.89
11504	Adamts1	A disintegrin-like and metallopeptidase (reprolysin type) type 1, motif 1					-1.55	
101401	Adamts9	A disintegrin-like and metallopeptidase (reprolysin type) type 1, motif 9				1.55	-1.55	
246747	Adig	Adipogenin				1.90		
11450	Adipoq	Adiponectin, C1Q and collagen domain containing				2.22		
11555	Adrb2	Adrenergic receptor, beta 2				1.51		
11556	Adrb3	Adrenergic receptor, beta 3				4.66		
140497	AF251705	cDNA sequence AF251705						1.61
67512	Agpat2	1-acylglycerol-3-phosphate O-acyltransferase 2				2.54		
231510	Agpat9	1-acylglycerol-3-phosphate O-acyltransferase 9	-1.55					
11625	Ahsg	Alpha-2-HS-glycoprotein			2.58		-3.10	

			Liver		Muscle		Adipose	
ID	Symbol	Name	Young	Old	Young	Old	Young	Old
380795	AI324046	Expressed sequence AI324046		2.35				
233066	AI428936	Expressed sequence AI428936		1.68				
11997	Akr1b7	Aldo-keto reductase family 1, member B7						-12.17
11657	Alb	Albumin			3.06	-5.13	-2.88	
26358	Aldh1a7	Aldehyde dehydrogenase family 1, subfamily A7						-1.57
107747	Aldh1l1	Aldehyde dehydrogenase 1 family, member L1				1.57		
621603	Aldh3b2	Aldehyde dehydrogenase 3 family, member B2		1.94				
230163	Aldob	Aldolase B, fructose-bisphosphate					-1.58	-1.98
11687	Alox15	Arachidonate 15-lipoxygenase		1.53				
71481	Alpk1	Alpha-kinase 1		2.46				
11699	Ambp	Alpha 1 microglobulin/bikunin					-1.96	
109959	Amy2a5	Amylase 2a5		-5.14				
11600	Angpt1	Angiopoietin 1					1.61	1.63
57875	Angptl4	Angiopoietin-like 4				1.88		
654812	Angptl7	Angiopoietin-like 7			1.55			
56642	Ankrd2	Ankyrin repeat domain 2 (stretch responsive muscle)				-1.51		
78321	Ankrd23	Ankyrin repeat domain 23		1.61				
319196	Ankrd5	Ankyrin repeat domain 5					1.57	
68743	Anln	Anillin, actin binding protein		2.26				
11754	Aoc3	Amine oxidase, copper containing 3				2.18		
20219	Apcs	Serum amyloid P-component		2.23				
11806	Apoa1	Apolipoprotein A-I			2.55	-2.27	-2.27	
11807	Apoa2	Apolipoprotein A-II			3.74		-2.94	
238055	Apob	Apolipoprotein B				-2.02	-2.11	
11814	Apoc3	Apolipoprotein C-III					-1.55	
11425	Apoc4	Apolipoprotein C-IV					-1.63	
11816	Apoe	Apolipoprotein E				1.55		
11818	Apoh	Apolipoprotein H			1.99		-2.11	
11833	Aqp8	Aquaporin 8	-1.66					
102910	Armcx4	Armadillo repeat containing, X-linked 4		1.89				
11883	Arsa	Arylsulfatase A		-1.58				
27053	Asns	Asparagine synthetase				2.22		
11898	Ass1	Argininosuccinate synthetase 1			1.50		-2.73	
11910	Atf3	Activating transcription factor 3					-1.75	
50770	Atp11a	ATPase, class VI, type 11A		1.83				
11937	Atp2a1	ATPase, Ca++ transporting, cardiac muscle, fast twitch 1		2.19				
242341	Atp6v0d2	ATPase, H+ transporting, lysosomal V0 subunit D2		2.60			-2.05	2.52
241633	Atp8b4	ATPase, class I, type 8B, member 4						1.60
100798	AU017193	Expressed sequence AU017193		1.78				
234564	AU018778	Expressed sequence AU018778				4.99		
692182	AY498738	cDNA sequence AY498738						-2.48
12007	Azgp1	Alpha-2-glycoprotein 1, zinc					-1.71	
26877	B3galt1	UDP-Gal:betaGlcNAc beta 1,3-galactosyltransferase, polypeptide 1		1.64				
26878	B3galt2	UDP-Gal:betaGlcNAc beta 1,3-galactosyltransferase, polypeptide 2				2.93		
14422	B4galnt2	Beta-1,4-N-acetyl-galactosaminyl transferase 2		2.12			1.89	2.36
56336	B4galt5	UDP-Gal:betaGlcNAc beta 1,4-galactosyltransferase, polypeptide 5					-1.50	
236149	BC014805	cDNA sequence BC014805		4.26				
667597	BC023105	cDNA sequence BC023105					-1.66	
228642	BC034902	cDNA sequence BC034902				2.81		
381680	BC055004	cDNA sequence BC055004						1.63
12051	Bcl3	B-cell leukemia/lymphoma 3					-1.79	
12053	Bcl6	B-cell leukemia/lymphoma 6	2.25	-1.64				
79362	Bhlhe41	basic helix-loop-helix family, member e41					1.85	
14705	Bscl2	Bernardinelli-Seip congenital lipodystrophy 2 homolog (human)				1.63		

			Liver		Muscle		Adipose	
ID	Symbol	Name	Young	Old	Young	Old	Young	Old
12262	C1qc	Complement component 1, q subcomponent, C chain				1.54		
12263	C2	Complement component 2 (within H-2S)				1.53		
12266	C3	Complement component 3				1.57		
12267	C3ar1	Complement component 3a receptor 1		-1.57				
12268	C4b	Complement component 4B (Childo blood group)				2.00		
54725	Cadm1	Cell adhesion molecule 1						1.85
70405	Calml3	Calmodulin-like 3					2.06	3.93
75600	Calml4	Calmodulin-like 4					1.56	
12332	Capg	Capping protein (actin filament), gelsolin-like		-1.70				
12346	Car1	Carbonic anhydrase 1		-2.36				
23831	Car14	Carbonic anhydrase 14		-1.68				
12349	Car2	Carbonic anhydrase 2		-1.64				
56078	Car5b	Carbonic anhydrase 5b, mitochondrial				2.89		
67896	Ccdc80	Coiled-coil domain containing 80				1.53		
20293	Ccl12	Chemokine (C-C motif) ligand 12					-1.72	
20296	Ccl2	Chemokine (C-C motif) ligand 2					-2.09	
18829	Ccl21a	Chemokine (C-C motif) ligand 21A						1.55
56221	Ccl24	Chemokine (C-C motif) ligand 24		-1.63				
56838	Ccl28	Chemokine (C-C motif) ligand 28					1.64	2.75
20302	Ccl3	Chemokine (C-C motif) ligand 3		-2.13			-2.18	
20304	Ccl5	Chemokine (C-C motif) ligand 5						1.61
20306	Ccl7	Chemokine (C-C motif) ligand 7		-2.34			-2.33	
20307	Ccl8	Chemokine (C-C motif) ligand 8				2.83	-3.44	
12428	Ccna2	Cyclin A2		-1.65				
12444	Ccnd2	Cyclin D2		-1.62				
12775	Ccr7	Chemokine (C-C motif) receptor 7						1.51
12475	Cd14	CD14 antigen		2.10				
17079	Cd180	CD180 antigen		-1.52				1.64
170776	Cd209c	CD209c antigen					-1.59	
170780	Cd209e	CD209e antigen					-1.58	
217303	Cd300a	CD300A antigen		-1.64				
217305	Cd300ld	CD300 molecule-like family member d		-1.50			-1.55	
12491	Cd36	CD36 antigen	-1.78					
12504	Cd4	CD4 antigen		-1.53				
12505	Cd44	CD44 antigen					-1.62	
12514	Cd68	CD68 antigen		-1.59		1.51		
12516	Cd7	CD7 antigen		-1.60				
16149	Cd74	CD74 antigen (invariant polypeptide of major histocompatibility complex)		-1.78				
12526	Cd8b1	CD8 antigen, beta chain 1						1.79
68764	Cdhr3	Cadherin-related family member 3						1.97
72040	Cdhr5	Cadherin-related family member 5						2.19
12575	Cdkn1a	Cyclin-dependent kinase inhibitor 1A (P21)	-2.23				-1.80	
12583	Cdo1	Cysteine dioxygenase 1, cytosolic				2.54		
26366	Ceacam10	Carcinoembryonic antigen-related cell adhesion molecule 10						-4.05
12606	Cebpa	CCAAT/enhancer binding protein (C/EBP), alpha				2.20		
12613	Cel	Carboxyl ester lipase		-5.11				
109901	Cela1	Chymotrypsin-like elastase family, member 1		-1.81			-1.62	
13706	Cela2a	Chymotrypsin-like elastase family, member 2A		-3.19				
67868	Cela3b	Chymotrypsin-like elastase family, member 3B		-2.01				
228094	Cerkl	Ceramide kinase-like		1.52				
104158	Ces3	Carboxylesterase 3				2.21		
67935	Ces7	Carboxylesterase 7						-4.54
14962	Cfb	Complement factor B				1.57		
11537	Cfd	Complement factor D (adipsin)				3.10		
12643	Chad	Chondroadherin					1.65	3.08

			Liver		Muscle		Adipose	
ID	Symbol	Name	Young	Old	Young	Old	Young	Old
320790	Chd7	Chromodomain helicase DNA binding protein 7					1.52	
12654	Chi3l1	Chitinase 3-like 1		8.98				
110902	Chrna2	Cholinergic receptor, nicotinic, alpha polypeptide 2 (neuronal)		-1.90				
12683	Cidea	Cell death-inducing DNA fragmentation factor, alpha subunit, effector A	-3.18	-2.33		2.40		
14311	Cidec	Cell death-inducing DFFA-like effector c	-2.77	-3.42		2.23		
12700	Cish	Cytokine inducible SH2-containing protein			1.56	1.90		
12715	Ckm	Creatine kinase, muscle		1.63				
58187	Cldn10a	Claudin 10A					1.83	
75677	Cldn22	Claudin 22					1.81	
17312	Clec10a	C-type lectin domain family 10, member A				1.61		
232413	Clec12a	C-type lectin domain family 12, member a		-1.50				1.64
94071	Clec2h	C-type lectin domain family 2, member h	1.65					
269799	Clec4a1	C-type lectin domain family 4, member a1		-1.80				
26888	Clec4a2	C-type lectin domain family 4, member a2		-2.02				
73149	Clec4a3	C-type lectin domain family 4, member a3		-1.69				
17474	Clec4d	C-type lectin domain family 4, member d					-2.56	
56620	Clec4n	C-type lectin domain family 4, member n		-2.13				
56644	Clec7a	C-type lectin domain family 7, member a						1.56
98985	Clp1	CLP1, cleavage and polyadenylation factor I subunit		1.58				
109791	Clps	Colipase, pancreatic		-4.41				
93673	Cml2	Camello-like 2					-1.95	
69049	Cml5	Camello-like 5		-2.46				
12797	Cnn1	Calponin 1						-2.22
12816	Col12a1	Collagen, type XII, alpha 1					-1.82	
12861	Cox6a1	Cytochrome c oxidase, subunit VI a, polypeptide 1				1.56		
109697	Cpa1	Carboxypeptidase A1		-5.78				
76703	Cpb1	Carboxypeptidase B1 (tissue)		-5.28				
12876	Cpe	Carboxypeptidase E						1.51
66871	Cpne8	Copine VIII		1.78				
227231	Cps1	Carbamoyl-phosphate synthetase 1					-1.93	
12903	Crabp1	Cellular retinoic acid binding protein I						2.41
12908	Crat	Carnitine acetyltransferase		-1.66				
74175	Crct1	Cysteine-rich C-terminal 1			4.64			
76737	Creld2	Cysteine-rich with EGF-like domains 2		1.52				
11571	Crisp1	Cysteine-rich secretory protein 1						-110.58
246277	Csad	Cysteine sulfinic acid decarboxylase		-2.10				
114564	Csprs	Component of Sp100-rs					-1.98	-1.51
13009	Csrp3	Cysteine and glycine-rich protein 3				-1.86		
66473	Ctrb1	Chymotrypsinogen B1		-4.50				
109660	Ctrl	Chymotrypsin-like		-3.97				
13034	Ctse	Cathepsin E		-2.30				
13038	Ctsk	Cathepsin K						1.62
13040	Ctss	Cathepsin S					-1.52	
16433	Cuzd1	CUB and zona pellucida-like domains 1					1.66	
14825	Cxcl1	Chemokine (C-X-C motif) ligand 1		2.34				
15945	Cxcl10	Chemokine (C-X-C motif) ligand 10		-2.78			-1.95	
55985	Cxcl13	Chemokine (C-X-C motif) ligand 13	-1.82					
57266	Cxcl14	Chemokine (C-X-C motif) ligand 14						1.75
13056	Cyb561	Cytochrome b-561		2.06				
13074	Cyp17a1	Cytochrome P450, family 17, subfamily a, polypeptide 1		1.57				-2.35
233005	Cyp2a22	Cytochrome P450, family 2, subfamily a, polypeptide 22	-5.09					
13088	Cyp2b10	Cytochrome P450, family 2, subfamily b, polypeptide 10	-1.90					
13089	Cyp2b13	Cytochrome P450, family 2, subfamily b, polypeptide 13		4.02				
13094	Cyp2b9	Cytochrome P450, family 2, subfamily b, polypeptide 9	-1.83	2.09				

			Liver		Muscle		Adipose	
ID	Symbol	Name	Young	Old	Young	Old	Young	Old
72082	Cyp2c55	Cytochrome P450, family 2, subfamily c, polypeptide 55		-2.05				
76279	Cyp2d26	Cytochrome P450, family 2, subfamily d, polypeptide 26					-1.50	
13105	Cyp2d9	Cytochrome P450, family 2, subfamily d, polypeptide 9		-1.51				
13106	Cyp2e1	Cytochrome P450, family 2, subfamily e, polypeptide 1				2.62		
13107	Cyp2f2	Cytochrome P450, family 2, subfamily f, polypeptide 2				2.61	2.34	
13109	Cyp2j5	Cytochrome P450, family 2, subfamily j, polypeptide 5						-2.02
13112	Cyp3a11	Cytochrome P450, family 3, subfamily a, polypeptide 11						-1.93
56388	Cyp3a25	Cytochrome P450, family 3, subfamily a, polypeptide 25					-2.27	
53973	Cyp3a41a	Cytochrome P450, family 3, subfamily a, polypeptide 41A		2.13				
100041375	Cyp3a41b	Cytochrome P450, family 3, subfamily a, polypeptide 41B		2.25				
277753	Cyp4a12a	Cytochrome P450, family 4, subfamily a, polypeptide 12a						-3.14
13118	Cyp4a12b	Cytochrome P450, family 4, subfamily a, polypeptide 12B						-2.60
13119	Cyp4a14	Cytochrome P450, family 4, subfamily a, polypeptide 14		-2.29				
666168	Cyp4a31	Cytochrome P450, family 4, subfamily a, polypeptide 31		-1.62				
100040843	Cyp4a32	Cytochrome P450, family 4, subfamily a, polypeptide 32		-1.60				
13124	Cyp8b1	Cytochrome P450, family 8, subfamily b, polypeptide 1		-2.19				
16007	Cyr61	Cysteine rich protein 61		-1.78				
229791	D3Bwg0562e	DNA segment, Chr 3, Brigham & Women's Genetics 0562 expressed					-1.80	
13142	Dao	D-amino acid oxidase					1.51	
76747	Dapl1	Death associated protein-like 1			5.46			
13170	Dbp	D site albumin promoter binding protein					1.55	
195208	Dcdc2a	Doublecortin domain containing 2a					1.84	3.03
654457	Defb26	Defensin beta 26						-6.71
545475	Defb28	Defensin beta 28						-3.80
360214	Defb39	Defensin beta 39						-5.36
654458	Defb43	Defensin beta 43						-2.96
72121	Dennd2d	DENN/MADD domain containing 2D					1.60	
13350	Dgat1	Diacylglycerol O-acyltransferase 1				1.77		
241452	Dhrs9	Dehydrogenase/reductase (SDR family) member 9					-1.55	
50781	Dkk3	Dickkopf homolog 3 (Xenopus laevis)				2.10		
12945	Dmbt1	Deleted in malignant brain tumors 1		3.43				
73712	Dmkn	Dermokine			2.00			
226049	Dmrt2	Doublesex and mab-3 related transcription factor 2						-1.74
330355	Dnahc6	Dynein, axonemal, heavy chain 6					1.79	
69387	Dnajb13	DnaJ (Hsp40) related, subfamily B, member 13						-1.53
30045	Dnajc12	DnaJ (Hsp40) homolog, subfamily C, member 12		2.94				
76088	Dock8	Dedicator of cytokinesis 8					-1.94	
319446	Dpep2	Dipeptidase 2					-1.78	2.21
71712	Dram1	DNA-damage regulated autophagy modulator 1				1.85		
213696	Duoxa1	Dual oxidase maturation factor 1					-1.64	
13586	Ear1	Eosinophil-associated, ribonuclease A family, member 1		-1.79			-3.03	
93726	Ear11	Eosinophil-associated, ribonuclease A family, member 11					-3.21	
13587	Ear2	Eosinophil-associated, ribonuclease A family, member 2		-1.51				
93719	Ear6	Eosinophil-associated, ribonuclease A family, member 6		-2.12				
74147	Ehhadh	Enoyl-Coenzyme A, hydratase/3-hydroxyacyl dehydrogenase		-1.98				
12686	Elovl3	Elongation of very long chain fatty acids (yeast)-like 3		-1.72				
170439	Elovl6	ELOVL family member 6, elongation of long chain fatty acids (yeast)						-2.09
13732	Emp3	Epithelial membrane protein 3		-1.57				
13844	Ephb2	Eph receptor B2					-1.56	
13850	Ephx2	Epoxide hydrolase 2, cytoplasmic				1.67		
382053	Es31	Esterase 31			1.90		-1.84	
14009	Etv1	Ets variant gene 1		-1.55				
14048	Eya1	Eyes absent 1 homolog (Drosophila)		-2.67				
14061	F2	Coagulation factor II					-1.55	

			Liver		Muscle		Adipose	
ID	Symbol	Name	Young	Old	Young	Old	Young	Old
14068	F7	Coagulation factor VII					-1.79	
14080	Fabp1	Fatty acid binding protein 1, liver			4.09		-2.68	
14079	Fabp2	Fatty acid binding protein 2, intestinal		-1.61				
14077	Fabp3	Fatty acid binding protein 3, muscle and heart		2.23				
11770	Fabp4	Fatty acid binding protein 4, adipocyte				1.69		
16592	Fabp5	Fatty acid binding protein 5, epidermal		2.87				
21884	Fabp9	Fatty acid binding protein 9, testis						-3.04
14085	Fah	Fumarylacetoacetate hydrolase				1.94		
104943	Fam110c	Family with sequence similarity 110, member C					-1.64	
58909	Fam13a	Family with sequence similarity 13, member A				2.16	1.60	
75429	Fam183b	Family with sequence similarity 183, member B					3.74	5.11
245386	Fam70a	Family with sequence similarity 70, member A						-1.52
67030	Fancl	Fanconi anemia, complementation group L		-1.63				
14104	Fasn	Fatty acid synthase				2.13		
270120	Fat3	FAT tumor suppressor homolog 3 (Drosophila)						2.20
14129	Fcgr1	Fc receptor, IgG, high affinity I						1.63
14131	Fcgr3	Fc receptor, IgG, low affinity III				1.54		
246256	Fcgr4	Fc receptor, IgG, low affinity IV						1.90
59083	Fetub	Fetuin beta					-1.51	
110135	Fgb	Fibrinogen beta chain			2.56		-2.59	
14168	Fgf13	Fibroblast growth factor 13					-1.53	
99571	Fgg	Fibrinogen gamma chain			2.50		-2.54	
68680	Fitm1	Fat storage-inducing transmembrane protein 1		-1.53				
14262	Fmo3	Flavin containing monooxygenase 3		2.65			1.91	
72007	Fndc3b	Fibronectin type III domain containing 3B		1.56				
320181	Fndc7	Fibronectin type III domain containing 7						2.71
14281	Fos	FBJ osteosarcoma oncogene		-2.11				
14293	Fpr1	Formyl peptide receptor 1		-1.65				
654820	G530011O06Rik	RIKEN cDNA G530011O06 gene		1.78			-1.73	1.64
14381	G6pdx	Glucose-6-phosphate dehydrogenase X-linked				1.65		
209239	Gan	Giant axonal neuropathy		1.58				
14456	Gas6	Growth arrest specific 6		1.58				
14468	Gbp1	Guanylate binding protein 1						-2.03
14473	Gc	Group specific component			2.86		-3.68	
14562	Gdf3	Growth differentiation factor 3						1.68
66569	Gdpd1	Glycerophosphodiester phosphodiesterase domain containing 1		-1.54				
14583	Gfpt1	Glutamine fructose-6-phosphate transaminase 1		1.53				
244757	Glb1l2	Galactosidase, beta 1-like 2				1.61		
73690	Glipr1	GLI pathogenesis-related 1 (glioma)						1.83
100038441	Gm10419	Predicted gene 10419					1.97	
100042314	Gm10639	Predicted gene 10639		-1.59				
100038559	Gm10673	Predicted gene 10673					2.28	
434033	Gm10879	Predicted gene 10879		-1.70				
236047	Gm10880	Predicted gene 10880		2.06			-2.34	
100043125	Gm11711	Predicted gene 11711		-2.37				
664840	Gm12643	Predicted gene 12643					1.74	
229599	Gm129	Predicted gene 129					1.54	
381346	Gm13194	Predicted gene 13194					1.57	
384515	Gm1419	Predicted gene 1419		2.07			-2.30	
385120	Gm1502	Predicted gene 1502		1.97			-1.97	
235952	Gm189	Predicted gene 189		2.31			-1.87	
100041482	Gm3365	Predicted gene 3365					1.65	
100041932	Gm3579	Predicted gene 3579	-1.61	1.62				1.56
100042539	Gm3893	Predicted gene 3893						1.56
194604	Gm46	Predicted gene 46						-5.11

			Liver		Muscle		Adipose	
ID	Symbol	Name	Young	Old	Young	Old	Young	Old
243420	Gm4964	Predicted gene 4964		1.79		2.32		
381484	Gm5150	Predicted gene 5150						1.83
434025	Gm5571	Predicted gene 5571		-1.58				-2.07
434037	Gm5574	Immunoglobulin kappa chain variable 12-47		2.65			-2.17	
434510	Gm5627	Predicted gene 5627					-1.65	
435373	Gm5666	Predicted gene 5666					1.55	
546164	Gm5921	Predicted gene 5921					1.52	
623114	Gm6394	Predicted gene 6394					1.76	
624219	Gm6484	Predicted gene 6484					-1.70	
627821	Gm6792	Predicted gene 6792					-1.79	
633457	Gm7112	Predicted gene 7112						7.51
640532	Gm7299	Predicted gene 7299					1.82	
665033	Gm7455	Predicted gene 7455					-1.74	
665378	Gm7609	Predicted gene 7609					-2.07	
667410	Gm8615	Glucosamine-6-phosphate deaminase 1 pseudogene		-1.75				
667718	Gm8780	Predicted gene 8780						1.77
668603	Gm9264	Predicted gene 9264					2.44	
225443	Gm94	Predicted gene 94			3.56			
667055	Gm9992	Predicted gene 9992		-1.60				
14677	Gnai1	Guanine nucleotide binding protein (G protein), alpha inhibiting 1				1.64		
14711	Gnmt	Glycine N-methyltransferase					-1.50	
14727	Gp49a	Glycoprotein 49 A					-1.60	
93695	Gpnmb	Glycoprotein (transmembrane) nmb					-2.61	1.54
239853	Gpr128	G protein-coupled receptor 128		2.77				
14765	Gpr50	G-protein-coupled receptor 50					-5.50	
237175	Gpr64	G protein-coupled receptor 64					1.65	1.62
243270	Gpr81	G protein-coupled receptor 81				2.60		
243385	Gprin3	GPRIN family member 3						-1.61
75512	Gpx6	Glutathione peroxidase 6	-1.76					
23893	Grem2	Gremlin 2 homolog, cysteine knot superfamily (Xenopus laevis)		1.51				
14857	Gsta1	Glutathione S-transferase, alpha 1 (Ya)	-1.59	-1.82				
14858	Gsta2	Glutathione S-transferase, alpha 2 (Yc2)	-1.55	-1.66				
14860	Gsta4	Glutathione S-transferase, alpha 4					1.56	
14866	Gstm5	Glutathione S-transferase, mu 5					1.55	
68312	Gstm7	Glutathione S-transferase, mu 7					1.51	1.55
14872	Gstt2	Glutathione S-transferase, theta 2		-1.72				
14874	Gstz1	Glutathione transferase zeta 1 (maleylacetoacetate isomerase)				1.53		
70676	Gulp1	GULP, engulfment adaptor PTB domain containing 1					1.55	
232493	Gys2	Glycogen synthase 2						-2.29
14960	H2-Aa	Histocompatibility 2, class II antigen A, alpha		-1.66				
84506	Hamp	Hepcidin antimicrobial peptide			3.47		-4.94	
15116	Has1	Hyaluronan synthase1					-1.53	
15139	Hc	Hemolytic complement					-1.81	
79221	Hdac9	Histone deacetylase 9					-1.58	
319169	Hist1h2ak	Histone cluster 1, H2ak		-1.82				
360198	Hist1h3a	Histone cluster 1, H3a		-1.62				
319149	Hist1h3d	Histone cluster 1, H3d		-1.63				
260423	Hist1h3f	Histone cluster 1, H3f		-1.60				
97908	Hist1h3g	Histone cluster 1, H3g		-1.64				
319154	Hist2h3b	Histone cluster 2, H3b		-1.70				
15077	Hist2h3c1	Histone cluster 2, H3c1		-1.63				
319162	Hist3h2a	Histone cluster 3, H2a		-1.57				
545370	Hmcn1	Hemicentin 1					-1.56	
15357	Hmgcr	3-hydroxy-3-methylglutaryl-Coenzyme A reductase		1.66				

			Liver		Muscle		Adipose	
ID	Symbol	Name	Young	Old	Young	Old	Young	Old
208715	Hmgcs1	3-hydroxy-3-methylglutaryl-Coenzyme A synthase 1		1.53				
15368	Hmox1	Heme oxygenase (decycling) 1					-1.59	
21410	Hnf1b	HNF1 homeobox B					1.66	
15445	Hpd	4-hydroxyphenylpyruvic acid dioxygenase					-1.60	
54486	Hpgds	Hematopoietic prostaglandin D synthase		-1.65				1.69
15442	Hpse	Heparanase					-1.53	
15458	Hpx	Hemopexin					-2.92	
15496	Hsd3b5	Hydroxy-delta-5-steroid dehydrogenase, 3 beta-isomerase 5		-2.26				
15507	Hspb1	Heat shock protein 1		-2.03				
330723	Htra4	HtrA serine peptidase 4				-1.67		
244653	Hydin	Hydrocephalus inducing						1.80
619313	I730030J21Rik	RIKEN cDNA I730030J21 gene		-2.87				
15937	Ier3	Immediate early response 3					-1.51	
65972	Ifi30	Interferon gamma inducible protein 30		-1.64				
213002	Ifitm6	Interferon induced transmembrane protein 6						-1.50
16006	Igfbp1	Insulin-like growth factor binding protein 1		2.21				
16008	Igfbp2	Insulin-like growth factor binding protein 2	1.52					
16019	Igh-6	Immunoglobulin heavy chain 6 (heavy chain of IgM)		2.51			-5.08	
380794	Ighg	Immunoglobulin heavy chain (gamma polypeptide)		3.05				
380820	IghmAC38.205.12	Ig mu chain V region AC38 205.12		2.04				
619916	Ighv1-72	Immunoglobulin heavy variable V1-72		2.22			-1.80	
380800	Ighvq52.3.8	Immunoglobulin heavy chain variable region Q52.3.8		1.63			-1.73	1.75
16069	Igj	Immunoglobulin joining chain						-1.55
243469	Igk	Immunoglobulin kappa chain complex		1.70		-4.11	-1.71	
16081	Igk-V1	Immunoglobulin kappa chain variable 1 (V1)					-2.30	
667881	Igk-V19-14	Immunoglobulin kappa chain variable 19 (V19)-14		1.80			-1.94	-1.57
108024	Igk-V19-20	Immunoglobulin kappa chain variable 19 (V19)-20		2.29				2.54
626583	Igk-V21-2	Immunoglobulin kappa chain variable 21 (V21)-2					-1.62	
16114	Igk-V28	Immunoglobulin kappa chain variable 28 (V28)		2.63			-1.59	
434586	Igkv4-71	Immunoglobulin kappa chain variable 4-71		2.02			-2.11	
16142	Igl-V1	Immunoglobulin lambda chain, variable 1					-2.86	-2.20
110612	Igl-V2	Immunoglobulin lambda chain, variable 2					-1.91	-4.36
16176	Il1b	Interleukin 1 beta					-2.42	
16177	Il1r1	Interleukin 1 receptor, type I		1.81				
16181	Il1rn	Interleukin 1 receptor antagonist					-1.54	
77125	Il33	Interleukin 33						1.51
16190	Il4ra	Interleukin 4 receptor, alpha					-1.64	
16197	Il7r	Interleukin 7 receptor					-1.59	
23918	Impdh2	Inosine 5'-phosphate dehydrogenase 2		1.55				
21743	Inmt	Indolethylamine N-methyltransferase		-1.51			1.90	
231070	Insig1	Insulin induced gene 1				1.63	-1.82	
68265	Iqcf3	IQ motif containing F3						-3.18
71780	Isyna1	Myo-inositol 1-phosphate synthase A1		4.08				
16411	Itgax	Integrin alpha X					-1.99	1.57
16414	Itgb2	Integrin beta 2					-1.62	
16427	Itih4	Inter alpha-trypsin inhibitor, heavy chain 4					-1.87	
217837	Itpk1	Inositol 1,3,4-triphosphate 5/6 kinase					-1.51	
70337	Iyd	Iodotyrosine deiodinase						1.95
16483	Kap	Kidney androgen regulated protein					-1.91	-6.40
16527	Kcnk3	Potassium channel, subfamily K, member 3					-1.79	
16529	Kcnk5	Potassium channel, subfamily K, member 5		-1.76				
240776	Kcnt2	Potassium channel, subfamily T, member 2		1.86				
64697	Keg1	Kidney expressed gene 1						-1.99
17311	Kitl	Kit ligand		-1.56				
83379	Klb	Klotho beta				3.06		

			Liver		Muscle		Adipose	
ID	Symbol	Name	Young	Old	Young	Old	Young	Old
16612	Klk1	Kallikrein 1		-1.67				
16644	Kng1	Kininogen 1			2.79	-2.56	-2.75	
385643	Kng2	Kininogen 2					-1.69	
16661	Krt10	Keratin 10			2.83			
406220	Krt77	Keratin 77			3.02			
223917	Krt79	Keratin 79				1.54		
67127	Lce1a1	Late cornified envelope 1A1			4.58			
16819	Lcn2	Lipocalin 2	-5.83	1.97				1.98
13863	Lcn5	Lipocalin 5					-2.76	
235435	Lctl	Lactase-like					-1.91	-2.20
16852	Lgals1	Lectin, galactose binding, soluble 1	-1.58					
56072	Lgals12	Lectin, galactose binding, soluble 12				2.80		
16890	Lipe	Lipase, hormone sensitive				1.90		
67717	Lipf	Lipase, gastric					-2.11	
100046275	LOC100046275	Similar to Igha protein		2.49		-2.21	-2.37	-2.39
100046496	LOC100046496	Similar to Ig kappa V-region 24B		1.79			-1.64	
100047053	LOC100047053	Similar to monoclonal antibody kappa light chain					3.33	
100047070	LOC100047070	Similar to Ig rearranged gamma chain mRNA, V-J-C region						-1.77
382693	LOC382693	Similar to immunoglobulin heavy chain		2.78				
435333	LOC435333	Similar to monoclonal antibody heavy chain		2.42				
641089	LOC641089	Similar to Ig heavy chain V region BCL1 precursor		2.42				
676175	LOC676175	Similar to Ig kappa chain V-V region MPC11 precursor					-8.37	
14245	Lpin1	Lipin 1		1.54				
319476	Lrtm1	Leucine-rich repeats and transmembrane domains 1	-1.91					
16987	Lss	Lanosterol synthase		1.67				
17001	Ltc4s	Leukotriene C4 synthase				1.64		
17068	Ly6d	Lymphocyte antigen 6 complex, locus D						-2.04
17071	Ly6f	Lymphocyte antigen 6 complex, locus F						-3.24
68468	Ly6g6c	Lymphocyte antigen 6 complex, locus G6C			2.93			
17076	Ly75	Lymphocyte antigen 75		1.52				
17085	Ly9	Lymphocyte antigen 9					-1.54	
114332	Lyve1	Lymphatic vessel endothelial hyaluronan receptor 1		-2.14				
17110	Lyz1	Lysozyme 1						-1.66
16658	Mafb	v-maf musculoaponeurotic fibrosarcoma oncogene family, protein B				1.83		
105853	Mal2	Mal, T-cell differentiation protein 2					-1.60	-1.82
72289	Malat1	Metastasis associated lung adenocarcinoma transcript 1 (ncRNA)		1.65				
11720	Mat1a	Methionine adenosyltransferase I, alpha					-1.86	
17189	Mb	Myoglobin		1.81				
17203	Mc5r	Melanocortin 5 receptor						1.59
17436	Me1	Malic enzyme 1, NADP(+)-dependent, cytosolic	-1.63					-1.59
17276	Mela	Melanoma antigen		-3.82				-2.16
17294	Mest	Mesoderm specific transcript					-1.92	
76293	Mfap4	Microfibrillar-associated protein 4						1.52
76574	Mfsd2a	Major facilitator superfamily domain containing 2A	-1.59					
17318	Mid1	Midline 1		1.85				
56727	Miox	Myo-inositol oxygenase						-3.48
387218	Mir26a-1	MicroRNA 26a-1					1.55	
751545	Mir505	MicroRNA 505		1.74				
100124467	Mir568	MicroRNA 568					1.57	
735265	Mir703	MicroRNA 703		1.52				
17345	Mki67	Antigen identified by monoclonal antibody Ki 67		-1.59				
67468	Mmd	Monocyte to macrophage differentiation-associated				1.61		
75104	Mmd2	Monocyte to macrophage differentiation-associated 2	-1.55	1.86				
17381	Mmp12	Matrix metallopeptidase 12					-3.24	1.75
17386	Mmp13	Matrix metallopeptidase 13		-3.55				

			Liver		Muscle		Adipose	
ID	Symbol	Name	Young	Old	Young	Old	Young	Old
17393	Mmp7	Matrix metallopeptidase 7					1.95	7.65
17395	Mmp9	Matrix metallopeptidase 9						-1.67
233549	Mogat2	Monoacylglycerol O-acyltransferase 2					-2.08	-2.14
66112	Mosc1	MOCO sulphurase C-terminal domain containing 1					-1.86	-1.90
59012	Moxd1	Monooxygenase, DBH-like 1	-1.69					
17476	Mpeg1	Macrophage expressed gene 1					-1.50	1.51
77037	Mrap	Melanocortin 2 receptor accessory protein				2.30		
17534	Mrc2	Mannose receptor, C type 2					-2.25	
68774	Ms4a6d	Membrane-spanning 4-domains, subfamily A, member 6D				1.63	-1.83	
109225	Ms4a7	Membrane-spanning 4-domains, subfamily A, member 7		-2.78				
64381	Ms4a8a	Membrane-spanning 4-domains, subfamily A, member 8A		-1.88				-1.54
17748	Mt1	Metallothionein 1	-2.45	2.45				
17751	Mt3	Metallothionein 3						1.94
17754	Mtap1a	Microtubule-associated protein 1 A					-1.65	
320923	Mtap7d3	MAP7 domain containing 3					1.64	
20771	Mucl1	Mucin-like 1					1.71	
17836	Mug1	Murinoglobulin 1					-2.32	
17835	Mug-ps1	Murinoglobulin, pseudogene 1			2.02		-2.47	
17840	Mup1	Major urinary protein 1					-2.60	-3.94
100039028	Mup11	Major urinary protein 11			2.52		-2.70	-3.26
17841	Mup2	Major urinary protein 2			2.47		-2.66	-2.20
381530	Mup20	Major urinary protein 20			2.73		-3.38	
17842	Mup3	Major urinary protein 3				-3.20	-3.04	
100041658	Mup7	Major urinary protein 7			2.52		-2.71	-3.12
17855	Mvk	Mevalonate kinase		1.53				
17869	Myc	Myelocytomatosis oncogene						1.79
17879	Myh1	Myosin, heavy polypeptide 1, skeletal muscle, adult		2.47				
17882	Myh2	Myosin, heavy polypeptide 2, skeletal muscle, adult		2.27				
17901	Myl1	Myosin, light polypeptide 1		2.84				
17897	Myl3	Myosin, light polypeptide 3				-1.50		
71602	Myo1e	Myosin IE						1.85
667838	Naip3	NLR family, apoptosis inhibitory protein 3		-1.82				-1.62
269642	Nat8l	N-acetyltransferase 8-like				1.95		
18030	Nfil3	Nuclear factor, interleukin 3, regulated					-1.81	
70701	Nipal1	NIPA-like domain containing 1		1.81				
93960	Nkd1	Naked cuticle 1 homolog (Drosophila)					-1.61	
18111	Nnat	Neuronatin				2.05		
18113	Nnmt	Nicotinamide N-methyltransferase				2.00		
70729	Nos1ap	Nitric oxide synthase 1 (neuronal) adaptor protein		1.66				
18133	Nov	Nephroblastoma overexpressed gene						-1.98
664883	Nova1	Neuro-oncological ventral antigen 1						-1.50
109648	Npy	Neuropeptide Y						-2.89
83961	Nrg4	Neuregulin 4				2.31		
60345	Nrip2	Nuclear receptor interacting protein 2					-2.08	
70021	Nt5dc2	5'-nucleotidase domain containing 2		-1.51				
53814	Oaz3	Ornithine decarboxylase antizyme 3						-2.46
23966	Odz4	Odd Oz/ten-m homolog 4 (Drosophila)				1.99		
99543	Olfml3	Olfactomedin-like 3					-1.51	
258459	Olfr1388	Olfactory receptor 1388					-1.69	
50914	Olig1	Oligodendrocyte transcription factor 1	-1.50					
13603	Opn3	Opsin 3				1.53		
18406	Orm2	Orosomucoid 2	-6.34	1.98			-1.60	
18407	Orm3	Orosomucoid 3	-2.48	3.06				
18414	Osmr	Oncostatin M receptor		1.56				
21906	Otop1	Otopetrin 1					-1.64	
18430	Oxtr	Oxytocin receptor					-1.78	

			Liver		Muscle		Adipose	
ID	Symbol	Name	Young	Old	Young	Old	Young	Old
233571	P2ry6	Pyrimidinergic receptor P2Y, G-protein coupled, 6					-1.57	
18478	Pah	Phenylalanine hydroxylase					-1.70	-2.31
75552	Paqr9	Progestin and adipoQ receptor family member IX					-2.12	-1.76
18534	Pck1	Phosphoenolpyruvate carboxykinase 1, cytosolic				3.47		
76477	Pcolce2	Procollagen C-endopeptidase enhancer 2		1.57			-1.57	
18546	Pcp4	Purkinje cell protein 4						-7.33
66425	Pcp4l1	Purkinje cell protein 4-like 1				-1.51		2.02
18563	Pcx	Pyruvate carboxylase				1.72		
18576	Pde3b	Phosphodiesterase 3B, cGMP-inhibited				2.67		
170676	Peg10	Paternally expressed 10					-1.83	-2.00
18628	Per3	Period homolog 3 (Drosophila)					1.53	
64058	Perp	PERP, TP53 apoptosis effector			1.86			
18631	Pex11a	Peroxisomal biogenesis factor 11 alpha		-1.58				
56744	Pf4	Platelet factor 4		-3.46				
110208	Pgd	Phosphogluconate dehydrogenase				1.58		
228829	Phf20	PHD finger protein 20					1.56	
237928	Phospho1	Phosphatase, orphan 1		-1.56				
170741	Pilrb1	Paired immunoglobin-like type 2 receptor beta 1		-1.65				
18782	Pla2g2d	Phospholipase A2, group IID						-1.55
27226	Pla2g7	Phospholipase A2, group VII		1.62				
231507	Plac8	Placenta-specific 8					-1.87	
18793	Plaur	Plasminogen activator, urokinase receptor					-1.50	
56193	Plek	Pleckstrin		-1.53			-1.62	
18815	Plg	Plasminogen					-2.04	
103968	Plin1	Perilipin 1				2.56		
69060	Pnlip	Pancreatic lipase		-3.45				
18946	Pnliprp1	Pancreatic lipase related protein 1		-3.24				
18947	Pnliprp2	Pancreatic lipase-related protein 2		-2.77				
116939	Pnpla3	Patatin-like phospholipase domain containing 3				2.42		
19016	Pparg	Peroxisome proliferator activated receptor gamma		-1.50		1.65		
19017	Ppargc1a	Peroxisome proliferative activated receptor, gamma, coactivator 1 alpha					1.75	
57349	Ppbp	Pro-platelet basic protein		-2.46				
96875	Prg4	Proteoglycan 4 (megakaryocyte stimulating factor)		1.88				
19088	Prkar2b	Protein kinase, cAMP dependent regulatory, type II beta				2.71		
19118	Prm1	Protamine 1						-9.54
19119	Prm2	Protamine 2						-3.74
19126	Prom1	Prominin 1						1.61
114228	Prss1	Protease, serine, 1 (trypsin 1)		-1.80				
21755	Prss39	Protease, serine, 39						-2.42
19218	Ptger3	Prostaglandin E receptor 3 (subtype EP3)						-1.76
64292	Ptges	Prostaglandin E synthase				1.59		
19220	Ptgfr	Prostaglandin F receptor						-1.84
19225	Ptgs2	Prostaglandin-endoperoxide synthase 2						-4.86
70757	Ptplb	Protein tyrosine phosphatase-like, member b				1.92		
19288	Ptx3	Pentraxin related gene					-2.11	
19296	Pvt1	Plasmacytoma variant translocation 1					-1.74	
110078	Pygb	Brain glycogen phosphorylase				1.58		
11287	Pzp	Pregnancy zone protein			2.52		-2.83	
57785	Rangrf	RAN guanine nucleotide release factor		1.79				
19662	Rbp4	Retinol binding protein 4, plasma				1.85		
63954	Rbp7	Retinol binding protein 7, cellular				1.97		
19683	Rdh16	Retinol dehydrogenase 16	-1.55				1.83	
19692	Reg1	Regenerating islet-derived 1		-2.03				
57264	Retn	Resistin				2.25		
57262	Retnla	Resistin like alpha		-3.17				
245195	Retnlg	Resistin like gamma		-1.94				-1.53

			Liver		Muscle		Adipose	
ID	Symbol	Name	Young	Old	Young	Old	Young	Old
67442	Retsat	Retinol saturase (all trans retinol 13,14 reductase)		-1.72				
50778	Rgs1	Regulator of G-protein signaling 1					-2.11	2.83
19734	Rgs16	Regulator of G-protein signaling 16					-1.75	
19735	Rgs2	Regulator of G-protein signaling 2						1.91
214951	Rhbdl1	Rhomboid, veinlet-like 1 (Drosophila)		-1.51				
19752	Rnase1	Ribonuclease, RNase A family, 1 (pancreatic)		-4.07				
497106	Rnase12	Ribonuclease, RNase A family, 12 (non-active)						-5.75
223881	Rnd1	Rho family GTPase 1					-1.69	
66889	Rnf128	Ring finger protein 128						2.71
19876	Robo1	Roundabout homolog 1 (Drosophila)	-1.62					
19885	Rorc	RAR-related orphan receptor gamma					1.57	
12394	Runx1	Runt related transcription factor 1					-1.76	
20201	S100a8	S100 calcium binding protein A8 (calgranulin A)					-1.84	
20202	S100a9	S100 calcium binding protein A9 (calgranulin B)					-1.78	
20208	Saa1	Serum amyloid A 1	-10.57	15.90				
20209	Saa2	Sserum amyloid A 2	-8.35	3.26			-4.71	
20210	Saa3	Serum amyloid A 3	-4.60	1.74			-2.31	1.66
71145	Scara5	Scavenger receptor class A, member 5 (putative)		1.72				
100306943	Scarna13	Small Cajal body-specific RNA 1	2.52			1.59		
20250	Scd2	Stearoyl-Coenzyme A desaturase 2						-1.97
30049	Scd3	Stearoyl-coenzyme A desaturase 3			2.47			
70061	Sdr9c7	4 short chain dehydrogenase/reductase family 9C, member 7		-1.69				
58210	Sectm1b	Secreted and transmembrane 1B					2.30	4.40
217847	Serpina10	Serine (or cysteine) peptidase inhibitor, clade A, member 10		1.63				
20700	Serpina1a	Serine (or cysteine) peptidase inhibitor, clade A, member 1A					-2.49	
20701	Serpina1b	Serine (or cysteine) preptidase inhibitor, clade A, member 1B			2.92		-2.71	
20702	Serpina1c	Serine (or cysteine) peptidase inhibitor, clade A, member 1C			3.79		-4.81	
20703	Serpina1d	Serine (or cysteine) peptidase inhibitor, clade A, member 1D					-1.93	
20704	Serpina1e	Serine (or cysteine) peptidase inhibitor, clade A, member 1E			2.97	-4.83	-3.01	
68348	Serpina1f	Serine (or cysteine) peptidase inhibitor, clade A, member 1F						-15.41
271047	Serpina3b	Serine (or cysteine) peptidase inhibitor, clade A, member 3B				1.53		
16625	Serpina3c	Serine (or cysteine) peptidase inhibitor, clade A, member 3C				1.73		
20714	Serpina3k	Serine (or cysteine) peptidase inhibitor, clade A, member 3K					-1.62	
20716	Serpina3n	Serine (or cysteine) peptidase inhibitor, clade A, member 3N				1.54		
12401	Serpina6	Serine (or cysteine) peptidase inhibitor, clade A, member 6					-2.25	
20708	Serpinb6b	Serine (or cysteine) peptidase inhibitor, clade B, member 6b		-1.87				
15160	Serpind1	Serine (or cysteine) peptidase inhibitor, clade D, member 1					-1.91	
18787	Serpine1	Serine (or cysteine) peptidase inhibitor, clade E, member 1						-1.71
20720	Serpine2	Serine (or cysteine) peptidase inhibitor, clade E, member 2		-1.65				
20377	Sfrp1	Secreted frizzled-related protein 1					-1.72	
20379	Sfrp4	Secreted frizzled-related protein 4						-1.80
14057	Sfxn1	Sideroflexin 1				2.16		
27219	Sgk2	Serum/glucocorticoid regulated kinase 2		-1.59				
268396	Sh3pxd2b	SH3 and PX domains 2B					-1.64	
66940	Shisa5	Shisa homolog 5 (Xenopus laevis)		1.60				
320832	Sirpb1a	Signal-regulatory protein beta 1A					-1.66	1.78
668101	Sirpb1b	Signal-regulatory protein beta 1B					-2.02	1.73
27401	Skp2	S-phase kinase-associated protein 2 (p45)		-1.58				
30925	Slamf6	SLAM family member 6		-1.74				
75345	Slamf7	SLAM family member 7		-1.68				

			Liver		Muscle		Adipose	
ID	Symbol	Name	Young	Old	Young	Old	Young	Old
20493	Slc10a1	Solute carrier family 10 (sodium/bile acid cotransporter), member 1					-2.21	
114644	Slc13a3	Solute carrier family 13 (sodium-dependent dicarboxylate), member 3		1.52				
237831	Slc13a5	Solute carrier family 13 (sodium-dependent citrate), member 5		2.42				
65221	Slc15a3	Solute carrier family 15, member 3					-1.57	
277898	Slc15a5	Solute carrier family 15, member 5				-1.64		-1.78
217316	Slc16a5	Solute carrier family 16 (monocarboxylic acid transporters), member 5	-2.22					
216227	Slc17a8	Solute carrier family 17 (sodium-dependent phosphate), member 8	-1.82	-1.54				
20512	Slc1a3	Solute carrier family 1 (glial high affinity glutamate), member 3				2.37		
55963	Slc1a4	Solute carrier family 1 (glutamate/neutral amino acid), member 4		1.93				
20514	Slc1a5	Solute carrier family 1 (neutral amino acid transporter), member 5				2.07		
20519	Slc22a3	Solute carrier family 22 (organic cation transporter), member 3	-1.65					
20520	Slc22a5	Solute carrier family 22 (organic cation transporter), member 5		-1.74				
13358	Slc25a1	Solute carrier family 25 (mitochondrial citrate transporter), member 1				1.91		
27376	Slc25a10	Solute carrier family 25 (mitochondrial dicarboxylate), member 10				1.98		
217593	Slc25a21	Solute carrier family 25 (mitochondrial oxodicarboxylate), member 21		-1.58				
227731	Slc25a25	Solute carrier family 25 (mitochondrial, phosphate carrier), member 25		-1.57				
26458	Slc27a2	Solute carrier family 27 (fatty acid transporter), member 2						-1.70
20505	Slc34a1	Solute carrier family 34 (sodium phosphate), member 1						-2.99
246049	Slc36a2	Solute carrier family 36 (proton/amino acid symporter), member 2				2.39		
224674	Slc37a1	Solute carrier family 37 (glycerol-3-phosphate transporter), member 1		2.09				
56857	Slc37a2	Solute carrier family 37 (glycerol-3-phosphate transporter), member 2						1.65
76257	Slc38a3	Solute carrier family 38, member 3					-1.62	
213053	Slc39a14	Solute carrier family 39 (zinc transporter), member 14		1.57				
14977	Slc39a7	Solute carrier family 39 (zinc transporter), member 7		1.52				
338365	Slc41a2	Solute carrier family 41, member 2		1.67				
100434	Slc44a1	Solute carrier family 44, member 1					1.75	
213603	Slc44a3	Solute carrier family 44, member 3				2.25		
20533	Slc4a1	Solute carrier family 4 (anion exchanger), member 1		-2.82				
63993	Slc5a7	Solute carrier family 5 (choline transporter), member 7					-3.38	
53896	Slc7a10	Solute carrier family 7 (cationic amino acid, y+ system), member 10				2.46		
105243	Slc9a3	Solute carrier family 9 (sodium/hydrogen exchanger), member 3					1.82	
28248	Slco1a1	Solute carrier organic anion transporter family, member 1a1		-3.20				
20568	Slpi	Secretory leukocyte peptidase inhibitor		1.60				
55994	Smad9	MAD homolog 9 (Drosophila)		-1.61				
17235	Smcp	Sperm mitochondria-associated cysteine-rich protein						-4.12
64075	Smoc1	SPARC related modular calcium binding 1				2.17		
58994	Smpd3	Sphingomyelin phosphodiesterase 3, neutral		1.86				
100310813	Snora16a	Small nucleolar RNA, H/ACA box 16A		1.68				
100302499	Snora3	Small nucleolar RNA, H/ACA box 3				2.13		
100306944	Snora73a	Small nucleolar RNA, H/ACA box 73a		1.77		1.64		
100306945	Snora73b	Small nucleolar RNA, H/ACA box 73b		1.71				
218739	Sntn	Sentan, cilia apical structure protein					2.88	9.61
216233	Socs2	Suppressor of cytokine signaling 2		1.83				
12702	Socs3	Suppressor of cytokine signaling 3					-1.72	
20660	Sorl1	Sortilin-related receptor, LDLR class A repeats-containing					-1.50	
67926	Spert	Spermatid associated						-2.43

			Liver		Muscle		Adipose	
ID	Symbol	Name	Young	Old	Young	Old	Young	Old
20728	Spic	Spi-C transcription factor (Spi-1/PU.1 related)		-2.10				
78709	Spink8	Serine peptidase inhibitor, Kazal type 8						-48.07
75526	Spinlw1	Serine protease inhibitor-like, with Kunitz and WAP domains 1 (eppin)						-1.99
629747	Spint3	Serine peptidase inhibitor, Kunitz type, 3						-3.29
20750	Spp1	Secreted phosphoprotein 1					-2.13	4.23
20753	Sprr1a	Small proline-rich protein 1A						-4.02
20755	Sprr2a1	Small proline-rich protein 2A1						-5.91
20775	Sqle	Squalene epoxidase		1.60				
94224	Srd5a2	Steroid 5 alpha-reductase 2					1.62	
68792	Srpx2	Sushi-repeat-containing protein, X-linked 2		-1.57				
20440	St6gal1	Seta galactoside alpha 2,6 sialyltransferase 1		1.65				
76630	Stambpl1	STAM binding protein like 1					-1.66	
56792	Stap1	Signal transducing adaptor family member 1						1.54
117167	Steap4	STEAP family member 4		2.24				
232533	Stk38l	Serine/threonine kinase 38 like		1.51				
69083	Sult1c2	Sulfotransferase family, cytosolic, 1C, member 2					1.91	
20860	Sult1e1	Sulfotransferase family 1E, member 1		6.50			1.64	
57430	Sult3a1	Sulfotransferase family 3A, member 1		14.28				
96935	Susd4	Sushi domain containing 4						1.93
68416	Sycn	Syncollin		-4.42				
20977	Syp	Synaptophysin					-1.51	
234724	Tat	Tyrosine aminotransferase					-1.71	
237052	Tceal1	Transcription elongation factor A (SII)-like 1					1.56	
66684	Tceal8	Transcription elongation factor A (SII)-like 8	-1.85					
21637	Tcrg-V3	T-cell receptor gamma, variable 3		-1.92				-1.58
21786	Tff3	Trefoil factor 3, intestinal	1.72					
21789	Tfpi2	Tissue factor pathway inhibitor 2					-1.53	
21828	Thbs4	Thrombospondin 4					-1.75	
21835	Thrsp	Thyroid hormone responsive SPOT14 homolog (Rattus)				2.12		
24001	Tiam2	T-cell lymphoma invasion and metastasis 2		-1.53				
211550	Tifa	TRAF-interacting protein with forkhead-associated domain		2.25				
276891	Timd4	T-cell immunoglobulin and mucin domain containing 4						-1.96
21857	Timp1	Tissue inhibitor of metalloproteinase 1					-2.34	2.00
21881	Tkt	Transketolase				1.72		
21897	Tlr1	Toll-like receptor 1						1.64
279572	Tlr13	Toll-like receptor 13		-1.58			-1.64	1.65
170744	Tlr8	Toll-like receptor 8		-1.86				
277203	Tm4sf19	Transmembrane 4 L six family member 19					-1.79	
56363	Tmeff2	Transmembrane protein with EGF-like and two follistatin-like domains 2					-1.52	
217203	Tmem106a	Transmembrane protein 106A				1.54		
215210	Tmem120a	Transmembrane protein 120A				1.66		
320782	Tmem154	Transmembrane protein 154						-1.51
208613	Tmem212	Transmembrane protein 212					1.71	3.08
57394	Tmem27	Transmembrane protein 27						-4.35
235135	Tmem45b	Transmembrane protein 45b				2.14		
50528	Tmprss2	Transmembrane protease, serine 2		1.51				
21928	Tnfaip2	Tumor necrosis factor, alpha-induced protein 2					-2.07	
21924	Tnnc1	Troponin C, cardiac/slow skeletal				-1.57		
21925	Tnnc2	Troponin C2, fast		1.59				
21957	Tnnt3	Troponin T3, skeletal, fast		1.97				
21958	Tnp1	Transition protein 1						-2.15
21959	Tnp2	Transition protein 2						-4.31
76757	Trdn	Triadin		3.17			-8.88	
83433	Trem2	Triggering receptor expressed on myeloid cells 2		-1.99			-1.59	1.93
22041	Trf	Transferrin				1.57		

			Liver		Muscle		Adipose	
ID	**Symbol**	**Name**	**Young**	**Old**	**Young**	**Old**	**Young**	**Old**
103964	Try5	Trypsin 5		-4.30				
22095	Tshr	Thyroid stimulating hormone receptor				2.59		
244152	Tsku	Tsukushin	-1.66					
269831	Tspan12	Tetraspanin 12				1.65		
12257	Tspo	Translocator protein				1.53		
22117	Tst	Thiosulfate sulfurtransferase, mitochondrial						1.56
22138	Ttn	Titin		1.69				
22139	Ttr	Transthyretin			2.41		-2.77	
22151	Tubb2a	Tubulin, beta 2A	-1.88					
237858	Tusc5	Tumor suppressor candidate 5				1.87		
22177	Tyrobp	TYRO protein tyrosine kinase binding protein				1.55		
22245	Uck1	Uridine-cytidine kinase 1				1.55		
223337	Ugt3a2	UDP glycosyltransferases 3 family, polypeptide A2						-2.34
22248	Unc119	Unc-119 homolog (C. elegans)						-1.73
381058	Unc93a	Unc-93 homolog A (C. elegans)		-1.55				
109637	Upk1a	Uroplakin 1A						-2.19
75083	Usp50	Ubiquitin specific peptidase 50					1.57	
380822	V165-D-J-C mu	IgM variable region		3.71				
22329	Vcam1	Vascular cell adhesion molecule 1		-2.13				
22361	Vnn1	Vanin 1		-1.79				-1.53
629756	Wfdc10	WAP four-disulfide core domain 10						-3.62
408190	Wfdc13	WAP four-disulfide core domain 13						-3.24
192201	Wfdc15b	WAP four-disulfide core domain 15B						-5.71
22403	Wisp2	WNT1 inducible signaling pathway protein 2					-1.82	
22630	Ywhaq	Tyr 3-monooxygenase/tryptophan 5-monooxygenase activation protein						1.51
58203	Zbp1	Z-DNA binding protein 1					-1.59	
170938	Zfp617	Zinc finger protein 617					1.53	
268670	Zfp759	Zinc finger protein 759					1.56	
69036	Zg16	Zymogen granule protein 16		-5.04				
226409	Zranb3	Zinc finger, RAN-binding domain containing 3						1.83

Appendix 1. Genotype-associated gene expression changes from microarray experiments

[1]Listed here are all genes whose expression changed with genotype, comparing *Myc*$^{+/-}$ mice with *Myc*$^{+/+}$ control mice at two ages (5 and 24 months) and three tissues (liver, skeletal muscle and white adipose). See Figure 4.1A for a schematic representation of all gene expression changes. Genes whose expression changed with age (vertical lines, Figure 4.1A) or tissue (horizontal lines, Figure 5A) were too numerous to list here. For the full dataset see the NCBI Gene Expression Omnibus (GEO) database (accession GSE55272). The numbers in the table designate fold-changes, where genes upregulated in *Myc*$^{+/+}$ *versus* *Myc*$^{+/-}$ animals (*i.e.* MYC activated genes) are shown with positive values and are shaded red. Conversely, genes upregulated in *Myc*$^{+/-}$ *versus* *Myc*$^{+/+}$ animals (*i.e.* MYC repressed genes) are shown with negative values and are shaded blue.

[2]The bottom row of the header summarizes the total number of genes in each column, using the same conventions as in Figure 4.1A. A 1.5-fold cutoff and a FDR threshold of <5% were used to calculate the number of genes changing expression. N=5-8 male animals in each group.

Appendix 2. Upstream regulators implicated by analysis of microarray data[1]

	Liver				Adipose				Skeletal Muscle			
	ΔGenotype[2]		ΔAge[3]		ΔGenotype[2]		ΔAge[3]		ΔGenotype[2]		ΔAge[3]	
Upstream Regulator	Young	Old	+/+	+/–	Young	Old	+/+	+/–	Young	Old	+/+	+/–
SREBF1	3.0	-2.9	1.0	0.0	3.4	3.6	-2.8	-2.2	0.0	-2.9	3.8	3.5
PPARG	3.3	1.1	-1.9	0.0	-1.1	3.0	-3.9	-2.3	0.0	-4.6	3.2	3.3
SREBF2	1.9	-3.3	1.1	0.0	2.6	2.9	-3.1	-2.1	0.0	-1.9	4.4	3.7
SCAP	2.1	-2.5	0.5	0.0	1.8	3.0	-3.2	-2.1	0.0	-2.2	4.1	3.1
INSIG1	-2.8	2.3	-3.7	-5.0	-4.1	-1.9	-0.5	-1.6	0.0	3.4	-5.7	-2.9
Tretinoin	2.5	2.0	5.1	6.6	3.5	-0.9	4.3	4.9	0.0	-4.3	3.0	0.8
INSIG2	0.0	2.6	0.7	0.0	-1.0	-2.2	2.2	0.7	0.0	2.2	-2.3	-1.9
THRB	1.7	-1.7	-0.1	0.0	-1.3	2.8	-1.8	-0.2	0.0	-2.2	0.7	0.0
PPARA	2.3	3.9	-1.2	2.4	-0.4	-0.4	-2.5	-1.2	0.2	-2.4	2.1	2.5
IL5	1.1	-1.4	6.0	4.8	3.5	2.0	3.3	2.4	0.0	-2.9	2.7	1.3
OSM	1.9	-2.4	5.8	4.4	3.7	2.8	3.0	1.3	-1.4	0.8	1.1	0.5
CSF2	1.4	0.2	8.3	7.7	5.2	-2.8	7.6	3.8	0.0	-2.9	4.6	1.9
MITF	0.0	2.4	2.2	0.0	0.9	-1.5	2.1	1.0	0.0	-1.9	2.6	1.8
NR1H3	0.0	-2.5	-0.5	0.0	-0.3	1.2	-0.5	-0.2	0.0	-2.0	1.9	1.5
Arachidonic acid	-1.1	2.1	2.2	0.8	0.2	-1.3	1.0	0.7	0.0	2.2	-1.3	-0.6
LDL	2.0	1.6	3.5	4.2	3.6	-1.4	3.2	1.0	0.0	-2.5	2.7	1.9
MAPK9	0.9	0.5	0.0	1.4	-0.1	2.4	0.1	0.8	0.0	-2.6	1.0	0.8
TGM2	0.0	1.9	5.3	5.6	4.4	0.7	5.5	4.0	0.0	-2.8	5.0	2.3
CD44	1.1	1.7	3.7	4.0	1.9	-2.4	4.5	1.5	0.0	-1.3	1.3	0.0
L-glutamic acid	2.4	0.9	2.6	0.0	1.7	1.8	-0.5	-0.4	0.0	-2.6	1.8	1.5
FGF21	0.0	-0.9	-0.2	0.0	0.0	1.7	-0.5	0.4	0.0	-2.6	1.0	0.7
ESR1	0.4	0.5	1.8	2.7	1.4	-2.2	0.2	-1.0	0.0	-2.6	0.2	0.0
EGR1	2.0	1.4	3.0	3.4	2.3	2.4	1.7	0.0	0.0	-1.4	0.4	-1.2
AICAR	0.8	1.5	-0.6	0.0	-1.7	-2.6	-0.1	-0.6	0.0	-1.1	0.0	0.0
ARNT2	0.0	2.7	0.0	0.0	2.9	0.0	2.7	2.7	0.0	-2.4	2.2	2.6
SIM1	0.0	2.7	0.0	0.0	3.1	0.0	2.8	3.0	0.0	-2.4	1.9	2.5
ATP7B	1.0	-2.7	-1.2	0.0	1.0	2.4	-3.0	-0.9	0.0	0.0	3.3	2.7
RAF1	1.2	2.6	2.2	4.0	2.2	0.5	1.0	0.3	0.0	-2.0	0.8	-1.2
HRG	0.0	2.4	3.6	3.4	1.9	-2.6	2.5	1.3	0.0	0.0	0.3	-2.1
IGF1	2.0	-1.9	2.1	0.0	2.9	0.7	1.5	-0.5	0.0	-2.5	-0.4	-0.9
IL4	1.2	2.0	4.7	4.8	4.0	0.5	3.6	0.1	0.0	-2.5	3.9	1.2
VEGFA	0.0	2.1	1.9	1.9	1.7	0.3	1.3	0.8	0.0	-2.6	-0.7	-2.5
Sterol	0.0	2.4	0.0	0.0	-1.2	-1.9	2.9	1.0	0.0	0.6	-1.5	0.0
CSF1	0.0	0.9	5.6	5.3	4.2	-1.6	4.0	1.9	0.0	-2.4	2.9	0.8
F2	2.6	1.3	5.4	0.0	3.4	1.3	4.2	1.5	0.0	-2.1	0.0	-1.3
HOXA10	-1.3	-1.4	-0.3	0.0	-0.1	0.4	-1.3	-2.2	0.0	3.0	-2.8	-1.0
MED13	-2.6	0.0	1.4	0.0	0.0	-2.2	3.2	1.3	0.0	2.5	-3.5	-2.3
Cholesterol	0.8	1.2	2.8	3.5	1.6	-3.3	3.1	2.1	0.0	0.2	0.3	-1.0
PPARGC1B	0.0	-2.7	0.7	0.0	0.9	0.0	-1.5	-0.1	0.0	-2.0	1.9	2.5
NR1I2	3.5	-1.0	2.2	0.0	-0.3	1.1	-3.1	-1.1	2.0	-2.6	2.5	0.0
CDKN1A	0.0	-1.9	-0.4	-1.5	-0.1	2.7	-1.9	0.0	0.0	0.0	0.0	0.0
PDGF BB	2.6	-1.0	4.2	0.0	4.6	-0.9	5.1	1.5	0.0	-2.7	0.2	-0.7
IL22	0.0	-2.9	3.7	2.9	1.7	-1.6	2.8	0.4	0.0	0.0	0.0	0.0
MAP2K1	0.0	0.7	4.0	0.0	2.9	-1.5	3.0	0.4	0.0	-2.4	1.3	0.0
MAP4K4	-2.6	0.0	1.5	0.0	1.5	-2.0	6.9	4.8	0.0	2.6	-0.5	-1.8
P38 MAPK	2.6	1.8	4.3	4.8	3.7	-0.8	5.1	1.8	0.0	-2.0	0.1	-0.8
IFNAR1	0.0	2.1	1.9	3.6	1.2	-0.4	4.0	3.9	0.0	-2.0	2.2	0.0
ANGPT2	2.0	0.7	2.7	0.0	2.6	2.4	0.3	-0.4	0.0	-1.4	0.1	-1.5
POR	-2.2	1.4	-2.5	-3.1	-2.6	-3.0	0.8	0.9	0.0	0.1	-2.9	-1.4
CFTR	-1.1	2.9	-2.0	0.0	-1.3	-0.4	-2.2	-0.8	0.0	-1.1	-0.1	0.0
STAT3	1.3	-1.6	5.4	4.1	3.7	-1.2	4.9	2.7	0.0	-1.7	1.0	-0.5
SLC13A1	-2.1	2.5	-1.3	0.0	-1.7	-1.9	0.0	0.0	0.0	0.0	0.6	-0.7

	Liver				Adipose				Skeletal Muscle			
	ΔGenotype[2]		ΔAge[3]		ΔGenotype[2]		ΔAge[3]		ΔGenotype[2]		ΔAge[3]	
Upstream Regulator	Young	Old	+/+	+/–	Young	Old	+/+	+/–	Young	Old	+/+	+/–
Interferon alpha	2.2	1.0	6.7	7.1	4.2	-1.9	7.0	5.9	0.0	-1.5	4.8	2.2
IL15	0.0	0.8	3.2	3.6	2.7	-1.3	3.9	1.8	0.0	-2.2	0.4	0.0
IL27	0.0	0.8	3.2	5.0	4.0	-1.5	5.7	4.2	0.0	-2.0	4.0	0.0
Carbohydrate	0.0	0.0	-2.3	0.0	0.0	2.2	0.0	0.3	0.0	-2.0	2.3	2.1
IRS1	0.0	-1.2	-1.4	0.0	1.7	0.9	0.3	-0.9	0.0	-2.1	1.4	0.1
APP	0.0	2.3	2.4	3.5	1.9	0.2	2.4	0.2	0.0	-1.7	0.7	-0.8
MYOD1	0.9	-2.3	2.7	0.0	0.4	-0.6	-1.0	-2.2	0.0	-1.3	2.2	3.9
CEBPA	2.7	-0.8	2.8	3.2	3.5	-0.4	1.6	0.4	0.0	-2.8	1.6	0.1
Ethanol	2.5	-2.0	3.9	2.2	1.0	-0.8	1.1	-0.5	0.0	-1.3	-0.5	-0.2
PTEN	-0.7	0.7	-0.7	-0.8	-1.2	-0.8	0.1	-0.6	0.0	2.6	-0.4	0.5
SRF	0.0	-0.7	2.3	-1.8	0.9	2.0	-1.0	-0.6	0.0	1.2	-0.9	0.0
APOE	0.0	-1.8	-3.6	-3.9	-2.7	1.8	-4.5	-2.6	0.0	0.4	-0.6	0.6
XBP1	0.0	-3.9	4.6	4.8	0.0	0.0	0.0	0.0	0.0	0.1	2.0	1.3
STAT5B	0.6	0.8	0.3	0.0	1.6	0.7	-1.2	-1.8	0.0	-2.5	2.0	1.9
IL6	1.6	-2.3	6.2	5.4	4.0	-1.0	5.3	1.6	-1.4	-0.6	1.3	1.0
ACACB	0.0	2.2	0.0	0.0	0.0	0.0	0.5	-0.2	0.0	1.7	0.0	-0.3
MAPK14	0.0	1.8	3.7	3.8	2.2	0.5	4.1	2.7	0.0	-1.6	0.5	-0.2
PI3K (complex)	1.8	1.3	4.6	0.0	3.2	-0.1	3.1	0.9	0.0	-2.4	0.9	-0.3
HRAS	0.0	1.4	2.9	3.3	2.5	1.6	3.1	0.5	0.0	-0.9	1.4	1.6
NCOA2	0.4	1.4	1.2	0.0	1.7	0.0	0.7	0.8	0.0	-2.4	1.6	1.8
SP1	0.0	-0.8	4.0	0.0	1.2	0.5	2.1	-0.5	0.0	-2.6	0.5	-0.4
Thyroid hormone	0.0	-0.9	-0.8	0.0	-1.1	0.7	-0.4	1.0	0.0	-2.2	-0.4	-1.4
CHUK	2.8	-0.7	4.7	4.9	4.0	-0.1	5.9	4.4	0.0	-3.0	1.3	0.0
D-fructose	0.0	-1.1	0.3	0.0	0.0	0.0	-1.7	-2.0	0.0	-2.6	2.9	0.0
STAT1	1.4	1.0	5.2	6.5	4.0	0.3	6.2	5.7	0.0	-2.4	3.6	1.4
IL2	0.4	-0.6	5.8	5.6	3.2	-1.3	6.2	3.7	0.0	-1.9	2.8	1.6
CSF3	0.0	-1.1	2.2	2.9	2.0	-1.3	2.6	1.6	0.0	-1.4	0.7	0.0
Beta-carotene	-2.0	-0.8	-0.1	0.0	-2.6	-2.6	2.0	2.2	0.0	0.3	-1.2	-0.8
SPI1	0.0	0.2	4.3	5.1	4.0	-1.5	4.7	4.4	0.0	-2.0	3.2	0.0
TGFB3	0.0	1.5	2.3	0.0	2.1	2.2	0.4	-0.7	0.0	0.0	-1.3	-0.7
VIMP	0.0	1.2	0.0	0.0	0.0	0.0	-0.7	0.0	0.0	2.4	-1.8	-1.1
ADRB	-2.2	1.9	-2.2	-1.1	-2.5	-1.7	1.1	0.0	0.0	0.0	-1.3	-1.1
Inosine	0.0	0.4	3.4	2.3	1.4	-0.3	2.2	1.9	0.0	-3.0	1.4	-1.3
LEP	0.0	0.9	4.4	4.4	2.3	-2.5	2.3	0.0	-0.4	0.2	0.8	-0.4
PRL	0.4	-1.1	2.5	0.0	2.3	-2.3	3.1	1.5	0.0	-0.3	0.0	-0.4
RIPK2	0.0	1.1	2.0	2.4	0.0	-2.0	1.8	0.0	0.0	0.4	0.0	0.0
TGFBR1	0.0	1.4	1.5	0.0	1.6	2.2	0.1	0.6	0.0	0.0	-2.3	0.0
LGALS3	0.0	1.3	0.2	0.0	-2.1	0.0	-0.9	1.3	0.0	-2.2	1.5	1.8
Ins1	1.6	-0.5	1.4	0.0	2.3	1.6	-0.6	-2.8	0.0	-1.4	0.2	-0.1
TGFB1	-0.5	-0.1	5.9	3.3	4.4	1.1	1.9	-1.0	0.0	-2.3	-0.4	-1.1
IL1B	2.5	-0.8	7.7	6.5	4.2	-1.0	7.0	3.5	-1.0	-1.7	2.5	0.7
IGE	0.0	1.3	2.8	2.0	2.2	-2.2	2.0	-0.2	0.0	0.0	2.1	0.0
TNFSF11	2.4	0.8	4.9	4.6	4.4	-0.7	3.4	1.4	0.0	-1.9	2.0	0.3
IKBKG	1.3	-1.5	3.9	4.3	2.6	-0.2	4.8	4.0	0.0	-1.7	1.3	0.0
CEBPB	2.0	-2.0	3.7	3.9	2.7	-0.5	2.2	1.3	0.0	-1.0	1.9	1.1
NOTCH1	2.2	0.9	1.5	2.1	0.6	0.5	2.3	-0.8	0.0	-2.0	1.8	0.1
SMARCB1	0.0	1.0	0.8	0.9	1.2	0.0	0.3	1.2	0.0	-2.4	1.4	0.0
TP53	1.0	-0.7	1.8	-0.9	1.3	0.6	-0.7	-0.7	0.5	-2.0	0.0	-0.5
LIF	-0.1	-0.4	1.3	2.2	3.2	-1.6	4.5	1.4	-2.2	-1.3	0.0	0.0
TNFSF12	0.0	2.4	3.8	4.8	4.7	-0.9	4.8	1.7	0.0	0.0	2.8	-0.4
IFNB1	0.0	2.9	2.7	5.5	1.2	0.1	4.0	4.8	0.0	-0.3	3.3	2.4
TICAM1	2.0	-0.1	4.8	5.8	2.8	1.2	5.5	5.3	0.0	-2.0	3.7	0.0
NFE2L2	3.1	-0.5	5.5	3.5	-0.5	-1.2	-3.2	-3.4	0.0	-1.6	2.3	1.8
IL13	0.7	1.3	3.6	3.3	3.5	-0.2	2.8	0.8	0.0	-1.9	3.0	0.4

	Liver				Adipose				Skeletal Muscle			
	ΔGenotype[2]		ΔAge[3]		ΔGenotype[2]		ΔAge[3]		ΔGenotype[2]		ΔAge[3]	
Upstream Regulator	Young	Old	+/+	+/–	Young	Old	+/+	+/–	Young	Old	+/+	+/–
N-cor	0.0	0.4	-2.0	0.0	-1.4	-0.4	0.0	0.4	0.0	2.5	-3.0	-1.8
MYC	-1.5	-0.9	-0.5	-0.4	-2.1	-1.1	-0.8	-2.5	0.0	1.3	0.5	0.9
CREB1	0.0	0.7	0.9	0.0	1.4	0.1	1.2	-1.0	0.0	-2.4	0.0	0.1
RAC1	0.0	0.7	2.5	0.0	2.8	2.6	1.4	0.3	0.0	0.0	0.4	0.0
CCL2	0.0	1.0	1.4	2.0	2.0	-1.1	4.0	2.2	0.0	1.1	-0.9	0.0
IRGM	0.0	-2.2	-4.2	-4.7	0.0	1.0	-3.9	-2.1	0.0	0.0	-2.7	0.0
HNF1A	0.0	-1.1	0.1	0.0	2.6	1.6	1.1	0.0	-2.4	0.5	0.0	0.0
S-adenosylmethionine	0.0	1.2	-0.6	0.0	-0.7	-2.0	-0.5	-0.3	0.0	0.0	0.0	1.7
HDAC	0.0	1.0	-1.4	0.0	-1.1	2.2	-1.6	-0.1	0.0	0.0	0.2	0.0
MYCN	0.0	-1.2	-3.6	-4.2	-2.6	-2.0	3.3	1.3	0.0	0.0	-1.0	-1.1
Corticosterone	0.0	0.3	2.1	0.0	-0.2	-2.8	1.4	-0.1	0.0	0.1	0.8	0.0
ATF4	1.1	-1.3	1.9	0.0	2.2	0.0	1.0	-1.9	0.0	-1.9	0.5	0.4
IFNG	1.2	1.7	8.0	9.8	5.4	0.0	10.8	8.9	0.0	-1.4	4.4	1.1
SPARC	0.0	2.7	-2.9	-2.3	0.0	0.4	-1.9	-1.7	0.0	0.0	-2.4	-1.7
XDH	0.0	-0.9	0.0	-0.5	-0.3	-0.2	2.2	2.4	0.0	2.0	-1.4	-2.1
FOXO1	-0.2	0.4	1.0	1.2	2.4	1.1	2.2	2.2	0.0	-1.6	1.1	1.3
IRF7	0.0	2.0	6.5	7.7	3.9	-1.1	7.1	7.1	0.0	0.0	4.9	3.2
HTT	0.0	-0.3	2.5	3.2	1.3	-2.3	1.7	0.9	0.3	-0.5	0.3	-0.7
TGFB2	0.0	0.1	0.5	0.0	2.7	1.1	-1.2	-1.9	0.0	-2.0	-1.3	-1.1
TLR	2.0	0.0	2.0	3.7	3.2	-1.1	4.6	2.8	0.0	-2.0	0.0	0.0
IFNAR	0.0	2.6	5.7	6.9	2.7	-0.4	6.5	6.6	0.0	0.0	5.3	3.6
STAT5A	2.4	-0.4	-0.2	0.0	1.7	0.0	-0.5	-1.5	0.0	-2.6	2.6	0.0
TRIM24	0.0	-1.9	-6.0	-6.4	-3.1	-1.1	-5.9	-6.4	0.0	0.0	-4.9	-3.2
KITLG	0.0	1.1	2.6	3.2	2.2	0.0	3.5	2.6	0.0	-1.9	0.0	0.0
JUN	-0.3	1.7	1.2	4.0	3.1	-0.5	1.5	-0.4	0.0	-0.8	-0.3	-1.2
ETS2	0.0	2.4	3.7	3.5	2.0	-0.6	2.4	2.9	0.0	0.0	0.9	0.0
RXRA	1.4	-0.6	0.1	2.3	0.0	0.0	-1.8	-1.9	0.0	-2.4	2.0	1.4
RELA	2.1	1.3	3.8	5.0	3.9	-0.9	6.2	3.3	0.0	-0.8	2.1	0.0
BAX	0.0	-0.5	2.7	4.0	1.5	-2.4	3.5	2.3	0.0	0.0	2.2	0.0
RARA	0.0	-0.9	0.0	0.0	0.5	0.0	0.6	0.0	0.0	-2.0	0.1	0.0
Sodium chloride	0.0	2.2	2.8	0.0	2.2	-0.8	1.9	2.2	0.0	0.0	0.0	0.0
SOCS1	0.0	-1.6	-4.1	-5.7	-3.3	-1.3	-4.9	-4.0	0.0	0.0	-2.8	0.0
Estrogen receptor	0.5	-1.8	0.0	0.0	-2.0	1.1	0.4	2.1	0.0	0.0	2.8	2.7
BMP7	0.6	0.0	-1.3	0.0	-0.9	-0.5	-0.3	0.3	0.0	-2.4	1.3	1.0
IRF1	0.0	1.6	3.1	5.4	3.2	-1.3	4.9	4.7	0.0	0.0	2.8	0.0
ABCB4	0.0	-2.2	-2.9	0.0	-2.8	0.7	-1.2	1.9	0.0	0.0	2.1	2.8
JAG2	0.0	-0.9	-1.0	-2.8	-2.4	2.0	-2.7	0.0	0.0	0.0	0.0	0.0
CREBBP	0.0	0.1	1.0	0.0	-0.3	-0.3	-0.1	-0.2	0.0	-2.4	2.0	0.0
ERK1/2	0.5	2.0	4.2	3.9	2.9	-0.8	4.3	1.3	0.0	-0.1	0.4	1.2
HMGN5	0.0	-2.8	0.0	0.0	0.0	0.0	0.0	0.0	0.0	0.0	0.0	0.0
TAF7L	0.0	0.0	0.0	0.0	0.0	2.8	0.0	3.0	0.0	0.0	0.0	0.0
NFkB (complex)	0.9	-0.1	6.1	7.4	5.2	-1.3	6.9	3.9	0.0	-1.5	2.9	0.0
MTORC1	0.0	-2.2	0.0	0.0	0.0	0.6	0.0	0.0	0.0	0.0	0.0	0.0
MKL1	0.0	0.4	1.1	-2.8	0.6	2.4	-1.4	-1.2	0.0	0.0	0.1	0.0
RORA	0.0	-0.1	0.9	-0.4	0.4	0.7	0.3	-0.3	0.0	-2.0	0.9	1.5
PKD1	0.0	2.7	-1.6	0.0	-0.1	0.0	0.0	0.6	0.0	0.0	0.0	0.0
HMGA1	0.0	2.4	-1.7	0.4	0.6	-0.3	1.2	0.7	0.0	0.0	-1.3	-0.9
CD38	0.2	-0.5	2.5	2.0	1.8	2.2	0.9	0.9	0.0	0.0	0.8	0.6
SMARCA4	0.3	-1.9	1.5	1.6	3.4	-0.8	0.1	0.7	0.0	0.0	0.9	0.6
CTNNB1	0.0	2.1	-0.2	0.0	2.0	0.6	1.3	0.1	0.0	0.0	-2.2	-1.4
Hydrocortisone	0.7	-0.1	-0.3	0.0	-0.5	-0.6	-0.9	-1.8	0.0	-2.0	0.0	0.0
PRKAA2	0.0	0.8	-0.8	0.0	-2.4	-1.5	-2.1	-2.4	0.0	-0.5	1.1	1.2
MAP2K3	0.0	2.0	1.8	0.0	0.9	-0.7	0.9	0.2	0.0	0.0	-0.5	-1.0
MGEA5	0.0	2.7	-1.7	0.0	0.0	0.0	1.3	1.3	0.0	0.0	-0.7	-0.7

	Liver				Adipose				Skeletal Muscle			
	ΔGenotype[2]		ΔAge[3]		ΔGenotype[2]		ΔAge[3]		ΔGenotype[2]		ΔAge[3]	
Upstream Regulator	Young	Old	+/+	+/–	Young	Old	+/+	+/–	Young	Old	+/+	+/–
Hydrogen peroxide	1.7	-0.2	5.6	5.1	3.8	1.2	3.8	1.2	0.0	-1.2	1.5	1.0
SIRT2	0.0	-2.6	0.0	0.0	0.7	0.0	-1.7	-2.0	0.0	0.0	1.4	0.0
FN1	0.0	0.2	4.0	0.0	3.2	-0.5	3.9	2.5	0.0	-2.0	0.0	0.0
CYP7A1	0.0	-2.6	0.0	0.0	1.1	0.0	0.0	0.0	0.0	0.0	2.4	0.0
NR1H	0.0	-2.2	-2.6	-4.2	-1.6	0.3	-3.4	-3.0	0.0	-0.1	-0.9	0.7
CREB	2.0	0.4	2.5	0.0	1.9	0.0	1.4	0.7	0.0	-2.2	2.1	1.4
E2F1	0.0	2.6	2.2	3.8	0.0	0.0	0.0	-1.8	0.0	0.0	2.1	2.5
TLR4	0.0	-0.3	5.2	5.2	3.8	0.6	6.1	5.2	0.0	-1.7	2.1	0.0
TAC1	0.0	2.6	0.0	0.0	2.0	0.0	2.6	0.0	0.0	0.0	0.0	-2.0
TNFRSF1A	2.6	-1.5	3.5	2.5	3.2	-1.0	3.0	0.6	0.0	0.0	1.8	0.0
FOXA2	0.0	0.2	-2.2	0.0	-1.2	2.0	-1.4	-1.7	-2.2	0.3	-0.7	2.3
TLR3	2.0	-0.2	5.1	5.8	4.9	-0.9	6.0	3.1	0.0	-1.4	0.5	0.4
CORT	0.0	-2.4	-2.2	-3.2	-2.6	0.0	-2.9	-0.7	0.0	0.0	0.0	0.0
TP73	0.0	0.0	2.0	2.6	0.7	2.4	-0.4	0.0	0.0	0.0	3.3	2.1
TET2	0.0	-0.4	3.4	2.1	3.6	-2.0	1.8	-1.0	0.0	0.0	0.0	0.0
TLR2	1.7	-0.5	1.9	2.6	2.8	0.0	3.5	1.7	0.0	-2.0	0.0	0.0
CYP19A1	0.0	0.2	0.0	0.0	0.0	-2.2	0.0	0.0	0.0	0.0	0.0	0.0
MBTPS1	0.0	-2.4	0.0	0.0	0.0	0.0	-2.2	0.0	0.0	0.0	2.2	0.6
ATF2	0.0	2.4	0.0	0.0	0.0	0.0	0.1	-0.8	0.0	0.0	0.0	0.2
PEX5L	0.0	2.4	-2.6	0.0	0.0	0.0	1.7	2.0	0.0	0.0	0.0	0.0
PTF1A	0.0	2.4	0.0	0.0	0.0	0.0	0.0	0.0	0.0	0.0	0.0	0.0
NCOA1	0.0	0.0	0.2	0.0	0.0	0.0	0.0	0.0	0.0	-2.4	0.0	0.0
RHOA	0.7	-0.2	2.0	2.0	1.7	2.2	0.9	-0.9	0.0	0.0	0.8	0.0
SOD2	0.0	0.2	1.4	0.0	0.7	-2.2	0.7	0.0	0.0	0.0	0.0	0.0
APOA1	0.0	-1.9	-1.7	-2.2	-2.9	0.0	-2.9	0.0	0.0	-0.5	-1.2	0.0
MYD88	2.4	0.0	6.3	6.7	4.3	0.3	5.9	4.1	0.0	-2.1	3.7	0.0
ERN1	0.0	-2.4	0.0	0.0	0.0	0.0	1.4	-0.3	0.0	0.0	-0.8	0.1
Hyaluronic acid	0.0	1.1	2.2	2.9	3.2	-1.3	2.4	0.7	0.0	0.0	0.3	0.0
IKBKB	1.9	-0.1	4.3	5.7	3.3	-0.3	5.7	4.1	0.0	-1.9	1.9	-1.1
ETS1	0.0	1.9	4.3	4.0	2.0	-0.4	4.3	2.9	0.0	0.0	0.8	0.0
IL3	0.0	0.2	4.0	3.3	1.5	0.0	3.9	1.3	0.0	-2.1	2.3	1.4
MET	0.0	2.1	3.5	4.0	1.5	0.2	3.3	1.7	0.0	0.0	1.6	1.8
TREM1	1.6	-1.1	2.1	1.9	2.9	-1.2	1.8	-0.5	0.0	0.0	0.8	-1.0
FGF2	0.3	0.6	3.2	0.0	2.3	1.3	2.5	0.8	0.0	-0.4	-1.5	-0.6
SMAD3	-0.2	1.9	2.2	0.0	3.5	0.4	0.8	-1.0	0.0	0.0	-1.7	-2.1
CCR2	0.0	2.0	1.7	3.2	2.1	-0.3	2.0	0.9	0.0	0.0	0.0	0.0
TLR9	2.0	-0.5	3.6	4.8	4.3	-0.1	4.9	2.8	0.0	-1.6	0.0	0.0
MTTP	0.0	0.1	0.0	0.0	0.0	0.0	-0.6	0.0	0.0	2.1	-1.9	-0.8
JAK2	2.2	0.3	3.5	3.2	2.8	-2.0	4.0	1.8	0.0	0.0	2.6	0.0
VIP	0.0	0.3	-2.1	-2.7	-2.0	1.8	-2.4	0.0	0.0	0.1	0.0	0.0
IDH1	0.0	0.0	0.0	0.0	0.0	0.0	-2.2	-2.0	0.0	-2.2	2.6	1.3
MAT1A	0.0	2.2	-0.3	0.0	-0.3	0.0	-1.6	0.4	0.0	0.0	-1.1	-1.0
AGPAT2	0.0	0.0	0.0	0.0	0.0	0.0	-1.3	-2.0	0.0	-2.2	1.9	1.3
WISP2	0.0	-2.2	-1.6	0.0	0.0	0.0	0.0	1.2	0.0	0.0	0.0	1.7
ANXA7	0.0	2.2	0.0	0.0	1.3	0.0	0.0	0.0	0.0	0.0	0.0	0.0
BID	0.0	0.0	2.7	2.5	3.0	-2.2	3.1	-0.6	0.0	0.0	0.0	0.0
SRC	0.0	1.5	0.5	2.0	2.1	0.8	2.5	0.0	0.0	0.0	0.0	0.0
Fe2+	0.0	2.2	-0.9	0.3	0.0	0.0	0.0	2.0	0.0	0.0	0.0	0.0
Farnesyl pyrophosphate	0.0	2.2	0.8	0.0	0.9	0.0	0.9	0.0	0.0	0.0	-1.3	0.0
PARP9	0.0	2.2	3.6	3.4	0.0	0.0	3.1	3.6	0.0	0.0	3.4	2.8
STK11	0.0	-2.2	1.1	0.0	0.9	0.0	0.5	1.8	0.0	0.0	1.0	-0.7
HMGB1	0.0	-0.2	1.6	0.0	1.9	2.0	2.7	0.0	0.0	0.0	2.2	0.0
IL11RA	0.0	2.2	2.2	2.4	3.0	0.0	2.6	0.0	0.0	0.0	0.0	0.0
STAT3	0.0	-2.2	0.0	0.0	2.4	0.0	0.0	-2.0	0.0	0.0	0.0	0.0

	Liver				Adipose				Skeletal Muscle			
	ΔGenotype[2]		ΔAge[3]		ΔGenotype[2]		ΔAge[3]		ΔGenotype[2]		ΔAge[3]	
Upstream Regulator	Young	Old	+/+	+/–	Young	Old	+/+	+/–	Young	Old	+/+	+/–
IL1	1.7	0.0	4.5	5.0	2.7	-0.4	4.6	3.2	0.0	-1.8	2.4	0.0
MLXIPL	0.0	0.0	-3.0	0.0	0.0	2.2	0.0	1.1	0.0	0.0	2.0	2.0
PIK3R1	0.0	2.2	1.2	0.0	1.9	0.0	1.4	0.8	0.0	0.0	1.7	0.0
Anandamide	0.0	2.2	0.0	0.0	0.5	0.0	0.0	0.0	0.0	0.0	0.0	0.0
RBL1	0.0	-2.2	-2.9	-2.9	-0.1	0.0	-0.9	0.0	0.0	0.0	0.0	0.0
CCND1	0.0	0.0	0.0	1.9	0.0	-2.2	1.7	-0.7	0.0	0.0	0.0	0.0
PTPN1	0.0	-2.2	0.0	0.0	-1.3	0.0	0.0	0.0	0.0	0.0	0.0	0.0
NR5A2	0.6	2.2	0.2	0.0	0.1	0.0	1.8	2.2	0.0	0.0	0.0	0.0
MEF2C	0.0	-2.2	0.0	0.0	-2.2	0.0	0.0	0.0	0.0	0.0	-0.1	1.6
5-hydroxytryptamine	0.0	2.1	1.1	0.0	0.3	0.0	1.4	0.0	0.0	0.0	0.0	0.0
PPARD	2.6	1.1	-0.7	0.0	-0.6	0.8	-0.8	-0.3	0.0	-0.1	0.4	1.9
MAPKAPK2	0.0	1.7	1.9	1.8	2.1	-0.3	3.1	2.7	0.0	0.0	1.2	0.0
LHX1	0.0	0.0	0.0	0.0	1.2	2.0	0.0	2.9	0.0	0.0	0.0	1.9
KDM5B	0.0	2.0	-0.9	-1.3	-0.1	0.0	1.9	2.7	0.0	0.0	-0.7	0.0
TNF	0.8	-0.8	7.9	9.3	7.5	-1.1	10.4	5.3	-0.7	0.2	2.3	-0.6
Gamma-linolenic acid	0.0	2.0	2.0	0.0	0.0	0.0	1.4	-0.4	0.0	0.0	0.0	0.0
Acetaldehyde	0.0	2.0	2.4	0.0	2.0	0.0	2.5	0.0	0.0	0.0	-1.9	-1.8
Arginine	0.0	-2.0	1.8	0.0	-0.3	0.0	1.4	0.0	0.0	0.0	0.0	1.7
NADPH oxidase	0.0	2.0	0.0	0.0	1.2	0.0	1.8	1.5	0.0	0.0	0.0	0.0
CYP51A1	0.0	2.0	-1.9	0.0	0.0	0.0	0.0	2.0	0.0	0.0	-2.6	-2.2
NOS3	0.0	-2.0	0.0	0.0	-0.4	0.0	-0.4	-1.0	0.0	0.0	0.0	0.0
PAPOLB	0.0	0.0	0.0	0.0	0.0	2.0	0.0	2.4	0.0	0.0	0.0	0.0
ENPP2	0.0	0.0	0.0	0.0	0.0	0.0	0.0	0.0	0.0	2.0	-2.1	0.0
JAG1	0.0	0.0	2.4	2.0	1.1	-2.0	1.8	0.0	0.0	0.0	0.0	0.0
CSF1R	0.0	0.0	2.6	2.2	1.3	-2.0	0.5	-0.5	0.0	0.0	0.0	0.0
MEDAG	0.0	0.0	0.0	0.0	0.0	0.0	-2.4	-2.0	0.0	-2.0	2.6	2.4
SOCS6	0.0	-2.0	1.9	1.1	0.0	0.0	0.0	1.5	0.0	0.0	0.0	0.0
Hbb-b2	0.0	1.0	4.0	4.6	2.3	-1.0	4.5	2.8	0.0	0.0	2.8	0.0
DMD	0.0	-2.0	0.0	0.0	0.0	0.0	-0.8	-1.1	0.0	0.0	0.1	1.0
TMEM173	0.0	0.0	0.0	0.0	0.0	-2.0	2.9	2.1	0.0	0.0	0.0	0.0
CASP1	0.0	0.0	0.0	0.0	0.0	0.0	-0.8	-1.3	0.0	-2.0	0.0	0.0
GRIP1	0.0	-2.0	-2.2	-2.9	-2.0	0.0	-2.6	0.0	0.0	0.0	0.0	0.0
NCOR1	-2.0	0.0	-0.4	0.0	-0.5	0.0	0.0	0.4	0.0	2.0	-0.5	-0.6
YBX2	0.0	0.0	0.0	0.0	0.0	2.0	0.0	2.2	0.0	0.0	0.0	0.0
NOS2	1.4	0.4	1.0	3.5	2.9	-1.1	2.4	1.9	0.0	0.5	-0.2	-1.0
NFKBIA	2.0	0.2	2.4	3.9	3.3	0.5	3.6	3.4	0.0	-1.3	-0.3	-2.4
PTPN6	0.0	0.0	-3.0	-3.0	-2.4	2.0	-3.1	-0.4	0.0	0.0	-2.2	0.0
PRKCB	0.0	-0.8	1.1	0.0	2.4	1.1	1.4	0.0	0.0	0.0	0.0	0.0
IL9	0.0	2.0	2.4	0.0	2.0	0.0	2.2	0.6	0.0	0.0	0.0	0.0
TGF beta	-0.1	0.4	2.0	0.0	2.1	1.6	1.1	0.2	0.0	0.0	-1.8	-2.4
Palmitic acid	0.8	-0.2	2.4	3.8	3.5	-0.8	3.7	1.6	0.0	-1.0	1.6	1.9
IRF3	0.0	1.8	5.0	5.7	2.3	-0.1	5.1	6.7	0.0	0.0	4.9	3.1
MOG	0.0	1.7	2.8	3.1	2.4	-0.3	3.3	1.4	0.0	0.0	2.2	1.8
CDKN1B	0.0	0.0	0.0	0.0	-2.4	1.9	-0.8	-0.6	0.0	0.0	-1.8	0.0
AKT1	0.6	1.2	2.2	3.4	3.0	0.2	1.5	-0.2	0.0	-0.4	0.1	-0.6
Jnk	0.0	0.9	4.5	0.0	3.0	1.0	4.3	2.2	0.0	0.0	-0.2	0.0
Progesterone	0.1	-0.7	1.4	2.5	2.4	0.0	2.1	0.8	0.0	1.1	-0.7	-0.9
IRF8	0.0	0.3	2.5	3.4	2.4	-0.9	3.6	1.8	0.0	-0.7	0.4	0.0
PARP1	0.0	1.4	2.5	4.3	2.4	0.4	2.6	0.9	0.0	0.0	3.0	2.0
TRPV4	0.0	0.7	1.9	2.1	3.1	-1.1	2.8	0.9	0.0	0.0	0.0	0.0
OLR1	0.0	0.7	3.1	2.6	2.8	-1.1	3.9	3.6	0.0	0.0	0.0	0.0
TCR	-1.0	-1.0	4.6	3.6	2.4	-0.8	4.5	1.9	0.0	0.0	2.0	0.5
NFKB1	0.0	1.1	3.8	4.1	3.4	-0.5	3.9	2.2	0.0	-0.2	1.8	0.0
RETNLB	0.0	0.9	4.7	3.8	4.8	-0.4	3.3	0.9	0.0	-0.4	1.1	-2.1

	Liver				Adipose				Skeletal Muscle			
	ΔGenotype[2]		ΔAge[3]		ΔGenotype[2]		ΔAge[3]		ΔGenotype[2]		ΔAge[3]	
Upstream Regulator	Young	Old	+/+	+/–	Young	Old	+/+	+/–	Young	Old	+/+	+/–
ITK	0.0	1.7	2.6	3.3	2.2	0.0	3.1	3.0	0.0	0.0	0.0	2.1
S100A4	0.0	1.7	3.0	0.0	2.2	0.0	2.5	2.4	0.0	0.0	0.2	-1.3
SOCS3	0.0	-1.6	-1.8	-3.1	-2.8	0.0	-3.0	-1.7	0.0	0.0	0.0	0.0
IL17A	2.4	-0.9	4.1	4.0	4.5	0.7	4.1	0.9	0.0	0.0	2.3	0.0
IL12 (complex)	0.0	-1.0	4.2	4.4	3.2	-0.6	3.8	1.7	0.0	0.0	2.8	0.0
PDGFB	0.0	-0.6	2.4	0.0	2.4	-1.0	3.4	0.3	0.0	0.0	-1.7	-2.3
NR4A3	0.0	-1.6	1.6	0.0	-2.8	0.0	0.6	1.8	0.0	0.0	-0.3	1.0
PTGS2	0.0	-0.1	2.9	3.0	2.1	-1.5	4.7	1.5	0.0	0.0	0.4	0.1
IFN alpha/beta	0.0	1.5	3.7	4.9	2.4	-0.1	4.0	4.4	0.0	0.0	2.9	1.8
NR1I3	2.9	-0.2	2.4	0.0	1.4	0.0	0.0	0.9	0.0	-1.4	1.9	0.0
BMP2	0.1	-0.2	-1.0	0.0	2.6	-0.4	0.0	0.0	0.0	-1.0	0.0	-1.0
BMP6	0.0	-0.4	0.8	0.8	2.8	1.1	0.4	-0.6	0.0	0.0	-1.2	-1.7
D-glucose	2.5	-0.1	1.3	0.0	2.3	1.4	1.5	1.7	0.0	-0.1	0.5	0.2
PRKCA	0.0	-1.0	2.9	0.0	2.9	0.6	3.2	0.5	0.0	0.0	0.8	0.0
Immunoglobulin	0.0	-0.5	-2.2	-0.7	-2.0	0.7	-0.2	-1.6	0.0	-0.3	-1.1	1.8
ERK	1.7	0.7	4.5	0.0	2.8	0.4	4.7	1.7	0.0	0.4	-0.3	-0.4
STAT	0.0	-1.5	0.0	2.6	2.4	0.0	2.4	0.0	0.0	0.0	2.6	0.0
Ursodeoxycholic acid	0.0	1.5	3.0	2.2	2.0	0.0	0.5	-0.3	0.0	0.0	0.7	0.0
ERBB4	0.0	0.2	-2.0	0.0	-2.1	-1.2	-1.3	-0.9	0.0	0.0	-0.3	-0.1
PTX3	0.0	-1.4	0.0	0.0	-2.5	0.0	-3.5	-2.1	0.0	0.0	-2.7	-1.9
Aldosterone	1.7	0.6	3.9	0.0	3.3	-0.3	3.4	2.2	0.0	-0.5	-1.3	-2.6
IFN gamma	0.0	0.9	3.4	4.4	3.1	-0.5	5.0	3.1	0.0	0.0	3.3	0.0
TNFRSF1B	2.0	-1.3	2.3	0.0	2.0	0.1	2.7	-0.1	0.0	0.0	0.0	0.0
LAMA5	0.0	1.3	0.0	2.6	2.2	0.0	3.4	1.8	0.0	0.0	0.0	0.0
IFI16	0.0	0.0	1.8	0.0	2.2	-1.3	2.2	0.8	0.0	0.0	1.8	0.9
SMAD4	0.0	1.3	1.2	0.0	2.3	0.0	-0.2	0.2	0.0	0.0	-1.7	-1.5
Alpha catenin	-1.1	0.6	-5.4	0.0	-5.1	-0.7	-4.8	-0.7	0.0	0.0	1.8	4.6
EGF	0.7	-0.1	4.5	5.0	4.5	0.6	3.7	0.3	0.0	-0.7	-0.8	-1.2
NFAT (family)	0.0	0.0	0.0	0.0	2.8	0.3	2.7	0.0	0.0	-1.0	0.0	0.0
ADA	0.0	-0.8	0.0	0.0	-2.2	0.4	-1.2	0.0	0.0	0.0	0.0	1.9
IL6R	2.2	-0.8	2.8	0.0	2.1	-0.4	1.4	-0.2	0.0	0.0	0.0	0.0
GFI1	0.0	-1.2	-2.2	-3.3	-2.9	0.0	-2.9	-1.2	0.0	0.0	0.0	0.0
SMAD2	0.0	1.2	3.2	0.0	2.6	0.0	0.0	0.0	0.0	0.0	0.0	-2.1
CG	1.4	0.0	3.2	0.0	4.2	1.0	1.8	-0.7	0.0	-0.1	-0.1	-0.6
GPX1	0.0	-0.9	-3.2	-2.6	-2.4	0.2	-1.9	-2.0	0.0	0.0	0.0	0.0
PLAU	0.0	0.0	3.6	2.5	2.3	1.1	2.6	1.7	0.0	0.0	0.9	0.0
CD2	0.0	1.1	2.3	3.5	2.4	0.0	4.3	2.3	0.0	0.0	0.0	0.0
DUSP1	0.0	-1.1	0.0	-3.0	-2.4	0.0	-2.2	0.0	0.0	0.0	0.0	0.0
AGT	1.9	0.5	5.4	5.1	3.9	-0.6	2.8	0.7	0.0	0.0	0.1	-0.7
THPO	0.0	1.1	0.0	1.8	2.2	0.0	0.9	-0.7	0.0	0.0	0.0	0.0
HMGN3	0.0	0.0	0.0	0.0	3.0	0.0	1.7	0.0	-2.2	1.1	-2.3	0.0
STAT4	0.0	-1.0	4.7	5.2	2.8	-0.1	1.9	1.4	0.0	0.0	3.2	0.6
NFYA	2.0	-1.1	2.5	0.0	2.2	0.0	0.0	0.0	0.0	0.0	0.7	1.2
VEGF	1.1	0.3	6.1	0.0	3.5	0.8	2.4	-0.4	0.0	0.0	0.0	-1.9
MAP2K1/2	0.0	1.0	2.4	0.0	2.4	0.0	2.8	1.2	0.0	0.0	0.0	0.0
TRAF6	0.0	1.0	3.1	3.3	2.3	0.0	3.0	0.0	0.0	0.0	0.0	0.0
MSTN	0.0	1.0	0.0	0.0	2.4	0.0	0.0	-0.6	0.0	0.0	1.8	1.2
PDGF (complex)	0.0	0.9	2.4	0.0	2.1	0.0	2.0	-0.1	0.0	0.0	0.0	-0.1
IL1R1	0.0	0.3	0.0	0.0	2.4	0.6	2.0	0.9	0.0	0.0	0.0	-2.0
IL1A	1.3	-0.2	5.0	0.0	4.1	-0.3	4.6	1.7	0.0	-0.4	0.0	-1.2
JAK1	0.0	0.9	2.0	3.7	2.3	0.0	4.0	3.1	0.0	0.0	2.7	2.0
IFNA2	1.3	0.0	7.1	7.5	2.9	0.9	6.2	5.4	0.0	0.0	4.7	3.0
CD3	0.0	-0.9	-2.8	-3.1	-2.4	0.0	-3.0	-1.1	0.0	0.0	-0.9	0.5
CXCL12	0.0	0.7	4.1	4.6	2.9	-0.2	4.4	3.2	0.0	0.0	2.5	2.1

	Liver				Adipose				Skeletal Muscle			
	ΔGenotype[2]		ΔAge[3]		ΔGenotype[2]		ΔAge[3]		ΔGenotype[2]		ΔAge[3]	
Upstream Regulator	Young	Old	+/+	+/–	Young	Old	+/+	+/–	Young	Old	+/+	+/–
CD5	0.0	-0.9	1.8	1.4	2.1	0.0	2.8	1.2	0.0	0.0	2.2	0.0
IL8	0.0	0.0	2.1	1.8	2.0	0.9	1.7	1.5	0.0	0.0	1.7	0.0
AGER	0.0	0.4	2.0	1.8	2.3	0.4	1.5	0.4	0.0	0.0	0.0	0.0
THBS4	0.0	-0.8	2.2	2.1	2.4	0.0	3.3	0.0	0.0	0.0	1.3	1.5
C5	1.0	-0.5	3.5	3.4	2.6	-0.2	3.0	0.5	0.0	0.2	0.0	0.0
HNF4A	2.4	0.6	-1.3	2.5	2.9	0.0	1.9	2.5	-2.2	-0.1	0.7	1.8
F7	0.0	0.7	0.0	0.0	2.2	0.0	1.9	0.0	0.0	0.0	0.0	0.0
AKT	2.3	0.1	2.9	2.6	2.3	0.7	1.3	-0.1	0.0	0.0	0.0	0.0
CCL5	0.0	0.7	3.5	2.9	3.0	0.0	2.9	1.0	0.0	0.0	0.0	0.0
EIF2AK2	2.0	0.7	4.7	4.1	2.5	0.0	2.6	1.5	0.0	0.0	0.9	0.4
IL12A	0.0	0.6	1.8	3.7	2.0	0.0	2.2	1.6	0.0	0.0	0.0	0.0
CEBPD	0.0	0.4	1.4	1.5	2.3	0.2	1.6	1.4	0.0	0.0	-1.2	0.0
CAT	0.0	0.0	-1.9	0.0	-2.8	0.5	-0.3	0.9	0.0	0.0	0.0	0.0
GDF2	0.0	0.0	-0.9	0.0	3.0	-0.5	0.1	-1.2	0.0	0.0	-1.0	-0.6
IKZF1	0.0	0.0	-2.3	-1.8	-3.0	-0.5	-1.9	-1.4	0.0	0.0	0.0	0.0
GM-CSF	0.0	0.5	2.3	0.0	2.8	0.0	3.3	0.0	0.0	0.0	0.0	0.0
ADAMTS12	0.0	0.4	-3.1	-3.0	-3.1	0.0	-3.7	-1.8	0.0	0.0	0.0	0.0
C3	0.0	-0.4	2.1	2.3	2.0	0.0	1.8	0.6	0.0	0.0	0.0	0.0
IL18	0.0	0.2	4.8	4.5	3.6	0.2	4.5	2.0	0.0	0.0	0.0	0.0
IL12B	0.0	0.4	3.0	3.9	2.8	0.0	4.0	3.0	0.0	0.0	2.7	0.0
CYP2E1	0.0	0.3	1.6	1.9	2.2	0.0	2.5	1.8	0.0	0.0	0.0	0.0
LTA	0.0	0.0	2.0	3.1	2.2	0.3	2.2	1.7	0.0	0.0	0.0	0.0
FCER1	0.0	0.3	3.8	3.1	2.4	0.0	3.4	1.3	0.0	0.0	0.0	0.0
Angiotensin II receptor	0.0	0.0	0.0	0.0	2.4	0.2	1.7	1.3	0.0	0.0	0.0	0.0
ZAP70	0.0	0.0	0.0	0.0	2.4	-0.2	0.0	-1.4	0.0	0.0	1.1	0.0
EBI3	0.0	0.1	3.0	3.0	2.4	0.0	2.6	1.9	0.0	0.0	2.8	0.0
NRG1	0.0	0.1	2.7	0.0	2.2	0.0	1.9	-0.3	0.0	0.0	0.0	0.2
Leukotriene D4	0.0	-0.1	2.4	0.0	2.1	0.0	4.2	2.4	0.0	0.0	0.5	0.0
PRKCE	0.0	0.0	2.1	2.9	2.4	0.0	2.0	-0.6	0.0	0.0	0.0	0.0
Indican	0.0	0.0	0.0	0.0	2.4	0.0	2.0	-0.4	0.0	0.0	0.0	0.0
10-nitrooleate	0.0	0.0	0.0	0.0	-2.0	0.0	-1.4	0.0	0.0	0.0	0.0	0.0
Choline	0.0	0.0	0.0	0.0	-2.2	0.0	0.0	0.0	0.0	0.0	0.0	0.0
NfkB-RelA	0.0	0.0	0.0	0.0	2.4	0.0	1.9	1.1	0.0	0.0	0.0	0.0
Fibrinogen	0.0	0.0	1.9	1.9	2.1	0.0	2.5	0.0	0.0	0.0	0.0	0.0
Smad	0.0	0.0	0.2	0.0	2.1	0.0	-0.5	0.0	0.0	0.0	-1.0	0.0
Ncoa-Nr1i3-Rxra	0.0	0.0	0.0	0.0	2.0	0.0	0.0	0.0	0.0	0.0	0.0	0.0
CXCL2	0.0	0.0	1.8	2.6	2.2	0.0	2.8	1.1	0.0	0.0	0.0	0.0
IL23A	0.0	0.0	2.6	2.6	2.4	0.0	3.2	0.0	0.0	0.0	0.0	0.0
CRH	0.0	0.0	0.0	0.0	2.2	0.0	0.0	0.0	0.0	0.0	0.0	0.0
CYBB	0.0	0.0	2.3	1.9	2.0	0.0	1.4	0.0	0.0	0.0	0.0	0.0
HSPD1	0.0	0.0	2.2	0.0	2.2	0.0	1.7	0.0	0.0	0.0	2.2	0.0
NOX4	0.0	0.0	1.1	0.0	2.4	0.0	2.2	0.9	0.0	0.0	0.0	0.0
PLA2G2D	0.0	0.0	0.0	-2.6	-2.2	0.0	-2.4	-0.3	0.0	0.0	0.0	0.0
C5AR1	0.0	0.0	3.4	2.8	2.4	0.0	2.5	1.4	0.0	0.0	0.0	0.0
FCGR3	0.0	0.0	2.2	1.1	2.0	0.0	1.5	0.0	0.0	0.0	0.0	0.0
Relaxin	0.0	0.0	0.0	0.0	-2.0	0.0	0.0	0.0	0.0	0.0	0.0	0.0
TCF 1/3/4	0.0	0.0	0.0	0.0	2.2	0.0	2.2	0.0	-2.0	0.0	-2.2	2.0
SOD	0.0	0.0	0.0	0.0	-2.2	0.0	-2.8	0.0	0.0	0.0	0.0	0.0
INHBB	0.0	0.0	0.0	0.0	2.0	0.0	0.3	-0.6	0.0	0.0	0.0	-0.6
IGF2	0.0	0.0	2.0	2.3	2.3	0.0	-0.1	-1.1	0.0	0.0	-1.1	-0.2
NGF	0.0	0.0	0.0	0.0	2.1	0.0	2.2	0.0	0.0	0.0	1.8	0.0
MAP3K5	0.0	0.0	2.6	0.0	2.0	0.0	2.6	0.6	0.0	0.0	0.0	-1.4
NTRK2	0.0	0.0	0.0	0.9	2.2	0.0	0.7	0.0	0.0	0.0	0.0	0.0
PIM1	0.0	0.0	0.0	0.0	2.2	0.0	2.0	0.0	0.0	0.0	0.0	0.0

	Liver				Adipose				Skeletal Muscle			
	ΔGenotype[2]		ΔAge[3]		ΔGenotype[2]		ΔAge[3]		ΔGenotype[2]		ΔAge[3]	
Upstream Regulator	Young	Old	+/+	+/–	Young	Old	+/+	+/–	Young	Old	+/+	+/–
BTK	0.0	0.0	2.0	1.4	2.2	0.0	1.5	0.0	0.0	0.0	0.0	0.0
RXRB	0.0	0.0	0.0	0.0	-2.0	0.0	-1.9	0.0	0.0	0.0	0.0	0.0
RPL13A	0.0	0.0	-2.4	-2.2	-2.2	0.0	-2.4	-0.8	0.0	0.0	0.0	0.0
CYR61	0.0	0.0	1.2	0.0	2.4	0.0	2.8	0.1	0.0	0.0	0.0	0.4
CAMP	0.0	0.0	2.0	1.6	2.2	0.0	2.0	0.6	0.0	0.0	0.0	0.0
DMP1	0.0	0.0	0.0	0.0	-2.4	0.0	-2.1	-2.2	0.0	0.0	0.0	0.0
SELPLG	0.0	0.0	3.4	3.2	2.1	0.0	3.5	1.7	0.0	0.0	2.8	2.1
CR1L	0.0	0.0	-2.0	0.0	-2.6	0.0	1.2	2.7	0.0	0.0	3.1	3.1
VGLL3	0.0	0.0	0.0	0.0	2.0	0.0	2.0	0.0	0.0	0.0	-2.1	-1.1
TRADD	0.0	0.0	2.1	2.1	2.6	0.0	3.1	1.7	0.0	0.0	2.4	0.0
COL18A1	0.0	0.0	-2.5	0.0	-2.1	0.0	-2.4	0.0	0.0	0.0	0.0	2.0
SERPINF1	0.0	0.0	-1.3	0.0	-2.2	0.0	-1.8	0.0	0.0	0.0	0.0	0.4
S100A8	0.0	0.0	2.2	2.2	2.2	0.0	1.6	0.0	0.0	0.0	0.0	0.0
S100A9	0.0	0.0	2.4	2.6	2.4	0.0	1.9	-0.2	0.0	0.0	0.0	0.0
CFB	0.0	0.0	2.1	0.0	2.4	0.0	2.4	2.2	0.0	0.0	0.0	0.0
USP18	0.0	0.0	-1.5	-2.8	-2.2	0.0	-2.9	-2.2	0.0	0.0	-2.2	0.0
WWTR1	0.0	0.0	0.0	0.0	2.0	0.0	0.0	0.0	0.0	0.0	0.0	0.0
HDAC2	0.0	0.0	0.0	0.0	-2.4	0.0	0.0	0.0	0.0	0.0	1.1	0.0
SMAD1	0.0	0.0	0.0	0.0	2.6	0.0	0.0	-2.0	0.0	0.0	-2.7	-2.2
OTX2	0.0	0.0	0.0	0.0	2.2	0.0	0.0	0.0	0.0	0.0	-2.1	0.0
GLI1	0.0	0.0	2.2	0.0	3.0	0.0	0.5	1.2	0.0	0.0	-0.2	-1.1
ID2	0.0	0.0	0.0	0.0	-2.0	0.0	-2.8	-1.6	0.0	0.0	0.0	0.0
DDIT3	0.0	0.0	0.0	0.0	2.4	0.0	0.7	0.9	0.0	0.0	0.0	0.0
T	0.0	0.0	0.0	0.0	2.0	0.0	0.4	0.0	0.0	0.0	0.0	0.0
SMARCD3	0.0	0.0	0.0	0.0	2.0	0.0	0.0	0.0	0.0	0.0	0.0	0.0
EEF1A2	0.0	0.0	-2.2	-2.2	-2.0	0.0	-2.2	-2.2	0.0	0.0	-2.0	0.0
IGF2BP1	0.0	0.0	0.0	0.0	2.4	0.0	0.0	-2.6	0.0	0.0	-2.2	-2.8
IFNGR1	0.0	0.0	2.7	3.0	2.0	0.0	2.5	0.0	0.0	0.0	0.0	0.0
OSMR	0.0	0.0	0.0	0.0	2.2	0.0	1.4	0.0	0.0	0.0	-1.2	0.0
TYROBP	0.0	0.0	0.0	3.0	2.6	0.0	3.8	0.0	0.0	0.0	0.0	0.0
CSF2RB	0.0	0.0	0.0	0.0	2.0	0.0	1.9	0.0	0.0	0.0	0.0	0.0
EDNRA	0.0	0.0	0.0	0.0	2.2	0.0	2.6	0.8	0.0	0.0	0.0	-2.0
IL17RA	0.0	0.0	2.3	1.9	2.6	0.0	3.0	0.0	0.0	0.0	0.0	0.0
TLR5	0.0	0.0	2.2	0.0	2.2	0.0	2.8	0.0	0.0	0.0	0.0	0.0
CTLA4	0.0	0.0	0.0	0.0	-2.2	0.0	-3.0	0.0	0.0	0.0	0.0	0.0
IGFBP7	0.0	0.0	-1.9	0.0	-2.0	0.0	-1.7	-0.5	0.0	0.0	0.0	0.0
TNNI3	0.0	0.0	0.0	2.2	2.0	0.0	2.4	1.3	0.0	0.0	0.0	0.0
GJA1	0.0	0.0	1.1	0.0	-2.2	0.0	0.0	0.1	0.0	0.0	0.0	0.0
SLC4A1	0.0	0.0	-1.1	-0.7	-2.0	0.0	0.0	-1.5	0.0	0.0	0.0	0.0

Appendix 2. Upstream Regulators Implicated by Analysis of Microarray Data

[1]IPA (Ingenuity) software was used to analyze microarray expression data sets to predict upstream regulators. All the values shown are z-scores generated by the software. Values greater than 2 or less than -2 are considered meaningful. Rows were sorted by the sum of absolute values of z-scores for the genotype effect in old (24 month old) mice, and all upstream regulators for which there is a meaningful difference between genotypes in at least one tissue are shown.

[2]Changes due to genotype (ΔGenotype columns). Red shading indicates a stronger effect in $Myc^{+/-}$ *versus* $Myc^{+/+}$ animals (*i.e.* effectors/regulators whose influence is more pronounced in $Myc^{+/-}$ tissues). Conversely, blue shading indicates a stronger effect in $Myc^{+/+}$ *versus* $Myc^{+/-}$ animals (*i.e.* effectors/regulators whose influence is more pronounced in $Myc^{+/+}$ tissues). The intensity of the shading illustrates the relative magnitude of the effect.

[3]Changes due to age (ΔAge columns). Red shading indicates a stronger effect in old (24 month old) relative to young (5 month old) animals (*i.e.* effectors/regulators whose influence is more pronounced in old tissues). Conversely, blue shading indicates a stronger effect in young *versus* old animals (*i.e.* effectors/regulators whose influence is more pronounced in young tissues). The intensity of the shading illustrates the relative magnitude of the effect.

Appendix 3. List of Primers Used in PCR Analysis[1]

#	Designation	Sequence	Notes
Primer pair 1[2]	MYCFLXS MYCFLXA	GCCCCTGAATTGCTAGGAAGACTG CCGACCGGGTCCGAGTCCCTATT	Intron 1 of *Myc*, 5' of the 5' Lox site, sense orientation. Intron 1 of *Myc*, 3' of the 5' Lox site, antisense orientation. Primer pair will amplify 378 bp fragment from $Myc^{+/+}$ (wild-type) chromosome, and nothing from the $Myc^{+/-}$ (deletion) chromosome, because primers flank 5' Lox site.
Primer pair 2[2]	MYCDELS MYCDELA	TCGCGCCCCTGAATTGCTAGGAA TGCCCAGATAGGGAGCTGTGATACTT	Intron 1 of *Myc*, 5' of the 5' Lox site, sense orientation. Downstream of *Myc*, 3' of the 3' Lox site, antisense orientation. Primer pair will amplify ~450 bp fragment from $Myc^{+/-}$ (deletion) chromosome, and nothing from the $Myc^{+/+}$ (wild-type) chromosome, because the primers are too far apart.
Primer pair 3	JSMYCX JSMYCY	CCTCGCGCCCCTGAA AACCGCTCAGATCACGACTCA	Intron 1 of *Myc*, 5' of the 5' Lox site, sense orientation. Intron 1 of *Myc*, 5' of the 5' Lox site, sense orientation. Used for qPCR of genomic DNA, as control in assays to quantify the efficiency of Cre-mediated deletion. Primer pair will detect all copies of *Myc* locus (both wild-type and deleted).
Primer pair 4	JSMYCN JSMYCB	TCCAAACCAGAAACTGAAACATGT ACAATGGGGTCATTTAGGAC	Downstream of *Myc*, 5' of the 3' Lox site, sense orientation. Downstream of *Myc*, 3' of the 3' Lox site, antisense orientation. Used for qPCR of genomic DNA, in assays to quantify the efficiency of Cre-mediated deletion. Primer pair will detect only the $Myc^{+/+}$ (wild-type) locus (and hence show 50% of the signal of primers X-Y if the deletion was complete).
Primer pair 5	XZMTCYTBAF XZMTCYTBAR	ACGAAGCCTAATATTCCGCCCAATC AAATGGGTGTTCTACTGGTTGGCCC	Sense orientation. Antisense orientation. In the cytochrome B gene of mitochondrial DNA. Used for qPCR of mitochondrial DNA.
Primer pair 6	XZMCMYC1F XZMCMYC1R	TTCCTTTGGGCGTTGGAAAC GCTGTACGGAGTCGTAGTCG	At the 3' end of *Myc* exon 1, sense orientation. In *Myc* exon 2, antisense orientation. Used for RT-qPCR of *Myc* mRNA. Primers span intron 1.
Primer pair 7	JHLSSF JHLSSR	GCACACCACAGACCTGAGTTTC CAGTGTGCTGAAGGAGAAACCAC	Sense orientation. Antisense orientation. Used for RT-qPCR of the mRNA of the *Lss* gene. Primers span an intron.
Primer pair 8	JHSQLEF JHSQLER	GTTGCGGATGGACTCTTCTCC GACCAGAACAAGCTCCGCA	Sense orientation. Antisense orientation. Used for RT-qPCR of the mRNA of the *Sqle* gene. Primers span an intron.
Primer pair 9	JHHMGCRF JHHMGCRR	GCTCGTCTACAGAAACTCCACG CTTCAGCAGTGCTTTCTCCGT	Sense orientation. Antisense orientation. Used for RT-qPCR of the mRNA of the *Hmgcr* gene. Primers span an intron.
Primer pair 10	JHMVDF JHMVDR	AGCTAGTCCACCGCTTCAACA CAAACTCAGCCACAGTGTCCTC	Sense orientation. Antisense orientation. Used for RT-qPCR of the mRNA of the *Myd* gene. Primers span an intron.

Primer pair 11	JHHMGCS1F JHHMGCS1R	GGAAATGCCAGACCTACAGGTG CTCGGAGAGCATGTCAGGCT	Sense orientation. Antisense orientation. Used for RT-qPCR of the mRNA of the *Hmgcs1* gene. Primers span an intron.
Primer pair 12	JHMVKF JHMVKR	CTTCAGCGACTGGACACGA AGAGCCATGCCTTCATTGC	Sense orientation. Antisense orientation. Used for RT-qPCR of the mRNA of the *Myk* gene. Primers span an intron.
Primer pair 13	JHIDI1F JHIDI1R	GCTCCTGTTACAGCAGAGATCAG GCTTCACACCAATGGCGTT	Sense orientation. Antisense orientation. Used for RT-qPCR of the mRNA of the *Idi1* gene. Primers span an intron.
Primer pair 14	JHSREBF2F JHSREBF2R	GAAAGAGCGGTGGAGTCCTTG CTGTACGACAAAGGGCACCA	Sense orientation. Antisense orientation. Used for RT-qPCR of the mRNA of the *Srebf2* gene. Primers span an intron.
Primer pair 15	P21MouseF P21MouseR	TCAGAGCCACAGGCACCAT TCCACGGGACCGAAGAGA	Sense orientation. Antisense orientation. Used for RT-qPCR of the mRNA of the *Cdkn1a* gene. Primers span an intron.
Primer pair 16	P16MouseF P16MouseR	CCAGGGCCGTGTGCAT TACGTGAACGTTGCCCATCA	Sense orientation. Antisense orientation. Used for RT-qPCR of the mRNA of the *Cdkn2a* gene. Primers span an intron.
Primer pair 17	MGAPDHF MGAPDHR	CGGCCGCATCTTCTTGTG GTGACCAGGCGCCCAATA	Sense orientation. Antisense orientation. Used for RT-qPCR of the mRNA of the *Gapdh* gene. Primers span an intron.

[1]All sequences are listed in the 5'->3' orientation.
[2]These primers pairs were used for genotyping of animals using tail snip DNA. Both primer pairs were included in the same PCR reaction.

AGE
DOI 10.1007/s11357-014-9618-3

The effects of aging on the expression of Wnt pathway genes in mouse tissues

Jeffrey W. Hofmann · Tony McBryan · Peter D. Adams · John M. Sedivy

Received: 21 June 2013 / Accepted: 12 January 2014

Abstract The Wnt signaling pathway is involved in the regulation of tissue patterning and organ development during embryogenesis and continues to contribute to the maintenance of tissue homeostasis in adulthood. Recently, Wnt signaling has also been implicated in the establishment and progression of replicative cellular senescence. Given the known roles of tissue homeostasis and cellular senescence in aging, we sought to determine whether Wnt signaling changes with age. We examined the expression of 84 Wnt pathway-related genes in the liver, lung, skeletal muscle, and brain tissue from young and old mice. Expression changes were compared with those seen in cellular senescence, and transcription factors that might mediate these changes were predicted bioinformatically. In aggregate, our data are indicative of a general decrease in Wnt signaling with age, especially in the lung and brain. Furthermore, the set of genes that are differentially expressed with age is distinct from the genes differentially expressed in cellular senescence. The transcription factors predicted to regulate these changes, Nf-κB, Myb, Nkx2-1, Nr5a2, and Ep300, are known to regulate inflammation, differentiation, lipid metabolism, and chromatin remodeling, all of which have previously been implicated in aging. Although our study does not address whether altered Wnt signaling is a cause or an effect of aging, the presence of a relationship between the two provides a starting point for further investigation.

Keywords Aging · Wnt pathway · Cellular senescence

Electronic supplementary material The online version of this article (doi:10.1007/s11357-014-9618-3) contains supplementary material, which is available to authorized users.

J. W. Hofmann · J. M. Sedivy (✉)
Department of Molecular Biology, Cell Biology and Biochemistry, Laboratories for Molecular Medicine, Brown University, Providence, RI 02903, USA
e-mail: john_sedivy@brown.edu

T. McBryan · P. D. Adams
Beatson Institute for Cancer Research and Institute for Cancer Sciences, University of Glasgow, Glasgow, UK

Introduction

Aging is a gradual deleterious process that underlies the pathogenesis of the majority of diseases responsible for human morbidity and mortality. Though the etiology of aging is not fully understood, there is abundant evidence that it is not simply caused by the accumulation of damage but rather is governed by genetic mechanisms (Kenyon 2010). Elucidation of these mechanisms would greatly accelerate our ability to formulate effective therapies to treat or prevent some of the most prevalent diseases of the modern world.

Aging of the cell can be broken down into two categories: chronological and replicative. Chronological aging is largely due to the accumulation of damaged or destructive molecules that impair the function of the cell, and it has the strongest effects in terminally differentiated cells which are unable to dilute these molecules through cell division. Replicative aging is the damage caused by proliferation such as shortening of telomeres. Replicative aging can ultimately result in replicative cellular

Published online: 01 February 2014

senescence, causing cells to cease proliferation and adopt the senescence-associated secretory phenotype, in which they secrete inflammatory molecules that damage their local environment. The proportion of cells that have entered replicative senescence increases with age, but the mechanisms underlying this progression are not fully understood (Krishnamurthy et al. 2004; Tchkonia et al. 2010; Wang et al. 2009).

Recent work has implicated the Wnt signaling pathway in replicative senescence and, thereby, aging (Ye et al. 2007). Though the Wnt pathway is mostly known for its role in morphogenic signaling during embryonic development, there are some reports of its involvement in homeostasis of adult tissues and stem cell maintenance (Alonso and Fuchs 2003; Boj et al. 2012; Hu et al. 2007; Reya et al. 2003). Wnt signaling naturally declines in senescent cells, and its repression induces cellular senescence (Ye et al. 2007). There is also evidence that dysfunctional Wnt signaling is pathogenic in many aging-related diseases. The decline of Wnt signaling with age contributes to the pathogenesis of osteoporosis (Almeida et al. 2007; Bennett et al. 2005), Alzheimer's disease, and Parkinson's disease (Berwick and Harvey 2012); increased Wnt signaling with age is thought to cause fibrosis in skeletal muscle, resulting in sarcopenia (Arthur and Cooley 2012); and a variant of TCF7L2, a transcriptional effector of the Wnt pathway, increases the risk of type II diabetes (Grant et al. 2006). Attaining a greater understanding of the relationship between aging and Wnt signaling in vivo would be valuable in the study of age-associated diseases and changes in physiology.

In the canonical Wnt signaling pathway, a soluble Wnt ligand binds to the Frizzled receptor (Fzd) and the LRP5/6 co-receptor on the plasma membrane, which activate the cytoplasmic protein Dishevelled (Dvl). Dvl inhibits the β-catenin (Ctnnb1) destruction complex (APC, GSK3β, and Axin), hence preventing the phosphorylation and consequent destruction of Ctnnb1. When it is stabilized as a result of active Wnt signaling, Ctnnb1 can translocate to the nucleus, form a complex with Lef and Tcf transcription factors, and thereby activate transcription of target genes such as c-Myc and Cyclin D1. To investigate the effects of age on Wnt signaling, we used quantitative PCR arrays to measure the expression of 84 relevant genes, including those listed above as well as other inhibitors, modulators, and effectors of Wnt signaling in young and old mice. Determining which genes are differentially expressed with age in various tissues in vivo has revealed novel tissue-specific mechanisms by which organ function and homeostasis decline with time, as well as a greater understanding of the roles of Wnt signaling in adult animals.

Experimental procedures

Gene expression analysis

Tissues were harvested from 5- and 36-month-old male C57BL/6J (Jackson Labs) mice purchased from the NIA and sacrificed in our facility and 24-month-old C57BL/6N (Charles River) mice that were bred and aged in our own facility. These two sub-strains of C57BL/6 differ by only 34 single nucleotide polymorphisms (SNPs) and 2 indels in coding regions and 146 SNPs and 54 indels in noncoding regions, none of which are within or near to any of the genes observed in this study (Simon et al. 2013); thus, variability due to strain is not expected to significantly affect our results. The following tissues were examined: liver, skeletal muscle, lung, and brain, although only liver and muscle were available from 24-month-old mice. Samples were homogenized in liquid nitrogen and then resuspended and further homogenized in TRIzol reagent according to the manufacturer's suggested protocol (Invitrogen). RNA was isolated using phenol chloroform extraction and purified using the RNeasy kit from QIAGEN. Quality of individual RNA preparations was verified using the Bioanalyzer (Agilent), and only samples with RIN>9 were used. Equal amounts of total RNA from ten 5- or 36-month-old mice, or five 24-month-old mice, were pooled, and then reverse transcription and quantitative PCR were performed in triplicate on the pooled samples. Gene expression was measured using the mouse Wnt signaling pathway RT^2 Profiler PCR Array (SABiosciences/QIAGEN, PAMM-043E-4) using the manufacturer's protocols. This array contains primers corresponding to 84 genes related to the Wnt pathway, five housekeeping genes for normalization, and positive and negative controls for the PCR reaction (raw data are provided in Table S1). Genes were considered to be differentially expressed if their expression differed by at least twofold in either direction between either 5- and 24- or 5- and 36-month-old mice, and that difference was statistically significant across technical replicates.

Transcription factor prediction

The Transfac software package was used to predict which transcription factors are most likely to cause the observed changes in gene expression. Promoter sequences were defined as −1,000 to +200 bp relative to the transcription start site, and loci within each promoter that were at least a 90 % match to a transcription factor binding site were identified and summed to create a score for each transcription factor for each gene. To predict whether each transcription factor regulates age-related changes in Wnt signaling, its scores for genes that were differentially expressed between 5- and 36-month-old mice were compared to its scores for genes that were not differentially expressed with age, and a two-tailed *t* test was used to determine whether the promoters of differentially expressed genes were more enriched for binding sites than promoters of non-differentially expressed genes.

Results

Assessment of variability

To verify that the detection of differentially expressed genes was not adversely affected by pooling samples from different animals, mRNA quantity of *Ccnd2* in the liver and *Lef1* in the lung was measured by qPCR on samples from individual animals (Fig. 1). Biological variability was low and the effect of age was similar to that observed in the pooled samples: average expression and standard deviation in arbitrary units for *Ccnd2* were 0.905±0.081 in young and 2.138±0.457 in old and for *Lef1* were 1.408±0.074 in young and 0.515±0.010 in old. This indicates that pooling of RNA samples from different animals is unlikely to reduce the accuracy of our findings.

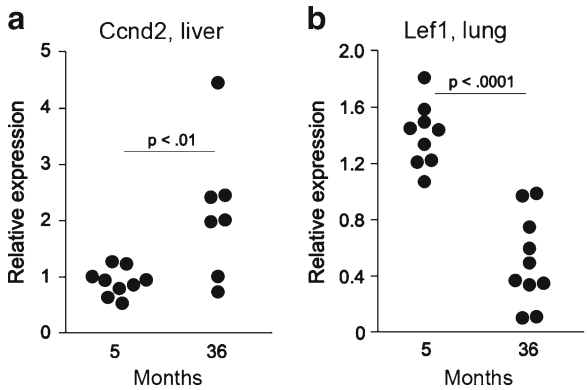

Fig. 1 Relative expression of *Ccnd1* and *Lef1* in the liver and lung, respectively, measured by qPCR of samples from 5- or 36-month-old male mice. Seven to ten individual mice were used for each group, and a two-tailed *t* test was used to compute *p* values. Expression is reported in arbitrary units, determined by normalization to *Gapdh* in each sample

Liver

Several genes related to Wnt signaling were differentially expressed with age in the liver, although the implications of these changes for Wnt pathway activity are somewhat contradictory and hence remain uncertain (Fig. 2a). *Wnt11* expression decreased with age, whereas *Wnt6* expression increased, and neither was among the Wnt ligands with high expression in the liver (Fig. 3a). Extracellular inhibitors of Wnt ligands had higher expression in the liver from older mice (*Frzb*, *Sfrp1*), which suggests less Wnt signaling. However, some positive mediators of Wnt signaling had greater expression in old liver (*Dvl*), while others had reduced expression (*Fzd2*, *Fzd3*). The same dichotomy was exhibited by the transcription factors that drive Wnt-dependent expression (*Lef1*, *Tcf3*). Among genes whose expression is regulated by Wnt signaling, *Ccnd1* and *Ccnd2* were upregulated in old mice. However, their transcriptional regulation is known to be multifactorial and could thus be driven by other means. In summary, we cannot draw strong conclusions about the effects of age on Wnt signaling in the liver from these data.

Brain

Wnt signaling appeared to decrease with age in the brain (Fig. 2b). All genes related to the Wnt pathway whose expression changed with age in the brain showed decreased expression in old mice. Among these genes was a positive mediator of Wnt signaling (*Dixdc1*), a transcriptional output (*Ccnd2*), two Wnt-dependent transcription factors (*Lef1*, *Tcf3*), and three Wnt ligands (*Wnt2*, *Wnt4*, *Wnt9a*). *Wnt4* was the Wnt ligand that had the greatest expression in the brain (Fig. 3b), so its decreased expression is particularly likely to indicate a functional effect on Wnt signaling in this tissue.

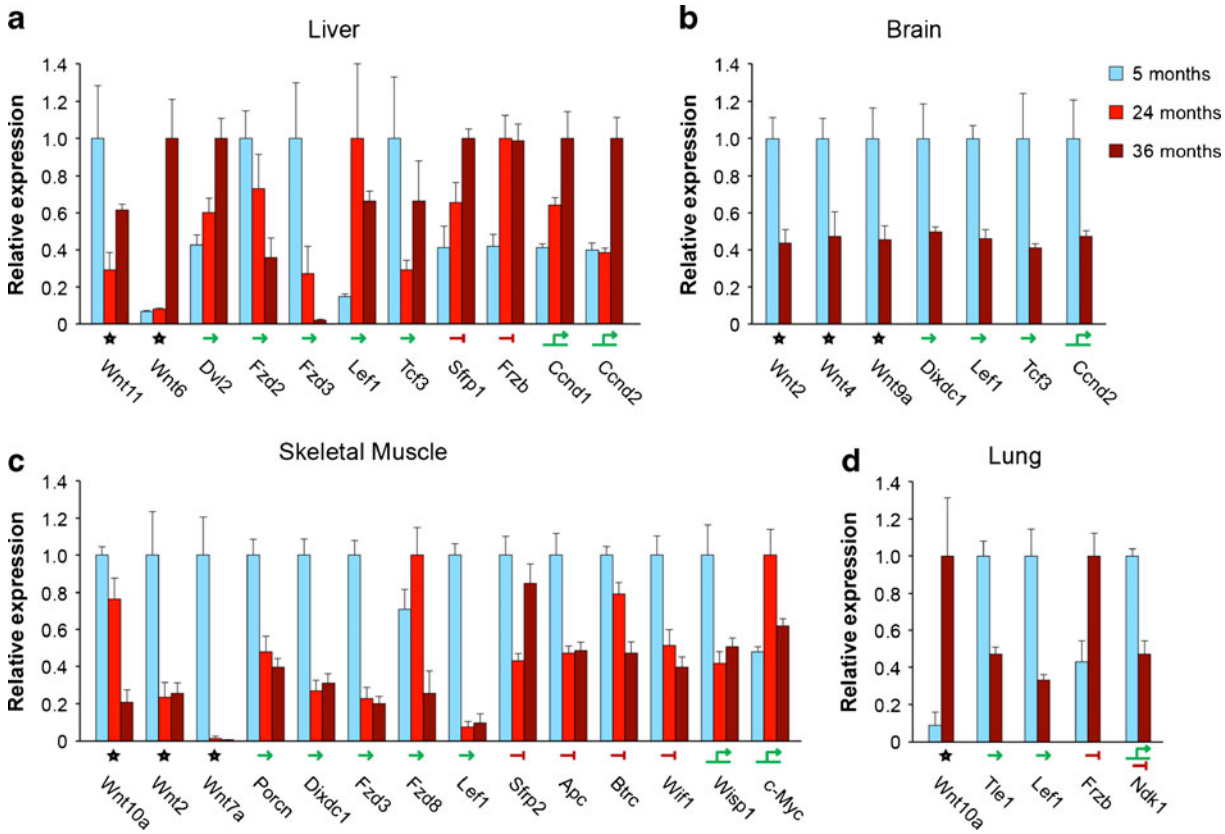

Fig. 2 Relative expression of genes that are differentially expressed between 5-month-old and either 24- or 36-month-old mice for the **a** liver, **b** brain, **c** muscle, or **d** lung. *Symbols* below each set of columns indicate whether it is a Wnt ligand (*star*), positive mediator of Wnt signaling (*green arrow*), inhibitor of Wnt signaling (*red inhibitory arrow*), or transcriptional output of Wnt signaling (*green promoter arrow*). Expression is listed in arbitrary units determined by normalization to the housekeeping genes *Gusb*, *Hprt*, *Hsp90ab1*, *Gapdh*, and *Actb* and further normalized to the age with the highest expression for each gene. *Error bars* represent the standard error among technical replicates

Skeletal muscle

All differentially expressed genes showed decreased expression in skeletal muscle except c-*Myc*. Both positive mediators and some inhibitors of Wnt signaling were represented (Fig. 2c). *Apc* and *Btrc* are part of the β-catenin destruction complex, and *Sfrp1* and *Wif1* directly inhibit Wnt ligands outside the cell. Their downregulation in old animals would be consistent with increased Wnt signaling. In contrast, *Dixdc1*, *Fzd3*, *Fzd8*, and *Lef1* all positively mediate Wnt signaling; *Porcn* is required for Wnt ligand synthesis; *Wnt10a*, *Wnt2*, and *Wnt7a* are Wnt ligands (though other Wnt ligands show higher expression in muscle; Fig. 3c); and *Wisp1* expression is a transcriptional output of Wnt signaling. Their downregulation collectively implies less Wnt signaling. Overall, the most likely explanation of these changes is that Wnt signaling is decreased, and therefore, less inhibition is needed to keep it in check. This is supported by the magnitude of the observed expression changes, namely, that the decreases in the expression of genes that positively affect Wnt signaling are more substantial than the decreases in the expression of inhibitors of the pathway. Although c-*Myc* expression is inconsistent with this interpretation, c-*Myc* is regulated by a diverse set of genes and physiologic parameters, and its upregulation with age may not be related to Wnt signaling.

Lung

Wnt signaling also decreased with age in the lung. *Tle1* and *Lef1*, which positively mediate Wnt signaling, showed decreased expression; *Frzb*, an extracellular Wnt ligand inhibitor, had greater expression; and *Nkd1*, whose expression is driven by Wnt signaling

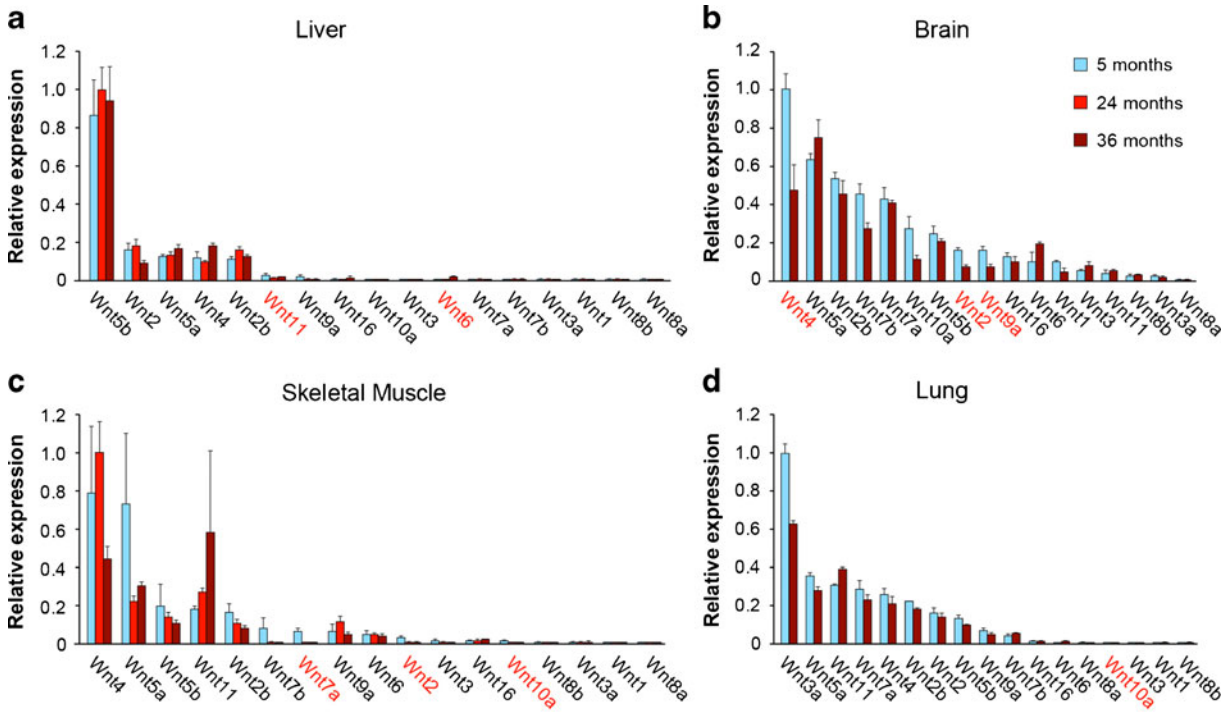

Fig. 3 Relative expression of Wnt ligands for 5-, 24-, or 36-month-old mice in the **a** liver, **b** brain, **c** muscle, or **d** lung, sorted by expression at 5 months. Genes that are differentially expressed between either 5- and 24- or 5- and 36-month-old mice have *red text*. *Error bars* represent the standard error among technical replicates

and also provides negative feedback, had decreased expression with age (Fig. 2d). All of these changes are indicative of reduced Wnt signaling. The Wnt ligand *Wnt10a* was upregulated in older animals but was one of the least expressed Wnt ligands in the lung. Although it is quite possible that the differential expression of *Wnt10a* has physiological significance, it is unlikely to represent overall pathway activity because it is opposed by several other components of the pathway that are expressed at much higher levels (Fig. 3d).

Transcription factor analysis

We used the bioinformatics package Transfac to predict which transcription factors (TFs) might regulate the genes that were differentially expressed with age in a manner consistent with the direction of change. TF-binding affinity was computed between each of 2,200 transcription factors and the promoter of each differentially expressed gene using known TF-binding sites in the Transfac database. For each transcription factor, the average score across differentially expressed genes was compared to that of genes in our dataset that were not differentially expressed. This analysis was performed on skeletal muscle since it had the greatest number of differentially expressed genes of all the tissues studied and therefore was most likely to yield reliable results. The transcription factors that are statistically more likely to regulate differentially expressed genes are NF-κB, Myb, Nkx2-1, Nr5a2, and Ep300 (Table 1). Neither a literature search nor the bioinformatics package Ingenuity (Ingenuity Systems) revealed existing experimentally validated evidence linking any of these transcription factors with the regulation of more than one of the differentially expressed genes. Thus, the transcription factors identified here are potentially novel regulators of the age-dependent Wnt signaling changes in skeletal muscle.

Comparison with cellular senescence

Wnt signaling has been implicated in regulating cellular senescence (Ye et al. 2007), and the frequency of senescent cells increases in several tissues with age (Krishnamurthy et al. 2004; Tchkonia et al. 2010; Wang et al. 2009). One possible hypothesis thus would be that the differential expression of Wnt pathway genes observed in this study reflects the changing proportion

Table 1 Transcription factors predicted to regulate Wnt pathway genes differentially expressed in the skeletal muscle

Transcription factor	*p* value	Differentially expressed score[a]	Non-differentially expressed score[a]	Function
NF-κB	0.019	0.269642	0	Inflammation
Myb	0.028	6.38036	4.281	Hematopoiesis, tumorigenesis
Nkx2-1	0.030	7.939676	5.936284	Thyroid and lung development
Nr5a2	0.043	2.404614	1.559868	Cholesterol metabolism, transport
Ep300	0.04	4.369797	3.115769	Chromatin remodeling

[a] Scores indicate similarity between the binding motif for that transcription factor and sequences in the promoter region of a gene, and the average scores from differentially expressed or non-differentially expressed genes are listed. Statistics were computed using a two-tailed *t* test

of senescent cells with age. To address this, the set of genes differentially expressed with age in our dataset was compared with a list of genes found to be differentially expressed in either oncogene-induced senescence or replicative senescence (Nelson et al. 2014). Additionally, the known transcriptional outputs of Wnt signaling that were differentially expressed in senescent cells (Nelson et al. 2014) were referenced in whole genome microarray data comparing gene expression in the liver, skeletal muscle, and adipose tissue of young and old mice (our unpublished data). In both comparisons of organismal aging and cellular senescence, no significant correlations were found for genes that comprise the Wnt signaling pathway. Therefore, the expression changes we have described above are unlikely to be caused by age-related increases in cellular senescence.

Discussion

Overall, our analysis indicates that Wnt signaling tends to decrease with age in mouse tissues. Although the effect of age on Wnt signaling in the liver was ambiguous, it is likely that it decreases with age in skeletal muscle, and there was clear repression with age in both the brain and lung. This repression of gene expression was distributed across the pathway, with decreases in Wnt ligands as well as both cytoplasmic and nuclear mediators of Wnt signaling. Although some of the differentially expressed Wnt ligands have low expression relative to other Wnt ligands expressed in the same tissue, evidence in the literature suggests that such "minor" ligands can affect the physiology of that tissue in a meaningful way. For example, Wnt7a is one of the Wnt ligands with the lowest expression in skeletal muscle, but its effects on muscle regeneration via stem cell activation (Le Grand et al. 2009) and activation of the mTOR pathway to induce muscle growth (von Maltzahn et al. 2012) have been well established. Consequently, it would not be surprising if the drastic decrease in Wnt7a expression with age we observed in skeletal muscle underlies the age-related impairment of this tissue.

Although Wnt signaling has been shown to decline in senescent cells and the number of senescent cells increases in many tissues with age, a comparison of the expression changes caused by either organismal aging or cellular senescence suggests that the effects of each on Wnt signaling are not related. This is consistent with the prevailing evidence that the frequency of senescent cells in tissues, even at advanced age, is likely to be quite low (Wang et al. 2009). In particular, skeletal muscle contains very few (if any) senescent cells, and their number does not seem to increase with age (Wang et al. 2009). Since the great majority of cells in skeletal muscle are mature myocytes (muscle fibers), the changes in the Wnt pathway we observed with age are likely attributable to this cell type.

To search for the cause of decreased Wnt signaling in old animals, we employed a computational approach to identify common regulators of differentially expressed genes. The transcription factors that were identified are known to regulate diverse biological functions, including inflammation, hematopoiesis, organ development, cholesterol metabolism, and chromatin remodeling. Both inflammation and chromatin remodeling are known to be inextricably tied to aging, so it would not be surprising if one or both of these were the cause of reduced Wnt signaling with age, potentially mediated by the transcriptional regulators NF-κB and/or Ep300. Additionally, our data suggest that the effects of processes like inflammation that are associated with aging

may be deleterious at least partially due to their interaction with Wnt signaling.

It has been well documented that Wnt signaling positively influences adult stem and progenitor cell maintenance (Hoffman et al. 2004; Kuhnert et al. 2004). This pathway has recently also emerged as potentially a key regulator of cellular senescence (Ye et al. 2007). Consistent with these anti-aging properties, several reports have documented that inherited genetic polymorphisms that result in reduced Wnt signaling are associated with premature aging phenotypes such as heart disease, metabolic syndrome, Alzheimer's disease, osteoporosis, and diabetes (De Ferrari et al. 2007; Gong et al. 2001; Mani et al. 2007; Soriano et al. 2001; Welters and Kulkarni 2008). This genetic evidence is consistent with the idea that maintenance of Wnt signaling is required for stem cell homeostasis and hence acts to delay aging processes. However, other lines of evidence suggest that over activation of the Wnt pathway can have pro-aging effects by promoting excessive tissue fibrosis (Chilosi et al. 2003) and thus accelerating the onset of tissue dysfunction and age-associated phenotypes (Brack et al. 2007; Liu et al. 2007). In sum, several different lines of evidence support the hypothesis that Wnt signaling impacts the aging processes. Whether Wnt signaling accelerates or delays aging and to what extent these effects are tissue specific remains to be worked out in detail. Our data presented here, based on expression analysis of Wnt pathway component genes in four major tissues of the mouse (liver, brain, skeletal muscle, and lung), are indicative of a general trend toward reduced activity of this pathway with age.

Acknowledgments Research in the Sedivy laboratory was supported by NIH/NIA grants R37 AG016694 and R01 AG035328 to J.M.S. J.W.H. was supported by a NRSA individual predoctoral MD/PhD fellowship from the NIH/NIA, F30 AG035592. J.M.S. was a senior scholar of the Ellison Medical Foundation and a recipient of the Glenn Award for Research on the Biological Mechanisms of Aging from the Glenn Foundation for Medical Research.

References

Almeida M, Han L, Martin-Millan M, O'Brien CA, Manolagas SC (2007) Oxidative stress antagonizes Wnt signaling in osteoblast precursors by diverting beta-catenin from T cell factor- to forkhead box O-mediated transcription. J Biol Chem 282(37):27298–27305

Alonso L, Fuchs E (2003) Stem cells in the skin: waste not, Wnt not. Genes Dev 17(10):1189–1200

Arthur ST, Cooley ID (2012) The effect of physiological stimuli on sarcopenia; impact of notch and Wnt signaling on impaired aged skeletal muscle repair. Int J Biol Sci 8(5):731–760

Bennett CN, Longo KA, Wright WS, Suva LJ, Lane TF, Hankenson KD, MacDougald OA (2005) Regulation of osteoblastogenesis and bone mass by Wnt10b. Proc Natl Acad Sci U S A 102(9):3324–3329

Berwick DC, Harvey K (2012) The importance of Wnt signalling for neurodegeneration in Parkinson's disease. Biochem Soc Trans 40(5):1123–1128

Boj SF, van Es JH, Huch M, Li VS, Jose A, Hatzis P, Mokry M, Haegebarth A, van den Born M, Chambon P et al (2012) Diabetes risk gene and Wnt effector Tcf7l2/TCF4 controls hepatic response to perinatal and adult metabolic demand. Cell 151(7):1595–1607

Brack AS, Conboy MJ, Roy S, Lee M, Kuo CJ, Keller C, Rando TA (2007) Increased Wnt signaling during aging alters muscle stem cell fate and increases fibrosis. Science 317(5839):807–810

Chilosi M, Poletti V, Zamo A, Lestani M, Montagna L, Piccoli P, Pedron S, Bertaso M, Scarpa A, Murer B et al (2003) Aberrant Wnt/beta-catenin pathway activation in idiopathic pulmonary fibrosis. Am J Pathol 162(5):1495–1502

De Ferrari GV, Papassotiropoulos A, Biechele T, Wavrant De-Vrieze F, Avila ME, Major MB, Myers A, Saez K, Henriquez JP, Zhao A et al (2007) Common genetic variation within the low-density lipoprotein receptor-related protein 6 and late-onset Alzheimer's disease. Proc Natl Acad Sci U S A 104(22):9434–9439

Gong Y, Slee RB, Fukai N, Rawadi G, Roman-Roman S, Reginato AM, Wang H, Cundy T, Glorieux FH, Lev D et al (2001) LDL receptor-related protein 5 (LRP5) affects bone accrual and eye development. Cell 107(4):513–523

Grant SF, Thorleifsson G, Reynisdottir I, Benediktsson R, Manolescu A, Sainz J, Helgason A, Stefansson H, Emilsson V, Helgadottir A et al (2006) Variant of transcription factor 7-like 2 (TCF7L2) gene confers risk of type 2 diabetes. Nat Genet 38(3):320–323

Hoffman J, Kuhnert F, Davis CR, Kuo CJ (2004) Wnts as essential growth factors for the adult small intestine and colon. Cell Cycle 3(5):554–557

Hu M, Kurobe M, Jeong YJ, Fuerer C, Ghole S, Nusse R, Sylvester KG (2007) Wnt/beta-catenin signaling in murine hepatic transit amplifying progenitor cells. Gastroenterology 133(5):1579–1591

Kenyon CJ (2010) The genetics of ageing. Nature 464(7288):504–512

Krishnamurthy J, Torrice C, Ramsey MR, Kovalev GI, Al-Regaiey K, Su L, Sharpless NE (2004) Ink4a/Arf expression is a biomarker of aging. J Clin Invest 114(9):1299–1307

Kuhnert F, Davis CR, Wang HT, Chu P, Lee M, Yuan J, Nusse R, Kuo CJ (2004) Essential requirement for Wnt signaling in proliferation of adult small intestine and colon revealed by adenoviral expression of Dickkopf-1. Proc Natl Acad Sci U S A 101(1):266–271

Le Grand F, Jones AE, Seale V, Scime A, Rudnicki MA (2009) Wnt7a activates the planar cell polarity pathway to drive the symmetric expansion of satellite stem cells. Cell Stem Cell 4(6):535–547

Liu H, Fergusson MM, Castilho RM, Liu J, Cao L, Chen J, Malide D, Rovira II, Schimel D, Kuo CJ et al (2007) Augmented

Wnt signaling in a mammalian model of accelerated aging. Science 317(5839):803–806

Mani A, Radhakrishnan J, Wang H, Mani MA, Nelson-Williams C, Carew KS, Mane S, Najmabadi H, Wu D, Lifton RP (2007) LRP6 mutation in a family with early coronary disease and metabolic risk factors. Science 315(5816):1278–1282

Nelson DM, McBryan T, Jeyapalan JC, Sedivy JM, Adams PD (2014) Comparative gene expression profiling reveals similarities and differences between oncogene-induced and replicative senescence. Age, (in press)

Reya T, Duncan AW, Ailles L, Domen J, Scherer DC, Willert K, Hintz L, Nusse R, Weissman IL (2003) A role for Wnt signalling in self-renewal of haematopoietic stem cells. Nature 423(6938):409–414

Simon MM, Greenaway S, White JK, Fuchs H, Gailus-Durner V, Wells S, Sorg T, Wong K, Bedu E, Cartwright EJ et al (2013) A comparative phenotypic and genomic analysis of C57BL/6J and C57BL/6N mouse strains. Genome Biol 14(7):R82

Soriano S, Kang DE, Fu M, Pestell R, Chevallier N, Zheng H, Koo EH (2001) Presenilin 1 negatively regulates beta-catenin/T cell factor/lymphoid enhancer factor-1 signaling independently of beta-amyloid precursor protein and notch processing. J Cell Biol 152(4):785–794

Tchkonia T, Morbeck DE, Von Zglinicki T, Van Deursen J, Lustgarten J, Scrable H, Khosla S, Jensen MD, Kirkland JL (2010) Fat tissue, aging, and cellular senescence. Aging Cell 9(5):667–684

von Maltzahn J, Bentzinger CF, Rudnicki MA (2012) Wnt7a-Fzd7 signalling directly activates the Akt/mTOR anabolic growth pathway in skeletal muscle. Nat Cell Biol 14(2):186–191

Wang C, Jurk D, Maddick M, Nelson G, Martin-Ruiz C, von Zglinicki T (2009) DNA damage response and cellular senescence in tissues of aging mice. Aging Cell 8(3):311–323

Welters HJ, Kulkarni RN (2008) Wnt signaling: relevance to beta-cell biology and diabetes. Trends Endocrinol Metab 19(10):349–355

Ye X, Zerlanko B, Kennedy A, Banumathy G, Zhang R, Adams PD (2007) Downregulation of Wnt signaling is a trigger for formation of facultative heterochromatin and onset of cell senescence in primary human cells. Mol Cell 27(2):183–196